STRUCTURE AND PROPERTIES OF SOME α-, β- AND γ-AGOSTIC ALKYL-TITANOCENE COMPLEXES

by

Alexandre F. Dunlop-Brière

A thesis submitted to the Department of Chemistry

In conformity with the requirements for

the degree of Doctor of Philosophy

Queen's University

Kingston, Ontario, Canada

(December, 2014)

Abstract

In chapter 2, the synthesis and NMR characterization of $[Cp_2TiCH_3(H_2O)]^+$ (**I**) is presented. In the presence of excess water, there is evidence of rapid H-exchange and H-bonding between coordinated and free water. At higher temperatures, **I** undergoes hydrolysis to produce methane.

In chapter 3, formation of $[Cp_2TiCH_2CHMeCMe_3]^+$ (**II**) via a controlled single 1,2-migratory insertion reaction of $[Cp_2TiMe]^+$ and 3,3-dimethyl-1-butene (3,3-DMB) at 205 K is presented. **II** exchanges between its two α-agostic isomers, with a preference for one agostic isomer over the other and also remains α-agostic under coordination of Et_2O.

In chapter 4, $[Cp_2TiCH_2CHMeSiMe_3]^+$ (**III**), a complex that is exchanging between γ- (ground state) and β- agostic isomers, is prepared by reaction of $[Cp_2TiMe]^+$ with 1 equivalent of trimethylvinylsilane at 205 K. There is exchange between β-H and γ-H from 215 K to 260 K but ^1H NMR data suggests no or very little increase in rate. $[Cp_2TiCH_2CHCD_3SiMe_3]^+$ undergoes a reversible and exclusive isotopomeric rearrangement to form specifically $[Cp_2TiCD_2CDCH_3SiMe_3]^+$ through a series of reversible β-H elimination, 2,1- and 1,2- migratory-insertion reactions (process 1). Deuteration of **III** at β- or γ- positions essentially shuts down the β-H/γ-H exchange, with a k_H/k_D of at least 13000 at 225 K. These results indicate that this latter exchange process is driven by H quantum mechanical tunneling (QMT).

Finally, chapter 5 presents is a re-investigation of **II** that unravels some exchange processes that were not detected in previous studies of **II**. EXSY and D-labeling (of β-Me in **II**) experiments suggest that **II** also undergoes process 1. Olefin dissociation from $[Cp_2TiH(CH_2=CMeCMe_3)]^+$ is faster than process 1 and EXSY correlations are seen intermolecularly between **II** and 2,3,3-TMB, as well as intramolecularly in 2,3,3-TMB (fastest exchange). In **II**-d_3, this rapid reversible olefin dissociation from the olefin-hydride complex coupled to process 1 leads to multiple isotopologuous rearrangements in 2,3,3-TMB before it can be re-incorporated in **II**, with similar overall rates of deuterium incorporation at all α- and β- sites in **II**-d_x (x = 0-6, statistical distribution with an average value of 3).

Co-Authorship

The current thesis is a manuscript based thesis. Michael C. Baird (supervisor) is a co-author for chapters 2-5 and Peter H. M. Budzelaar is a co-author for chapters 3-5. Professor Budzelaar is responsible for all DFT calculations and related discussion. I performed the experimental work under the supervision of Professor Baird.

Acknowledgements

First and for most, I would like to thank my PhD supervisor Professor Michael C. Baird for mentoring me throughout my PhD program. It has been a great learning experience and his guidance, wisdom and friendship as a PI were much appreciated and proved to be a crucial factor in the accomplishment of this journey. Naturally also, an exceptional thanks to our collaborator, Peter H. M. Budzelaar, who did all the computational calculations in our work. His incomparable expertise and wisdom shed light on a lot of complicated issues we were hesitant on, and his help was often essential to solve problems that could not be addressed experimentally.

I would also like to give a special note of appreciation to our NMR specialist Dr. Françoise Sauriol who taught me everything I needed to know about NMR to accomplish my very heavily NMR-oriented research project. She has always been there to consult, support and help me with technical issues but also with spectral interpretations, and her friendship and enthusiasm were much appreciated during all these years.

I would also like to thank all other professors and members of the Department of Chemistry at Queen's University who have helped training me in many different ways, academically but professionally also. I would like to address a special thanks to Dr. Igor Kozin who taught me a lot about lab organization, team leadership and general professionalism through teaching assistantship in his laboratories. I would also like to thank Dr. Alexei Neverov and Mark Raycroft for their help for solving kinetics in a project. This PhD program would not have been the same without the amazing past and current members of the Baird lab, a big thanks to them for their support, useful discussions and friendships.

Finally, I would like to thank all my friends, my partner and my family for their support throughout my PhD.

Table of Contents

List of Figures

List of Tables

List of Abbreviations

Chapter 1

M	metal center (general)
R	alkyl or H atom (general)
P	polymeryl growing chain
Cp	cyclopentadienyl ligand, $[\eta^5\text{-}(C_5H_5)]^-$
C(1) or α-C	carbon directly bonded to M, or terminal olefinic carbon (methylene)
C(2) or β-C	carbon two-bond away from M or internal olefinic carbon (methine)
C(3) or γ-C	methyl carbon 3 bonds away from M, or C(2)-attached methyl carbon in olefin
dmpe	$Me_2PCH_2CH_2PMe_2$
1A (fig. 1.6)	Cp_2MR_2
1B (fig. 1.6)	$[Cp_2MR]^+$
1C (fig. 1.6)	$[Cp_2MR(CH_2{=}CHR')]^+$
1D (fig. 1.6)	$[Cp_2MCH_2CHRR']^+$
1E (fig. 1.6)	$[Cp_2M\{(CH_2CHR')_nCH_2CHRR'\}]^+$
1F (fig. 1.6)	$[Cp_2MR]^+$
1G (fig. 1.6)	β-agostic $[Cp_2MCH_2CHRR']^+$
□	Coordination site which is vacant or occupied by a loosely bonded molecule
MAO	methylaluminoxane
Cp'	$[\eta^5\text{-}(C_5H_3Me_2)]^-$
Cp''	$[\eta^5\text{-}\{C_5H_4(CH_2Ph)\}]^-$
Cp*	pentamethylcyclopentadienyl anion, $C_5Me_5^-$
DMP	2,4-dimethyl-1-pentene
SI	Supporting information

NOESY	Nuclear Overhauser Effect spectroscopy
EXSY	Exchange Spectroscopy
HSQC	Heteronuclear single quantum coherence spectroscopy
HMBC	Heteronuclear multiple-bond correlation spectroscopy
COSY	Correlation spectroscopy

Chapter 2

R	alkyl or H atom (general)
Cp	cyclopentadienyl ligand, $[\eta^5\text{-}(C_5H_5)]^-$
C(1) or α-C	carbon directly bonded to M, or terminal olefinic carbon (methylene)
C(2) or β-C	carbon two-bond away from M or internal olefinic carbon (methine)
C(3) or γ-C	methyl carbon 3 bonds away from M, or C(2)-attached methyl carbon in olefin
M	metal center (general)
DMP	2,4-dimethyl-1-pentene
DMH	2,4-dimethyl-1-heptene
I	solvent-separated ion pair $[Cp_2Ti(Me)(CD_2Cl_2)][B(C_6F_5)_4]$
II	contact ion pair $[Cp_2Ti(Me)B(C_6F_5)_4]$
III	dinuclear species $[Cp_2Ti(Me)(\mu\text{-}Me)Ti(Me)Cp_2][B(C_6F_5)_4]$
IV	$[Cp_2Ti(Me)(H_2O)][B(C_6F_5)_4]$
NOESY	Nuclear Overhauser Effect spectroscopy
EXSY	Exchange Spectroscopy
HSQC	Heteronuclear single quantum coherence spectroscopy
HMBC	Heteronuclear multiple-bond correlation spectroscopy
COSY	Correlation spectroscopy

Chapter 3

R	alkyl or H atom (general)
Cp	cyclopentadienyl ligand, $[\eta^5\text{-}(C_5H_5)]^-$
M	metal center (general)
C(1) or α-C	carbon directly bonded to M, or terminal olefinic carbon (methylene)
C(2) or β-C	carbon two-bond away from M or internal olefinic carbon (methine)
C(3) or γ-C	methyl carbon 3 bonds away from M, or C(2)-attached methyl carbon in olefin
P	polymeryl growing chain
A	α-agostic species of the type $[Cp_2M\text{-}\eta^2\text{-}(CH_2CHRP)]^+$
B	β-agostic species of the type $[Cp_2M\text{-}\eta^2\text{-}(CH_2CHRP)]^+$
DMP	2,4-dimethyl-1-pentene
DMB	3,3-dimethyl-1-butene
I	solvent-separated ion pair $[Cp_2Ti(Me)(CD_2Cl_2)][B(C_6F_5)_4]$
II	$[Cp_2TiCH_2CHMe^tBu]^+$
III	$[Cp_2TiCH_2CH_2{}^tBu]^+$
IV	$[Cp_2Ti(CH_2CHMe^tBu)(Et_2O)]^+$
IIa	α-agostic isomer of **II** in which Ha is agostic (dominant, C(1) = S chiral configuration)
IIb	α-agostic isomer of **II** in which Hb is agostic (minor, C(1) = R chiral configuration)
NOESY	Nuclear Overhauser Effect spectroscopy
EXSY	Exchange Spectroscopy
HSQC	Heteronuclear single quantum coherence spectroscopy
HMBC	Heteronuclear multiple-bond correlation spectroscopy
COSY	Correlation spectroscopy

Chapter 4

R	alkyl, aryl or H atom (general)
Cp	cyclopentadienyl ligand, $[\eta^5\text{-}(C_5H_5)]^-$
M	metal center (general)
WCA	weakly coordinating anion
C(1) or α-C	carbon directly bonded to M, or terminal olefinic carbon (methylene)
C(2) or β-C	carbon two-bond away from M or internal olefinic carbon (methine)
C(3) or γ-C	methyl carbon 3 bonds away from M, or C(2)-attached methyl carbon in olefin
P	polymeryl growing chain
A	$[Cp_2M(Me)(\eta^2\text{-}CH_2{=}CHR)]^+$
B	$[Cp_2MCH_2CHMeR]^+$
C	$[Cp_2Zr(\text{tethered olefin})]^+$
DMP	2,4-dimethyl-1-pentene
a (fig. 4.1)	$[Cp_2ZrMe\text{-}\eta^2\text{-}(DMP)]^+$
b (fig. 4.1)	$[Cp_2ZrMe\text{-}\eta^1\text{-}(DMP)]^+$
D	α-agostic species of the type $[Cp_2M\text{-}\eta^2\text{-}(CH_2CHRP)]^+$
E	β-agostic species of the type $[Cp_2M\text{-}\eta^2\text{-}(CH_2CHRP)]^+$
DMB	3,3-dimethyl-1-butene
TMVS	trimethylvinylsilane
I	solvent-separated ion pair $[Cp_2Ti(Me)(CD_2Cl_2)][B(C_6F_5)_4]$
II	$[Cp_2TiCH_2CHMe^tBu]^+$
IIa	α-agostic isomer of **II** in which Ha is agostic (dominant, C(1) = S chiral configuration)
IIb	α-agostic isomer of **II** in which Hb is agostic (minor, C(1) = R chiral configuration)

III	$[Cp_2TiCH_2CHMeSiMe_3]^+$
III-d_3	$[Cp_2TiCH_2CH(CD_3)(SiMe_3)]^+$
IV	$[Cp_2TiH(CH_2{=}CMeSiMe_3)]^+$ with olefinic methylene proximal to hydride
IVa	$[Cp_2TiH(CH_2{=}CMeSiMe_3)]^+$ with olefinic methylene distal to hydride
V	$[Cp_2TiCMe_2SiMe_3)]^+$
VI	$[Cp_2Ti(\eta^2\text{-}H_2)(\eta^3\text{-}(CH_2)_2CSiMe_3)]^+$
VIa	$[Cp_2Ti(\eta^2\text{-}H_2)(\eta^3\text{-}(CH_2)_2CSiMe_3)]^+$ in which the carbon proximal to H_2 ligand in **VI** is distal to H_2 ligand (results from allyl ligand rotation)
VII	β-agostic $[Cp_2TiCH_2CHMeCH_2CHMe_2]^+$
I-d_3	$[Cp_2Ti(CD_3)(CD_2Cl_2)][B(C_6F_5)_4]$
VIII	$[Cp_2TiH(CH_2{=}CMeSiMe_3)]^+$ from which H-quantum tunneling is thought to happen, with one of the H-atoms on the olefinic Me at only 1.61 Å of the hydride
NOESY	Nuclear Overhauser Effect spectroscopy
EXSY	Exchange Spectroscopy
HSQC	Heteronuclear single quantum coherence spectroscopy
HMBC	Heteronuclear multiple-bond correlation spectroscopy
COSY	Correlation spectroscopy

Chapter 5

R	alkyl, aryl or H atom (general)
Cp	cyclopentadienyl ligand, $[\eta^5\text{-}(C_5H_5)]^-$
M	metal center (general)
WCA	weakly coordinating anion
C(1) or α-C	carbon directly bonded to M, or terminal olefinic carbon (methylene)
C(2) or β-C	carbon two-bond away from M or internal olefinic carbon (methine)
C(3) or γ-C	methyl carbon 3 bonds away from M, or C(2)-attached methyl carbon in olefin

P	polymeryl growing chain
DMP	2,4-dimethyl-1-pentene
A	α-agostic species of the type $[Cp_2M\text{-}\eta^2\text{-}(CH_2CHRP)]^+$
B	β-agostic species of the type $[Cp_2M\text{-}\eta^2\text{-}(CH_2CHRP)]^+$
3,3-DMB	3,3-dimethyl-1-butene
2,3,3-TMB	2,3,3-trimethyl-1-butene
TMVS	trimethylvinylsilane
I	solvent-separated ion pair $[Cp_2Ti(CH_3)(CD_2Cl_2)][B(C_6F_5)_4]$
I-CD_3	$[Cp_2Ti(CD_3)(CD_2Cl_2)][B(C_6F_5)_4]$
II	$[Cp_2TiCH_2CHMe^tBu]^+$
IIa or **α-IIa**	α-agostic isomer of **II** in which Ha is agostic (dominant, C(1) = S chiral configuration)
IIb or **α-IIb**	α-agostic isomer of **II** in which Hb is agostic (minor, C(1) = R chiral configuration)
β-II	β-agostic isomer of **II**
γ-II	γ-agostic isomer of **II**
II-CD_3	$[Cp_2TiCH_2CH(CD_3)(CMe_3)]^+$ (and other β-methyl isotologues CH_mD_n (m, n = 0-3; m + n = 3)
a	$[Cp_2TiCH_2CD(CD_2H)CMe_3]^+$ (and other β-methyl isotologues CH_mD_n (m, n = 0-3; m + n = 3)
b	$[Cp_2Ti\{CH(a)D(b)\}CH(CD_2H)CMe_3]^+$ (and other β-methyl isotologues CH_mD_n (m, n = 0-3; m + n = 3)
c	$[Cp_2Ti\{CH(a)D(b)\}CD(CH_2D)CMe_3]^+$ (and other β-methyl isotologues CH_mD_n (m, n = 0-3; m + n = 3)
d	$[Cp_2Ti\{CD(a)H(b)\}CH(CD_2H)CMe_3]^+$ (and other β-methyl isotologues CH_mD_n (m, n = 0-3; m + n = 3)
e	$[Cp_2Ti\{CH(a)D(b)\}CD(CH_2D)CMe_3]^+$ (and other β-methyl isotologues CH_mD_n (m, n = 0-3; m + n = 3)

III	$[Cp_2TiCH_2CHMeSiMe_3]^+$
III-CD_3	$[Cp_2TiCH_2CH(CD_3)(SiMe_3)]^+$
IV	$[Cp_2TiH]^+$
V	$[Cp_2TiCH_2CH_2CMe_3]^+$
α-V	α-agostic isomer of **V**
β-V	β-agostic isomer of **V**
VI	$[Cp_2TiH(CH_2=CMeCMe_3)]^+$
VII	$[Cp_2TiCMe_2(CMe_3)]^+$
VIII	$[Cp_2Ti(\eta^2\text{-}H_2)\{\eta^3\text{-}(CH_2)_2CCMe_3\}]^+$
NOESY	Nuclear Overhauser Effect spectroscopy
EXSY	Exchange Spectroscopy
HSQC	Heteronuclear single quantum coherence spectroscopy
HMBC	Heteronuclear multiple-bond correlation spectroscopy
COSY	Correlation spectroscopy

Chapter 6

R	alkyl, aryl or H atom (general)
Cp	cyclopentadienyl ligand, $[\eta^5\text{-}(C_5H_5)]^-$
M	metal center (general)
3,3-DMB	3,3-dimethyl-1-butene
2,3,3-TMB	2,3,3-trimethyl-1-butene
TMVS	trimethylvinylsilane
II	$[Cp_2TiMe(H_2O)]^+$
II	$[Cp_2TiCH_2CHMe^tBu]^+$

III	$[Cp_2TiCH_2CHMeSiMe_3]^+$
IV and **IV'**	diastereotopic pair of $[Cp_2TiCH_2CHMeCH_2CHMeCH_2CH_2Me]^+$
V and **V'**	diastereotopic pair of $[Cp_2TiCH(SiMe_3)(CH_2CH_2CHMeSiMe_3)]^+$
VI	$[Cp_2TiCH_2CHMeSiEt_3]^+$
II-Et_2O	$[Cp_2Ti(CH_2CHMe^tBu)(Et_2O)]^+$
III-Et_2O	$[Cp_2Ti(CH_2CHMeSiMe_3)(Et_2O)]^+$
VI-Et_2O	$[Cp_2Ti(CH_2CHMeSiEt_3)(Et_2O)]^+$
CB	2-chlorobutane
II-CB	$[Cp_2Ti(CH_2CHMeCMe_3)(ClCHMeEt)]^+$
NOESY	Nuclear Overhauser Effect spectroscopy
EXSY	Exchange Spectroscopy
HSQC	Heteronuclear single quantum coherence spectroscopy
HMBC	Heteronuclear multiple-bond correlation spectroscopy
COSY	Correlation spectroscopy

Chapter 1

Introduction

1.1 General introduction to d^0 group IV metallocene catalyzed polymerization of aliphatic 1-alkenes

It has now been over 50 years since Karl Ziegler and Giulio Natta received the Nobel Prize of Chemistry, in 1963. Their achievement resides in the development of coordination polymerization, a form of olefin addition polymerization. They pioneered the development of a unique class of supported heterogeneous catalysts capable of polymerizing ethylene, propylene and other 1-alkenes in a stereo-regular (tacticity, see Figure 1.1 below) and mostly linear fashion (meaning no branching, see Figure 1.1), with allowing the resulting plastic to gain excellent mechanical and heat-resistance properties.

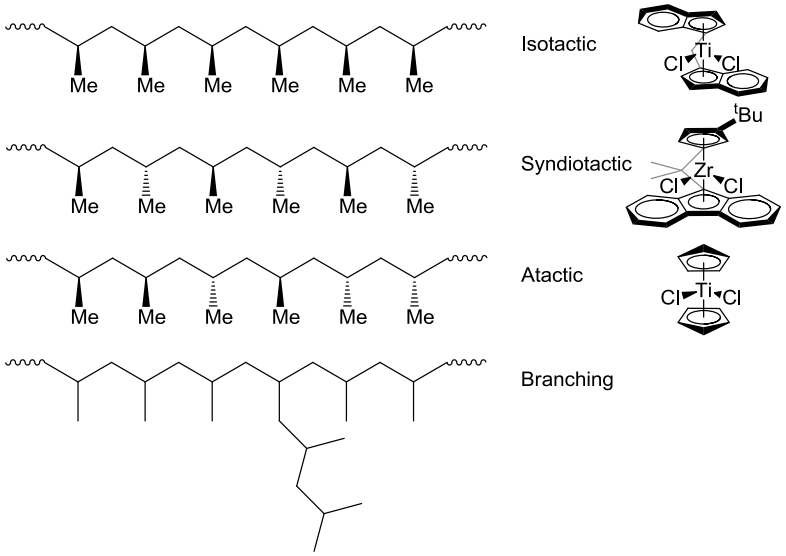

Figure 1.1. Some polypropene microstructures typically seen for metallocene catalyzed polymerization. From top to bottom (left) are examples of two stereo-regular polypropylene chains (isotactic and syndiotactic), of a stereo-random but linear one (atactic) with an example (right) of a precatalyst that leads to these specific microstrucutre when properly activated,[1] and a schematic representation of branching.

Among the different classes of catalysts that were derived from the original heterogenous Ziegler-Natta catalysts, d^0 group IV metallocene catalysts and related complexes have drawn substantial attention in recent years, with their scope in industry still expected to increase significantly.[2] Because they are homogeneous, they not only offer an extraordinary reaction efficiency, but they are also easily tuned by spectator ligand modifications, such as those shown in Figure 1.1.[3] This type of ancillary ligand modification offers a variable control on stereoselectivity at olefin insertion and on activity, two essential properties for producing polymers of high quality. Modifications on the ancillary ligands to affect the resulting polymers is a vast field in chemistry and leads to a broad array of fascinating coordination and polymerization chemistry stories, but their detailed study is beyond the scope of this thesis.

In addition to this ease of customizability of the catalysts (and thus of tacticity in the resulting polymers), it has long been recognized that the use of homogeneous catalysts also generally leads to much narrower molecular weight distributions for the polymer chains it produces than do heterogeneous catalysts.[4] The mechanism of Ziegler-Natta heterogeneous catalysis remains a subject of discussion to this day because of the challenges surrounding characterization of heterogeneous systems. However, it is generally accepted that this difference between the molecular weight distributions of polymers produced with the classical Ziegler-Natta heterogeneous catalysts versus that of polymers produced with homogeneous metallocene-derived catalysts originates from the variability in activity of the different active sites present in heterogeneous systems.[5]

While the mechanistic study of heterogeneous systems is rather difficult, an NMR mechanistic study of a model system for homogeneous catalysts is much easier and proves useful in extending the understanding and knowledge of these catalyst systems in general. With polyethylene and polypropylene production reaching more than 100 million tons yearly,[6] these catalyst systems are well worth studying to gain a deeper knowledge about their fundamental polymerization

mechanism and some of their side reactions, with perhaps an impending rational improvement of their design as ultimate goal. The various reaction intermediates of interest are very prone to fast degradation or polymerization and thus are especially challenging to study experimentally; special strategies need to be employed to directly study and follow these reactions by NMR methods to fill the still existing literature gap.[7]

The interest of this work was focused on characterizing some rare and fundamental intermediates thought to exist transiently during the polymerization reactions, on examining their chemical reactivity and on comparing the results with what has been seen or hypothesized in the literature. In addition, because there are many mechanistic similarities between all these systems in terms of general polymerization, the findings for the relatively simple catalyst system studied in this thesis are hoped to be the basis for understanding similar reactions and intermediates in more complex systems. While ancillary ligands will certainly affect accessibility to certain reaction paths and intermediates via steric and electronic effects, it is hypothesized here that at least some of the findings will be transposable to other catalyst systems.

While the polymerization process itself is not the focus of interest here, it is important to understand some basics of coordination polymerization to grasp the relevance of this work. Thus some selected topics relevant to the work presented in this thesis will be briefly examined.

1.2 Agostic interactions

1.2.1 General description of agostic interactions

Because the metal centers in d^0 group IV alkyl-metallocenes are quite Lewis acidic and have vacant accepting orbitals, it is not uncommon to obtain complexes in which the alkyl ligand is chelated to the metal center via an agostic interaction, and thus it is important to have a good understanding of what their nature and properties. Agostic interactions are often described as a specific type of σ-bond complex, a 3-center-2-electron bond between a hydrogen, a carbon and a

metal atom, a comparable type of bond to that known for alkane (Figure 1.2) or H_2 σ-bond coordination complexes.[8]

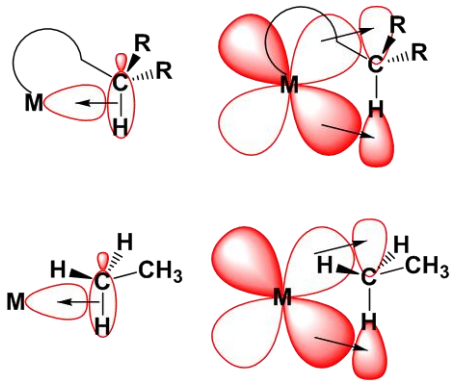

Figure 1.2. Schematic representation of interaction modes of bonding, involving C-H σ donation to a vacant accepting orbital on the metal (M) center (top-left) and back-donation to the corresponding C-H σ* from a filled orbital (of π symmetry relative to CH bond) on M (top-right). The circular linker between the metal and the CH of interest represents an alkyl group. Also shown are related interactions seen in ethane σ-complexes, with σ donation from the CH bond (left) to a vacant accepting orbital on the metal (M) center (bottom-left) and back-donation to the corresponding C-H σ* from a filled orbital (of π symmetry relative to CH bond) on M (bottom-right).

In an agostic interaction, the electron density normally attributed to a C-H bond gets partly delocalized over a Lewis-acidic metal's accepting orbital to form an interaction that is covalent in nature (Figure 1.2). For general cases where d-electrons are available on the metal center, back-donation to the C-H σ* orbital can also occur if the metal has populated orbitals with proper symmetry, potentially leading to weakening or breakage of the C-H bond to result in a hydride-alkyl complex instead (not seen for the d^0 alkyl metallocene complexes presented in this thesis).

1.2.2 Special nomenclature for chelating agostic interactions

The various types of chelating agostic interactions are named according to the number of bonds that separate the CH bond of interest from the metal center through the alkyl backbone, following Greek letters in their alphabetic order.[8a] Thus, an agostic interaction occurring through an H-atom attached to the first carbon (C(1)) directly attached to the metal center is called an α-agostic interaction, one that occurs through the second C-atom (C(2)) from the metal center a β-agostic

interaction, one originating from an H on C(3) a γ-agostic interaction, and so on (Figure 1.3). When drawing agostic structures, a half-arrow pointing from the agostic H atom to the metal center is used to depict the agostic interaction, as shown in Figure 1.3.

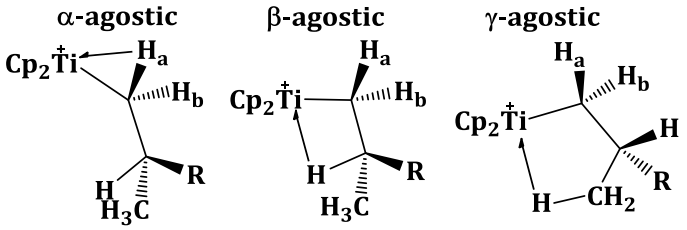

Figure 1.3. Schematic representation of different types of agostic interactions seen for alkyl-titanocene complexes (R = H or alkyl).

1.2.3 Some interesting structural features of agostic interactions

Typically, the M-H distance for agostic interactions will be between 1.8 and 2.3 Å and a M-H-C angle below 140° (and generally above ~90°),[8b,9] but, for α-agostic interactions, the situation is a bit different and this M-H distance have been reported to be up to ~2.5 Å for certain Ti complexes.[10] The acute M-H-C angle seen in agostic interactions generally leads to comparable M-H and M-C distances and this is a critical criterion in identifying agostic interactions.[8b] The covalent electron donation to the metal center seen in agostic interactions results in C-H bond weakening generally elongating the C-H bond to 1.1-1.2 Å,[11] corresponding to a ~1-10% elongation relative to the normal non-agostic C-H bond. The C-H bond weakening is easily identified by NMR; a significant drop in the $^{1}J_{CH}$ coupling constant is key evidence in assigning a particular CH to an agostic interaction, generally around 50 - 110 Hz for typical agostic bonds (sp^3 CH bonds have $^{1}J_{CH}$ ~ 120-130 Hz[12]). Additionally, the agostic interaction causes the involved CH to resonate at lower frequency in infrared spectroscopy, a feature that can sometimes be used as a spectroscopic signature of agostic interactions.[8]

1.2.4 Estimating the strength of agostic interactions

From a computational and experimental perspective, estimating the strength of a chelating agostic interaction on its own is not trivial as it often involves geometric modifications that also affect energetic factors in the rest of the complex.[9,13] McGrady and Scherer have proposed that the chief driving force for adoption of α- or β- agostic geometry might often originate mostly from delocalization of the electron pair attributed to the M-C_α σ-bond to the metal center over the accepting C-H anti-bonding orbital (σ*) of the agostic CH of question for d^0 metals.[14] This opposes the commonly accepted concept of extra stabilization brought by σ-bond electron donation to the Lewis acidic metal (which they however recognize is also participating in the interaction) in agostic interactions. The exact nature, strength and driving force of chelating agostic geometries in d^0 complexes are still a matter of debate amongst computational chemists, but details of the advanced computational methods for study of these complexes are beyond the scope of this thesis.

From an experimental perspective, in order to eliminate some of these undesirable variables, it is thus useful to look at alkane σ-complexes to have an idea of the strength of purely agostic interactions. As shown in Figure 1.2, alkane σ-complexes differ from typical agostic complexes examined thus far by the absence of chelation. As so, alkane σ-complexes have the advantage of having no chelation-related electronic effects suggested by McGrady to contribute to the stability of agostic interactions. Thus, probing the bond strength in σ-alkane complexes provides a realistic estimate of the enthalpy stabilizing contribution of purely agostic interactions.

Using photoacoustic calorimetry, Burkey et al. measured the enthalpy of CO dissociation from $M(CO)_6$ (M = Cr, Mo, W) in heptane allowing them to determine indirectly the σ-complex bond strength for that solvent: 9.6 ± 2.3, 8.7 ± 2.7 and 13.4 ± 2.8 kcal/mol, for Cr, Mo and W, respectively (eq. 1.1).[15]

$$M(CO)_6 \xrightarrow{C_7H_{16}} M(CO)_5(C_7H_{16}) + CO \qquad (1.1)$$

Similarly, others also established an ethane binding energy of 9.7 ± 3 kcal/mol to $W(CO)_5$ in the gas phase by time resolved IR spectroscopy following photolysis of $W(CO)_6$ in an ethane matrix,[16] a case that was later re-studied by the same authors and refined to (7.4 ± 2) kcal/mol.[17] In that latter paper, the binding energy for propane, n-butane, n-pentane and n-hexane were reported at 8.1 ± 2, 9.1 ± 3, 10.6 ± 3 and 10.8 ± 3 kcal/mol, respectively. The values obtained for ethane agree well with what others have recently found using computational methods, leading to similar bond enthalpies (5.2-9.1 kcal/mol).[18] This is also consistent with what other computational chemists have estimated for this type of σ-complex[19] but also chelating agostic interactions,[8,13-14,20] between ~1 and 15 kcal/mol. Thus, agostic interactions are generally found to be weak and it is not surprising that other weak interactions in a complex, such as π-stacking [21] or weak π-donation from a ligand,[22] can compete with agostic interactions.

1.2.5 Processes involving competition between different agostic conformations

In cases where there is more than one CH bond available for donation to the metal center, as in CH_2 and CH_3 groups, exchange between different agostic conformations of degenerate or nearly degenerate free energy can occur because the barrier for exchange between these different agostic conformations is generally low. In these cases, exchange between hydrogen atoms in agostic and non-agostic positions occurs rapidly and the spectral properties of the observed agostic CH_x (x = 2 or 3) are the weighted average of agostic and non-agostic spectral properties. Thus the NMR spectral data can sometimes appear deceptively normal (not agostic) for the agostic CH_x, relative to what is expected for the non-agostic CH_x of question.[23] There are, however, ways around that problem, as discussed below.

It has been long known that, for systems in which H is in exchange with D for occupation of equivalent sites, D tends to accumulate in positions where the bond force constant is the strongest since the gap between zero point energy difference between H-X and D-X (X = C, M or other

heteroatom) is smaller for lower vibrational frequency.[24] Thus, D will accumulate in non-agostic positions when an H/D exchange exists between the agostic and non-agostic sites (see Figure 1.4).

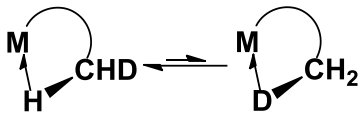

Figure 1.4. Simple schematic representation of preference of H over D for agostic interactions (curved M-C bond = alkyl linkage).

In non-agostic alkanes, a H → D substitution will result in a small NMR chemical shift of neighboring atoms relative to the un-substituted alkane, a phenomenon called chemical shift isotope effect.[25] These chemical shift isotope effects are well known and are, for most practical considerations, roughly additive when more than one isotopic substitution affects the observed nucleus (Figure 1.5).[25]

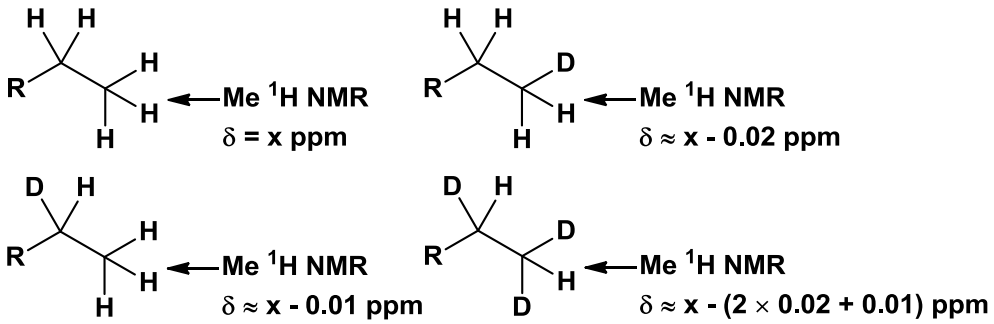

Figure 1.5. Examples of what normal chemical shift isotope effects are roughly expected to be for H → D geminal and vicinal H → D substitutions in common alkanes.

The magnitude of the chemical shift isotope effect on a given observed nucleus decreases with increasing number of bonds separating this latter from the atom that was substituted with its isotope. For example, it is generally accepted that chemical shift isotope effect on neighboring ^{1}H-atoms for a H → D substitution in common alkanes is upfield relative to the un-substituted species, by roughly ~0.02 and ~0.01 ppm for a H atom that is two (geminal) and three (vicinal) bonds away from the substitution position (Figure 1.5), respectively, although the bond angles or dihedral angles in a particular species are known to affect slightly the magnitude of chemical shift isotope

effects.[24b,26] Chemical shift isotope effect on neighboring ^{13}C-atoms for a H → D substitution in alkanes is upfield relative to un-substituted species, by roughly ~0.3 and ~0.1 ppm for a ^{13}C nucleus that is 1 and 2 bonds away from the substitution position, respectively.

Partial deuteration is a useful tool to probe for agostic interaction in degenerate agostic CH_x (x = 2, 3). It takes advantage of the slight preference of D for non-agostic position, as shown in Figure 1.4. As formerly mentioned, the observed δ of a particular degenerate agostic CH_x is a weighted average between non-agostic and agostic δ contributions, which are usually very different from each other. Partial deuteration disrupts the degeneracy of the agostic CH_x interaction, with the hydrogen spending more time than deuterium in the agostic site. Deuteration therefore shifts the equilibrium between these sites for the observed H with resulting chemical shift isotope effects that are larger than what is seen in common alkanes, because of a larger contribution of the agostic δ contribution to its weight averaged δ. Because processes of this type (Figure 1.4) are at equilibrium, temperature will significantly affect the H-agostic to D-agostic ratio, and therefore the magnitude of the chemical shift isotope effect at different temperatures will differ.

For example, $[(C_5H_4Me)_2Zr(CH_2CH_2R)(PMe_3)]^+$ (R = H or Et) was previously studied and found β-agostic in the solid state.[27] Since the H atoms of β-CH_2 are degenerate and can both occupy the agostic position, it was not completely clear whether the agostic interaction persisted in solution. A partial isotopic substitution was performed at β-CH_2 to form the isotopologue $[(C_5H_4Me)_2Zr(CH_2CDHR)(PMe_3)]^+$. [27] The geminal chemical shift isotope effects were -0.40 ppm at 0 °C and -0.63 ppm at -90 °C for R = Et, as well as -0.13 ppm at 25 °C and -0.19 ppm at -60 °C for R = H. This is far more than what is expected for a normal geminal chemical shift isotopic effect (~0.02 ppm), and as explained above, highly dependent on temperature. The interaction was therefore confirmed to persist in solution.

Another way around the degenerate agostic CH_x problem is system dependent; in the case of a β-agostic interaction, the α-carbon also experiences some changes. Indeed, upon β-agostic

conformation adoption, the α-carbon gains significant sp^2 hybridization character from Ti-C(1)-C(2) bond angle deformation[28] and/or double bond character between C(1) and C(2) (from negative hyperconjugation interaction),[14,29] easily captured by NMR with $^1J_{CH}$ revolving around ~140-160 Hz, as opposed to the ~120-130 Hz commonly found for sp^3 hybridized carbons.[12] For example, in one of the first known cases of an agostic interaction studied by single-crystal X-ray diffraction, the β-agostic complex [$TiCl_3$(dmpe)Et] (dmpe = $Me_2PCH_2CH_2PMe_2$), the $^1J_{CH}$ of the agostic Me was ~127 Hz, a rather ordinary value for sp^3 hybridized carbons (~120-130 Hz), while the $^1J_{CH}$ of the α-CH_2 of the Et ligand, 150 Hz, lays within the range expected for an sp^2 hybridised CH_2 group (~140-165 Hz), and it was therefore evidence of degenerate β-agostic interaction. The crystal structure of this complex was unambiguous; the β-agostic nature of the complex was evident and it was rationalized that $^1J_{CH}$ of the agostic Me deceptively appeared normal because its $^1J_{CH}$ was a weighted average between two non-agostic (large $^1J_{CH}$) and one agostic (small $^1J_{CH}$) sites on the NMR time scale. This goes to show how ambiguous and subtle the assignment to an agostic structure can be for cases containing degenerate H which are in rapid exchange between agostic and non-agostic sites.

There are also cases for which the competition for the agostic position occurs between H-atoms that are not on the same carbon. In an early example, Etienne *et al.* reported a niobium complex that underwent an exchange between an α-agostic conformation and a β-agostic conformation (schematic representation shown in Figure 1.6), with a preference for the β-agostic conformation (ΔG = 2.2 kcal/mol at 193 K).[30] This type of exchange was also later reported in a similar tantalum complex.[31]

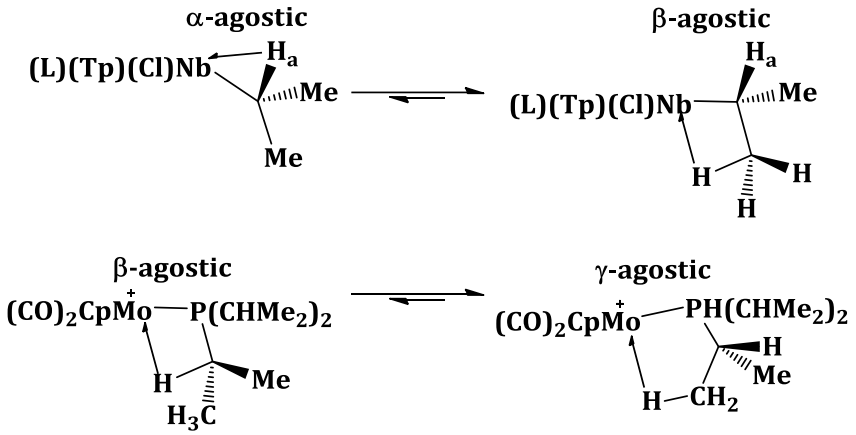

Figure 1.6. Schematic representation of exchange between α- and β- agostic structures seen in ref. 30 (top) and between β- and γ- agostic structures seen in ref. 32 (bottom). Tp = hydridotris(3,5-dimethylpyrazolyl)borate; L = PhC≡CMe

Much more recently, a complex was isolated and an X-ray crystal structure was obtained for both its β-agostic and γ-agostic conformations (Figure 1.6, ΔG calculated at 0.6 kcal/mol in favor of the γ-agostic conformation).[32] Interestingly, the two types of crystals obtained had such contrasting electronic properties that they differed in color; the β-agostic ones were orange while the γ-agostic ones were blue. This underlines the importance of the agostic conformation(s) and their influence on electronic properties, and thus potentially on the reactivity of a complex. The authors proposed a new nomenclature for the different agostic conformation, calling them "agostomers", and using the same Greek letter convention (α-agostomer for an α-agostic conformation, β-agostomer for a β-agostic conformation and so on).[32] As will be discussed below, different agostomers do indeed have a different chemistry and roles in the d^0 group IV metallocene-catalyzed olefin polymerization cycle.

1.3 The cycle of d^0 group IV metallocene-catalyzed olefin-polymerization

1.3.1 General mechanism of d^0 group IV metallocene-catalyzed polymerization of olefins

It is thought that the polymerization mechanism initially involves a very fast reversible olefinic coordination (step 2 in Figure 1.7) to the cationic alkyl-metallocene center (1B), quickly followed by a migratory-insertion (step 3 in Figure 1.7) to leave an empty coordination site for another incoming olefin in the resulting intermediate, 1D, and so on (step 4 in Figure 1.7). [23,33]

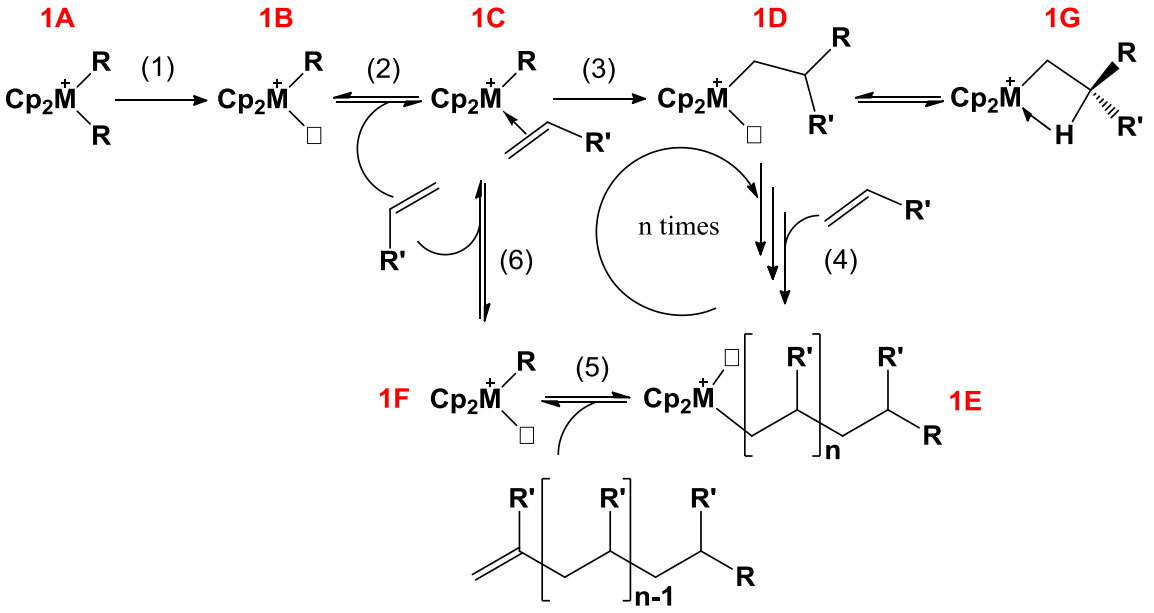

Figure 1.7. General d^0 group IV metallocene-catalyzed olefin-polymerization schematic representation. Above, R and R' = H, Me or other alkyls, and M = Ti, Zr or Hf. The empty boxes attached to M^+ above represent coordination sites that are vacant or occupied by a loosely bonded solvent molecule. Here, **1B** and **1F** are labelled differently because the R group generally differ in those intermediates. Whereas **1B** tends to have R = Me, **1F** has R = H (from β-H elimination in **1E**) or CH_2CH_2R' (from chain transfer of **1E** by direct reaction with a monomer CH_2=CHR') in general.

This ultimately leads to a very rapid alkyl chain growth and eventually to termination by chain transfer or β-elimination, where an active cationic alkyl-metallocene catalyst is regenerated (step 5 in Figure 1.7). When sterics are not too imposing on the Cp and on the growing alkyl-chain, there is usually equilibrium of the active alkyl-metallocene species with an inactive β-agostic species (1G in Figure 1.7) that is thought to serve as the resting state of the cycle and often leads to undesirable side-reactions.[8b,9,14,23,28-29,33d,34] The β-agostomer precedes β-H elimination, which in

turn leads to side reactions such as olefin loss and chain transfer, chain-walking and hydrogen loss to form a polymerization-inactive allylic complex, as will be discussed in much detail in subsequent chapters. Thus, in most cases, the β-agostomer leads to lower catalytic polymerization activity, polymer branching, higher polymer polydispersity index and/or stereoerror introduction. While Figure 1.7 provides a good simplified overview of the catalytic cycle for the polymerization of olefins by d^0 group IV metallocenes, things are a bit more complex than they appear there.

The following subsections will explore in more detail some important reactions and intermediates of this simplified reaction scheme, with special emphasis on material most relevant for the research presented later in this thesis and that is not covered in the introduction of these chapters.

1.3.2 Catalyst activation

Catalyst activation is a very extensive subject on its own and is simply too broad to be fully covered here. Chen and Marks performed an extensive review in 2000 of the topic and the reader interested in learning more details on the topic is invited to refer to that paper,[35] which is the main foundation for this subsection. Nevertheless, it is important to cover fundamental aspects of it as it helps understanding the nature and properties of the catalysts, as well as their catalytic activity.

Early work in the late 1950s on developing the use of group IV metallocene dichloride species for polymerization of olefins involved reactions with alkylaluminum chloride, inspired by the co-catalysts classically used in the heterogeneous Ziegler-Natta systems. While these alkylaluminum chlorides were rather sluggish polymerization cocatalysts, they enabled initial investigations of the underlying principles of coordination polymerization. It was known early on, through isotopic labeling of the alkyl chains on the cocatalysts, that the alkyl chains were incorporated in the polymer chains obtained from these types of catalysts,[36] but there was a lot of speculation about what the mechanism was, what was the active catalyst species.

Although their work was initially focused on heterogeneous systems, it was Cossee, and soon after Arlman, that first proposed that the growing alkyl chain was attached to a Ti atom that had a vacant coordination site next to that of the alkyl where an olefin could come in and coordinate to the metal center for subsequent migratory-insertion, as described in Figure 1.7.[33a-c,37] Since at the time chemists were working with dichlorotitanocene as starting material, this result implied that a ligand exchange between the alkyl-aluminum chlorides and the titanium center. It was long speculated that the active species was a cationic alkyltitanocene species with a vacant coordination site for the incoming olefin to bind to. On top of initially providing the alkyl ligand to the Ti center by ligand exchange in the initial stage of the polymerization, the aluminum center was also thought to act as a Lewis acid to abstract a chloride ion from Ti, making the latter cationic and providing a vacant site for olefin coordination.

However, it was not until 1985 that direct evidence of this cationic nature of the active titanocene was provided, with the crystal structure of the ion pair $[AlCl_4][Cp_2Ti(C(SiMe_3)CMePh)]$, resulting from reaction of dichlorotitanocene, methyldichloroaluminum and trimethyl-(phenylethynyl)silane (eq. 1.2).[38]

$$Cp_2TiCl_2 + AlCl_2Me + Ph_3C{\equiv}CSiMe_3 \longrightarrow [Cp_2Ti\{C(SiMe_3){=}C(Me)(Ph)\}][AlCl_4] \quad (1.2)$$

While the ligand $(C(SiMe_3)CMePh)$ in the reported structure was not a simple alkyl chain as expected in polymerization of aliphatic olefins, this mono-insertion species provided strong evidence that chloride ion abstraction and formation of a cationic species was key in formation of the active catalyst. As a follow up, Eisch *et al.* studied the dynamic equilibrium they discovered exists between the contact ion pair (**CIP**) and the solvent-separated ion pair of $[Cp_2TiR]^+$ and $[AlCl_4]^-$ by variable temperature NMR, for R = Cl, Me and CH_2SiMe_3 (Figure 1.8, see next page).[39] Unsurprisingly, their results suggested that more polar solvents are better at solvating the ion pairs, forming larger proportions of the solvent-separated ion pair. Additionally, they also suggested that the solvent-separated ion pair is more active for ethylene polymerization than the contact ion pair,

and this is something that was crucial in rationally improving co-catalysts used to activate metallocenes for polymerization. It became clear that poorly coordinating anions were preferable for facilitating formation of the solvent-separated ion pair and thus approach and coordination of an incoming olefin.

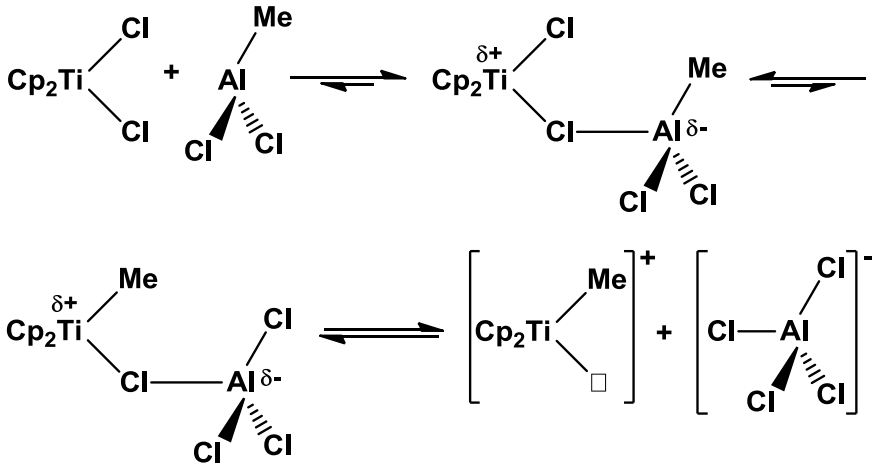

Figure 1.8. Overall process proposed by Eisch *et al.* for dichlorotitanocene activation by dichloromethylaluminum.[39] Their results suggest that the solvent-separated ion pair species are more active than the contact ion pair species for polymerization of ethylene in this system.

Prior to this work, some progress had already been made toward developing a more efficient co-catalyst. It was in 1976 that Vollmer *et al.* pushed the boundaries of these systems and developed what would be the next big thing at the time,[40] methylaluminoxane (MAO), which is still very much present in the current literature. They discovered that pretreatment of trimethylaluminum with 0.2-0.5 eq. of water produced a co-catalyst that was much superior to previous ones and that was sufficiently activating to react with dimethyl-titanocene and zirconocene, with no need for chlorine atoms on Ti/Zr or Al. The material resulting from this controlled hydrolysis is heterogeneous and polymeric in nature, and thus its structure and composition are still unknown, although they have been investigated theoretically.[41] Its general molecular formula is therefore generally just written as $[\text{-Al(Me)-O-}]_n$ for simplicity, even if it is likely not a very accurate or complete representation of the actual structure of MAO. Nevertheless, MAO is still considered a fairly good activator for group IV homogeneous olefin polymerization catalysts in general, but generally requires high Al:M

ratios for high efficiency (M = Ti, Zr, Hf), up to10^4:1 for some catalysts.[35] While recent advances in catalyst development by Eisen *et al.* allowed getting reasonable polyethylene polymerization activity with a Al:Ti ratio down to 8:1,[42] MAO is still a poorly suited cocatalyst for NMR studies of the type described in this thesis.

Another chief class of co-catalyst that greatly contributed to developing and understanding homogeneous group IV metallocene-based catalysts are the perfluoroaryl boranes. The most well known of them certainly is tris(pentafluorophenyl)borane and it was also the first of the class to be used. $B(C_6F_5)_3$ acts as a Lewis acid to abstract a Me from a dimethylmetallocene to yield an active $[Cp_2MMe]^+$ center, and a counteranion, namely $[BMe(C_6F_5)_3]^-$ (eq. 1.3).[43]

$$Cp_2MMe_2 + B(C_6F_5)_3 \rightarrow [Cp_2MMe][MeB(C_6F_5)_3] \qquad (1.3)$$

In their work, Marks *et al.* were able to obtain the crystal structures of a series of these ion pairs; these complexes are also easily studied by NMR means to probe their behavior in solution. This was a major advancement in the rational development and understanding of these systems, and it triggered a renewed interest in studying them.

In the solid state, it turned out that there is in most of the ion pairs studied by Marks *et al.* a coordinative interaction between these ions and the resulting complex, $Cp'_2ZrMe\text{-}\mu\text{-}Me\text{-}B(C_6F_5)_4$) ($Cp' = [\eta^5\text{-}(1,2\text{-}Me_2C_5H_3)]^-$), as a connection between the Zr and B atoms via a bridging agostic-Me (Figure 1.9).

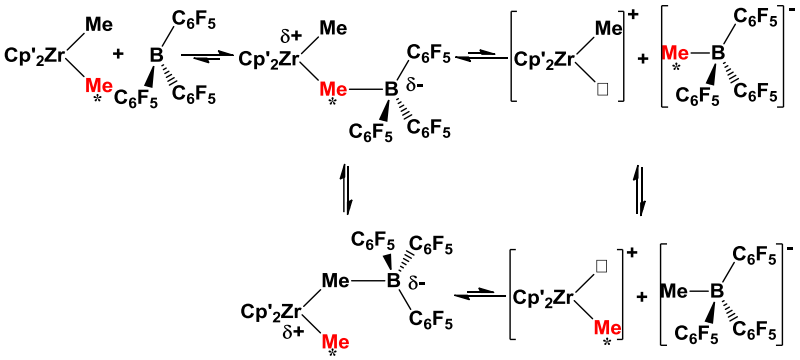

Figure 1.9. Exchange processes by ion-pair dissociation and Me-Me exchange reported by Marks *et al.* for the catalyst system $[Cp'_2ZrMe][MeB(C_5F_6)_3]$ $Cp' = [\eta^5\text{-}(1,2\text{-}Me_2C_5H_3)]^-$.

In Cp'$_2$ZrMe-μ-Me-B(C_6F_5)$_4$), the distance separating the carbon of μ-Me from Zr is elongated by ~0.3 Å relative to the adjacent terminal Zr-Me, but the B-Me distance was found to be elongated by ~0.03 Å only when compared with a non-interacting B-Me bond of free [MeB(C_6F_5)$_3$]$^-$ (the structural details of free [MeB(C_6F_5)$_3$]$^-$ were obtained from the bridged system [{($C_6H_3Me_2$)$_2$ZrMe)}$_2$-μ-F]$^+$ + [MeB(C_6F_5)$_3$]$^-$, where the association of the metal centers through μ-Me prevented a direct approach of the cationic metal center to the Me of free [MeB(C_6F_5)$_3$]$^-$). Their NMR study suggested that, at room temperature or lower, the structure is relatively static in solution, and likely resembled that in the crystal structure. However, at higher temperatures, they observed reversible ion-pair dissociation as well as a slower exchange between the Zr- and B-bonded Me, as shown in Figure 1.9.

In another catalyst system, addition of 0.5 eq. of B(C_6F_5)$_3$ to Cp'$_2$ZrMe$_2$ (Cp'' = [η^5-{C_5H_4(CH_2Ph)}]$^-$) resulted in formation of a Zr dimeric species bridged through an agostic Me, [(Cp'$_2$ZrMe)$_2$-μ-Me]$^+$, whereas adding 1 eq led to an equilibrium mixture of [Cp'$_2$ZrMe]$^+$ and Cp$_2$ZrMe-μ-Me-B(C_6F_5)$_3$ (see Figure 1.10).[44]

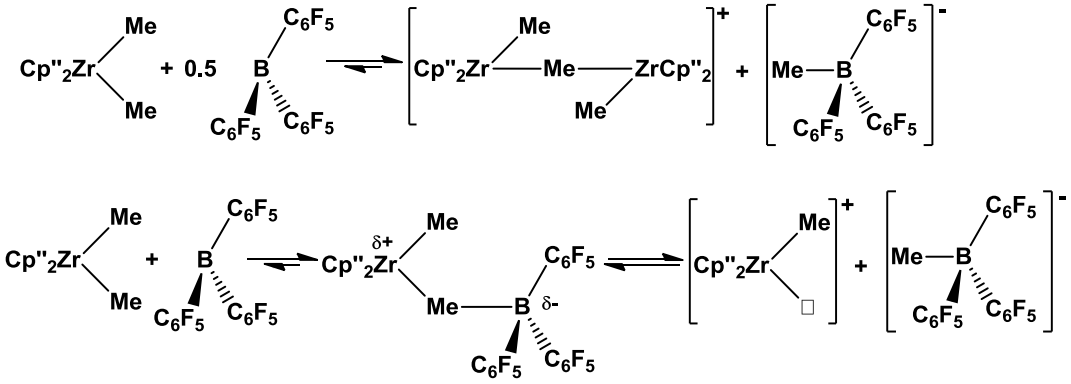

Figure 1.10. Formation of [(Cp''$_2$ZrMe)$_2$-μ-Me]$^+$, [Cp''$_2$ZrMe]$^+$ (a solvent separated ion pair) and Cp$_2$ZrMe-μ-Me-B(C_6F_5)$_4$ (a contact ion pair) from reaction of B(C_6F_5)$_3$ and Cp''$_2$ZrMe$_2$. Cp'' = [η^5-{C_5H_4(CH_2Ph)}]$^-$.[44]

In this same paper, the author also compared the use of $B(C_6F_5)_3$ as an activator for Cp'_2ZrMe_2 to the use of $[Ph_3C][B(C_6F_5)_4]$. $[Ph_3C][B(C_6F_5)_4]$ was first described by Chien *et al.*[45] and found to react with group IV dimethylmetallocene as in eq. 1.4.

$$Cp_2ZrMe_2 + [Ph_3C][B(C_6F_5)_4] \longrightarrow [Cp_2ZrMe][B(C_6F_5)_4] + Ph_3CMe \quad (1.4)$$

In this type of reaction, the products are less strongly associated with the resulting metallocene cationic center. This greatly simplifies NMR studies of subsequent reactions with olefins as the counter anion, $[B(C_6F_5)_4]^-$, is weakly coordinating, in contrast to $[MeB(C_6F_5)_3]^-$.[46] In the solid state, there is evidence that the association occurs through a dative interaction of the fluorine atoms on $[B(C_6F_5)_4]^-$ with the metal center.[43b] The relevant bond lengths suggest a rather weak interaction.

1.3.3 Olefin coordination to species of the type $[Cp_2M(alkyl)]^+$ (M = Ti, Zr, Hf)

In the 1980s, Bercaw *et al*. characterized one of the first olefin coordinated Cp-sandwich complexes of titanium(II).[47] However, this type of complex is not a good representation of typical olefin complexes of Ti(IV) and is of lesser relevance when it comes to study polymerization intermediates, since the metal centers employed in these reaction are of lower oxidation state. Group IV d^2 metallocene have electrons available for back bonding stabilizing interactions with the olefin (see Figure 1.11 (to the right), the metal's d-electrons are partially donated to the olefinic ligand and populates its π* molecular orbital), as opposed to the cationic group IV d^0 alkyl-metallocene polymerization-active catalysts of interest.[48]

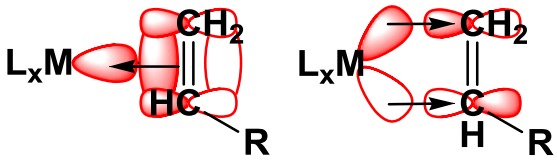

Figure 1.11. Schematic representation of olefin complexes showing 2 modes of coordination: olefin σ-donation to M (left), and d-π* back-bonding donation from d-electrons on M to the accepting π* orbital on the olefin (right).

In the late 1990s and early 2000s, Jordan and his group took a step in the quest for isolation of olefin complex of d^0 group IV metallocenes, using alkoxy-alkene-chelation to stabilize the desired olefinic complexes (Figure 1.12.a.).[49] At about the same time, Casey[50] (Figure 1.12.b.), Royo[51] (Figure 1.12.d.) and Bercaw[52] (Figure 1.12.c.) groups also came up with a chelation strategy that included alkyl-alkene and Cp-attached olefins chains.

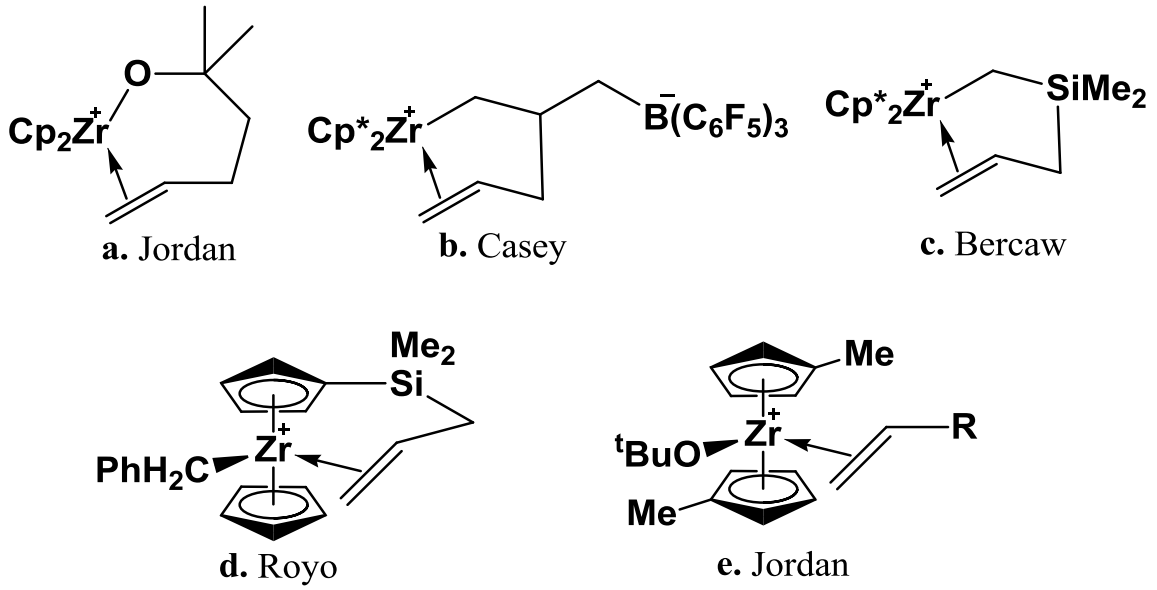

Figure 1.12. Examples of d^0 zirconocene-olefin complexes developed by Jordan,[49,53] Casey,[50] Bercaw[52] and Royo[51] groups in late 90's early 2000's. In e: R= H, Me, ^{n}Bu, $CH_2{}^t$Bu, CH_2SiMe_3.

The latter model systems were perhaps a more realistic representation of the real group IV d^0 metallocene-catalyzed olefin polymerization than that of Jordan; it involved the same type of metal-ligand bonds and only carbon atoms were involved, as in conventional alkene-polymerization systems of interest. The oxygen atom directly bonded to the metal center in the chelating alkoxy-alkene chain system not only differs in electronegativity with a carbon atoms found in alkyls, but it also contains electron lone pairs, conceivably affecting the electronic properties of the metal center.

However, from alkoxy- to alkyl- chelated olefinic complexes, the penalty in free energy associated with ligand-dissociation of the chelate as well as the bond strain restrictions of chelates

most likely modify the dynamics and structures of such complexes. Jordan and co-workers stated in a more recent publication that it is unlikely that these complexes behave in the same way as non-chelated group IV metal d^0 alkene-alkyl-metallocene complex:[53] "*As chelation may influence the structure, dynamics, and reactivity of d^0 metal-alkene complexes, it is desirable to study non-chelated systems to probe the fundamental features of the d^0 metal-alkene interaction.*"

They therefore reported, in the same publication, a series of non-chelated alkoxy-alkenes of the type $[(C_5H_4Me)_2Zr(O^tBu)(CH_2{=}CHR)]^+$ (Figure 1.12.e), with R= H, Me, ^{n}Bu, $CH_2{}^t$Bu, CH_2SiMe_3, by reversible reaction of $[(C_5H_4Me)_2Zr(O^tBu)]^+$ with the desired olefin, via eq. 1.5.

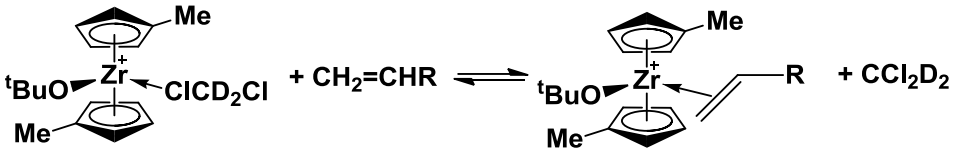

(1.5)

Some of the NMR properties of the olefins were significantly affected by coordination in unsymmetrical olefins (for R = Me, ^{n}Bu, $CH_2{}^t$Bu, CH_2SiMe_3); the internal olefinic carbon was shifted downfield by 15-30 ppm, the terminal olefin carbon was shifted upfield by 10-25 ppm and the internal vinylic hydrogen was shifted downfield by 1.5-1.8 ppm, although the terminal vinylic H were not greatly affected. This NMR data suggested unsymmetrical olefin bonding, with the distance between C(1) and Zr larger than that between C(2) and Zr, and polarization of the double bond upon coordination, consistent with NMR data from former systems (as those seen in Figure 1.12.a-d). It was concluded that there is partial positive charge buildup at C(2) and partial negative charge buildup at C(1) perhaps well described by the resonant forms shown in eq. 1.6.

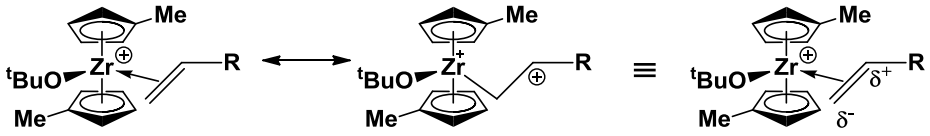

(1.6)

On the other hand, the J_{CH} and J_{HH} of the vinylic carbons and hydrogens of the coordinated olefin remained very similar to what they were in the free olefin. Jordan *et al.* thus concluded that there was no significant vinylic carbon re-hybridization upon olefin coordination, i.e. they remained

mostly sp^2 hybridized. These results were very exciting and provided new insights in olefin bonding to d^0 metals.

The quest for a more realistic model of the alkyl-alkene-metallocene catalytic polymerization intermediate was therefore still deserving attention and research. The Baird group came up with a different strategy for the observation of the desired intermediates. Prior to the work presented in this thesis, the Baird lab's former members managed to perform a low temperature NMR study of a non-chelated complex of the type $[Cp_2ZrMe(olefin)]^+$ $[[B(C_6F_5)_4]^-]$.[54] In order to slow down the migratory insertion step for the detection of the alkyl-alkene complex shown as 1C in Figure 1.7, the sample's temperature was lowered (180 K to 225 K) and an olefin that does not easily polymerize or undergo migratory-insertion reaction readily was then carefully added to the catalyst solution ($[Cp_2ZrMe][B(C_6F_5)_4]$). The olefin used, 2,4-dimethyl-1-pentene (DMP), contained two substituent positions on C(2) to increase the migratory insertion energy barrier by steric means. This permitted characterization by low temperature NMR techniques of the desired alkyl-alkene metallocene complex, $[Cp_2ZrMe(DMP)]^+$ (Figure 1.13).[54]

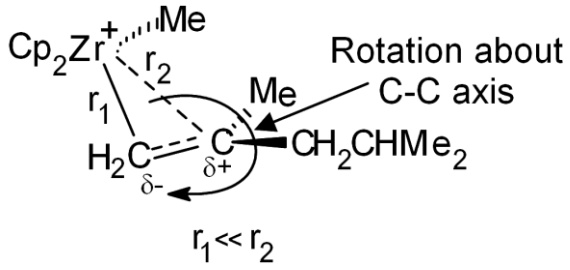

Figure 1.13. Earlier successful observation of alkyl-alkene group IV metallocene. DFT calculations and ^{13}C-NMR spectroscopy suggest a highly polarized bond for which the distance from Zr to C(1) is much shorter than that to C(2) and a rotation of Me and CH_2CHMe_2 groups around the C(1)-C(2) axis is supported by ^1H NMR data.

This first ever observed non-chelated alkyl-alkene complex of group IV metallocene had an unusual near η^1 fashion mode of coordination to DMP. As indicated by the terminal methylene $^2J_{HH}$ coupling constant and by a supportive DFT study the hybridization of the C(1) carbon (α) seemed to be midway between sp^3 and sp^2. Additionally, conspicuous Exchange Spectroscopy

(EXSY) exchange phenomena indicated significant loss of double bond character between C(1) and C(2) upon coordination. An exchange was observed between the olefinic terminal hydrogen atoms of the coordinated and free DMP, and more interestingly, a mutual exchange between the olefin methylene protons of free DMP was also observed. Along with the coalescence of the coordinated DMP olefinic terminal H-NMR signals under increasing temperature, these former exchange phenomena were attributed to a rotation of the Me and CH_2CHMe_2 groups (on C(2)) of DMP around the C(1)-C(2) axis relative to the olefinic methylene hydrogen atoms under coordination, in addition to a fast exchange with the free DMP.[54-55] This type of chemistry was not previously observed by Jordan for the non-chelating alkoxy-alkene-zirconocene complex formerly reported and presented in Figure 1.12.e,[53] and this goes to show the importance of the discovery and how subtly the electronic and steric factor can affect these systems. This type of rotation around the C(1)-C(2) is suggestive of a nearly η^1 σ-bonded alkene ligand with the bonding occurring mostly through C(1), inferring highly asymmetric olefin coordination mode.

Furthermore, the results suggested polarization of the C(1)-C(2) bond resulting in C(2) having significant carbocationic character as indicated by a significant downfield shift of C(2) (58.9 ppm). In the context of a general olefin polymerization cycle, it is thought that this carbocationic character at C(2) upon olefin coordination would increase the Lewis acidity of C(2), which in turn would lead to rapid migratory-insertion reaction with the adjacent alkyl-ligand. That property is thought to be a crucial property for catalytic efficacy in the polymerization of various olefins and was consequently an important discovery.

Despite these exciting results, the complex shown in Figure 1.13 was a poor model for the full cycle of catalytic olefin-polymerization reactions since it does not undergo migratory-insertion reactions (Figure 1.14) at the temperatures of interest (185 K-225 K) as in step 3 of Figure 1.7. The steric inaccessibility of C(2) resulted instead in γ-proton abstraction on the Me attached to C(2) (C(3)) by the methyl ligand, leading to formation and rapid release of methane, as well as the corresponding resonant η^3-allylic species as shown below in Figure 1.14.

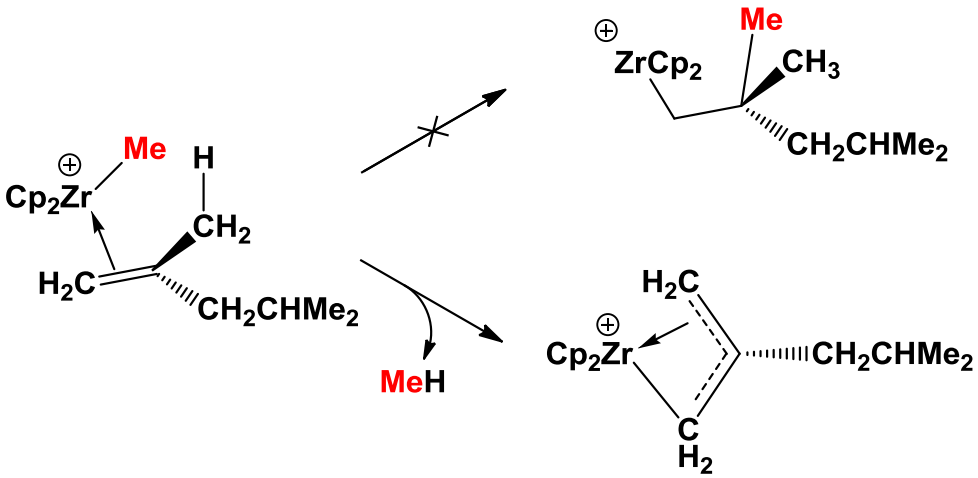

Figure 1.14. Allylic species formation (bottom) via γ-proton abstraction on the Me attached to C(2) (C(3)) by the methyl ligand (red). The top path shown expected to happen in d^0 metallocene-catalyzed olefin-polymerization reactions was not observed.

Nevertheless, this system is still to date the most realistic d^0 alkyl-olefin-metallocene known. A follow-up study of the reaction of DMP with $[Cp_2TiMe]^+$ did result in migratory-insertion, but this initial reaction was rapidly followed by a cascade of interesting new reactions that made it impossible to observe the alkyl-titanocene complex expected from direct migratory-insertion reaction.[55] This unprecedented chemistry triggered the interest for the work presented in this thesis, as will be discussed in subsequent chapters.

1.3.4 Migratory-insertion reaction

As d^0 metallocene-catalyzed olefin-polymerization was developed, four different reaction mechanisms have been proposed for the migratory-insertion step of the catalytic cycle. The earliest one was proposed by Breslow and Newburg,[56] and soon after by Arlman and Cossee [33a-c,57] in the early 1960's and involves a direct migration of the alkyl to the C(2) of a coordinated olefin via a 4 center transition state (Figure 1.15a).

a. Cosse-Arlman direct insertion mechanism

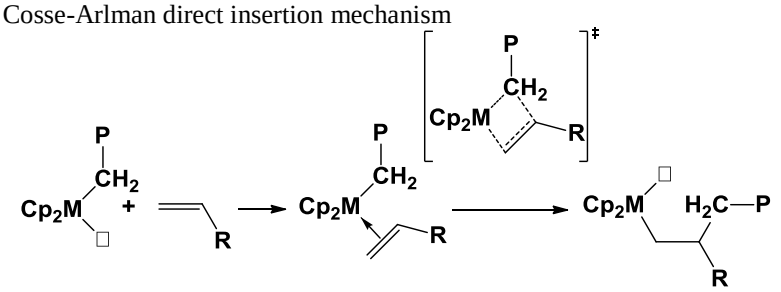

a. Green-Rooney-Brookhart ground and transition state α-agostic interaction mechanism

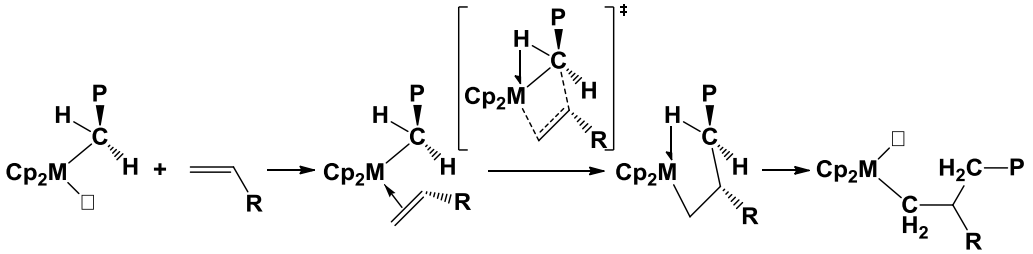

Figure 1.15. Different mechanisms proposed in the past for the migratory-insertion reaction of olefin-monomers incorporation in the growing polymeryl chain (P).

A proposition by Green, Rooney and Brookhart was also brought forward as α-agostic interactions were discovered for a Ti-complex,[28,58] as an alternative mechanism: in this model, the migratory-insertion reaction is assisted by an α-agostic interaction that develops and persists through the migratory-insertion reaction to stabilize the developing positive charge at the metal center (and thus lower the free energy of activation), effectively becoming a γ-agostic by the end of it (Figure 1.15b).[23,58-59] In the most widely accepted version of this mechanism, the polymeryl growing chain would then re-arrange to a β-agostomer in most cases since more stable (resting

state),[8b,9,14,23,28-29,33d,34] and subsequently would accommodate for the next incoming olefin monomer for the next insertion step, and so on. Some α-site D-labelling experiments in which a kinetic isotopic effect was observed originally showed that α-agostic did indeed assist the migratory-insertion reaction.[33d,60] In addition, computational chemists proposed α-agostic interactions to effectively lower the activation barrier of olefin insertion and it was also proposed to influence and enhance stereoselectivity in these reactions quite early in this investigation of the assistance role of α-agostic interactions in migratory-insertion reactions,[20b,61] a proposition also broadly supported by others in the late 1990s, [20a,34d,62] which lead to its acceptance as the correct mechanism of reaction. [1,8b,34h,63] The α-agostic interaction is thought to help moving the polymeryl chain attached to the α-carbon away from the approaching olefin, and that the chelating nature of the polymeryl ligand would firmly lock it in place relative to the Cp ligands and incoming olefin, providing extra control for the orientation of the olefin and thus, on the stereochemistry of the subsequent migratory-insertion reaction.[23] On the other hand β-agostomers generally serve as resting states for these catalytic olefin-polymerization systems, for electronic reasons,[8b,9,14,23,28-29,33d,34] but also lead to side-reactions since they lead to β-H elimination, as will be discussed in subsequent chapters.[60a,60b]

In the following chapters, a rare example of a chiral α-agostic complex will be covered, as well as an even more extraordinarily rare example of a chiral γ-agostic complex. Both complexes resulted from single insertion reactions and therefore, the latter γ-agostic complex is effectively the only example to our knowledge for group IV metallocenes in which the γ-agostic interaction persists after insertion and can be characterized by NMR. The two complexes' empirical formulas are different by only one atom, and their structural agostic difference is most interesting: their differences in agostic conformation lead to exciting differences in chemical properties and reactivity.

1.4 A note about the format and nomenclature of this thesis

This thesis is manuscript-based; it includes three published papers and one submitted manuscript. The supporting information (SI) files of these manuscripts are included as appendixes at the end of the thesis. The SI of the manuscript in chapter 2 is found in appendix A, the SI of the manuscript in chapter 3 is found in appendix B, the SI of the manuscript in chapter 4 is found in appendix C and the SI of the manuscript in chapter 5 is found in appendix D.

The nomenclature used in these various manuscripts involves usage of the same Roman numerals for representing different compounds, and the same numbering for Figures, Schemes and tables that are different from one paper to another. To avoid confusion, the compounds found in the list of abbreviations are presented by chapter, and it is stated here that these abbreviations are chapter-specific and remain local to that specific chapter, i.e. they do not apply to other chapters. Additionally, Figure, Scheme and Table numbering is preceded by the chapter number, or the Appendix letter. Thus the number for Figure 3 of chapter 4 is 4.3, the one for Figure 1 of Appendix C is C1, etc.

Finally, each chapter has its own local reference section. The numbers for these citations and references are only applicable within the same chapter.

1.5 References

1. Coates, G. W., *Chem. Rev. (Washington, D. C.)* **2000,** *100* (4), 1223.

2. Tullo, A. H., *Chemical & Engineering News* **2010,** *88* (42), 10.

3. Alt, H. G.; Koeppl, A., *Chem. Rev. (Washington, D. C.)* **2000,** *100* (4), 1205.

4. Zucchini, U.; Cecchin, G., *Adv. Polym. Sci.* **1983,** *51* (Ind. Dev.), 101.

5. Stevens, M. P., *Polymer Chemistry: an introduction*. third ed.; Oxford University Press, Inc.: 1999.

6. Iwashita, A.; Chan, M. C. W.; Makio, H.; Fujita, T., *Catal. Sci. Technol.* **2014,** *4* (3), 599.

7. (a) Chirik, P. J., *Organometallics* **2010,** *29* (7), 1500;(b) Busico, V., *Dalton Trans.* **2009,** (41), 8794.

8. (a) Green, J. C.; Green, M. L. H.; Parkin, G., *Chem. Commun. (Cambridge, U. K.)* **2012,** *48* (94), 11481;(b) Brookhart, M.; Green, M. L. H.; Parkin, G., *Proc. Natl. Acad. Sci. U. S. A.* **2007,** *104* (17), 6908.

9. Lein, M., *Coord. Chem. Rev.* **2009,** *253* (5+6), 625.

10. Mashima, K.; Nakamura, A., *J. Organomet. Chem.* **1992,** *428* (1-2), 49.

11. Thakur, T. S.; Desiraju, G. R., *Chem. Commun. (Cambridge, U. K.)* **2006,** (5), 552.

12. Reich, H. J., **2014**.

13. Bolton, P. D.; Clot, E.; Adams, N.; Dubberley, S. R.; Cowley, A. R.; Mountford, P., *Organometallics* **2006,** *25* (11), 2806.

14. Scherer, W.; McGrady, G. S., *Angew. Chem., Int. Ed.* **2004,** *43* (14), 1782.

15. Morse, J. M., Jr.; Parker, G. H.; Burkey, T. J., *Organometallics* **1989,** *8* (10), 2471.

16. Ishikawa, Y.; Brown, C. E.; Hackett, P. A.; Rayner, D. M., *Chem. Phys. Lett.* **1988,** *150* (6), 506.

17. Brown, C. E.; Ishikawa, Y.; Hackett, P. A.; Rayner, D. M., *J. Am. Chem. Soc.* **1990,** *112* (7), 2530.

18. Da Silva, J. C. S.; De Almeida, W. B.; Rocha, W. R., *Chem. Phys.* **2009,** *365* (1-2), 85.

19. (a) Gittermann, S. M.; Letterman, R. G.; Jiao, T.; Leu, G.-L.; DeYonker, N. J.; Webster, C. E.; Burkey, T. J., *J. Phys. Chem. A* **2011,** *115* (32), 9004;(b) Cobar, E. A.; Khaliullin, R. Z.;

Bergman, R. G.; Head-Gordon, M., *Proc. Natl. Acad. Sci. U. S. A.* **2007,** *104* (17), 6963;(c) Chan, B.; Ball, G. E., *J. Chem. Theory Comput.* **2013,** *9* (5), 2199.

20. (a) Fan, L.; Harrison, D.; Woo, T. K.; Ziegler, T., *Organometallics* **1995,** *14* (4), 2018;(b) Woo, T. K.; Fan, L.; Ziegler, T., *Organometallics* **1994,** *13* (6), 2252;(c) von Frantzius, G.; Streubel, R.; Brandhorst, K.; Grunenberg, J., *Organometallics* **2006,** *25* (1), 118.

21. Clot, E.; Eisenstein, O.; Dube, T.; Faller, J. W.; Crabtree, R. H., *Organometallics* **2002,** *21* (3), 575.

22. Boncella, J. M.; Cajigal, M. L.; Abboud, K. A., *Organometallics* **1996,** *15* (7), 1905.

23. Brookhart, M.; Green, M. L. H., *J. Organomet. Chem.* **1983,** *250* (1), 395.

24. (a) Calvert, R. B.; Shapley, J. R.; Schultz, A. J.; Williams, J. M.; Suib, S. L.; Stucky, G. D., *J. Am. Chem. Soc.* **1978,** *100* (19), 6240;(b) Smirnov, S. N.; Golubev, N. S.; Denisov, G. S.; Benedict, H.; Schah-Mohammedi, P.; Limbach, H.-H., *J. Am. Chem. Soc.* **1996,** *118* (17), 4094;(c) Jankowski, S., *Annu. Rep. NMR Spectrosc.* **2009,** *68*, 149.

25. Jameson, C. J. In *Isotope effects on chemical shifts and coupling constants*, John Wiley & Sons Ltd.: 2012; pp 2197-2214.

26. (a) Batiz-Hernandez, H.; Bernheim, R. A., *Progr. Nucl. Magn. Resonance Spectrosc.* **1967,** *3*, 63;(b) Hansen, P. E., *Annu. Rep. NMR Spectrosc.* **1983,** *15*, 105;(c) Lambert, J. B.; Greifenstein, L. G., *J. Am. Chem. Soc.* **1974,** *96* (16), 5120.

27. Jordan, R. F.; Bradley, P. K.; Baenziger, N. C.; LaPointe, R. E., *J. Am. Chem. Soc.* **1990,** *112* (3), 1289.

28. Dawoodi, Z.; Green, M. L. H.; Mtetwa, V. S. B.; Prout, K.; Schultz, A. J.; Williams, J. M.; Koetzle, T. F., *J. Chem. Soc., Dalton Trans.* **1986,** (8), 1629.

29. Scherer, W.; Herz, V.; Hauf, C., *Struct. Bonding (Berlin, Ger.)* **2012,** *146* (Electron Density and Chemical Bonding I), 159.

30. Jaffart, J.; Mathieu, R.; Etienne, M.; McGrady, J. E.; Eisenstein, O.; Maseras, F., *Chem. Commun. (Cambridge)* **1998,** (18), 2011.

31. Fryzuk, M. D.; Johnson, S. A.; Rettig, S. J., *J. Am. Chem. Soc.* **2001,** *123* (8), 1602.

32. van der Eide, E. F.; Yang, P.; Bullock, R. M., *Angew. Chem., Int. Ed.* **2013,** *52* (39), 10190.

33. (a) Cossee, P., *Tetrahedron Lett.* **1960,** (No. 17), 12;(b) Cossee, P., *J. Catal.* **1964,** *3* (1), 80;(c) Arlman, E. J.; Cossee, P., *J. Catal.* **1964,** *3* (1), 99;(d) Grubbs, R. H.; Coates, G. W., *Acc. Chem. Res.* **1996,** *29* (2), 85.

34. (a) Brookhart, M.; Green, M. L. H.; Wong, L. L., *Prog. Inorg. Chem.* **1988,** *36*, 1;(b) Scherer, W.; Sirsch, P.; Shorokhov, D.; Tafipolsky, M.; McGrady, G. S.; Gullo, E., *Chem. - Eur. J.* **2003,** *9* (24), 6057;(c) Clot, E.; Eisenstein, O., *Struct. Bonding (Berlin, Ger.)* **2004,** *113* (Principles and Applications of Density Functional Theory in Inorganic Chemistry II), 1;(d) Lohrenz, J. C. W.; Woo, T. K.; Ziegler, T., *J. Am. Chem. Soc.* **1995,** *117* (51), 12793;(e)

Jensen, V. R.; Koley, D.; Jagadeesh, M. N.; Thiel, W., *Macromolecules* **2005,** *38* (24), 10266;(f) Mitoraj, M. P.; Michalak, A.; Ziegler, T., *Organometallics* **2009,** *28* (13), 3727;(g) Laine, A.; Linnolahti, M.; Pakkanen, T. A.; Severn, J. R.; Kokko, E.; Pakkanen, A., *Organometallics* **2010,** *29* (7), 1541;(h) Laine, A.; Linnolahti, M.; Pakkanen, T. A.; Severn, J. R.; Kokko, E.; Pakkanen, A., *Organometallics* **2011,** *30* (6), 1350;(i) Scherer, W.; Priermeier, T.; Haaland, A.; Volden, H. V.; McGrady, G. S.; Downs, A. J.; Boese, R.; Blaeser, D., *Organometallics* **1998,** *17* (20), 4406;(j) Brookhart, M.; Lincoln, D. M.; Volpe, A. F., Jr.; Schmidt, G. F., *Organometallics* **1989,** *8* (5), 1212;(k) Shultz, L. H.; Brookhart, M., *Organometallics* **2001,** *20* (19), 3975.

35. Chen, E. Y.-X.; Marks, T. J., *Chem. Rev. (Washington, D. C.)* **2000,** *100* (4), 1391.

36. (a) Natta, G., *J. Polym. Sci.* **1959,** *34*, 21;(b) Chien, J. C. W., *J. Am. Chem. Soc.* **1959,** *81*, 86.

37. Arlman, E. J., *J. Catal.* **1964,** *3* (1), 89.

38. Eisch, J. J.; Piotrowski, A. M.; Brownstein, S. K.; Gabe, E. J.; Lee, F. L., *J. Am. Chem. Soc.* **1985,** *107* (24), 7219.

39. Eisch, J. J.; Pombrik, S. I.; Zheng, G. X., *Organometallics* **1993,** *12* (10), 3856.

40. Andresen, A.; Cordes, H. G.; Herwig, J.; Kaminsky, W.; Merck, A.; Mottweiler, R.; Pein, J.; Sinn, H.; Vollmer, H. J., *Angew. Chem. Int. Ed.* **1976,** *15* (10), 630.

41. Glaser, R.; Sun, X., *J. Am. Chem. Soc.* **2011,** *133* (34), 13323.

42. Shoken, D.; Sharma, M.; Botoshansky, M.; Tamm, M.; Eisen, M. S., *J. Am. Chem. Soc.* **2013,** *135* (34), 12592.

43. (a) Yang, X.; Stern, C. L.; Marks, T. J., *J. Am. Chem. Soc.* **1991,** *113* (9), 3623;(b) Yang, X.; Stern, C. L.; Marks, T. J., *J. Am. Chem. Soc.* **1994,** *116* (22), 10015.

44. Bochmann, M.; Green, M. L. H.; Powell, A. K.; Sassmannshausen, J.; Triller, M. U.; Wocadlo, S., *J. Chem. Soc., Dalton Trans.* **1999,** (1), 43.

45. Chien, J. C. W.; Tsai, W. M.; Rausch, M. D., *J. Am. Chem. Soc.* **1991,** *113* (22), 8570.

46. (a) Krossing, I.; Raabe, I., *Angew Chem Int Ed Engl* **2004,** *43* (16), 2066;(b) Chen, Y.-X.; Metz, M. V.; Li, L.; Stern, C. L.; Marks, T. J., *J. Am. Chem. Soc.* **1998,** *120* (25), 6287.

47. Cohen, S. A.; Auburn, P. R.; Bercaw, J. E., *J. Am. Chem. Soc.* **1983,** *105* (5), 1136.

48. (a) Dewar, M. J. S., *Bull. Soc. Chim. Fr.* **1951**, C71;(b) Chatt, J.; Duncanson, L. A., *J. Chem. Soc.* **1953**, 2939;(c) Hartley, F. R., *Angew. Chem., Int. Ed. Engl.* **1972,** *11* (7), 596.

49. (a) Wu, Z.; Jordan, R. F.; Petersen, J. L., *J. Am. Chem. Soc.* **1995,** *117* (21), 5867;(b) Carpentier, J.-F.; Maryin, V. P.; Luci, J.; Jordan, R. F., *J. Am. Chem. Soc.* **2001,** *123* (5), 898;(c) Carpentier, J.-F.; Wu, Z.; Lee, C. W.; Stroemberg, S.; Christopher, J. N.; Jordan, R. F., *J. Am. Chem. Soc.* **2000,** *122* (32), 7750.

50. (a) Casey, C. P.; Carpenetti, D. W., II; Sakurai, H., *J. Am. Chem. Soc.* **1999,** *121* (40), 9483;(b) Casey, C. P.; Carpenetti, D. W., II, *Organometallics* **2000,** *19* (19), 3970;(c) Casey, C. P.; Klein, J. F.; Fagan, M. A., *J. Am. Chem. Soc.* **2000,** *122* (18), 4320;(d) Casey, C. P.; Fagan, M. A.; Hallenbeck, S. L., *Organometallics* **1998,** *17* (3), 287;(e) Casey, C. P.; Carpenetti, D. W., II; Sakurai, H., *Organometallics* **2001,** *20* (20), 4262;(f) Casey, C. P.; Hallenbeck, S. L.; Wright, J. M.; Landis, C. R., *J. Am. Chem. Soc.* **1997,** *119* (41), 9680;(g) Casey, C. P.; Hallenbeck, S. L.; Pollock, D. W.; Landis, C. R., *J. Am. Chem. Soc.* **1995,** *117* (38), 9770;(h) Casey, C. P.; Fisher, J. J., *Inorg. Chim. Acta* **1998,** *270* (1,2), 5.

51. Galakhov, M. V.; Heinz, G.; Royo, P., *Chem. Commun. (Cambridge)* **1998,** (1), 17.

52. Brandow, C. G.; Mendiratta, A.; Bercaw, J. E., *Organometallics* **2001,** *20* (20), 4253.

53. Stoebenau, E. J., III; Jordan, R. F., *J. Am. Chem. Soc.* **2006,** *128* (25), 8162.

54. (a) Vatamanu, M.; Stojcevic, G.; Baird, M. C., *J. Am. Chem. Soc.* **2008,** *130* (2), 454;(b) Sauriol, F.; Wong, E.; Leung, A. M. H.; Donaghue, I. E.; Baird, M. C.; Wondimagegn, T.; Ziegler, T., *Angew. Chem., Int. Ed.* **2009,** *48* (18), 3342.

55. Sauriol, F.; Sonnenberg, J. F.; Chadder, S. J.; Dunlop-Briere, A. F.; Baird, M. C.; Budzelaar, P. H. M., *J. Am. Chem. Soc.* **2010,** *132* (38), 13357.

56. Breslow, D. S.; Newburg, N. R., *J. Am. Chem. Soc.* **1959,** *81*, 81.

57. Cossee, P., *Tetrahedron Lett.* **1960,** (No. 17), 17.

58. Dawoodi, Z.; Green, M. L. H.; Mtetwa, V. S. B.; Prout, K., *J. Chem. Soc., Chem. Commun.* **1982,** (24), 1410.

59. Laverty, D. T.; Rooney, J. J., *J. Chem. Soc., Faraday Trans. 1* **1983,** *79* (4), 869.

60. (a) Krauledat, H.; Brintzinger, H. H., *Angewandte Chemie-International Edition in English* **1990,** *29* (12), 1412;(b) Piers, W. E.; Bercaw, J. E., *J. Am. Chem. Soc.* **1990,** *112* (25), 9406;(c) Fink, G.; Muelhaupt, R.; Brintzinger, H. H.; Editors, *Ziegler Catalysts: Recent Scientific Innovations and Technological Improvements*. Springer: 1995; p 511 pp;(d) Leclerc, M. K.; Brintzinger, H. H., *J. Am. Chem. Soc.* **1995,** *117* (5), 1651.

61. (a) Prosenc, M. H.; Janiak, C.; Brintzinger, H. H., *Organometallics* **1992,** *11* (12), 4036;(b) Janiak, C., *J. Organomet. Chem.* **1993,** *452* (1-2), 63;(c) Woo, T. K.; Fan, L.; Ziegler, T., *Organometallics* **1994,** *13* (2), 432;(d) Meier, R. J.; van Doremaele, G. H. J.; Iarlori, S.; Buda, F., *J. Am. Chem. Soc.* **1994,** *116* (16), 7274;(e) Axe, F. U.; Coffin, J. M., *J. Phys. Chem.* **1994,** *98* (10), 2567;(f) Kawamura-Kuribayashi, H.; Koga, N.; Morokuma, K., *J. Am. Chem. Soc.* **1992,** *114* (7), 2359;(g) Weiss, H.; Ehrig, M.; Ahlrichs, R., *J. Am. Chem. Soc.* **1994,** *116* (11), 4919.

62. (a) Yoshida, T.; Koga, N.; Morokuma, K., *Organometallics* **1995,** *14* (2), 746;(b) Margl, P.; Lohrenz, J. C. W.; Ziegler, T.; Bloechl, P. E., *J. Am. Chem. Soc.* **1996,** *118* (18), 4434;(c) Thorshaug, K.; Stovneng, J. A.; Rytter, E.; Ystenes, M., *Macromolecules* **1998,** *31* (21), 7149.

63. Resconi, L.; Cavallo, L.; Fait, A.; Piemontesi, F., *Chem. Rev. (Washington, D. C.)* **2000,** *100* (4), 1253.

Chapter 2

Synthesis and Properties of $[Cp_2Ti(Me)(H_2O)][B(C_6F_5)_4]$*

2.1 Abstract

Treatment of water-stable Cp_2TiMe_2 with $[Ph_3C][B(C_6F_5)_4]$ in CD_2Cl_2 gives the solvent-separated ion pair $[Cp_2Ti(Me)(CD_2Cl_2)][B(C_6F_5)_4]$, which reacts rapidly with water at 205 K to give the corresponding aqua complex $[Cp_2Ti(Me)(H_2O)][B(C_6F_5)_4]$. The latter has been characterized by ^1H and ^{13}C NMR spectroscopy at 205 K and is a rare, possibly unique, example of a complex containing aqua and methyl ligands within the coordination sphere of a titanium(IV) complex.

2.2 Introduction

The orange compound Cp_2TiMe_2 exhibits properties surprisingly different from those of its colorless heavy homologues, Cp_2ZrMe_2 and Cp_2HfMe_2. For instance, while the latter two compounds are thermally stable to at least 80 °C and are readily manipulated at ambient temperature,[1a,b] Cp_2TiMe_2 can be manipulated at ambient temperature but is also found to decompose erratically and apparently auto-catalytically at this temperature.[1b,c-f] Curiously, Cp_2TiMe_2 is most fragile when isolated as a solid, frequently turning black during attempts at purification.[1b,c-f] It is thus best stored as THF or toluene solutions, where dilution seems to prevent autocatalytic decomposition processes that probably involve radical species.[1g-i]

Another significant difference between Cp_2TiMe_2, on one hand, and Cp_2ZrMe_2 and Cp_2HfMe_2 on the other has to do with their protolytic reactivities. Although Cp_2ZrMe_2 and Cp_2HfMe_2 are very sensitive to water and alcohols, giving methane and metal products containing oxo, hydroxyl, or

* The manuscript presented in chapter 2 was published at: Dunlop-Brière, A. F.; Baird, M. C. *Organometallics* **2010**, *29*, 6117.

alkoxy ligands,[2] the synthesis of Cp_2TiMe_2 involves methylation of Cp_2TiCl_2 with 2 equiv of methyl lithium *followed by hydrolysis*, after which workup yields the orange product.[1b,c-i] Thus, Cp_2TiMe_2 is stable to water.

We have recently reported the syntheses and properties of the methyl alkene complexes $[Cp_2Zr(Me)(CH_2{=}CMeR)][B(C_6F_5)_4]$ (R=CH_2CHMe_2, CH_2CMeCH_2Et), prepared by methyl carbanion abstraction from Cp_2ZrMe_2 by $[Ph_3C][B(C_6F_5)_4]$ in CD_2Cl_2 to give *inter alia* the solvent-separated ion pair $[Cp_2Zr(Me)(CD_2Cl_2)][B(C_6F_5)_4]$, followed by substitution of CD_2Cl_2 by the alkene.[3a,b] Such alkene complexes are of interest for several reasons: (a) they are alkyl alkene complexes of a type intermediate in coordination polymerization reactions but never previously observed because of their high proclivities to migratory insertion, (b) they contain a novel near η^1 mode of alkene coordination, and (c) the C(1)-C(2) π bonds are sufficiently weak that the =C(Me)R groups rotate relative to the terminal $=CH_2$ groups.[3a,b]

Embarking on a similar investigation of the analogous titanium system, we have utilized the reaction of Cp_2TiMe_2 with $[Ph_3C][B(C_6F_5)_4]$ in CD_2Cl_2 to form mixtures of what we believe to be the solvent-separated ion pair $[Cp_2Ti(Me)(CD_2Cl_2)][B(C_6F_5)_4]$ (**I**), the contact ion pair $[Cp_2Ti(Me)B(C_6F_5)_4]$ (**II**), and, when a deficiency of $[Ph_3C][B(C_6F_5)_4]$ is used, the dinuclear species $[Cp_2Ti(Me)(\mu\text{-}Me)Ti(Me)Cp_2][B(C_6F_5)_4]$ (**III**).[3c] While **III** was readily identified on the basis of its ^1H NMR spectrum,[3c] such was not the case with the two mononuclear species. Noting,[3] however, that Cp chemical shifts in metallocene compounds are generally strongly influenced by inductive effects,[3d,4] we believed it reasonable to assign the less shielded Cp resonance at δ 6.72 to the cationic species **I** and the more shielded Cp resonance at δ 6.33 to the neutral species **II**. Similar assignments had been suggested for the analogous zirconium compounds $[Cp_2ZrMe(solvent)][B(C_6F_5)_4]$ (solvent=CD_2Cl_2, C_6D_5Cl) and $Cp_2ZrMeB(C_6F_5)_4$,[3a,b] and thus **I** was thought to contain a solvent-separated, or outer-sphere, ion pair, while **II** was thought to contain a contact, or inner-sphere, ion pair in which, presumably, the anion coordinates via one or more fluorine atoms.[3c]

Unfortunately, consistent with the literature cited above, we found that attempts to purify Cp_2TiMe_2 resulted frequently but erratically in its decomposing to a black material.[3c] The compound could therefore not be reliably obtained free of traces of ethyl ether or water, present during its synthesis, or of toluene, the solvent in which it was stored. Wondering, therefore, about the possible ramifications of having low, variable amounts of water present during the synthesis of, for example $[Cp_2Ti(Me)(CD_2Cl_2)][B(C_6F_5)_4]$, we have investigated and report herein the chemistry of $[Cp_2Ti(Me)(CD_2Cl_2)][B(C_6F_5)_4]$ with water.

2.3 Experimental Section

All syntheses were carried out under dry, deoxygenated argon using standard Schlenk line techniques. Argon was deoxygenated by passage through a heated column of BASF copper catalyst and then dried by passing through a column of activated 4 Å molecular sieves. Handling of Cp_2TiMe_2 was done in an MBraun Labmaster glovebox, and the compound was stored in toluene under argon in a freezer. NMR spectra were recorded using a Bruker AV600 spectrometer, ^1H and ^{13}C NMR data being referenced to TMS via the residual proton signals of the deuterated solvent. $[Ph_3C][B(C_6F_5)_4]$ was purchased from Asahi Glass Company and used as obtained, and CH_3Li was purchased from Aldrich. Cp_2TiMe_2 was synthesized from Cp_2TiCl_2 and methyllithium, as described elsewhere,[1b,c-i] and was stored in toluene solution at -30 °C. Dichloromethane-d_2 was dried by storage over activated 3 Å molecular sieves.

Solutions for NMR studies were prepared using a 2 mL aliquot of a toluene solution containing ~16.5 μmol of Cp_2TiMe_2 per mL of toluene. The toluene was removed rapidly under reduced pressure at ~323 K, and the residue was taken into the glovebox and dissolved in a solution containing 45 mg (excess) of $[Ph_3C][B(C_6F_5)_4]$ in 0.6 mL of CD_2Cl_2 to give a yellow-orange solution. The mixture was then syringed into a rubber septum sealed NMR tube (under Ar), which was taken quickly out of the glovebox and immersed within 2-4 min in a dry ice/acetone bath (195 K). The NMR tube was placed in the precooled (185-205 K) probe of the NMR spectrometer, and

a ^{1}H NMR spectrum was run. The tube was then removed from the probe to the dry ice/acetone bath, and several aliquots of water (molar ratio **I**:H_2O ≈ 1:0.3-1:1.5)[5a] were added to the cold solution. The tube was shaken vigorously at 195 K to induce mixing and placed back in the probe at 205 K, and NMR spectra were obtained at various time intervals and temperatures. Nuclear Overhauser Effect spectroscopy (NOESY) experiments were typically performed with mixing times between 0.2 and 0.6 seconds, while measured t1 relaxation times were typically ranging between 0.1 s and 1 s. In NOESY spectra presented are phased to get the diagonal to be negative and thus, correlations that are of the same colour as the diagonal are also negative (EXSY correlations), and those that are of a different colour than the diagonal are positive (NOE).

2.4 Results and Discussion

Reactions of Cp_2TiMe_2 with $[Ph_3C][B(C_6F_5)_4]$ in CD_2Cl_2, carried out at ~293 K as described in the Experimental Section, gave dark orange-brown solutions. NMR spectra of these reaction mixtures at 205 K (see Figure A1 of the Appendix A (Appendix A) for a typical spectrum) were found generally to exhibit resonances of the product of methyl abstraction by trityl ion, $CMePh_3$ (δ 7.0-7.3, m, Ph; 2.13, s, Me), in addition to resonances that we have previously suggested[3c] are attributed to the solvent-separated ion pair $[Cp_2TiMe(CD_2Cl_2)][B(C_6F_5)_4]$ (**I**, ^{1}H NMR: δ 6.72 (Cp), 1.63 (Me); ^{13}C NMR: δ 128.1 ($^1J_{CH}$ 176 Hz, Cp), 75.7 ($^1J_{CH}$ 129 Hz, Me)) and the contact ion pair $[Cp_2TiMeB(C_6F_5)_4]$ (**II**, ^{1}H NMR: δ 6.33 (Cp), 1.24 (Me); ^{13}C NMR: δ 117.4 ($^1J_{CH}$ 176 Hz, Cp), 62.8 ($^1J_{CH}$ 126 Hz, Me)). If a deficiency of $[Ph_3C][B(C_6F_5)_4]$ was used, the dinuclear species $[\{Cp_2TiMe\}_2(\mu\text{-Me})][B(C_6F_5)_4]$ (**III**, ^{1}H NMR: δ 6.21 (Cp), 0.61 (Me), -1.28 (μ-Me); ^{13}C NMR: δ 115.6 (Cp), 55.8 ($^1J_{CH}$ 127 Hz, Me)), 44.2 ($^1J_{CH}$ 138 Hz, μ-Me)) was also present.[3c]

Figure 2.1 illustrates a ^{1}H NMR spectrum of a Cp_2TiMe_2/ $[Ph_3C][B(C_6F_5)_4]$ reaction mixture in which the dinuclear species $[\{Cp_2TiMe\}_2(\mu\text{-Me})][B(C_6F_5)_4]$ was absent. As can be seen, complexes **I** and **II** were present in an approximate ratio of 3:1, and addition of ~0.3 mol of H_2O per mole of **I** at 205K (Figure 2.1.b) resulted in diminution of the resonances of **I**, by about 30%,[6] but not those

of **II**. New Cp and Ti-Me resonances appeared at δ 6.44 and 1.33, respectively (ratio 10:3), in addition to a new, broader resonance integrating for 2H at δ 4.74. Reaction with additional aliquots of water (Figure 2.1.b-d) resulted in proportional decreases in the resonances of **I** and increases in the resonances of **IV**, but again in very little changes in the intensities of the resonances of **II**.

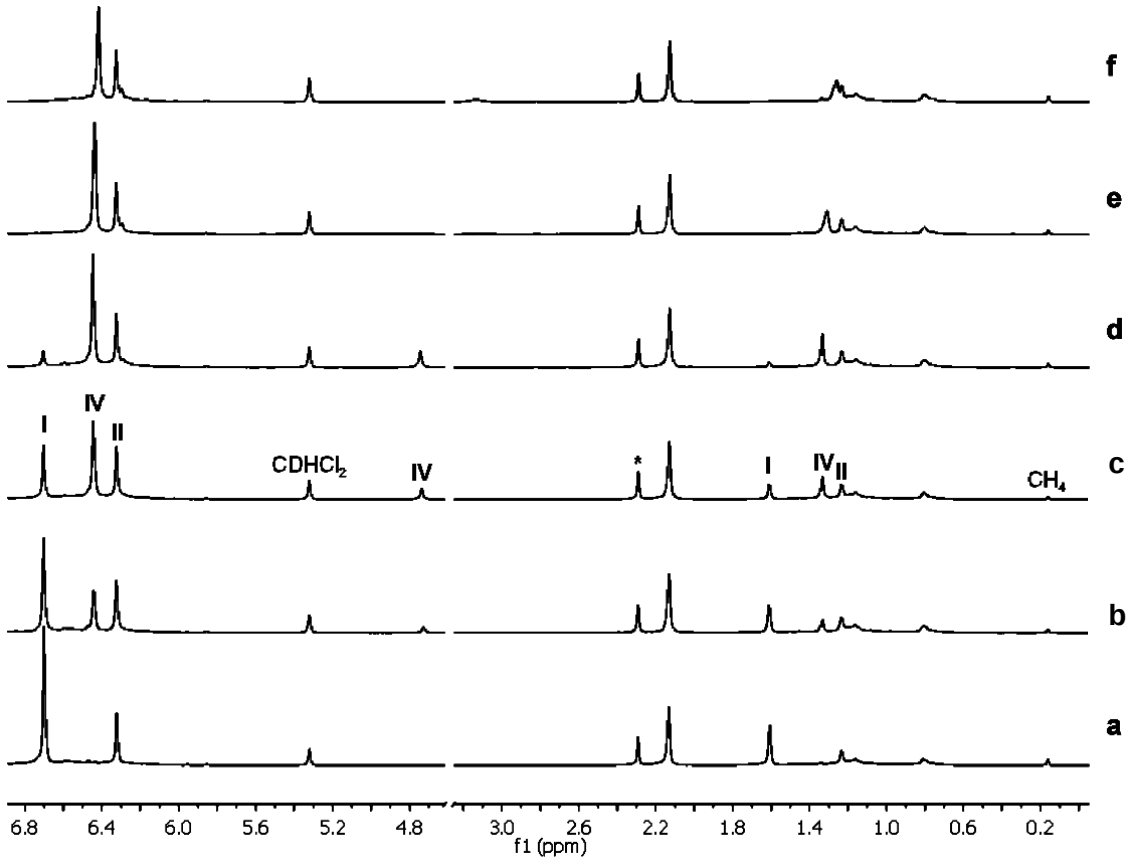

Figure 2.1. ^{1}H NMR spectra in the Cp and methyl regions (CD_2Cl_2, 205 K) of (a) a typical mixture of **I** and **II** and after the addition of ~0.3 (b), ~0.6 (c), ~0.9 (d), ~1.2 (e), and ~1.5 (f) equiv of water per **I** (* = resonance of residual toluene).

A NOESY experiment of the reaction mixture (available in the Appendix A (Appendix A) as Figure A2) demonstrated that the three resonances at 6.44, 4.74, and 1.33 all belonged to the same molecule, while a modified[†] Heteronuclear single quantum coherence spectroscopy (HSQC)

[†] In the modified HSQC experiment, the proton and carbon decouplers were turned off during the evolution and the acquisition, respectively. This resulted in signals in the 2D spectrum that are projections of the ^{13}C satellites (a doublet) seen in the ^{1}H NMR axis and carry the carbon multiplicity in the ^{13}C axis, which varies with the number of H attached to it.

experiment of a similar reaction mixture showed that the resonance at δ 4.77 was not coupled to any carbon atoms and was therefore to be assigned to coordinated water rather than some hydrocarbon fragment. The Cp and methyl ^{13}C chemical shifts obtained from the HSQC experiment (Appendix A, Figure A3) were δ 117.6 ($^{1}J_{CH}$ 175.7 Hz) and 61.1 ($^{1}J_{CH}$ 132.0 Hz), respectively. These are very similar to the data for compounds **I**-**III**, and we note that all of the methyl $^{1}J_{CH}$ values are typical of literature data.[7] Thus, the product is identified as $[Cp_2Ti(Me)(H_2O)][B(C_6F_5)_4]$ (**IV**), which is a rare, possibly unique, example of a complex containing aqua and methyl ligands within the inner coordination sphere of a titanium(IV) complex.

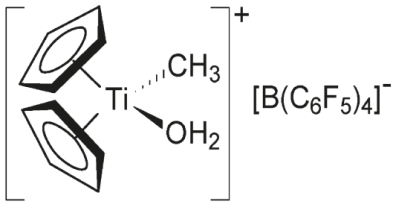

IV

Interestingly, while addition of a slight excess of water (Figure 2.1.e) to the reaction mixture had little effect on the Cp and methyl resonances of **II** and caused only small, upfield shifts of those of **IV**, the resonance of the coordinated water disappeared and a new, broad resonance appeared at δ ~3.15. On the addition of further water (Figure 2.1 f), the resonance at δ ~3.15 became stronger and is tentatively attributed to free water. That the resonance is broad while that of the coordinated water of **IV** cannot be observed suggests strong hydrogen bonding and exchange between the two sites.

As has been mentioned above, Cp chemical shifts in metallocene compounds are generally strongly influenced by inductive effects,[4] and we have previously utilized this correlation to distinguish between the resonances of **I** and **II**.[3] On this basis we note that coordinated water of **IV** (δ_{Cp} 6.44) appears to be intermediate in donor properties between those of the neutral CD_2Cl_2 (δ_{Cp} 6.71) and the $[B(C_6F_5)_4]^-$ (δ_{Cp} 6.32) and chloride (δ_{Cp} 6.23[3c]) anions.

While **IV** is reasonably stable for hours at 205 K, its resonances slowly weaken and the singlet resonance of methane appears at δ 0.16 (note the weak methane resonance in Figure 2.1); the decomposition of **IV** is more rapid at 225 K, with the methane resonance now at δ 0.17. Using D_2O instead of H_2O, the Cp and Ti-Me resonances but not the aqua resonance of **IV** were observed at 205 K, and warming to 225 K now resulted in a quadrupolar broadened methane resonance, which sharpened on further warming to 298 K to a 1:1:1: triplet ($^2J_{HD}$ 1.9 Hz) at δ 0.20 (Figure A4 in Appendix A). Thus, as anticipated, the decomposition does indeed involve transfer of a proton from water (see below) to the methyl ligand. While we were not able to identify the titanium-containing product(s), a number of new Cp resonances appeared in the region δ 6-7 (Figure A5), and we note that the initially formed species would probably be $[Cp_2Ti(OH)(CD_2Cl_2)][B(C_6F_5)_4]$. This might well convert to the dinuclear species $[Cp_2Ti(\mu\text{-}OH)_2TiCp_2][B(C_6F_5)_4]_2$ and, ultimately, perhaps, to oxide clusters of the types $Cp_6Ti_6(\mu\text{-}O)_8$ and $Cp_8Ti_8(\mu\text{-}O)_{12}$, which have been reported previously.[8]

The contrast between Cp_2TiMe_2 and **IV** with regard to susceptibilities of their methyl ligands to undergo protonolysis is quite notable, especially since the positive charge of **IV** should render its methyl ligand much less carbanionic in character and thus less susceptible to protonolysis. The proton transferred must originate in the coordinated water, and, consistent with this hypothesis, we note that the coordinated water molecules in $[Cp_2Ti(H_2O)_2]^{2+}$ are much more acidic than is bulk water, with pK_{a1} ~3.51 and pK_{a2} ~4.35.[9]

Finally, we note that the much greater reactivity of what we believe to be the cationic, solvent-separated ion pair **I** than of the contact ion pair **II** with water is paralleled in the relative reactivities of these two complexes (and their zirconocene analogues) with alkenes.[3] We have noted instances where the reactivities of two analogous solvent-separated and contact ion pair complexes can be directly compared, it does appear from this work and elsewhere[3] that anion-cation separation is a key feature in enhancing coordination of neutral ligands to cationic metallocene complexes.

2.5 Acknowledgment

M.C.B. gratefully acknowledges the Natural Science and Engineering Research Council of Canada and Queen's University for funding of this research.

2.6 References

1. (a) Samuel, E.; Rausch, M. D. *J. Am. Chem. Soc.* **1973**, *95*, 6263. (b) Alt, H. G.; Di Sanzo, F. P.; Rausch, M. D.; Uden, P. C. *J. Organomet. Chem.* **1976**, *107*, 257. (c) Clauss, K.; Bestian, H. *Justus Liebigs Ann. Chem.* **1962**, *654*, 8. (d) Erskine, G. J.; Wilson, D. A.; McCowan, J. D. *J. Organomet. Chem.* **1976**, *114*, 119. (e) Erskine, G. J.; Hartgerink, J.; Weinberg, E. L.; McCowan, J. D. *J. Organomet. Chem.* **1979**, *170*, 51. (f) Razuvaev, G. A.; Mar'in,V. P.; Andrianov,Y. A. *J. Organomet. Chem.* **1979**, *174*, 67. (g) Razuvaev, G. A.; Mar'in, V. P.; Drushkov, O. N.; Vyshinskaya, L. I. *J. Organomet. Chem.* **1982**, *231*, 125. (h) Li, H.; Neckers, D. C. *Can. J. Chem.* **2003**, *81*, 758. (i) Dollinger, L. M.; Ndakala, A. J.; Hashemzadeh, M.; Wang, G.;Wang,Y.; Martinez, I.; Arcari, J. T.; Galluzzo, D. J.; Howell, A. R.; Rheingold, A. L.; Figuero, J. S. *J. Org. Chem.* **1999**, *64*, 7074. (j) Payack, J. F.; Hughes, D. L.; Cai, D.; Cottrell, I. F.; Verhoeven, T. R. *Organic Syntheses*; Collect. 2004; Vol. *10*, p 355.

2. (a) Wailes, P. C.; Weigold, H.; Bell, P. *J. Organomet. Chem.* **1972**, *34*, 155. (b) Fronczek, F. R.; Baker, E. C.; Sharp, P. R.; Raymond, K. N.; Alt, H. G.; Rausch, M. D. *Inorg. Chem.* **1976**, *15*, 2284, and references therein. (c) Yakelis, N. A.; Bergman, R. G. *Organometallics* **2005**, *24*, 3579, and references therein.

3. (a) Vatamanu, M.; Stojcevic, G.; Baird, M. C. *J. Am. Chem. Soc.* **2008**, *130*, 454. (b) Sauriol, F.;Wong, E.; Leung, A. M. H.; Elliott Donaghue, I.; Baird, M. C.;Wondimagegn, T.; Ziegler, T. *Angew. Chem., Int. Ed.* **2009**, *48*, 3342. (c) Sauriol, F.; Sonnenberg, J. F.; Chadder, S. J.; Dunlop-Brière, A. F.; Baird, M. C.; Budzelaar, P.H.M. *J. Am. Chem. Soc.* **2010**, *132*, 13357. (d) Reviewers have expressed the opinion that the arguments for the identification of **I** and **II** are not compelling, suggesting that one of them might be $Cp_2TiMeCl$,[3d] a potential product of degradation in the solvent, CD_2Cl_2, or (unspecified) dinuclear species containing bridging anions. We find, however, that the Cp and methyl resonances of $Cp_2TiMeCl$ are observed at δ 6.23 and 0.65, respectively, and thus this compound is clearly not present in our reaction mixtures. A reasonable dinuclear candidate might be $[Cp_2TiMe]_2(\mu\text{-O})$, but this compound would exhibit Cp and Me resonances at δ 5.82 and 0.52, respectively,[3e-i] and clearly is also not present. Other unacceptable potential candidates are $[Cp_2TiCl]_2(\mu\text{-O})$,[3g] for which the Cp resonance would be observed at δ 6.30 albeit unaccompanied by a methyl resonance, and $Cp_2TiMeOTiClCp_2$, for which the Cp resonances would be observed at δ 5.98 and 6.14, the methyl resonance at δ 0.67.[3g] Thus all suggested alternative identifications of **I** or **II** are not observed. Beachell, H. C.; Butter, S. A. *Inorg. Chem.* **1965**, 4, 1133. (e) Surer, H.; Claude, S.; Jacot-Guillarmod, A. Helv. *Chim. Acta* **1978**, 61, 2956. (f) Hughes, D. L.; Payack, J. F.; Cai, D.; Verhoeven, T. R.; Reider, P. J. *Organometallics* **1996**, 15, 663. (g) Huffman, M.; Payack, J. PCT Int. Appl. WO 2000024748 A1 20000504, 2000. (h) Berget, P. E.; Schore, N. E. *Organometallics* **2006**, 25, 552. (i) Berget, P. E.; Schore, N. E. *Organometallics* **2006**, 25, 2398.

4. Gray, D. R.; Brubaker, C. H. *Inorg. Chem.* **1971**, *10*, 2143.

5. (a) A standard solution of water in CD_2Cl_2 was prepared, by dissolving 31 μL of H_2O in 10 mL of CD_2Cl_2 at 20 °C; CH_2Cl_2 has a solubility[5b] of 0.2-0.24 wt %, or ~3.2 μL of H_2O per mL of CD_2Cl_2. After an initial ^1H NMR spectrum of a Cp_2TiMe_2/$[Ph_3C][B(C_6F_5)_4]$ mixture was obtained, 0.05 mL of the standard H_2O/CD_2Cl_2 solution was syringed into 0.6 mL of the Cp_2TiMe_2/ $[Ph_3C][B(C_6F_5)_4]$ mixture in CD_2Cl_2 at 195 K solution for an approximate molar ratio of Ti:H_2O ≈ 4:1, making it a solution containing 0.24 μL of H_2O per mL of CH_2Cl_2. This is about 13 times less concentrated than the 20 °C saturated solution concentration (3.18 μL per mL). (b) For the solubility of H_2O in CH_2Cl_2, see: http://www.trimen.pl/witek/ciecze/old_liquids.html, http://macro.lsu.edu/HowTo/solvents/Dichloromethane.htm.

6. This experiment provides evidence for the stoichiometry of the reaction with water, a result confirmed by similar experiments involving other proportions of added water.

7. Courtot, P.; Pichon, R.; Salaun, J. Y.; Toupet, L. *Can. J. Chem.* **1991**, *69*, 661.

8. (a) Bottomley, F.; Drummond, D. F.; Egharevba, G. O.; White, P. S. *Organometallics* **1986**, *4*, 1620. (b) Heshmatpour, F.; Wocadlo, S.; Massa, W.; Dehnicke, K.; Bottomley, F.; Day, R. W. Z. *Naturforsch., B: Chem. Sci.* **1994**, *49*, 827.

9. Toney, J. H.; Marks, T. J. *J. Am. Chem. Soc.* **1985**, *107*, 947.

Chapter 3

α- and β-Agostic Alkyl-Titanocene Complexes*

3.1 Abstract

*Reaction of $[Cp_2Ti(Me)(CD_2Cl_2)]^+$ **(I)** with 3,3-dimethyl-1-butene at 205 K produces the α-agostic insertion product $[Cp_2TiCH_2CHMe^tBu]^+$ **(III)** in which the chirality at C(2) induces preferential binding of one of the diastereotopic α-H atoms; subsequent coordination of ethyl ether to **III** leaves the α-agostic interaction weakened but intact. On warming, **III** undergoes β-hydrogen elimination and the resulting hydride reacts further with excess 3,3-dimethyl-1-butene to form the β-agostic species $[Cp_2TiCH_2CH_2^tBu]^+$. NMR data and calculated (DFT) energies support the assignments.*

3.2 Introduction

An area of active research in recent years has involved the utilization of cationic metallocene complexes $[Cp'_2M(Me)]^+$ (Cp' = substituted cyclopentadienyl; M = Ti, Zr, Hf; Me = methyl) as catalysts for the polymerization of alkenes CH_2=CHR (R = H, alkyl, aryl).[1] The generally accepted mechanism of chain growth involves repeated olefin coordination and migratory insertion steps, the latter being facilitated by α-agostic interactions as in **A** (P = polymeryl). Complementary β-agostic species (**B**) are believed to serve as resting states during propagation.[2]

Scheme 3.1. α- and β- agostic intermediates thought to exist during group IV metallocenes-catalyzed olefin-polymerization

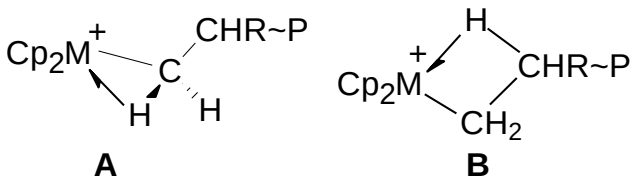

* The manuscript presented in chapter 3 was published at: Dunlop-Brière, A. F.; Budzelaar, P. H. M.; Baird, M. C., *Organometallics* **2012**, *31*, 1591.

Although neither olefin complexes nor either class of agostic species have been observed in active group IV metallocene catalyst systems, there is considerable theoretical evidence for such species and all three types of complexes have been reported for early transition metal complexes which are not particularly active in catalysis.[3,4]

We have recently reported that $[Cp_2Zr(Me)(CD_2Cl_2)]^+$ reacts with 2,4-dimethyl-1-pentene (DMP) to give a novel alkyl-olefin complex, $[Cp_2Zr(Me)(DMP)]^+$, which does not undergo migratory insertion.[5] In surprising contrast, the analogous reaction of DMP with $[Cp_2Ti(Me)(CD_2Cl_2)]^+$ results, via a complex cascade of reactions, in a β-agostic alkyl complex (of type **B**) that corresponds to the product of double propene insertion into $[Cp_2TiMe]^+$.[6] Thus by utilizing olefins which do not readily undergo polymerization via a coordination polymerization process, normally unobservable olefin and agostic intermediates are sufficiently stable at low temperatures that they can be characterized and studied.

We now report that reaction of $[Cp_2Ti(Me)(CD_2Cl_2)]^+$ with the sterically hindered olefin 3,3-dimethyl-1-butene (DMB) leads to an observable *single insertion*, α-*agostic* metal alkyl complex, of type **A**. DMB seems not to be known to undergo homo-polymerization via a coordination polymerization mechanism,[7] and it therefore seemed likely that multiple insertion reactions of this olefin are difficult and that again it might be possible to study interesting olefin and/or agostic intermediates.

3.3 Results and Discussion

On reaction of a mixture of the solvent-separated ion pair $[Cp_2TiMe(CD_2Cl_2)][B(C_6F_5)_4]$ (**I**)[6] with DMB in CD_2Cl_2 at 195-205 K, the ^1H resonances of **I** were replaced by those of a new species (**II**). On standing at 205 K, but more rapidly at higher temperatures, these resonances were in turn replaced by those of another new species (**III**).

Compound **II** was identified as the 1,2-insertion product $[Cp_2TiCH_2CHMe^tBu]^+$ based on NMR data (for details see the Appendix B). Of particular relevance are the resonances of the

diastereotopic α-CH_2 protons at δ −1.66 and 5.97, separated by more than 7 ppm and exhibiting an abnormally low value of the geminal coupling constant (3.7 Hz). The $^1J_{CH}$ values of these hydrogens are also markedly different, 104 and 133 Hz, respectively; in contrast, the β-CH is normal (δ 2.85, $^1J_{CH}$ 129 Hz). All this strongly suggests the presence of an α-agostic interaction (i.e. structure type **A**). A similarly negative chemical shift was noted previously for the β-agostic hydrogen of $[Cp_2Ti(CH_2CHMeCH_2CHMe_2)]^+$, and was attributed to ring current effects arising from close proximity to the Cp rings[6] (negative chemical shifts are not observed in agostic group 4 metal compounds which do not contain Cp rings[3,6]).

Although the diastereotopic α-CH_2 protons cannot undergo mutual exchange, one might anticipate that they would alternate between agostic and non-agostic positions, i.e. that the complex would equilibrate between structures **IIa** and **IIb**. The fact that α-H(a) and α-H(b) exhibit very different chemical shifts and $^1J_{CH}$ coupling constants suggests, however, that one of these conformations is strongly preferred.

Scheme 3.2. Schematic representation of the agostomeric exchange between α-agostic **IIa**, the dominant agostic conformation of **II**, and α-agostic **IIb**, the second most favored agostomer of **II**. The labeling of Ha and Hb is independent of chirality at C2 since by definition Ha is the α hydrogen that spends the most time involved in the agostic interaction for an enantiomer or the other, and Hb is the α hydrogen that spends the least time involved in the agostic interaction, regardless of the chirality at C2.

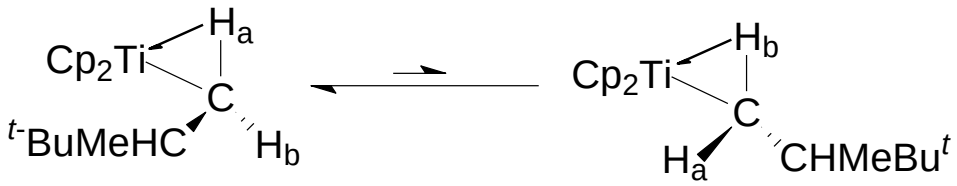

IIIa **IIIb**

DFT calculations were carried out to gain a better understanding of the structure and bonding in **II** and related species (see the Appendix B for details of the calculations). Figure 3.1 shows the structure of **IIa** optimized at the b3-lyp/TZVP level.

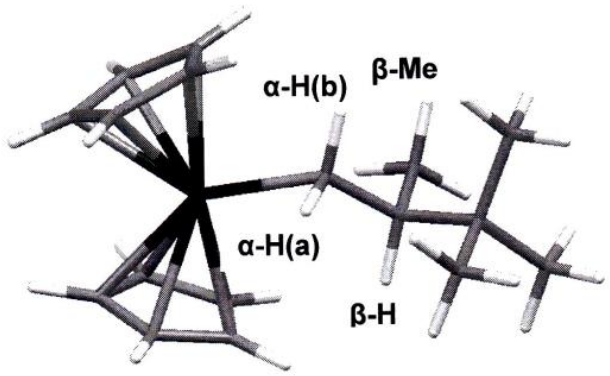

Figure 3.1. Optimized geometry (b3-lyp/TZVP) for **IIa** (white = H, grey = C, black = Ti).

In this structure, the Ti-Cα bond length is 2.099 Å, significantly shorter than has been calculated for the very similar but β-agostic species $[Cp_2TiCH_2CHMeCH_2CHMe_2]^+$ (2.169 Å) and $[Cp_2TiEt]^+$ (2.155 Å).[6] The reason for the difference presumably lies in the fact that the latter two complexes are both β-agostic; formation of α-agostic interactions result in shorter metal-carbon σ bonds as has been observed elsewhere.[3b,8]

The H atom labeled α-H(a) is positioned so as to occupy a vacant receptor orbital on the titanium[9] and, at 2.041 Å, the clearly agostic Ti-H distance is considerably less than the non-agostic Ti-α-H(b) distance of 2.696 Å. Interestingly, the α-H(a)-(α-C)-(β-C)-(β-H) and α-H(b)-(α-C)-(β-C)-(β-H) dihedral angles are 58.4° and 176.8°, respectively, and thus one anticipates that $^3J_{\alpha\text{-H(a)-}(\beta\text{-H})}$ will be considerably smaller than $^3J_{\alpha\text{-H(b)-}(\beta\text{-H})}$; the experimental values are ~4 Hz and 11.4 Hz, respectively.

Other features of note and possibly contributing to the stability of this conformation, the Ti-(α-C)-(β-C)-(β-Me) dihedral angle is 89.0°, and thus the β-Me group is anti to the agostic hydrogen atom and is in staggered position relative to both Cp groups.

According to our computational results, conformation **IIa** is marginally more stable (0.8 kcal/mol) than an alternative, **IIb**, which is similar but in which the β-Me group is *syn* to the agostic hydrogen atom although it still occupying an essentially staggered position with respect to the Cp groups. While many of the structural parameters of **IIb** are generally similar to those of **IIa**, we note that the α-H(a)-(α-C)-(β-C)-(β-H) and α-H(b)-(α-C)-(β-C)-(β-H) dihedral angles of **IIb** are 58.4° and 70.1°, respectively, from which one would expect two rather similar (and small) $^{3}J_{HH}$ vicinal coupling constants. This is not as observed, and thus the experimental NMR data are much more consistent with conformation **IIa**.

The 0.8 kcal/mol energy difference between **IIa** and **IIb** would result in a **IIa**:**IIb** ratio of ~6:1, sufficient for the more stable conformation to dominate the NMR parameters. Interestingly, however, the calculated chemical shifts of the α-H atoms of **IIa** are δ −2.82 and 10.9 (Δδ ~13.7 ppm) while the corresponding calculated values of $^{1}J_{CH}$ are 80 and 138 Hz (ΔJ = 58 Hz). These differences are significantly greater than those observed experimentally and thus the observed NMR parameters, while weighted toward those of the more highly populated conformation **IIa**, appear to be averages of the parameters of both conformations.

The α-agostic structure observed for **II** is very interesting, as most coordinatively unsaturated metal alkyl compounds bearing β-hydrogens prefer β- over α-agostic structures.[2,10] However, the calculated free energy of the β-agostic structure of **II** is ~4 kcal/mol *higher* than that of **IIa**, a preference which is undoubtedly a result of steric factors arising from the presence of the methyl and *t*-Bu groups on the β-carbon atom. A β-agostic structure would force the methyl and *t*-Bu groups into close proximity to the Cp rings, generating repulsive contacts which are avoided in the α-agostic structures. The promotion of α- over β-agostic structures by steric factors has been observed with other ligand systems.[10]

Conversion of **II** to **III** occurred smoothly at 205-220 K, and **III** was identified by NMR spectroscopy as $[Cp_2TiCH_2CH_2{}^tBu]^+$. Complex **III** undoubtedly forms via β-hydrogen elimination

from **II** to give 2,3,3-trimethyl-1-butene and $[Cp_2TiH]^+$, followed by insertion of DMB (present in excess). The negative chemical shift of the β-CH_2 hydrogens (δ −0.61) and the large $^1J_{CH}$ (145 Hz) of the α-CH_2 hydrogens strongly imply a β-agostic structure[2,6] but $^1J_{\beta\text{-}CH}$ (117 Hz) of **III** is considerably greater than in $[Cp_2TiCH_2CHMeCH_2CHMe_2]^+$.[6] Thus the observed NMR parameters of **III** are averages of those of rapidly exchanging agostic and non-agostic β-H atoms. Calculated energies (5.1 kcal/mol in favor of β-agostic, with a barrier of 4.0 kcal/mol for agostic/non-agostic exchange) support this interpretation.

In an effort to induce, for purposes of comparison, formation of a non-agostic derivative of **II**, we reacted **II** with ethyl ether. The reaction proceeded smoothly at 205 K to give $[Cp_2TiCH_2CHMe^tBu(Et_2O)]^+$ (**IV**), the ^1H and ^{13}C NMR spectral data of which are described in the Appendix B. Of some surprise, the data indicate strongly that **IV** is also α-agostic.

Thus the chemical shifts of the diastereotopic α-CH_2 protons are δ −0.31 and 4.97, with $^1J_{CH}$ being 107 and 131 Hz, respectively. In contrast, the β-CH is normal (δ 2.55, $^1J_{CH}$ 123 Hz) as are the other chemical shifts and coupling constants. The downfield chemical shift (1.35 ppm) and the increase in $^1J_{CH}$ (4 Hz) of the α-agostic hydrogen relative to the corresponding data for **II** suggests a weakened agostic interaction, presumably because of steric effects and/or reduction of the Lewis acidity of the titanium following ether coordination.

DFT calculations on **IV** were carried out, and the optimized structure is shown in Figure 3.2. Important bond lengths and angles are given in the Appendix B.

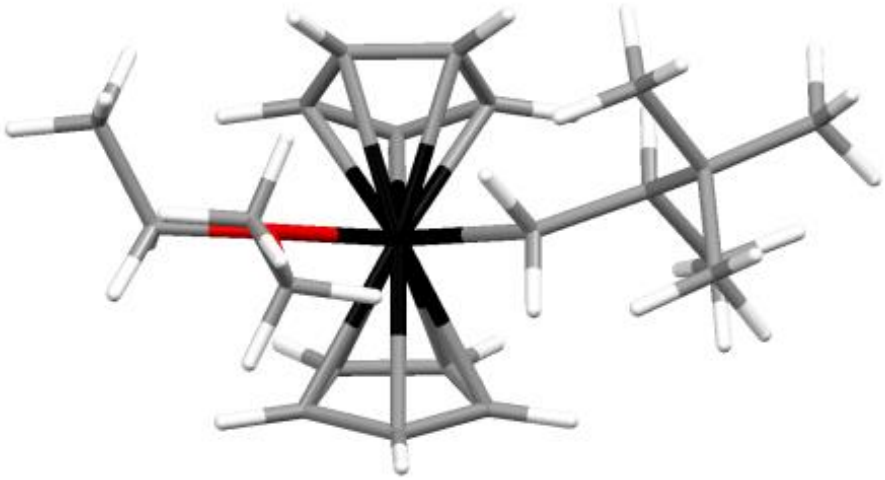

Figure 3.2. Optimized geometry for $Cp_2Ti(CH_2CHMeBu^t)(Et_2O)]^+$ (white = H, grey = C, red = O, black = Ti).

In this structure, the Ti-α-C bond length is 2.172 Å, significantly longer than was calculated for **II**, while the Ti-α-H distances are 2.419 and 2.655 Å, both much longer than the agostic Ti-H distance in **II**. The agostic hydrogen atom is positioned between the other donor atoms, appropriately to interact with central b_2 orbital of the Cp_2Ti^{2+} moiety,[9] although the orientation does not appear to be as favorable as in **IIa**.

Complex **IV** is thermally more stable than is **II**, and resists significant β-hydrogen elimination at 235 K for at least 25 min. The greater stability presumably arises because the coordinated ether occupies the metal orbital necessary for β-H elimination to occur in order to form 2,3,3-trimethyl-1-butene and $[Cp_2TiH]^+$. In addition, the coordinated ether may also provide steric hindrance to the β-agostic conformation required for β-H elimination.

3.4 Conclusion

In summary, our results clearly demonstrate the delicate balance between electronic factors (β-agostic preferred, as in **III**) and steric effects (β,β-disubstitution favoring α-agostic conformations, as in **II**) for these highly unsaturated and reactive metal alkyls. Furthermore, and in contrast to the situation with e.g. ethylene and α-olefins where barriers for all steps in the polymerization process are too low for intermediates to be observable, we show in this and in previous publications[5,6] that utilization of olefins which do not readily undergo coordination polymerization makes possible studies of normally unobservable, olefin and α- and β-agostic intermediate complex. In these cases, barriers to insertion steps are sufficiently high that important intermediates can be observed and characterized at low temperatures.

Interestingly, for the α-agostic species studied here, chirality in the alkyl ligand results in one α-agostic structure being favored over the other. To our knowledge, this type of behavior has not been observed previously although it has obvious implications in understanding the role(s) of α-agostic interactions during stereoselective polymerization of prochiral olefins by chiral metallocene polymerization catalysts.[1-3] Our findings support the viable existence of intermediates of the type $[Cp_2Ti(\alpha\text{-agostic-alkyl})(olefin)]^+$, and may also prove relevant in the gaining of understanding of chain-end control on tacticity.[1a,c,d]

3.5 Acknowledgements

MCB gratefully acknowledges the Natural Science and Engineering Research Council of Canada, the Canada Foundation for Innovation and Queen's University for funding of this research. PHMB thanks the Natural Science and Engineering Research Council of Canada, the Canada Foundation for Innova-tion, the Manitoba Research and Innovation Fund and SABIC Petrochemicals Europe for financial support.

3.6 References

1. For useful reviews see (a) Bochmann, M. *J. Chem. Soc., Dalton Trans*. **1996**, 255. (b) Resconi, L.; Camurati, I.; Sudmeijrt, O. *To-pics Catalysis* **1999**, *7*, 145. (c) Coates, G. W. *Chem. Rev*. **2000**, *100*, 1223. (d) Resconi, L. ; Cavallo, L.; Fait, A. ; Piemontesi, F. *Chem. Rev*. **2000**, *100*, 1253. (e) Chen, E. Y.-X. ; Marks, T. J. *Chem. Rev*. **2000**, *100*, 1391. (f) Rappé, A. K. ; Skiff, W. M. ; Casewit, C. J. *Chem. Rev*. **2000**, *100*, 1435. (g) Bochmann, M. *J. Organomet. Chem.* **2004**, *689*, 3982. (h) Fujita, T.; Makio, H. *Comp. Organomet. Chem.* III, chap. 11.20, *Crabtree, R. H.; Mingos, D. M. P. editors*, Elsevier, Amsterdam, **2007**. (i) Froese, R. D. J. in Computational Modeling for Homogeneous and Enzymatic Catalysis, editors Morokuma, K.; Musaev, D. G. **2008**, 149. Wiley-VCH, Weinheim, Germany. (j) Busico, V. *Macromol. Chem. Phys.* **2007**, *208*, 26. (k) Wilson, P. A.; Hannant, M. H.; Wright, J. A.; Cannon, R. D.; Bochmann, M. *Macromol. Symp.* **2006**, *236* (Olefin Polymerization), 100. (l) Alt, H. G.; Licht, E. H.; Licht, A. I.; Schneider, K. J. *Coord. Chem. Rev.* **2006**, *250*, 2. (m) Tullo, A. H. *C&EN* **2010**, *88* (42), 10. (n) Bochmann, M. *Organometallics* **2010**, *29*, 4711.

2. For reviews of agostic complexes, see (a) Brookhart, M.; Green, M. L. H.; Wong. L.-L. *Prog. Inorg. Chem.* **1988**, *36*. 1. (b) Grubbs, R. H.; Coates, G. W. *Acc. Chem. Res.* **1996**, *29*, 85.(c) Scherer, W.; McGrady, G. S. *Chem. Eur. J.* **2003**, *9*, 6057. (d) Clot, E.; Eisenstein, O. *Struct. Bonding (Berlin)* **2004**, *113*, 1. (e) Scherer, W.; McGrady, G. S. *Angew. Chem., Internat. Ed.* **2004**, *43*, 1782. (f) Brookhart, M.; Green, M. L. H.; Parkin, G. *Proc. Nat. Acad. Sci*. **2007**, *104*, 6908. (g) Lein, M. *Coord. Chem. Rev.* **2009**, *253*, 625.

3. (a) Dawoodi, Z.; Green, M. L. H.; Mtetwa, V. S. B.; Prout, K. *J. Chem. Soc., Chem. Commun.* **1982**, 802. (b) Dawoodi, Z.; Green, M. L. H.; Mtetwa, V. S. B.; Prout, K.; Schultz, A. J.; Williamns, J. M.; Koetzle, T. F. *J. Chem. Soc., Dalton Trans.* **1986**, 1629. (c) McGrady, G. S.; Downs, A. J.; Haaland, A.; Scherer, W.; McKean, D. C. *Chem. Commun.* **1997**, 1547. (d) Cotton, F. A.; Petrukhina, M. A. *Inorg. Chem. Commun.* **1998**, *1*, 195. (e) Scherer, W.; Priermeier, T.; Haaland, A.; Volden, H. V.; McGrady, G. S.; Downs, A. J.; Boese, R.; Bläser, D. *Organometallics* **1998**, *17*, 4406. (f) Scherer, W.; Hieringer, W.; Spiegler, M.; Sirsch, P.; McGrady, G. S.; Downs, A. J.; Haaland, A.; Pedersen, B. *Chem. Commun.* **1998**, 2471. (g) Haaland, A.; Scherer, W.; Ruud., K.; McGrady, G. S.; Downs, A. J.; Swang, O. *J. Am. Chem. Soc.* **1998**, *120*, 3762. (h) Scherer, W.; Sirsch, P.; Shorokhov, D.; Tafipolsky, M.; McGrady, G. S.; Gullo, E. *Chem. Eur. J.* **2003**, *9*, 6057. (i) Jordan, R. F.; Bradley, P. K.; Baenziger, N. C.; LaPointe, R. E. *J. Am. Chem. Soc.* **1990**, *112*, 1289.

4. For examples of metallocene olefin complexes, see (a) Casey, C. P.; Carpenetti, D. W. *Organometallics* **2000**, *19*, 3970. (b) Car-pentier, J. F.; Wu, Z.; Lee, C. W.; Strömberg, S.; Christopher, J. N.; Jordan, R. F. *J. Am. Chem. Soc.* **2000**, *122*, 7750, and references therein. (c) Brandow, C. G.; Mendiratta, A.; Bercaw, J. E.*Organometallics* **2001**, *20*, 4253. (d) Casey, C. P.; Carpenetti, D. W.; Sakurai, H. *Organometallics* **2001**, *20*, 4262. (e) Stoebenau, E. J.; Jordan, R. F. *J. Am. Chem. Soc.* **2006**, *128*, 8162. (f) Stoebenau, E. J.; Jordan, R. F. *J. Am. Chem. Soc.* **2006**, *128*, 8638. (g) Hunter, W. E.; Hrncir, D. C.; Bynum, R. V.; Penttila, R. A.; Atwood, J. L. *Organometallics* **1983**, *2*, 750. (h) Guzei, I. A.; Stockland, R. A.; Jordan, R. F. *Acta Cryst.* **2000**, *C56*, 635.

5. (a) Vatamanu, M.; Stojcevic, G.; Baird, M. C. *J. Amer. Chem. Soc*. **2008**, *130*, 454. (b) Sauriol, F.; Wong, E.; Leung, A. M. H.; Elliott Donaghue, I.; Baird, M. C.; Wondimagegn, T.; Ziegler, T. *Angew. Chem., Int. Ed.* **2009**, *48*, 3342.

6. Sauriol, F.; Sonnenberg, J. F.; Chadder, S. J.; Dunlop-Brière, A. F.; Baird, M. C.; Budzelaar, P. H. M. *J. Am. Chem. Soc*. **2010**, *132*, 13357.

7. Copolymers with ethylene are formed in this way. See (a) Kissin, Y. V.; Goldman, A. S. *Macromol. Chem. Phys.* **2009**, *210*, 1942. (b) Ketley, A. D.; Moyer, J. D. *J. Poly. Sci. Part A:* **1963**, *1*, 2467.

8. (a) Etienne, M. *Organometallics* **1994**, *13*, 410. (b) Mena, M.; Pellinghelli, M. M.; Royo, P.; Serrano, R.; Tiripicchio. A. *J. Chem. Soc., Chem. Comm.* **1986**, *14*, 1118.

9. (a) Lauher, J. W.; Hoffmann, R. *J. Am. Chem. Soc*. **1976**, *98*, 1729. (b) Albright, T. A.; Burdett, J. K.; Whangbo, M.-H. "Orbital Interactions in Chemistry", Wiley, 1985, p. 393.

10. A number of computational papers consider the interplay between α- and β-agostic species. See: (a) Nifant'ev, I. E.; Ustynyuk, L. Y.; Laikov, D. N. *Organometallics* **2001**, *20*, 5375. (b) Jensen, V. R.; Koley, D.; Jagadeesh, M. N.; Thiel, W. *Macromolecules* **2005**, *38*, 10266. (c) Graf, M.; Angermund, K.; Fink, G.; Thiel, W.; Jen-sen, V. R. *J. Organomet. Chem.* **2006**, *691*, 4367. (d) Karttunen, V. A.; Linnolahti, M.; Pakkanen, T. A.; Severn, J. R.; Kokko, E.; Maaranen, J.; Pitkänen, P. *Organometallics* **2008**, *27*, 3390. (e) Mitoraj, M. P.; Michalak, A.; Ziegler, T. *Organometallics* **2009**, *28*, 3727. (f) Laine. A.; Linnolahti, M.; Pakkanen, T. A.; Severn, J. R.; Kokko, E.; Pakkanen, A. *Organometallics* **2010**, *29*, 1541.

Chapter 4

$[Cp_2TiCH_2CHMe(SiMe_3)]^+$, an alkyl-titanium complex which (a) exists in equilibrium between a β-agostic and a *lower energy* γ-agostic isomer and (b) undergoes hydrogen atom exchange between α-, β- and γ-sites via a combination of conventional β-hydrogen elimination-reinsertion and a non-conventional, CH bond activation process which involves proton tunnelling*

4.1 Abstract

*The compound $[Cp_2Ti(Me)(CD_2Cl_2)][B(C_6F_5)_4]$ reacts with trimethylvinylsilane (TMVS) to form the 1,2-insertion product $[Cp_2TiCH_2CHMe(SiMe_3)]^+$ (**III**), which exists in solution as equilibrating β- and γ-agostic isomers. In addition, while free rotation of the β-methyl group results in a single, averaged γ-H atom resonance at higher temperatures, decoalescence occurs below ~200 K and the resonance of the γ-agostic hydrogen atom at δ ~–7.4 is observed. Reaction of $[Cp_2Ti(CD_3)(CD_2Cl_2)]^+$ with TMVS results in the formation of $[Cp_2TiCH_2CH(CD_3)(SiMe_3)]^+$, which converts, via reversible β-elimination, to an equilibrium mixture of specifically $[Cp_2TiCH_2CH(CD_3)(SiMe_3)]^+$ and $[Cp_2TiCD_2CD(CH_3)(SiMe_3)]^+$. Complementing this conventional process, EXSY experiments show that the β-H atom of $[Cp_2TiCH_2CHMe(SiMe_3)]^+$ undergoes exchange with the three hydrogen atoms of the β-methyl group (β-H/γ-H exchange) but not with the two α-H atoms. This exchange process is completely shut down when*

* The manuscript presented in chapter 4 was published at: Dunlop-Brière, A. F.; Budzelaar, P. H. M.; Baird, M. C. *Journal of the American Chemical Society* **2013**, *135(46)*, 17514.

*$[Cp_2TiCH_2CH(CD_3)(SiMe_3)]^+$ is used, suggesting an H/D kinetic isotope effect much larger (apparently >16000) than the maximum possible for an over-the-barrier process. It is proposed that β-H/γ-H exchange is facilitated by quantum mechanical proton tunnelling in which a hydrogen atom of the 2-methyl group of the alkene-hydride deinsertion product $[Cp_2TiH\{CH_2=CMe(SiMe_3)\}]^+$ undergoes reversible exchange with the hydride ligand via the allyl dihydrogen species $[Cp_2TiH_2\{(\eta^3\text{-}CH_2C(SiMe_3)CH_2\}]^+$. Complementing these findings, DFT calculations were carried out to obtain energies and NMR parameters for all relevant species and thence to obtain better insight into the agostic preference(s) of complex **III** and the observed exchange processes. In all cases where comparisons between experimental and calculated data were possible, agreement was excellent.*

4.2 Introduction

There has in recent years been considerable interest in the utilization of metallocene complexes of the types $Cp_2M(Me)(WCA)$ or $[Cp_2M(Me)(solvent)]WCA$ (M = Ti(IV), Zr(IV), Hf(IV); Me = methyl; WCA = weakly coordinating anion such as $B(C_6F_5)_4^-$) as catalysts for the coordination polymerization of alkenes CH_2=CHR (R = H, alkyl, aryl).[1] It is universally accepted that the initial steps of such polymerization processes involve coordination of the alkene to generate a cationic intermediate $[Cp_2M(Me)(\eta^2\text{-}CH_2=CHR)]^+$ (**A**), which undergoes subsequent migratory insertion to give an alkyl intermediate of type **B** (vacant site possibly occupied by alkene, solvent molecule or WCA).

Scheme 4.1. d^0 methyl-olefin-metallocene (**A**) and alkyl-metallocene (**B**) intermediates thought to exist during olefin-polymerization reaction catalyzed by group IV d^0 metallocene

Until recently, NMR studies of d^0 metallocene-based alkene polymerization catalyst systems had never provided direct evidence for alkyl alkene intermediates such as type **A**, presumably because (a) a lack of π back donation from d^0 metal ions results in weak alkene-metal bonding and (b) activation energies for migratory insertion processes involving e.g. ethylene, propylene and 1-alkenes are very low. Thus, species of type **A** are too short lived to be observed although complexes of type **C**, stabilized by chelation and other means, have been reported.[2]

Scheme 4.2. Chelation-stabilized alkyl-olefin-zirconocene intermediate

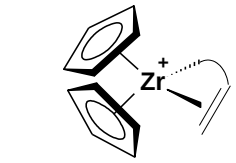

In **C**, tethering of the alkene apparently prevents rearrangement to the four-centred transition state necessary for migratory insertion to occur.

As we have recently observed, however, there is an alternative to tethering, as in **C**, to make possible the observation of alkyl alkene complexes of type **A**: one can utilize alkenes which do not readily undergo migratory insertion reactions, i.e. are generally non-polymerizable via a coordination polymerization process.[3] Thus, for instance, $[Cp_2Zr(Me)(CD_2Cl_2)][B(C_6F_5)_4]$ reacts with 2,4-dimethyl-1-pentene (DMP) to form $[Cp_2Zr(Me)(DMP)][B(C_6F_5)_4]$, which can be studied via NMR spectroscopy at low temperatures.[3] DFT calculations suggested that the activation energy for migratory insertion of the DMP ligand is relatively high, largely because the two substituents on C(2) provide steric hindrance which raises the energy of the migratory insertion transition state.[3] Thus $[Cp_2Zr(Me)(DMP)]^+$ was characterized by a series of low temperature 1D and 2D NMR experiments, supported by DFT calculations, which suggested that the alkene bonding mode is highly asymmetric, with the Zr-C(1) distance significantly shorter than the Zr-C(2) distance and, apparently, a high degree of carbocationic nature for C(2). Thus, the structure appears to be

described more appropriately as in **b** of Figure 4.1, analogous to intermediates during carbocationic polymerization of 2,2-disubstituted 1-alkenes,[4] rather than as the conventional η^2 structure **a**.

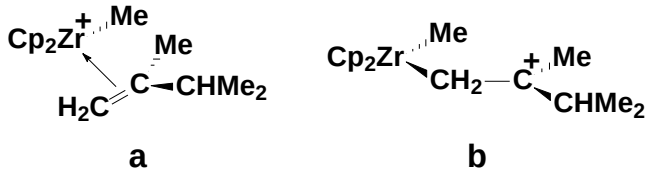

Figure 4.1. Alternative structures of $[Cp_2Zr(Me)(DMP)]^+$.

Consistent with this hypothesis, there occurs rotation of the R(Me)C= group along the C(1)-C(2) axis and relative to the $=CH_2$ group, implying significant loss of C=C double bond character in the near-η^1 coordinated alkene.[3]

During a coordination polymerization process, propagation following the formation of **B** involves a succession of analogous alkene coordination and migratory insertion steps, the insertions being facilitated by α-agostic interactions as in **D** (P = polymeryl) with complementary β-agostic species (**E**) serving as resting states during propagation.[5]

Scheme 4.3. α-agostic (D) and β-agostic (E) intermediates thought to exist in coordination polymerization processes

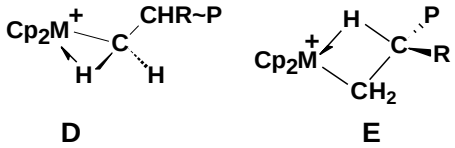

The α- and β-agostic modes of bonding, denoted by the half arrows in **D** and **E**, involve donation of electron density from respectively delocalized H-C(1) and H-C(2)-C(1) σ bonding molecular orbitals to a vacant orbital on the highly Lewis acidic metal ion.[5] Agostic complexes are well known for late transition metal compounds,[5q,r] and a small number of β-agostic zirconocene complexes of the type $[Cp_2ZrRL]^+$ (R = Et, CH_2CH_2Ph, $CH_2CH_2CMe_3$, CH_2CHMe_2; L = PMe_3 MeCN) are known.[6a,b,d] Zirconocene(IV) complexes containing α-agostic interactions of type **D** seem to be

unknown and titanocene(IV) complexes containing α- or β-agostic complexes of types **D** and **E** have also until very recently[6e,f] not been characterized. As with species of types **A** and **B**, activation energies for migratory insertion processes involving readily polymerized alkenes such as ethylene, propylene and 1-alkenes are sufficiently low that lifetimes of species **D** and **E** are too short for them to be observed.

Recognizing, as outlined above, that coordination of alkenes which are non-polymerizable via a coordination polymerization process can generate d^0 metal alkene complexes which are sufficiently stable at low temperatures that they can be characterized and studied, we attempted to synthesize the analogous titanocene(IV) complex $[Cp_2Ti(Me)(DMP)]^+$ by reacting DMP with $[Cp_2Ti(Me)(CD_2Cl_2)][B(C_6F_5)_4]$ (**I**). Instead we obtained, via a complex cascade of reactions, the cationic species $[Cp_2Ti(CH_2CHMeCH_2CHMe_2)]^+$, identified as a β-agostic metal alkyl complex of type **E**.[6e] The new complex was characterized by the complete analysis of a series of 1D and 2D NMR spectra, and a mechanism for its formation which involved an ε-agostic intermediate and a 1,5 metal shift was formulated on the basis of DFT calculations.[6e]

Pursuing this theme, we subsequently investigated the reaction of **I** with another type of sterically hindered alkene, 3,3-dimethyl-1-butene (3,3-DMB). This alkene also seems not to be known to undergo homo-polymerization via a coordination polymerization mechanism,[6f] and it therefore seemed likely that multiple insertion reactions would again be difficult and that it might be possible once more to study interesting alkene and/or agostic complexes. Reaction proceeded readily in CD_2Cl_2 at 195-205 K but resulted, via an η^2-3,3-DMB complex according to DFT calculations, in the formation of a *single insertion*, α-*agostic* metal alkyl complex, $[Cp_2TiCH_2CHMe^tBu]^+$ (**II**), of type **D**. Interestingly, although the diastereotopic α-CH_2 protons could not undergo mutual exchange, NMR spectral evidence and DFT calculations suggested that they alternated between agostic and non-agostic positions, i.e. that **II** equilibrated between structures **IIa** and **IIb** in a windshield wiper-like fashion.[6f]

Scheme 4.4. Schematic representation of the agostomeric exchange between α-agostic **IIa**, the dominant agostic conformation of **II**, and α-agostic **IIb**, the second most favored agostomer of **II.** Determination of which α-H is labeled H_a or H_b is dependent on chirality at C2. For a given chiral configuration (R or S) at C2, H_a is defined here as the α-H which spends the most time in the agostic configuration and H_b is the other proton, which is less agostic than the former.

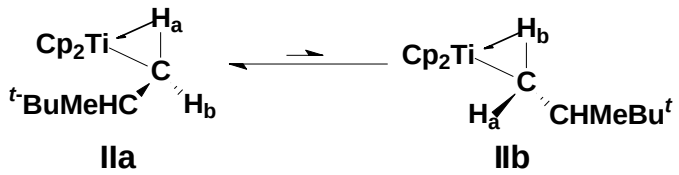

The fact that α-H(a) and α-H(b) exhibited very different chemical shifts and $^1J_{CH}$ coupling constants suggested, however, that one of these conformations was strongly preferred. Characteristic of the agostic hydrogen atoms in these titanocene compounds are their negative ^{1}H NMR chemical shifts, resulting from ring current effects from the Cp rings; non-metallocene group 4 agostic compounds exhibit positive ^{1}H NMR chemical shifts.[6e,f]

The α-agostic structure observed for **II** was also very interesting because most coordinatively unsaturated metal alkyl compounds bearing β-H atoms prefer β- over α-agostic structures.[5,6a-c,7] However, DFT calculations suggested that the β-agostic structure of **II** is destabilized by steric factors arising from the presence of the methyl and *t*-Bu groups on the β-carbon atom; a β-agostic structure would force the methyl and *t*-Bu groups into close proximity to the Cp rings, generating repulsive contacts which are avoided in the α-agostic structures. The promotion of α- over β-agostic structures by steric factors had been observed with other ligand systems,[5,7] but our results clearly demonstrated the delicate balance between electronic factors (β-agostic generally preferred) and steric effects (β,β-disubstitution favoring α-agostic conformations as in **II**) for highly unsaturated and reactive alkyl metallocenium cations. Furthermore, as noted above, utilization of alkenes which do not readily undergo coordination polymerization makes possible studies of normally unobservable α- and β-agostic intermediate species. In these cases, barriers to subsequent monomer insertion steps are sufficiently high that important intermediates can be observed and characterized at low temperatures.

We now report a similar study of the reaction of **I** with trimethylvinylsilane (TMVS), another alkene which seems not to be readily polymerized via coordination polymerization processes[8] although a few rather "normal" η^2-complexes are known;[9a-d] in addition, copolymerization with ethylene, presumably via a coordination polymerization process, has been reported.[9e] Given the similarity of TMVS to 3,3-DMB, we anticipated further opportunities to study agostic species, and we have not been disappointed.

4.3 Experimental

All syntheses were carried out under dry, deoxygenated argon using standard Schlenk line techniques, using argon deoxygenated by passage through a heated column of BASF copper catalyst and then dried by passing through a column of activated 4A molecular sieves, or an MBraun Labmaster glove box. NMR spectra were recorded using a Bruker AV600 spectrometer, ^1H, ^2H, and ^{13}C NMR data being referenced to TMS via the residual proton signals of the solvent. $[Ph_3C][B(C_6F_5)_4]$ was purchased from Asahi Glass Company and used as obtained, while CH_3Li, CD_3Li and trimethylvinylsilane (TMVS) were purchased from Aldrich. Cp_2TiMe_2 was synthesized from Cp_2TiCl_2 and CH_3Li, as described previously,[6e,f] and was stored in ethyl ether solution (~40.5 mM) under argon at −30 °C. Dichloromethane-d_2 was dried by storage over activated 3A molecular sieves.

Solutions containing $[Cp_2Ti(Me)(CD_2Cl_2)][B(C_6F_5)_4]$ (**I**) for NMR studies were prepared as follows. An aliquot of Cp_2TiMe_2 in ethyl ether (0.7 mL, ~0.03 mmol) was taken from the stock solution, the solvent was removed quickly and the residue was dissolved in 0.5 mL of CD_2Cl_2. To this was added a solution of $[Ph_3C][B(C_6F_5)_4]$ (35-55 mg, ~0.04-0.06 mmol) in 0.6 mL of CD_2Cl_2 in the glove box. The mixture was then syringed into a rubber septum sealed NMR tube, and the NMR tube was taken quickly out of the glove box and immersed within 2 min in a dry ice/acetone bath (195 K). The NMR tube was placed in the pre-cooled (185-205 K) probe of the NMR spectrometer, and a ^1H NMR spectrum was run. The tube was then removed from the probe to the

dry ice/acetone bath, and aliquots of the TMVS (molar ratio **I**:alkene ≈ 1:0.5 to 1:1.1) were added to the cold solution. The tube was shaken vigorously at 195 K to induce mixing and placed back in the probe at 185-215 K, and NMR spectra were obtained at various time intervals and temperatures. Note that although solutions of **I** prepared as above always contained relatively small amounts of $[Cp_2TiMe\{B(C_6F_5)_4\}]$,[6e,f] the latter did not react with TMVS under the experimental conditions used here. NOESY experiments were typically performed with mixing times between 0.2 and 0.6 seconds, while measured t1 relaxation times were typically ranging between 0.1 s and 1 s. In NOESY spectra presented are phased to get the diagonal to be negative and thus, correlations that are of the same colour as the diagonal are also negative (EXSY correlations), and those that are of a different colour than the diagonal are positive (NOE correlations).

Geometry optimizations were carried out with Turbomole[10a,b] using the TZVP basis[10c] and the b-p functional[10d-f] (without RI approximation) in combination with an external optimizer (PQS OPTIMIZE).[10j,k] Vibrational analyses were carried out for all stationary points to confirm their nature (1 imaginary frequency for transition states, none for minima). Final energies were obtained using the TZVPP basis[11a] and a COSMO solvent correction (ε = 9.1, CH_2Cl_2).[11b] These were combined with thermal corrections (enthalpy and entropy, 225 K, 1 bar) from the TZVP vibrational analyses to arrive at the final free energies. To account for the reduced freedom of movement in solution, entropy contributions to the free energies were scaled to 2/3 of their gas-phase values.[11c,d] To evaluate the sensitivity to method and basis sets, separate calculations were carried out (1) following the same procedure but with the b3-lyp[10f-i] functional used throughout and (2) by recalculation at the b-p/TZVP geometries of improved single-point energies using Gaussian,[11e] the M06 functional, the (m)aug-cc-pVTZ basis set,[12,13] and a PCM(dichloromethane) solvent correction. The results of these test calculations did not differ dramatically from the b-p/TZVPP/COSMO//b-p/TZVP results, and therefore only the latter will be discussed in the text.

We found earlier that prediction of NMR parameters works better when using a hybrid functional, and therefore separate optimizations were carried out at the b3-lyp/TZVP level, followed by evaluation of chemical shifts (GIAO method[10m-p]) and scalar coupling constants[10q-t] using Gaussian, a TZVP basis set on Ti and the IGLO-III[11f] basis set on Si, C and H, in combination with the functional B3LYP.[10g,i,l] The counteranion used experimentally, $[B(C_6F_5)_4]^-$, was not included in the calculations because it is not currently feasible to explore the many relative orientations of cation and anion which are possible, and then average the results to obtain chemical shifts. In any case, in a relatively polar solvent like dichloromethane, ion pair association would be expected to be relatively loose and the agreement between observed and calculated chemical shifts is such that the counteranion does not appear to greatly influence the NMR parameters of the cation. For full results of the calculations, see Tables C1-C4 in Appendix C.

4.4 Results and Discussion

4.4.1 NMR evidence for agostic structures

The species obtained in reactions of Cp_2TiMe_2 with a slight excess of $[Ph_3C][B(C_6F_5)_4]$ have been described previously.[6e,f] In addition to Ph_3CMe, the product of methyl carbanion abstraction, mixtures of the solvent separated, ionic $[Cp_2Ti(Me)(CD_2Cl_2)][B(C_6F_5)_4]$ (**I**) and the contact ion pair $[Cp_2TiMe\{B(C_6F_5)_4\}]$ are formed and it is the former which reacts with alkenes. Bright yellow NMR samples were prepared as described in the Experimental Section and were placed in the probe of a 600 MHz NMR spectrometer preset to 205 K. The ^{1}H NMR spectra were found to exhibit resonances of the products: $CMePh_3$ at δ 7.0-7.3 (m), 2.13 (s); **I** at δ 6.72 (Cp), 1.63 (Me); $[Cp_2TiMe\{B(C_6F_5)_4\}]$ at δ 6.33 (Cp), 1.24 (Me). See Appendix C, Figure C1b.

The addition of a sub-stoichiometric amount of TMVS to a mixture of **I** and $[Cp_2TiMe\{B(C_6F_5)_4\}]$ in CD_2Cl_2 at 195 K followed by raising the temperature to 215 K resulted in weakening of the resonances of **I** and the appearance of well resolved resonances at δ 6.07 (s, 10H), 4.41 (m, 1H), 4.30 (m, 1H), 0.21 (s, 9H) and −0.36 (m, 1H) (Appendix C, Figures C1c, C2),

attributable to a new species **III**. The resonances at δ 6.07 and 0.21 are clearly to be attributed to Cp and Me_3Si groups, respectively, the others to single hydrogen atoms on C(1) (α-H_a, α-H_b) and C(2) (β-H); the negative chemical shift suggests that one of them might be agostic.[6e,f] We were surprised not to observe a 3H resonance for the β-methyl group (γ-H) but, on raising the temperature above 205 K, a very broad, 3H resonance began to appear at δ ~–0.7 to ~–0.9; this shifted to lower field and narrowed as the temperature was raised to 250 K. Concurrent with these changes, the resonance at δ –0.36 shifted upfield and, at 270 K, the two resonances had crossed over and the 3H methyl resonance had decoalesced to a doublet (J 6.9 Hz) (Figure 4.2).

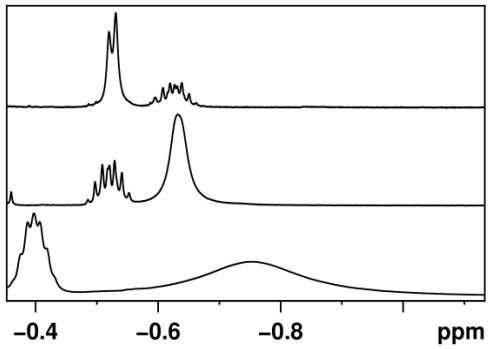

Figure 4.2. Changes in the ^{1}H NMR spectrum of III in the temperature range 225 K (bottom), 250 K (middle) and 270 K (top).

Full consideration of the structural and dynamic exchange implications of a series of 1D and 2D NMR experiments at various temperatures, complemented by DFT calculations, are presented below. One readily concludes that **III** is to be identified as $[Cp_2TiCH_2CHMe(SiMe_3)]^+$, the product of a single 1,2-insertion of TMVS into the Ti-Me bond of **I** (Scheme 4.5).

Scheme 4.5. Formation of III via the reaction of **I** with TMVS.

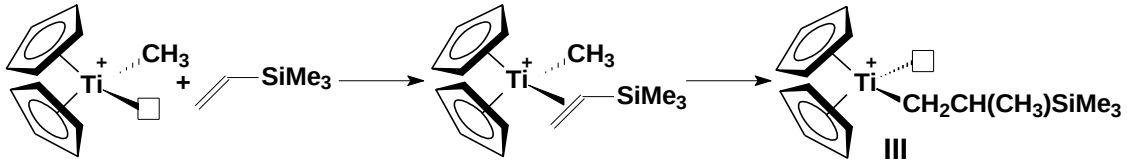

Because C(2) is chiral, the pair of hydrogen atoms on C(1), α-H_a and α-H_b, are diastereotopic, explaining the observation of separate resonances for these hydrogen atoms and hence the presence of three 1H resonances. Correlation spectroscopy (COSY) spectra over a range of temperatures exhibit correlations between the resonances at δ 4.41, 4.30 and −0.36 (Appendix C, Figure C3), and the mutual couplings of 8.7 Hz between the resonances at δ 4.41 and 4.30 confirm assignments of these to α-H_a and α-H_b. Although the very broad β-methyl resonance exhibits no COSY correlations below about 245 K, it does exhibit a correlation (^{3}J 6.9 Hz) at higher temperatures with the resonance at δ −0.49 (Appendix C, Figure C.4), which is attributed to the β-H atom on C(2). The latter resonance also exhibits quite different vicinal couplings to the α-CH resonances at δ 4.41 (7.9 Hz) and 4.30 (12.7 Hz), suggesting that the two vicinal angles of the dominant agostic structure are quite different. Experimental chemical shift and coupling constant data for **III** at 215 K are given in Table 4.1, where they are compared with data calculated for the γ-agostic isomer of **III** (see below and Appendix C, Table C.3).

Table 4.1. Observed and calculated (for γ-agostic structure) NMR data for **III** at 215 K.

Group	^{1}H		^{13}C ($^1J_{CH}$)[a]		Other	
	Exp.	Calc.	Exp.	Calc.	Exp.	Calc.
α-H_a	4.41	4.78	102.9 (150)	107.5 (148.3)	$^2J_{HH}$ 8.9, $^3J_{HH}$ 7.8	$^2J_{HH}$ –9.5, $^3J_{HH}$ 7.3
α-H_b	4.31	4.77	102.9 (147)	107.5 (142.7)	$^2J_{HH}$ 8.9, $^3J_{HH}$ 12.6	$^2J_{HH}$ –9.5, $^3J_{HH}$ 13.1
β-H	–0.36	0.03	–1.8 (133)	7.7 (124.8)	$^3J_{HH}$ 12.6, 7.8, 6.9	$^3J_{HH}$ 13.1, 7.3, 7.0
β-Me	–0.78	–0.94[c]	34 (133)[d]	34.2 (122.6)	$^3J_{HH}$ 6.9	$^3J_{HH}$ 7.0
Me_3Si[b]	0.21	0.42	–2.2 (122)	–0.8		
Cp	6.07	6.23	112.3	124.4		

[a] ^{13}C data from HSQC and Heteronuclear multiple-bond correlation spectroscopy (HMBC) spectra shown in Appendix C, Figures S5-S7. [b] ^{29}Si resonance was observed at δ –22.3 (^{1}H-^{29}Si HMBC; see Appendix C, Figure C8). [c] Calculated individual shifts: δ 2.9, 1.4, –7.2 (see Figure 4.3). [d] ^1J determined at 250 K.

The temperature dependences evident in Figure 4.2 are reflected in the NMR parameters in general. Thus the Cp and Me_3Si resonances shift downfield to δ 6.14 and 0.26, respectively, on raising the temperature to 250 K. The α-CH resonances also shift downfield, albeit at different rates, and overlap significantly at δ ~4.4 at 250 K although there is no change in the α-CH_a-α-CH_b geminal coupling constant. The vicinal coupling of 12.6 Hz between α-H_b and β-H remains essentially unchanged in the temperature range 215-250 K, but that between α-H_a and β-H decreases from 7.8 Hz to 7.4 Hz and that between β-H and the β-Me hydrogens decreases from 6.9 Hz to 6.8 Hz over the same temperature range. In addition, $^1J_{CH}$ for the β-H atom of **III** is 131, 133 and 137 Hz at 205 K, 225 K and 250 K, respectively, but that of $[Cp_2TiCH_2CH(CD_3)(SiMe_3)]^+$ (**III**-d_3; see below) is 128 Hz at 225 K and 130 Hz at 250 K while $^1J_{CH}$ of the methyl resonances of **III** and **III**-d_3 (see below) at 250 K are ~133 Hz and 126 Hz, respectively. These differences are all quite small but several appear to be significant and suggest that the NMR parameters are to be

interpreted as weighted averages of two or more species involved in temperature-dependent equilibria.

Observation of negative chemical shifts for the resonances of the β-H atom and the β-methyl group suggests that these hydrogen atoms experience β- and γ-agostic character, respectively, and the observed variations of chemical shifts as the temperature changes (Figure 4.2) suggest that there is equilibration between β- and γ-agostic structures with *the latter* being unexpectedly[5,6a-c,7] of lower energy as indicated in Scheme 4.6.

Scheme 4.6. Exchange between β- and γ-agostic isomers of **III** via the non-agostic isomer.

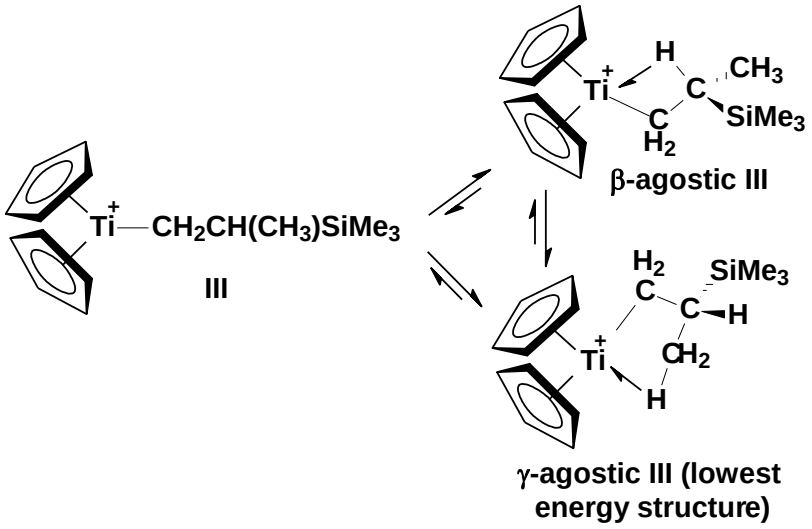

Interestingly, the extreme broadening of the resonance of the three γ-H atoms of the β-methyl group suggests that they are exchanging between non-equivalent positions at intermediate temperatures; presumably one of the methyl hydrogen atoms is γ-agostic at any one time. Consistent with this conclusion, reduction of the temperature below 205 K resulted in decoalescence of the broad methyl resonance shown in Figure 4.2 and, below 180 K, a broad new 1H resonance appeared at δ ~–7.4 (Figure 4.3).

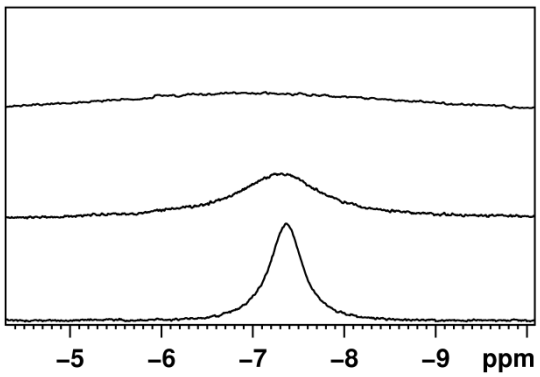

Figure 4.3. ^{1}H NMR spectra of $[Cp_2TiCD_2CDCH_3(SiMe_3)]^+$ (δ −4.5 to −10) at 190 K (top), 181 K (middle) and 172 K (bottom), showing emergence of the resonance of the agostic hydrogen as the temperature decreases.

This resonance exhibited correlations in a NOESY experiment with a partially obscured 1H resonance at δ ~3.0 and a similar but completely obscured resonance at δ ~1.5. These results are consistent with the presence of two diastereotopic, non-agostic methyl hydrogen atoms, with normal chemical shifts, and a γ-agostic hydrogen atom (chemical shift of δ ~–7.4) with a sufficiently strong agostic bond to titanium that methyl rotation is slow on the NMR time scale at this low temperature. Supporting this conclusion, DFT calculations suggest that the chemical shifts of the agostic and the two non-agostic hydrogen atoms are δ –7.2, 2.9 and 1.4, respectively (average δ –0.9; compare with Figure 4.2).

With the calculated chemical shifts of the agostic and non-agostic γ-H atoms in γ-agostic **III** in hand (see above and footnote c of Table 4.1), we calculated also (see Appendix C, Table C3) the chemical shifts of the non-agostic β-H atom in γ-agostic **III** (δ 0.03) and of the agostic β-H atom (δ –4.34) and non-agostic γ-H atoms (average δ 1.76) of β-agostic **III**. Assuming that the intrinsic chemical shifts are temperature independent and that the observed chemical shifts are weighted averages of the two exchanging species in Scheme 4.2, we have utilized the experimental and computed chemical shift data to determine the equilibrium constants for isomerization between the β-agostic **III** and γ-agostic **III** isomers at several temperatures and thence to determine thermodynamic data for the isomerization reaction. From a linear regression of $\Delta G = \Delta H - T\Delta S$

(deduced from equilibrium constants) vs temperature, we find ΔG for the conversion of β-agostic **III** to γ-agostic **III** to be −0.59 kcal/mol at 225 K compared with a calculated value of −1.9 kcal/mol (see below). In addition, ΔH for the β-agostic to γ-agostic conversion is −1.79±0.05 kcal/mol, and ΔS is −5.3±0.5 cal/mol·K, with $R^2 = 0.9924$.

Although agostic β-methyl groups in ethyltitanium complexes have been characterized crystallographically, such compounds are fluxional in solution and only fully coalesced, dynamic NMR spectra have previously been observed.[5m] In contrast, cobalt(III) and palladium(II) complexes of the types $[CpCoL(CH_2CH_3)]^+$ and $[Pd(\alpha\text{-diimine})(CH_2CH_3)]^+$ contain β-methyl groups for which NMR evidence of restricted methyl rotation has been obtained.[5q,r] Cooling solutions of these to ~200 K or ~143 K, respectively, results in decoalesence of the β-methyl resonances to three distinct, single hydrogen atom resonances, one of which exhibits a high field chemical shift and a much reduced value of $^1J_{CH}$, both characteristic of a β-agostic hydrogen atom and similar to the behaviour of **III** although the latter could not be studied at temperatures sufficiently low that $^1J_{CH}$ could be determined.

4.4.2 Additional, unanticipated exchange processes

Consistent with the assignments in Table 4.1, NOESY experiments run at various temperatures (Appendix C, Figures C9-C15) generally exhibited positive NOE correlations between the resonances of α-H_a, α-H_b, β-H and the Cp and $SiMe_3$ groups. Surprisingly, however, the β-methyl resonance exhibited a *negative* correlation with the resonance of the β-H atom, as is clear from Figure 4.4 (inset of Figure C10 of the Appendix C). This result implies an exchange process (quite different from that shown in Scheme 4.2) in which the β-H atom undergoes exchange with the three hydrogen atoms of the β-methyl group (β-H/γ-H exchange) but *not* with the two α-H atoms. At first sight the apparent hydrogen atom exchange might seem to be rationalized on the basis of reversible β-H elimination to give first an alkene hydride species **IV** and thence a symmetric tertiary alkyl isomer **V** (Scheme 4.3).

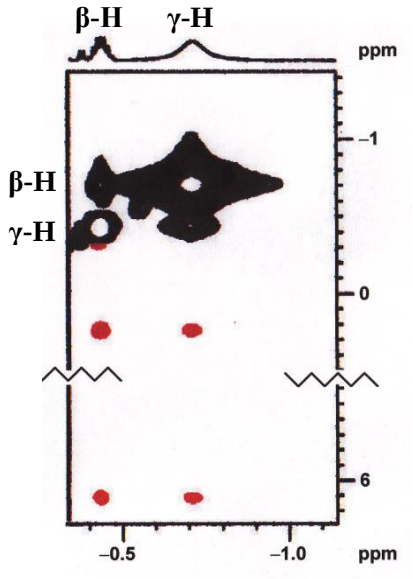

Figure 4.4. Partial NOESY spectrum of **III** at 235 K, showing the negative (black) EXSY correlations between the broad resonances of the β-H and the γ-H atoms at δ –0.43 and –0.71, respectively; NOEs with the relatively narrow $SiMe_3$ and Cp resonances at δ 0.25 and 6.1, respectively, are also apparent (red). For the full spectrum, see Appendix C, Figure C10.

Scheme 4.7. β-Elimination mechanism for exchange between the β-H atom and the hydrogen atoms of the β-methyl group.

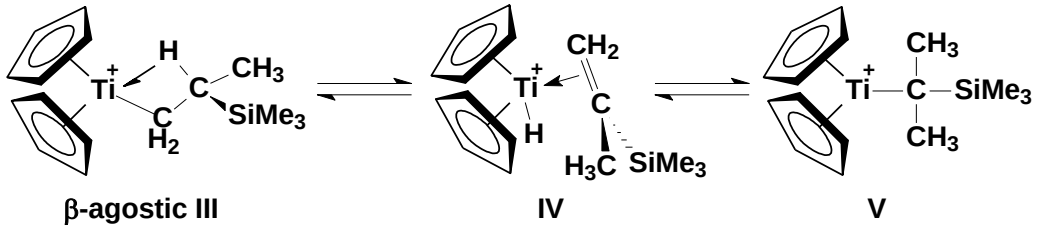

However, since the two α-methyl groups of the intermediate **V** are identical, any of the six β-H atoms could migrate to titanium to regenerate **IV** and, since two of the hydrogen atoms of one of the methyl groups of **V** are derived from the α-CH_2 group, this process would result in exchange of the β-H and β-Me atoms with the α-H atoms also. Since no EXSY correlation involving the α-CH_2 group is observed in the temperature range 215-245 K, the mechanism shown in Scheme 4.7 cannot apply.

An alternative process would involve isomerisation of **III** via CH activation of the $CH_2CHMeSiMe_3$ ligand to give the allylic dihydrogen species **VI** as in Scheme 4.8.

Scheme 4.8. Allylic dihydrogen mechanism for exchange between the β-H atom and the hydrogen atoms of the β-methyl group.

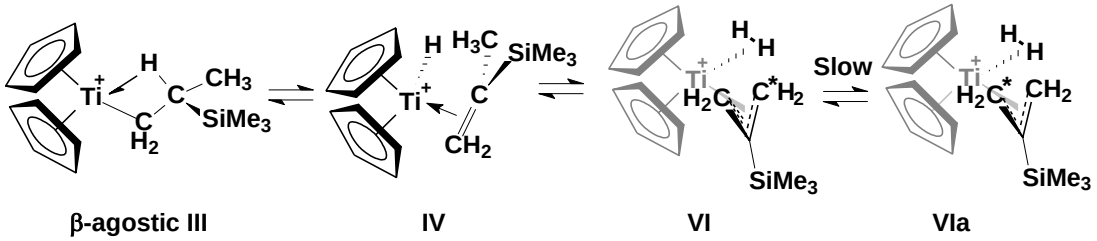

Similar transformations have been hypothesized to occur during metallocene-catalyzed propylene polymerization in order to account for the formation of dormant allylic species and the concomitant formation of H_2 as a by-product,[1b,5j,14] and we note that rotation of the methyl group

of **IV** and of the dihydrogen ligand of **VI** would enable exchange of both of the hydrogen atoms of the latter with the hydrogen atoms of the methylene group proximal to the H_2 ligand (C^*H_2). In contrast, exchange involving the α-CH_2 group of **III** would require reorganization of **VI** to **VIa**, and this may well be a relatively slow process given that the three receptor orbitals of the bent Cp_2Ti(IV) fragment ($1a_1$, b_2, $2a_1$) all lie in the plane perpendicular to the Cp-Ti-Cp plane.[15] Thus the termini of the allyl ligand should remain non-equivalent, as shown, and this would result in exchange involving the hydrogen atoms of the α-CH_2 group being slower, as is observed.

Although the similar complex $[Cp_2TiCH_2CHMe^tBu]^+$ (**II**), which assumes an α-agostic lowest energy structure,[6f] does not appear to exhibit analogous β-H/γ-H exchange at 215 K, we have previously observed exchange at 205 K between the β-H atom, the three γ-H atoms of the β-methyl group, two hydrogen atoms of the α-CH_2 group and the six hydrogen atoms of the two terminal methyl groups of the compound $[Cp_2Ti(CH_2CHMeCH_2CHMe_2)]^+$ (**VII**).[6e]

Scheme 4.9. Structure of $[Cp_2Ti(CH_2CHMeCH_2CHMe_2)]^+$ (**VII**)

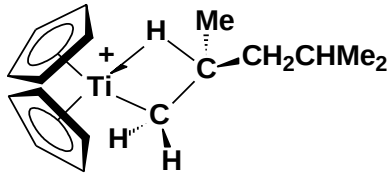

VII

Consistent with the mechanism shown in Scheme 4.8, **VII** also underwent degradation to the corresponding allylic compound $[Cp_2Ti\{\eta^3\text{-}(CH_2)_2CCH_2CHMe_2\}]^+$ and, presumably, H_2 although the latter was not detected. Reversible β-H elimination-reinsertion and allylic dihydrogen mechanisms, analogous to those shown in Schemes 4.7 and 4.8, respectively, were considered for this system also and circumstantial evidence that the latter pertains was obtained although a computational study found in favor of the β-H elimination-reinsertion mechanism of Scheme 4.7.

While exchange of the β-Me and the β-H atoms with the hydrogen atoms of the α-CH_2 group is not apparent in NOESY spectra in the temperature range 215-245 K, close inspection of NOESY

spectra run at 255 K and 260 K (Appendix C, Figures C12, C14) does reveal negative EXSY correlations between the resonance of the β-methyl group and the resonances of the α-CH_2 group, which have converged at this temperature. These observations suggest that relatively slow α-H/β-H exchange does occur at higher temperatures, presumably via species **VIa**. Unfortunately thermal decomposition of **III** above 250 K complicated interpretations of the NMR experiments undertaken.

To further investigate the exchange processes, we therefore conducted an experiment utilizing a deuterated analogue of **I**, $[Cp_2Ti(CD_3)(CD_2Cl_2)][B(C_6F_5)_4]$. On reaction of **I**-$d_3$ with TMVS at 205 K, a ^{1}H NMR spectrum of the reaction mixture exhibited initially the expected Cp, α-CH_a, α-CH_b, β-CH and $SiMe_3$ resonances peaks of **III**-d_3, the relative Cp:α-CH_2:$SiMe_3$:β-CH:β-Me integrations being 10:2:9:1.1:~0. The temperature was raised to and held at 225 K for several hours, and the resonance of the β-Me group was observed to rise out of the baseline, indicating slow, at least partial replacement of deuterium by hydrogen atoms. Furthermore, as the broad resonance of the β-Me resonance grew in, the α-CH_a, α-CH_b and β-CH resonances weakened proportionately while always maintaining essentially identical intensities.

The three resonances also retained their initial multiplet patterns, there being no evidence for the appearance of α-CHD or α-CH_2 doublets attributable to the presence of the isotopomers $[Cp_2TiCHDCH(CHD_2)SiMe_3]^+$ or $[Cp_2TiCH_2CD(CHD_2)SiMe_3]^+$, respectively, in the product. Assuming a normal deuterium isotope upfield shift of ~0.02 ppm,[16] the presence of $[Cp_2TiCHDCH(CHD_2)SiMe_3]^+$ or $[Cp_2TiCH_2CD(CHD_2)SiMe_3]^+$ would have been apparent because of the appearance of new resonances and/or altering of the relative intensities of the components of the three multiplets. The redistribution reaction proceeded more rapidly at higher temperatures, e.g. 245 K, and was readily followed by ^{2}D NMR spectroscopy which confirmed that α-CD_a, α-CD_b and β-CD resonances increased in intensity at essentially equal rates during the reaction.

Interestingly, the Cp resonance of **III**-d_3 at δ 6.10 also weakened and a new Cp resonance at δ 6.05 grew in. The sum of the intensities of the two Cp resonances remained constant at 10H relative to the 9H intensity of the Me_3Si resonance, for which no new resonance could be resolved, and thus the reaction being monitored appears to be that shown in Scheme 4.10 rather than a process involving random replacement of α- or β-H atoms.

Scheme 4.10. Deuterium redistribution in III-d_3.

$$[Cp_2TiCH_2CH(CD_3)SiMe_3]^+ \rightleftharpoons [Cp_2TiCD_2CD(CH_3)SiMe_3]^+$$

The disappearance of $[Cp_2TiCH_2CH(CD_3)(SiMe_3)]^+$ and the apparent appearance of solely the isotopomeric product $[Cp_2TiCD_2CD(CH_3)(SiMe_3)]^+$ were monitored for 7 h at 225 K, and Figure 4.5 shows plots for the decrease with time of the integrated intensities of $[Cp_2TiCH_2CH(CD_3)(SiMe_3)]^+$ (as the average of the intensities of the α-CH_a, α-CH_b and Cp resonances, normalized to the Me_3Si resonance as 9H), and for the concomitant increase with time of the Cp resonance at δ 6.05 of $[Cp_2TiCD_2CD(CH_3)(SiMe_3)]^+$.

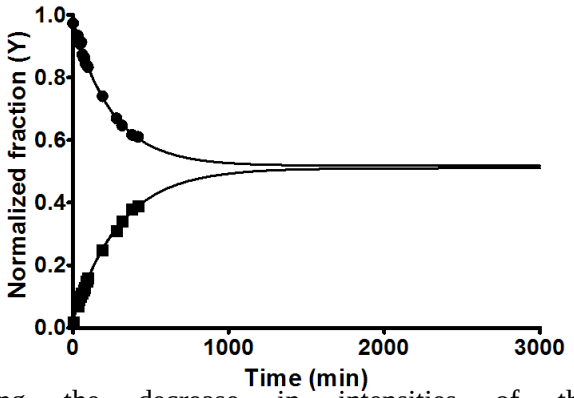

Figure 4.5. Plots showing the decrease in intensities of the resonances of $[Cp_2TiCH_2CH(CD_3)(SiMe_3)]^+$ (upper) and the increase in intensity of the Cp resonance of $[Cp_2TiCD_2CD(CH_3)(SiMe_3)]^+$ (lower) with time at 225 K.

As can be seen, loss of $[Cp_2TiCH_2CH(CD_3)(SiMe_3)]^+$ and growth of $[Cp_2TiCD_2CD(CH_3)(SiMe_3)]^+$ both appear to exhibit exponential behaviour while the isotopic redistribution process clearly had not reached equilibrium within the 7 h over which the reaction

was monitored. The data were therefore, using Prism software,[17a] treated as a reversible, first order process (eq 4.1).[17b]

$$[Cp_2TiCH_2CH(CD_3)(SiMe_3)]^+ \underset{k_{-1}}{\overset{k_1}{\rightleftharpoons}} [Cp_2TiCD_2CD(CH_3)(SiMe_3)]^+ \qquad (4.1)$$

$$Y' = \frac{k_1 e^{-(k_1+k_{-1})(t+a)} + k_{-1}}{k_1+k_{-1}} \qquad (4.2)$$

$$Y'' = k_1 \frac{1-e^{-(k_1+k_{-1})(t+a)}}{k_1+k_{-1}} \qquad (4.3)$$

Here, Y′ and Y″ represent the normalized fractions of $[Cp_2TiCH_2CH(CD_3)(SiMe_3)]^+$ and $[Cp_2TiCD_2CD(CH_3)(SiMe_3)]^+$, respectively, as a function of time, t. From an iterative best fit analysis of the data for the former (eq 4.2), the forward and reverse rate constants, k_1 and k_{-1} were found to be (1.92 ± 0.08) × 10^{-3} min^{-1} and (2.1 ± 0.2) × 10^{-3} min^{-1}, respectively, and hence the equilibrium constant K = (0.93 ± 0.14) (R^2 = 0.995). From a similar analysis of the data for the product (eq 4.3), the forward and reverse rate constants k_1 and k_{-1} were found to be (1.70 ± 0.07) × 10^{-3} min^{-1} and (1.6 ± 0.2) × 10^{-3} min^{-1}, respectively, and hence the equilibrium constant K = (1.04 ± 0.17) (R^2 = 0.9982). Averaging the two values of K, one obtains an equilibrium constant K_{eq} = 0.99 ± 0.15, which does not differ from unity by a statistically significant amount.

In chemical reactions involving equilibration of hydrogen and deuterium atoms among chemically non-equivalent sites, it has been well-established that the heavier isotope accumulates in those positions where the carbon-hydrogen bonds are strongest.[18a-c] This occurs because of reduction in vibrational energy (zero-point energy) when the heavier deuterium atom is substituted for the lighter hydrogen atom at a site with the highest bond stretching force constant. While calculations suggest that **III**-d_3 prefers by 0.14 kcal/mol the isotopomeric structure containing agostic CH_3 rather than agostic CD_3 interactions (see below), which would be consistent with this

argument, the uncertainties in the experimental measurements of Figure 4.5 are such that we cannot conclude therefrom with certainty which γ-agostic structure is preferred.

That said, the subtle but significant differences between the Cp resonances of **III** and its deuterated analogue seem to confirm that conversion from $Cp_2TiCH_2CH(CD_3)(SiMe_3)]^+$ to $[Cp_2TiCD_2CD(CH_3)(SiMe_3)]^+$ (Scheme 4.10) results in a shift of the equilibrium (à la Scheme 4.6) toward the anticipated γ-H agostic isomer. Consistent with this, the temperature variation of the ^1H NMR spectrum of **III**, in which the contribution of the γ-H agostic isomer to the averaged NMR parameters increases and that of the β-H agostic isomer decreases as the temperature decreases, shows that the Cp chemical shift of the γ-H agostic isomer lies at lower field than does the Cp resonance of the β-H agostic isomer (δ 6.07 at 215 K vs 6.14 at 250 K). Furthermore, as noted above, while $^1J_{CH}$ for the β-H atom of **III** is 131, 133 and 137 Hz at 205 K, 225 K and 250 K, respectively, that of $[Cp_2TiCH_2CH(CD_3)(SiMe_3)]^+$ is 128 Hz at 225 K and 130 Hz at 250 K while $^1J_{CH}$ of the methyl resonances of **III** and $[Cp_2TiCD_2CD(CH_3)(SiMe_3)]^+$ at 250 K are ~133 Hz and 126 Hz, respectively.

In the same vein, while deuteration of the β-methyl group results in essentially no change in the α-CH_a and α-CH_b chemical shifts ($\Delta\delta \leq 0.01$ ppm) relative to those of **III**-d_0, the β-H resonance shifts upfield by ~0.07 ppm at 225 K, indicating a greater contribution of the β-agostic isomer to the (averaged) β-H chemical shift. Similarly the β-Me (γ-H) resonance of $[Cp_2TiCD_2CD(CH_3)(SiMe_3)]^+$ at 250 K is shifted upfield by ~0.08 ppm relative to that of **III**-d_0, suggesting an analogous shift to the γ-H agostic structure. Assuming that intrinsic chemical shifts change by –0.01 ppm per vicinal D atom,[16,18a-c] we performed an analysis of the type discussed above for deducing equilibrium constants from comparisons of weighted-average observed with calculated β-H/γ-H chemical shifts. For purely β- and γ-agostic structures of the **III**-d_3 isotopomers at various temperatures, a difference in ΔG value of ~0.12 kcal/mol was obtained for the β- and γ-agostic isomers of $[Cp_2TiCH_2CH(CD_3)(SiMe_3)]^+$ at 225 K,[18d] in excellent agreement with the value

of ~0.14 kcal/mol calculated between the γ-agostic isomers of $[Cp_2TiCH_2CH(CD_3)(SiMe_3)]^+$ and $[Cp_2TiCD_2CD(CH_3)(SiMe_3)]^+$ (see Appendix C, Figure C16). Likewise, the free energy increase in the β-agostic conformation (in $[Cp_2TiCD_2CD(CH_3)(SiMe_3)]^+$) due to β-deuteration is experimentally estimated at ~0.30 kcal/mol compared with a calculated value of ~0.29 kcal/mol (Appendix C, Table C2).

In the case of $[Cp_2TiCD_2CD(CH_3)(SiMe_3)]^+$, in which random exchange between the α-CH_a, the α-CH_b, the β-H and the three γ-D atoms of the β-CD_3 group might seem possible, the deuterium atoms migrate from the methyl group to the other sites. Concurrently, because agostic bonding involving the γ-H atoms becomes more preferred relative to the newly formed β-agostic deuterium atom as the isotope redistribution proceeds, the position of equilibrium of Scheme 4.6 changes such that K becomes larger. Similarly, during the isotopic redistribution shown in Scheme 4.10, the averaged Cp resonance of $[Cp_2TiCH_2CH(CD_3)(SiMe_3)]^+$ (δ 6.10) is replaced by the averaged Cp resonance of $[Cp_2TiCD_2CD(CH_3)(SiMe_3)]^+$ (δ 6.05), consistent with the γ-agostic isomer being more favoured in the latter.

The deuterium rearrangement process, which is significantly slower than either the exchange shown in Scheme 4.6 or the β-H/γ-H exchange, could proceed via either or both of the mechanisms shown in Schemes 4.7 and 4.8. While the process shown in Scheme 4.7 cannot, for reasons discussed above, rationalize the low temperature β-H/γ-H exchange, high temperature NOESY experiments indicate that relatively slow α-H/β-H exchange does occur above ~250 K and, therefore, the process shown in Scheme 4.7 may well be involved in deuterium redistribution. Indeed, it provides a better rationale for the slow, highly selective deuterium redistribution observed, as shown in Scheme 4.11.

Scheme 4.11. Mechanism for selective isotope redistribution.

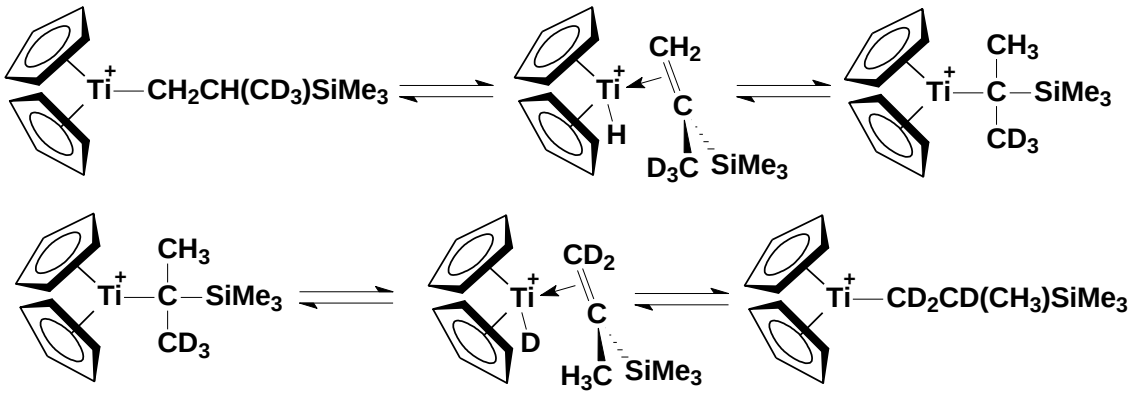

In contrast, the allyl-dihydrogen mechanism of Scheme 4.8 seems less likely to be applicable to the isotope exchange because the presumed intermediacy of the HD-allyl species should result in a relatively random β-H/γ-H redistribution of deuterium isotopes during the higher temperature exchange process (Scheme 4.12).

Scheme 4.12. Mechanism for random isotope H-D redistribution.

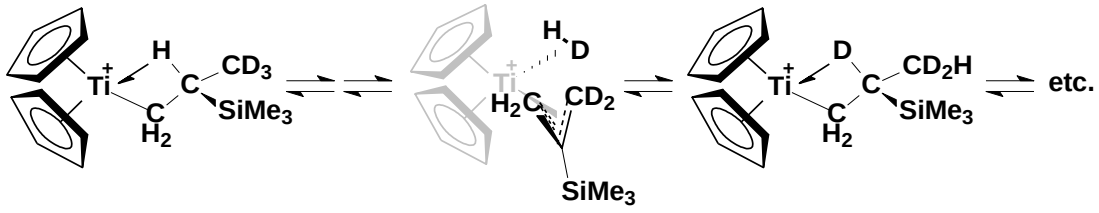

There remains to be rationalized the fact that the low temperature exchange process which involves the β-H atom and the three γ-H atoms of the β-methyl group *but not the α-CH_2 atoms* of **III**-d_0, revealed in EXSY experiments of **III**-d_0, does not give rise to a corresponding process in **III**-d_3 which results in preferential redistribution of deuterium atoms to the β-C site. Instead of relatively rapid deuterium enrichment at the β-CH position, we observe much slower redistribution

of deuterium atoms to all of the α-CH_a, α-CH_b and β-CH sites at comparable rates. In other words, while specific β-H/γ-H exchange is facile, specific β-H/γ-D exchange is not.

This observation seems to imply an unusually large kinetic isotope effect (KIE)[19-22] for the β-H/γ-H exchange process, much larger than the maximum primary KIE expected over the temperature range studied here (KIE 10-15) on the basis of zero-point energy differences and an "over-the-barrier" reaction involving C-H bond cleavage.[19] The KIE may be estimated by noting that the β-H/γ-H exchange happens within the approximate boundaries ~0.63 Hz (from the mixing time in the EXSY experiment) < exchange rate < 6.9 Hz (the $^3J_{H(\beta)-H(\gamma)}$ coupling constant observed at 250 K) in the temperature range 215 K to 260 K, corresponding to a life time of ~1.6 s. In direct contrast, as noted above for the process shown in Scheme 4.10, there was no evidence for the formation of $[Cp_2TiCH_2CD(CHD_2)SiMe_3]^+$ over 7 h (25,200 s) at 225 K, suggesting a KIE of >16000 for β-H/γ-H exchange.

The only reasonable explanation that we see for this observation is a significant contribution of quantum mechanical tunnelling during the exchange process.[19] While the apparent KIE seems very large, the magnitude is not, in fact, without precedent.[19c,d,21a-c] Indeed, for previously studied examples of H(D) abstractions for which the KIEs are sufficiently large that deuterium abstraction does not occur, the term "all-or-nothing" isotope effect has been coined.[19d]

In addition to abnormally large H/D KIEs, tunnelling processes generally result also in reaction rates which are significantly higher than those anticipated on the basis of known (or calculated) thermal barriers; they also exhibit little temperature dependence.[19,21] As will be shown below in connection with Figure 4.7, the barrier to β-H/γ-H exchange is calculated to be ~16.5 kcal/mol which would result in reaction rates varying between 6.5×10^{-5} s^{-1} and 2.0×10^{-2} s^{-1} in the temperature range 215 K to 260 K,[23a] a factor of ~300; this range is significantly higher than the maximum factor of ~12 (6.9/0.63) found here. Furthermore the rate of reaction found here at e.g. 215 K, >0.63 s^{-1}, is far higher than the rate anticipated for a barrier of 16.5 kcal/mol.[23a]

Tunnelling of hydrogen atoms has occasionally been observed in organometallic and related systems,[20] an example being thermal rearrangement reactions of the cluster compounds $M_3(CO)_{10}(\mu\text{-H})(\mu\text{-COH})$ (M = Ru, Os) to the dihydrides $M_3(CO)_{11}H(\mu\text{-H})$. These reactions exhibit very large KIEs which are clearly manifested when the μ-COH ligand is replaced by μ-COD.[20b,c] A lower limit KIE of ~47 was measured for the ruthenium compound but a much larger KIE was clearly operative in the case of the osmium analogue *for which the rearrangement of the deuterated species was shut down completely*, much as is observed here.

In a similar vein, albeit involving a very different type of chemistry, an apparently very large KIE is involved during the dissociative chemisorption of molecular hydrogen on a palladium surface.[20d] Whereas H_2 sorption at low temperatures results in H_2 dissociation and hydrogen atom combination with O atoms to form H_2O, which is desorbed at higher temperatures, D_2 sorption results solely in D_2 desorption at higher temperatures. Thus a KIE, which could not be measured, strongly suppresses D_2 dissociation and results in a significant alteration of the kinetic branching ratio in this system also. *A process involving a deuterated species is again shut down completely.* Thus "all-or-nothing" isotope effects are well established factors in organometallic and hydride chemistry.

Much closer to the chemistry involved in the β-H/γ-H exchange of **III**, quantum mechanical tunnelling is believed to be a major factor during methane σ-bond metathesis reactions with methyl compounds of the type Cp'_2MCH_3 (Cp′ = Cp or substituted Cp; M = Sc, Y, Lu), shown in eq 4.4.[21]

$$Cp'_2MCH_3 + CD_4 \rightarrow Cp'_2MCD_3 + CH_3D \qquad (4.4)$$

A number of mechanisms have been considered, with that shown in Scheme 4.13 having attracted considerable attention and being of probable relevance here.

Scheme 4.13. Mechanism for σ-bond metathesis of methane and d^0/f^o methyl compounds.

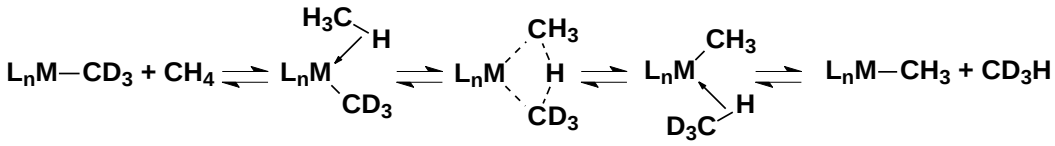

Here a hydrogen moves reversibly from a σ-bonded CH_4 ligand, via a near linear C--H--C transition state (TS), to a -CD_3 group which becomes a σ-bonded CHD_3 ligand. Consideration of the charge distributions involved suggests that the reactions essentially involve proton transfer between pairs of methyl carbanions.[21d]

Tunnelling has not been demonstrated explicitly for these reactions, but was invoked because experimentally determined activation barriers were considerably lower (by up to ~12 kcal/mol) than those predicted on the basis of DFT calculations.[21a-c] In addition, it was noted that the overall process involves considerable hydrogenic motion in the TS and thus may be expected to exhibit considerable light atom tunnelling behaviour. KIEs of up to three orders of magnitude in the temperature range 300-400 K were estimated to account for the discrepancies in calculated and observed rate constants.[21a-c]

4.4.3 Computational Studies of III

Computational studies (DFT) were performed to obtain more insight into the agostic preference(s) of complex **III** and to rationalize the observed exchange processes. Total energies and free energies as well as structural drawings for all species considered are provided in the Appendix C (Tables C1, C2; Figure C17).

The calculations yielded separate local minima corresponding to one γ-agostic, one β-agostic and two α-agostic structures and, in agreement with the experimental results, the γ-agostic structure was found to be lowest in free energy followed by the β-agostic structure (+1.9 kcal/mol) and the two α-agostic structures 3.0 and 4.2 kcal/mol higher than the γ-agostic structure. Transition states

for interconversions between the various agostic species were located, and the network connecting them is summarized in Figure 4.6.

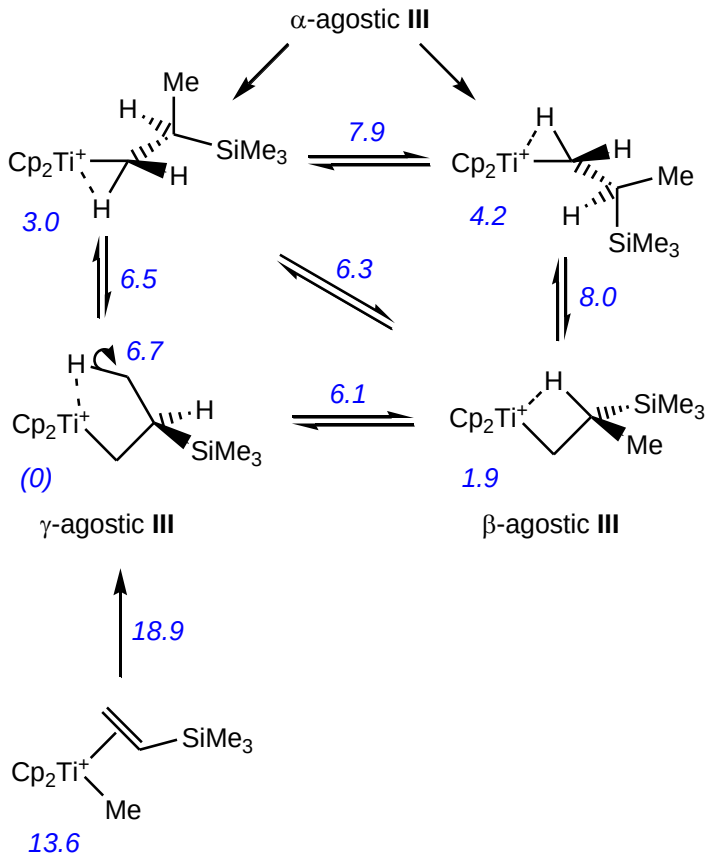

Figure 4.6. Calculated free energies of the agostic structures of III. Free energies (225 K) in kcal/mol; energies at arrows correspond to transition states relative to γ-agostic III at zero.

As can be seen, the methyl alkene intermediate complex of Scheme 4.5 and the barrier to insertion to form γ-agostic **III** lie at +13.6 and +18.9 kcal/mol mol, respectively. Thus migratory insertion and deinsertion have barriers of 5.3 and 18.9 kcal/mol respectively, and the insertion process of Scheme 4.5 is therefore rapid and essentially irreversible once the TMVS complex has formed.

Three different paths were identified for exchange of γ-agostic **III** with its α-agostic and β-agostic analogues: in-place methyl rotation, reversible conversion to the β-agostic structure, and reversible conversion to the more stable of the two α-agostic structures. The calculated barriers for

these three processes are essentially equal, 6.7, 6.1 and 6.5 kcal/mol respectively, and agree well with the barrier for γ-H coalescence estimated from the ^{1}H NMR data (~7 kcal/mol).[23b] The satisfyingly close agreement between calculated and experimental evidence lends credence to the appropriateness of our computational methodology.

The two different conventional hydrogen exchange paths of Schemes 4.7 and 4.8 were studied in detail and are summarized in Figure 4.7 for the all-H system **III** and in Appendix C, Figure C16 for the deuterated system **III**-d_3.

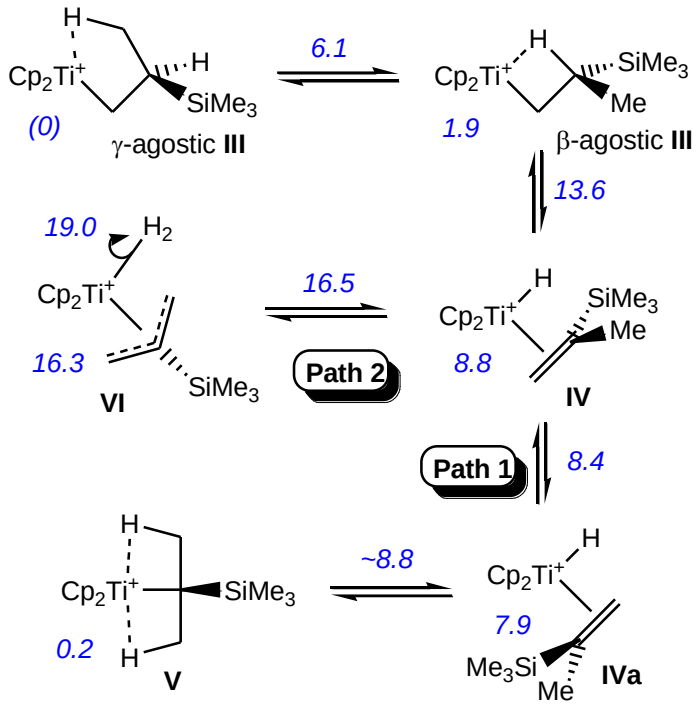

Figure 4.7. Calculated conventional paths for intramolecular hydrogen exchange in $[Cp_2TiCH_2CH(Me)(SiMe_3)]^+$. Free energies (225 K) in kcal/mol; energies at arrows correspond to transition states relative to γ-agostic III at zero.

As is shown, both paths begin with conventional β-hydrogen elimination which involves a transition state (TS) 13.6 kcal/mol above γ-agostic **III**. Path 1 (corresponding to Scheme 4.7), then continues with alkene rotation and reinsertion. These steps appear to be facile and to remain below the level of the original β-elimination TS. The free energy profile for alkene rotation in **IV** to

rotamer **IVa** seems rather flat and we could not locate a well-defined transition state for this step, but the highest point is calculated to be 8.4 kcal/mol above γ-agostic **III**. Rather surprisingly, the resulting tertiary alkyl insertion product **V**, which might be expected to be destabilized because of steric crowding, is in fact strongly stabilized by two β-agostic interactions and lies only 0.2 kcal/mol above γ-agostic **III**. Thus it seems likely that β-elimination of all of the six equivalent methyl hydrogens of **V** should be equally facile and would provide a mechanism for intramolecular hydrogen exchange between the α-, β- and γ-hydrogen atoms.

This path thus appears to provide an energetically feasible path for the observed H/D exchange between $[Cp_2TiCH_2CH(CD_3)(SiMe_3)]^+$ and $[Cp_2TiCD_2CD(CH_3)(SiMe_3)]^+$ (see Figure C16). There are significant isotope effects; for example the conversion of β-agostic **III** to **IV** has a barrier of 13.6 kcal/mol, which becomes 13.7 kcal/mol for its CD_3 deuterated isotopomer and 14.6 kcal/mol for the CD_2CD isotopomer (much as anticipated[20a]). However, these differences of up to 1 kcal/mol would result in a KIE of up to ~5, i.e. far too little to correspond to the dramatic difference in behaviour between **III** and **III**-d_3. We also calculate a slight preference (~0.14 kcal/mol) for the γ-H over γ-D agostic structure, corresponding to a predicted population of 58:42 at equilibrium (225 K). This appears to be reasonably compatible with the results in Scheme 4.11 although, as mentioned above, it implies an equilibrium constant for eq 1 somewhat larger than that suggested by the data in Figure 4.5.

The alternative Path 2 involves the allyl-dihydrogen species of Scheme 4.8 being formed from the same intermediate (hydride)(alkene) complex **IV** as in Path 1. The mechanism shown in Figure 4.7 is the most reasonable conventional path we can think of that would rationalize our observation of β-H/γ-H exchange without the exchange involving also the α-CH atoms. Furthermore, as we have noted above, this type of transformation enjoys substantial precedents.[14]

Indeed, Zhu and Ziegler have studied formation of allyl-dihydrogen complexes from sterically less encumbered alkenes,[14f] finding transition states for β-elimination and allyl formation steps at

respectively ~8-16 kcal/mol and 10-14 kcal/mol above the β-agostic alkyl precursor (compared with our values of 13.6 and 16.5 kcal/mol, respectively). They also found that most allyl-dihydrogen complexes were only ~5-8 kcal/mol above the alkyl precursor but, not surprisingly, that steric hindrance strongly disfavours formation of the allyl-dihydrogen species. In this context, our system appears to fall in the "sterically hindered" category because of the $SiMe_3$ group, with allyl-dihydrogen complex formation endergonic by 16.3 kcal/mol. It follows that the relatively high energy Path 2, involving β-H/γ-H exchange via the allyl-dihydrogen intermediate **VI**, would be preempted by the lower-energy Path 1 involving doubly β-agostic insertion product **V**. The β-H/γ-H exchange should proceed at about the same rate as exchange with the α-CH hydrogen atoms, which is not as indicated by the EXSY results, and exchange involving **III**-d_3 would, subject to any conventional KIEs, result in full deuterium scrambling at a rate comparable to the β-H/γ-H exchange. This also is not observed.

Instead all exchange involving the α-CH hydrogen atoms is relatively slow and, for the conversion of $[Cp_2TiCH_2CH(CD_3)(SiMe_3)]^+$ to $[Cp_2TiCD_2CD(CH_3)(SiMe_3)]^+$ via species **V**, we estimate a barrier of 18 kcal/mol from the first-order rate constant k_1 and the deuterium exchange data of Figure 4.5.[23c] This experimental barrier is significantly higher than the barrier calculated for the conversion of β-agostic **III** to **IV** (13.6 kcal/mol) and suggests a computationally unappreciated impediment to alkene rotation. While it is known that many DFT functionals underestimate barriers for hydrogen transfer reactions,[24a] the difference between calculated and observed barriers might also be due to external factors. For instance, the alkene rotation in **IV** to give **IVa**, a key step in Path 1 of Figure 4.7, involves a significant geometric rearrangement and might well be hindered in solution by ion pair formation with the very bulky $[B(C_6F_5)_4]^-$ counteranion. This factor was not taken into account in the isolated cationic species which we use in our computational model, and we note possible precedents for strong counteranion interactions impacting on internal molecular motions of metallocenium cations.[24b] In contrast, all other steps studied here result in relatively

modest changes in the overall shape of the cation and would hence be much less affected by the close presence of the counteranion.

However if, in reality, alkene rotation in **IV** has for whatever reason a barrier of ~18 kcal/mol and is thus the rate-limiting step for any process involving **V** as an intermediate, then reactions involving the (allyl)(dihydrogen) complex **VI** as an intermediate would be kinetically viable because of the lower barrier (16.5 kcal/mol). Path 2 would then be feasible as providing a mechanism for the observed β-H/γ-H exchange process, although we still have an apparent conundrum because it would remain unclear (a) why the calculated activation energy of ~16.5 kcal/mol above γ-agostic **III** is so much higher than the apparent activation energy for β-H/γ-H exchange determined on the basis of the rate of this reaction at 215 K (~12 kcal/mol; see above) and (b) why this path would not be available for the conversion of $[Cp_2TiCH_2CH(CD_3)(SiMe_3)]^+$ to specifically $[Cp_2TiCD_2CD(CH_3)(SiMe_3)]^+$.

4.4.4 Quantum mechanical proton tunnelling?

In considering a tentative rationale, we have noted above that our experimental results seemingly require a sufficiently large KIE that quantum mechanical tunnelling must be operative at some point during the β-H/γ-H exchange process. In addition, as with the σ-bond metathesis reactions of Scheme 4.13, the experimentally determined activation barrier is significantly lower, by ~9 kcal/mol, than the calculated barrier. This again suggests quantum mechanical tunnelling.

For tunnelling to occur, the reaction coordinate must correspond to mostly hydrogen motion with little heavy-atom movement,[19] as in Scheme 4.13 for methane metathesis. In addition, the thermal barrier to hydrogen transfer must be high but narrow, with width comparable to the de Broglie wavelength of the hydrogen atom (1-2 Å)[19a,b] or, from a different perspective, comparable to the sum of the van der Waals radii[25] of the atoms concerned. The de Broglie wavelength, coupled with the substantial mass differences between the isotopes of hydrogen H and D, leads to sizeable KIE values that greatly facilitate the investigation of tunneling processes. When dealing with

reactions involving proton transfer over such distances, it is almost incumbent on one to consider tunnelling as being involved mechanistically.

The characteristics of reactions involving proton tunnelling have been subjected to very careful scrutiny in connection with a variety of enzymatically catalyzed processes[21e,22] for which H/D tunnelling is frequently characterized by unusually large KIEs. In such cases, proton transfer is considered to involve strongly hydrogen-bonded systems characterized by a double minimum potential with a medium-high barrier, as in Figure 4.8 which illustrates a system involving collinear proton transfer via tunnelling.[21e,26] As we show below, a similar double potential wall probably applies to the β-H/γ-H exchange under consideration here.

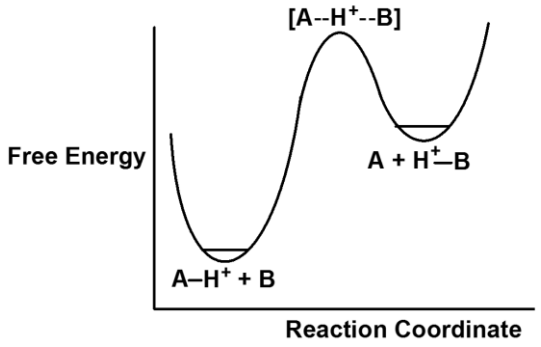

Figure 4.8. A double minimum free energy curve of type proposed for proton exchange in many enzymatic systems (A, B = C, N, O)

Although it was initially not clear to us just where tunnelling might be involved during β-H/γ-H exchange, β-hydrogen elimination/insertion reactions normally exhibit conventional KIEs[20a] and tunnelling is presumably not at play during the conversion of β-agostic **III** to **IV**. It therefore seems likely that the apparently very large KIE reflects tunnelling during exchange of the methyl hydrogen atoms and the hydride ligand of **IV**.

We have therefore investigated more closely the potential energy surface involved as **IV** isomerizes to the allyl dihydrogen species **VI** as in Figure 4.7. The optimized structure of **IV** has a very asymmetric mode of coordination of the alkene to the titanium (Figure 4.9).

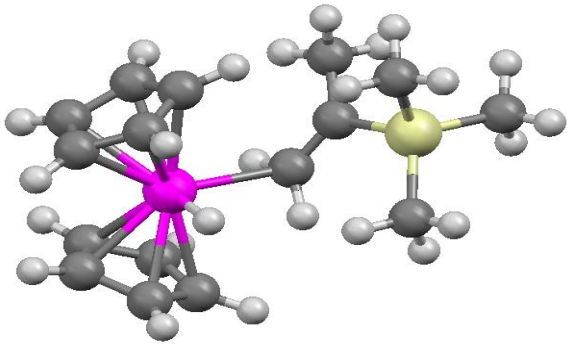

Figure 4.9. Structure of **IV**

The structure of **IV** contains the expected bent Cp-Ti-Cp motif with the Ti-H and Ti-C(1) bonds lying essentially on the plane bisecting the Cp_2Ti group. The hydride ligand lies at ~90° to the C_2 axis of the Cp_2Ti group, the Ti-H distance being 1.683 Å, while C(1) lies a few degrees off the C_2 axis. The Ti-C(1) and Ti-C(2) bond lengths are 2.42 Å and 3.40 Å, respectively, and while there are few relevant structural data available in the literature for comparisons, both are much longer than expected for Ti-C σ bonds and the Ti-C(1) bond length is comparable to Cp-Ti π bond lengths.[27a] The Ti-C(1)-C(2) bond angle is 125.4°, and thus the alkene is coordinated in an extremely asymmetric fashion.

The structure of **IV** is thus very similar to that of $[Cp_2Zr(Me)(DMP)]^+$, shown in Figure 4.1. Both exhibit very asymmetric coordination modes, induced apparently by the presence of two substituents on C(2). Indeed, presumably because of the smaller size of the titanium atom and the larger groups on C(2) of **IV**, the latter compound is more distorted from an η^2 mode of coordination than is $[Cp_2Zr(Me)(DMP)]^+$. Interestingly, since rapid rotation of the R(Me)C= group along the C(1)-C(2) axis and relative to the $=CH_2$ group of $[Cp_2Zr(Me)(DMP)]^+$ is observed,[3] rotation about the C(1)-C(2) bond of **IV** should also be facile. Thus a requisite for β-H/γ-H exchange via tunneling, close mutual approach of the hydride ligand and a γ-hydrogen on the β-methyl group, is seemingly made possible by rotation about the Ti-C(1), C(1)-C(2) and C(2)-Me bonds.

As pointed out above, these structural features are consistent with the fact that 2,2-disubstituted 1-alkenes readily undergo carbocationic rather than coordination insertion polymerization.[4] Indeed, intermediates having the type of near η^1 carbocationic structure shown in Figure 4.1 are believed to be involved as end groups during carbocationic polymerization reactions of 2,2-disubstituted 1-alkenes.[4] The significant degree of positive charge results in the hydrogen atoms of such end groups being strongly acidic[4] as indicated by the fact that that chain transfer during e.g. carbocationic isobutene polymerization occurs via deprotonation of a chain end by the very weakly basic isobutene.[4] Thus, of great relevance here (see below), the β-methyl hydrogen atoms of **IV** should be strongly acidic.

Searching the energy profile linking **IV** and **VI**, we found a shallow local minimum, **VIII**, shown in Figure 4.10 and lying ~2.4 kcal/mol above **IV**.

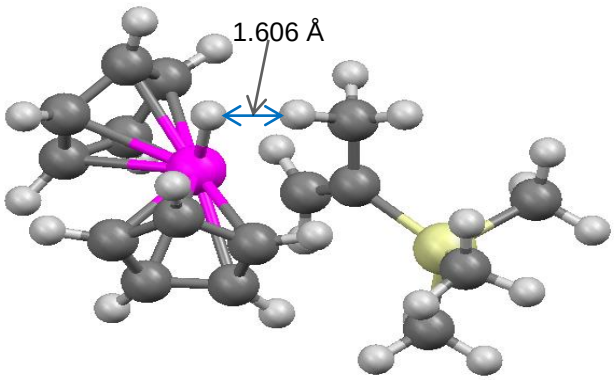

Figure 4.10. Structure of **VIII**.

In **VIII**, the Ti-H bond length is 1.685 Å, essentially unchanged from **IV**, while the Ti-C(1) and Ti-C(2) bond lengths are respectively 2.73 Å and 2.74 Å, marginally longer than the distance between the Ti and the carbon of the β-Me group, 2.73 Å. Thus the three titanium-carbon distances in the incipient η^3-allylic titanium intermediate are nearly identical and, while longer than e.g. the titanium-carbon distances in compounds of the type $Cp_2Ti(\eta^3$-allylic),[27b] they are significantly less than the sum of the van der Waals radii of carbon and titanium (~3.9 Å).[25]

In addition we note the very close approach of a methyl hydrogen atom to the hydride ligand, the resulting H-H distance being 1.606 Å. This is considerably less than the sum of the van der Waals radii of ~2.18-2.40 Å for two hydrogen atoms,[25a] and is probably a result of electrostatic attraction between the acidic γ-hydrogen (see above) and the negatively charged hydride.

This result is certainly consistent with the apparent involvement of quantum mechanical tunnelling during β-H/γ-H exchange and, in addition, the H(hydride)-H-C angle is nearly linear (166.4°). Thus the system seems ideally set up to facilitate proton tunneling of the type discussed above in connection with the exchange of Scheme 4.13 and that observed previously in enzymatically catalyzed processes.[21e,22]

We visualize a σ-bond metathesis-like process in which **VIII** (which appears to be thermally accessible from γ-agostic **III**) and a species similar to **VI** reside in potential wells much as in Figure 4.7, with **VIII** being the lower energy species. Transfer of a methyl hydrogen atom as a proton to the somewhat negatively charged hydride ligand to give a dihydrogen ligand would appear to be feasible and, given the dimensions of **VIII** (Figure 4.10), such a proton transfer must involve tunneling. While the energy calculated for dihydrogen complex **VI** seems too high for it specifically to be capable of significant existence, in fact the lifetime of the putative dihydrogen species need only be sufficiently long that the dihydrogen ligand can assume an η^2 structure in which the two hydrogen atoms are equivalent. Then both would have equal probability of transferring to the "allylic" carbon atom and, given that the methyl group undergoes free rotation, a tunneling route to β-H/γ-H exchange is available.

Finally, we note that return of a proton from a dihydrogen ligand would be facilitated by the fact that dihydrogen ligands in cationic complexes are invariably strongly acidic.[28] Thus β-H/γ-H exchange in **III** is rationalized on the basis of reversible tunneling involving proton exchange between two acidic partners, much as in both methane σ-bond metathesis (Scheme 4.13) and several strongly hydrogen-bonded systems in enzymatically catalyzed processes.[21e,22,26]

4.5 Conclusion

The compound $[Cp_2Ti(Me)(CD_2Cl_2)][B(C_6F_5)_4]$ (**I**) reacts with trimethylvinylsilane (TMVS) to form the 1,2-insertion product $[Cp_2TiCH_2CHMe(SiMe_3)]^+$ (**III**) which undergoes a most unusual array of exchange processes. Variable temperature NMR studies show, for instance, that **III** exists as equilibrating β- and γ-agostic isomers with, surprisingly, the latter preferred by ~0.6-1.9 kcal/mol. In addition, while free rotation of the β-methyl group results in a single averaged γ-H atom resonance at higher temperatures, decoalescence occurs below ~200 K and the resonance of the γ-agostic H atom at δ ~–7.2 can be observed. Free energy barriers to β-agostic/γ-agostic exchange and γ-H exchange (i.e. in-place β-methyl rotation) are both 6-7 kcal/mol. Reaction of $[Cp_2Ti(CD_3)(CD_2Cl_2)]^+$ with TMVS resulted in the formation of $[Cp_2TiCH_2CH(CD_3)(SiMe_3)]^+$ which in turn converts slowly, via a reversible β-hydrogen elimination-reinsertion process, specifically to $[Cp_2TiCD_2CD(CH_3)(SiMe_3)]^+$. No other isotopomers were formed in this process which has a barrier of ~18 kcal/mol.

Finally, and most interesting of all, EXSY studies show that the β-H atom of **III** undergoes facile exchange with the three hydrogen atoms of the β-methyl group (β-H/γ-H exchange) but *not* with the two α-H atoms. This exchange process is therefore very different from that involving deuterium atom redistribution, and must also be associated with a very high kinetic isotope effect (KIE) because it is completely shut down when $[Cp_2TiCH_2CH(CD_3)(SiMe_3)]^+$ is used. A reversible β-hydrogen elimination-reinsertion process does not seem to be involved in the β-H/γ-H exchange, but rather an allylic CH activation process similar to that posited previously to occur during metallocene-catalyzed propylene polymerization in order to account for the formation of dormant allylic species and the concomitant formation of H_2 as a by-product.[1b,5j,14] On the basis of an unusually large kinetic isotope effect and other factors, it is proposed that that quantum mechanical proton tunnelling is involved during the β-H/γ-H exchange and, possibly, during allylic CH activation processes in general.

Complementing the variable temperature NMR studies, DFT calculations were carried out to obtain energies and NMR parameters for all relevant and thence to obtain better insight into the agostic preference(s) of complex **III** and the observed exchange processes. NMR chemical shifts and coupling constants were also calculated and, in all cases where comparisons between experimental and calculated data were possible, agreement was excellent.

The ordering of stabilities of the agostic structures of **III**, observed and calculated, is different from those observed previously for $[Cp_2TiCH_2CHMeCH_2CHMe_2]^+$ and $[Cp_2TiCH_2CH_2Bu^t]^+$ (β-agostic preferred) and **II** (α-agostic preferred).[6e,f] Judging from models, this is mainly a steric effect, a result of decreasing cone angles in the order β-Bu^t > β-$SiMe_3$ >> β-H since, as noted elsewhere, an electronic preference for β-agostic structures generally holds true.[5,6a-c,7] However, a β-agostic structure forces the other two groups at a β-carbon atom to be in close contact with the Cp rings while, in contrast, crowding is a little less severe in the γ-agostic structure, and is lowest in the α-agostic structure of **II** in which the distance between the Cp_2Ti fragment and the substituents is maximized. The extreme crowding in **II** therefore results in the α-agostic structure being preferred, but the smaller cone angle of the Me_3Si group compared with the Me_3C group results in less crowding near the metal center for **III** with the result that this compound prefers the γ-agostic structure by a small margin. Reducing the size of the β-substituents even more leads to the "normal" β-agostic structures observed for $[Cp_2TiCH_2CHMeCH_2CHMe_2]^+$ and $[Cp_2TiCH_2CH_2Bu^t]^+$.

4.6 Acknowledgements

MCB gratefully acknowledges the Natural Science and Engineering Research Council of Canada and Queen's University for funding of this research. PHMB thanks the Natural Science and Engineering Research Council of Canada, the Canada Foundation for Innovation, the Manitoba Research and Innovation Fund and SABIC Petrochemicals Europe for financial support. We thank Dr. Alexei Neverov and Mr. Mark Raycroft for assistance running GraphPad Software Prism, and A.D.-B. thanks Queen's University for a Carrel Graduate Fellowship.

4.7 References

1. For useful reviews see (a) Bochmann, M. *J. Chem. Soc., Dalton Trans*. **1996**, 255. (b) Resconi, L.; Camurati, I.; Sudmeijrt, O. *Topics Catalysis* **1999**. *7*, 145. (c) Coates, G. W. *Chem. Rev*. **2000**, *100*, 1223. (d) Resconi, L. ; Cavallo, L.; Fait, A. ; Piemontesi, F. *Chem. Rev*. **2000**, *100*, 1253. (e) Chen, E. Y.-X. ; Marks, T. J. *Chem. Rev*. **2000**, *100*, 1391. (f) Rappé, A. K. ; Skiff, W. M. ; Casewit, C. J. *Chem. Rev*. **2000**, *100*, 1435. (g) Bochmann, M. *J. Organomet. Chem.* **2004**, *689*, 3982. (h) Fujita, T.; Makio, H. *Comp. Organomet. Chem.* III, chap. 11.20, *Crabtree, R. H.; Mingos, D. M. P. editors*, Elsevier, Amsterdam, 2007. (i) Froese, R. D. J. in Computational Modeling for Homogeneous and Enzymatic Catalysis, editors Morokuma, K.; Musaev, D. G. **2008**, 149. Wiley-VCH, Weinheim, Germany. (j) Busico, V. *Macromol. Chem. Phys.* **2007**, *208*, 26. (k) Wilson, P. A.; Hannant, M. H.; Wright, J. A.; Cannon, R. D.; Bochmann, M. *Macromol. Symp.* **2006**, *236* (Olefin Polymerization), 100. (l) Alt, H. G.; Licht, E. H.; Licht, A. I.; Schneider, K. J. *Coord. Chem. Rev*. **2006**, *250*, 2.

2. (a) Casey, C. P.; Carpenetti, D. W. *Organometallics* **2000**, *19*, 3970. (b) Carpentier, J. F.; Wu, Z.; Lee, C. W.; Strömberg, S.; Christopher, J. N.; Jordan, R. F. *J. Am. Chem. Soc.* **2000**, *122*, 7750, and references therein. (c) Brandow, C. G.; Mendiratta, A.; Bercaw, J. E. *Organometallics* **2001**, *20*, 4253. (d) Casey, C. P.; Carpenetti, D. W.; Sakurai, H.; *Organometallics* **2001**, *20*, 4262. (e) Stoebenau, E. J.; Jordan, R. F. *J. Am. Chem. Soc.* **2006**, *128*, 8162. (f) Stoebenau, E. J.; Jordan, R. F. *J. Am. Chem. Soc*. **2006**, *128*, 8638.

3. (a) Vatamanu, M.; Stojcevic, G.; Baird, M. C. *J. Amer. Chem. Soc*. **2008**, *130*, 454. (b) Sauriol, F.; Wong, E.; Leung, A. M. H.; Elliott Donaghue, I.; Baird, M. C.; Wondimagegn, T.; Ziegler, T. *Angew. Chem., Int. Ed.* **2009**, *48*, 3342.

4. Baird, M. C. *Chem. Rev*. **2000**, *100*, 1471.

5. For reviews of agostic complexes, see (a) Brookhart, M.; Green, M. L. H. *J. Organomet. Chem.* **1983**, *250*, 395. (b) Brookhart, M.; Green, M. L. H.; Wong. L.-L. *Prog. Inorg. Chem.* **1988**, *36*. 1. (c) Grubbs, R. H.; Coates, G. W. *Acc. Chem. Res.* **1996**, *29*, 85. (d) Scherer, W.; McGrady, G. S. *Chem. Eur. J*. **2003**, *9*, 6057. (e) Clot, E.; Eisenstein, O. *Struct. Bonding (Berlin)* **2004**, *113*, 1. (f) Scherer, W.; McGrady, G. S. *Angew. Chem., Internat. Ed.* **2004**, *43*, 1782. (g) Brookhart, M.; Green, M. L. H.; Parkin, G. *Proc. Nat. Acad. Sci*. **2007**, *104*, 6908. (h) Lein, M. *Coord. Chem. Rev.* **2009**, *253*, 625. For computational papers discussing the importance of β-agostic structures during metallocene-induced alkene polymerization, see (i) Lohrenz, J. C. W.; Woo, T. K.; Ziegler, T. *J. Amer. Chem. Soc*. **1995**, *117*, 12793. (j) Jensen, V. R.; Koley, D.; Jagadeesh, M. N.; Thiel, W. *Macromolecules*, **2005**, *38*, 10266. (k) Mitoraj, M. P.; Michalak, A.; Ziegler, T. *Organometallics* **2009**, *28*, 3727. (l) Scherer, W.; Herz, V.; Hauf, C. *Struct. Bonding* **2012**, *146*, 159. (m) Laine, A.; Linnolahti, M.; Pakkanen, T. A.; Severn, J. R.; Kokko E.; Pakkanen, A. *Organometallics* **2010**, *29*, 1541. (n) Laine, A.; Linnolahti, M.; Pakkanen, T. A.; Severn, J. R.; Kokko E.; Pakkanen, A. *Organometallics* **2011**, *30*, 1350. (o) Dawoodi, Z.; Green, M. L. H.; Mtetwa, V.; Prout, K.; Schultz, A. J.; Williams, J. M.; Koetzle, T. F. *J. Chem. Soc., Dalt.* **1986**, 1629. (p) Scherer, W.; Priermeier, T.; Haaland, A.; Volden, H. V.; McGrady, G. S.; Downs, A. J.; Boese, R.; Bläser, D. *Organometallics* **1998**, *17*, 4406. For papers describing specifically late transition metal agostic complexes, see (q) Brookhart, M.; Lincoln, D. M.; Volpe. A. F.; Schmidt, G. F. *Organometallics* **1989**, *8*, 1212. (r) Shultz, L. H.; Brookhart, M. *Organometallics* **2001**, *20*, 3975.

6. (a) Jordan, R. F.; Bradley, P. K.; Baenziger, N. C.; Lapointe, R. E. *J. Am. Chem. Soc.* **1990**, *112*, 1289. (b) Alelyunas,Y. W.; Guo,Z.; Lapointe, R. E.; Jordan, R. F. *Organometallic* **1993**, *12*, 544. (c) Alelyunas, Y. W.; Baenziger, N. C.; Bradley, P. K.; Jordan, R. F. *Organometallics* **1994**, *13*, 148. (d) Guo, Z.; Swenson, D. C.; Jordan, R. F. *Organometallics* **1994**, *13*, 1424. (e) Sauriol, F.; Sonnenberg, J. F.; Chadder, S. J.; Dunlop-Brière, A. F.; Baird, M. C.; Budzelaar, P. H. M. *J. Am. Chem. Soc*. **2010**, *132*, 13357. (f) Dunlop-Brière, A. F.; Baird, M. C.; Budzelaar, P. H. M. *Organometallics*, **2012**, *31*, 1591.

7. A number of computational papers consider the interplay between α- and β-agostic species. See: (a) Nifant'ev, I. E.; Ustynyuk, L. Y.; Laikov, D. N. *Organometallics* **2001**, *20*, 5375. (b) Graf, M.; Angermund, K.; Fink, G.; Thiel, W.; Jensen, V. R. *J. Organomet. Chem.* **2006**, *691*, 4367. (c) Karttunen, V. A.; Linnolahti, M.; Pakkanen, T. A.; Severn, J. R.; Kokko, E.; Maaranen, J.; Pitkänen, P. *Organometallics* **2008**, *27*, 3390.

8. TMVS is polymerized via anionic initiation. See (a) Rickle, G. K. *J. Macromol. Sci.-Chem.* **1986**, *A23*, 1287. (b) Oku, J.-I.; Hasegawa, T.; Takeuchi, T.; Takai, M. *Polymer Journal* **1991**, *23*, 1377. (c) Gan, Y.; Prakash, S.; Olah, G. A.; Weber, W. P.; Hogen-Esch, T. E. *Macromol.* **1996**, *26*, 8285. (d) Rangou, S.; Shishatskiy, S.; Filiz, V.; Abetz, V. *Eur. Poly. J.* **2011**, *47*, 723.

9. For examples, see (a) Peng, T.-S.; Arif, A. M.; Gladysz, J. A. *Helv. Chim. Acta* **1992**, *75*, 442. (b) Lenges, C. P.; White, P. S.; Brookhart, M. *J. Am. Chem. Soc*. **1998**, *120*, 6965. (c) Böhm, V. P. W.; Brookhart, M. *Angew. Chem., Internat. Ed.* **2001**, *40*, 4694. (d) Hapke, M.; Weding, N.; Spannenberg, A. *Organometallics* **2010**, *29*, 4298. (e) Lipponen, S. H.; Seppälä, J. V. *Organometallics* **2011**, *30*, 528.

10. (a) Ahlrichs, R.; Armbruster, M. K.; Bachorz, R. A.; Bär, M.; Baron, H.-P.; Bauernschmitt, R.; Bischoff, F. A.; Böcker, S.; Crawford, N.; Deglmann, P.; Della Sala, F.; Diedenhofen, M.: Ehrig, M.; Eichkorn, K.; Elliott, S.; Friese, D.; Furche, F.; Glöss, A.; Haase, F.; Häser, M.; Hättig, C.; Hellweg, A.; Höfener, S.; Horn, H.; Huber, C.; Huniar, U.; Kattannek, M.; Klopper, W.; Köhn, A.; Kölmel, C.; Kollwitz, M.; May, K.; Nava, P.; Ochsenfeld, C.; Öhm, H.; Pabst, M.; Patzelt, H.; Rappoport, D.; Rubner, O.; Schäfer, A.; Schneider, U.; Sierka, M.; Tew, D. P.; Treutler, O.; Unterreiner, B.; von Arnim, M.; Weigend, F.; Weis, P.; Weiss, H.; Winter, N. *Turbomole* Version 5; Theoretical Chemistry Group, University of Karlsruhe, **2002**. (b) Treutler, O.; Ahlrichs, R. *J. Chem. Phys.* **1995**, *102*, 346. (c) Schäfer, A.; Huber, C.; Ahlrichs, R. *J. Chem. Phys.* **1994**, *100*, 5829. (d) Becke, A. D. *Phys. Rev. A* **1988**, *38*, 3098. (e) Perdew, J. P. *Phys. Rev. B* **1986**, *33*, 8822. (f) All Turbomole calculations were performed with the functionals "b-p" and "b3-lyp" of that package, which are similar (but not identical) to the Gaussian "BP86" and "B3LYP" functionals. (g) Lee, C.; Yang, W.; Parr, R. G. *Phys. Rev. B* **1988**, *37*, 785. (h) Becke, A. D. *J. Chem. Phys.* **1993**, *98*, 1372. (i) Becke, A. D. *J. Chem. Phys.* **1993**, *98*, 5648. (j) *PQS* version 2.4; Parallel Quantum Solutions: Fayetteville, AR, 2001 (the Baker optimizer is available separately from PQS upon request). (k) Baker, J. *J. Comput. Chem.* **1986**, *7*, 385. (l) Stephens, P. J.; Devlin, F. J.; Chabalowski, C. F.; Frisch, M. J. *J. Phys. Chem.* **1994**, *98*, 11623. (m) McWeeny, R. *Phys. Rev.* **1962**, *126*, 1028; (n) Ditchfield, R. *Mol. Phys.* **1974**, *27*, 789; (o) Dodds, J. L.; McWeeny, R.; Sadlej, A. J. *Mol. Phys.* **1980**, *41*, 1419; (p) Wolinski, K.; Hilton, J. F.; Pulay, P. *J. Am. Chem. Soc.* **1990**, *112*, 8251. (q) Helgaker, T.; Watson, M.; Handy, N. C. *J. Chem. Phys.* **2000**, *113*, 9402; (r) Sychrovsky, V.; Grafenstein, J.; Cremer, D. *J. Chem. Phys.* **2000**, *113*, 3530; (s) Barone, V.; Peralta, J. E.; Contreras, R. H.; Snyder, J. P. *J. Phys. Chem. A* **2002**, *106*, 5607; (t) Peralta, J. E.; Contreras, R. H.; Cheeseman, J. R.; Frisch, M. J.; Scuseria, G. E. *Chem. Phys. Lett*. **2003**, *375*, 452.

11. (a) Weigend, F.; Furche, F.; Ahlrichs, R. *J. Chem. Phys.* **2003**, *119*, 12753. (b) Klamt, A.; Schürmann, G. *J. Chem. Soc. Perkin Trans. 2* **1993**, *5*, 799. (c) Tobisch, S.; Ziegler, T. *J. Am. Chem. Soc.* **2004**, *126*, 9059. (d) Raucoules, R.; De Bruin, T.; Raybaud, P.; Adamo, C. *Organometallics* **2009**, *28*, 5358. (e) Gaussian 03, Revision C.02, Frisch, M. J.; Trucks, G. W.; Schlegel, H. B.; Scuseria, G. E.; Robb, M. A.; Cheeseman, J. R.; Montgomery, Jr., J. A.; Vreven, T.; Kudin, K. N.; Burant, J. C.; Millam, J. M.; Iyengar, S. S.; Tomasi, J.; Barone, V.; Mennucci, B.; Cossi, M.; Scalmani, G.; Rega, N.; Petersson, G. A.; Nakatsuji, H.; Hada, M.; Ehara, M.; Toyota, K.; Fukuda, R.; Hasegawa, J.; Ishida, M.; Nakajima, T.; Honda, Y.; Kitao, O.; Nakai, H.; Klene, M.; Li, X.; Knox, J. E.; Hratchian, H. P.; Cross, J. B.; Bakken, V.; Adamo, C.; Jaramillo, J.; Gomperts, R.; Stratmann, R. E.; Yazyev, O.; Austin, A. J.; Cammi, R.; Pomelli, C.; Ochterski, J. W.; Ayala, P. Y.; Morokuma, K.; Voth, G. A.; Salvador, P.; Dannenberg, J. J.; Zakrzewski, V. G.; Dapprich, S.; Daniels, A. D.; Strain, M. C.; Farkas, O.; Malick, D. K.; Rabuck, A. D.; Raghavachari, K.; Foresman, J. B.; Ortiz, J. V.; Cui, Q.; Baboul, A. G.; Clifford, S.; Cioslowski, J.; Stefanov, B. B.; Liu, G.; Liashenko, A.; Piskorz, P.; Komaromi, I.; Martin, R. L.; Fox, D. J.; Keith, T.; Al-Laham, M. A.; Peng, C. Y.; Nanayakkara, A.; Challacombe, M.; Gill, P. M. W.; Johnson, B.; Chen, W.; Wong, M. W.; Gonzalez, C.; and Pople, J. A. Gaussian, Inc., Wallingford C. T. **2004**. (f) Kutzelnigg, W.; Fleischer, U.; Schindler, M. "*The IGLO-Method: Ab Initio Calculation and Interpretation of NMR Chemical Shifts and Magnetic Susceptibilities*", in: Diehl, P.; Flück, E.; Günther, H.; Kosfeld, R.; Seelig, J. (eds) "*NMR basic principles and progress*", Springer-Verlag, Heidelberg, **1990**, vol. *23*.

12. (a) Papajak, E.; Leverentz, H. R.; Zheng, J.; Truhlar, D. G. *J. Chem. Theory Comput.* **2009**, *5*, 1197. (b) Papajak, E.; Truhlar, D. G. *J. Chem. Theory Comput.* **2010**, *6*, 597. (c) Dunning, T. H.; *J. Chem. Phys.* **1989**, *90*, 1007. (d) Kendall, R. A.; Dunning, T. H.; Harrison, R. J. *J. Chem. Phys.* **1992**, *96*, 6796. (e) Woon, D. E.; Dunning, T. H. *J. Chem. Phys. 98*, 1358 (**1993**). (f) Dunning, T. H.; Peterson K. A.; Wilson, A. K. *J. Chem. Phys.* 2001, *114*, 9244. (g) Balabanov N. B.; Peterson K. A. *J. Chem. Phys*, **2005**, *123*, 064107

13. (a) Feller, D. *J. Comp. Chem.* **1996**, *17*, 1571. (b) Schuchardt, K. L.; Didier, B. T.; Elsethagen, T.; Sun, L.; Gurumoorthi, V.; Chase, J.; Li, J.; Windus, T. L. *J. Chem. Inf. Model.*, **2007**, *47*, 1045.

14. (a) Margl, P. M.; Woo, T. K.; Blöchl, P. E.; Ziegler, T. *J. Am. Chem. Soc.* **1998**, *120*, 2174. (b) Margl, P. M.; Woo, T. K.; Ziegler, T. *Organometallics* **1998**, *17*, 4997. (c) Resconi, L. *J. Molec. Catal., A* **1999**, *146*, 167. (d) Longo, P.; Grisi, F.; Guerra, G.; Cavallo, L. *Macromolecules*, **2000**, *33*, 4647. (e) Moscardi, M.; Resconi, L.; Cavallo, L. *Organometallics* **2001**, *20*, 1918. (f) Zhu, C.; Ziegler, T. *Inorg. Chim. Acta* **2003**, *345*, 1. (g) Pilme, J.; Busico, V.; Cossi, M.; Talarico, G. *J. Organomet. Chem.* **2007**, *692*, 4227.

15. (a) Lauher, J. W.; Hoffmann, R. *J. Am. Chem. Soc.* **1976**, *98*, 1729. (b) Albright, T. A.; Burdett, J. K.; Whangbo, M.-H. "Orbital Interactions in Chemistry", Wiley, 1985, p. 393.

16. For relevant reviews on the influence of isotope effects on chemical shifts, see (a) Batiz-Hernandez, H.; Bernheim, R. A. *Prog. NMR Spectrosc.*, **1967**, *3*, 63. (b) Hansen, P. E. *Annual Reports on NMR Spectroscopy* **1983**, *15*, 105.

17. (a) GraphPad Software Prism Version 3.02. The a parameters in each equation are the calculated offsets from the initial starting times of the reactions since each had already started prior to the first acquisition point. The values obtained by iteration are (9.9 ± 3.8) min for Y′

and 15.2 ± 2.9 min for Y″. (b) Espenson, J. H. Chemical Kinetics and Reaction Mechanisms, McGraw Hill, New York, 1981, p. 42. (c) Espenson, J. H. Chemical Kinetics and Reaction Mechanisms, McGraw Hill, New York, 1981, chap. 6.

18. For relevant reviews on the influence of isotope effects on chemical equilibria, see (a) Jameson, C. J. *Isotopes in Physical and Biomedical Science, Vol. 2*, edited by Buncel, E.; Jones, J. R. Elsevier, 1991, p. 1. (b) Jameson, C. J. *Encycl. Nuc Mag. Res.* **1996**, *4*, 2638. (c) Jankowski, S. *Annual Reports on NMR Spectroscopy* **2009**, *68*, 149. (d) Experimental values obtained from linear regressions of $\Delta G = \Delta H - T\Delta S$ (from equilibrium constants) against temperature, where ΔH is the enthalpy difference between γ- and β- agostic conformations (−1.40±0.04 kcal/mol for $[Cp_2TiCH_2CH(CD_3)(SiMe_3)]^+$ and −2.69±0.03 kcal/mol for $[Cp_2TiCD_2CD(CH_3)(SiMe_3)]^+$) and ΔS is the analogous entropy difference (−4.2±0.1 cal/(mol·K) for $[Cp_2TiCH_2CH(CD_3)(SiMe_3)]^+$ and −8.0±0.1 cal/(mol·K) for $[Cp_2TiCD_2CD(CH_3)(SiMe_3)]^+$) with R^2 of 0.9934 and 0.9991 and $\Delta G_{\beta\text{-}\rightarrow\gamma\text{-agostic}}$ at 225 K of −0.46 kcal/mol and −0.89 kcal/mol, respectively). These $\Delta(\Delta G_{\beta\text{-}\rightarrow\gamma\text{-agostic}})$ experimental and calculated values correspond to a change in the $\frac{\beta-\text{agostic}}{\gamma-\text{agostic}}$ contribution ratio by a factor of ~0.39 and of ~0.37 (225 K), respectively, going from $[Cp_2TiCH_2CH(CD_3)(SiMe_3)]^+$ to $[Cp_2TiCD_2CD(CH_3)(SiMe_3)]^+$, consistent with the significant difference observed in their respective Cp chemical shifts. Assuming that the changes in $\Delta G_{\beta\text{-}\rightarrow\gamma\text{-agostic}}$ of **III**-d_3 relative to that of **III**-d_0 originate primarily from the increase in free energy of the D-agostic conformer of question, we obtain a 0.12 kcal/mol experimental increase in free energy of the γ-D-agostic conformation at 225 K, in very close agreement with the computed 0.14 kcal/mol discussed above. Likewise, the free energy increase in the β-agostic conformation due to β-deuteration is experimentally estimated at 0.30 kcal/mol, calculated to be 0.29 kcal/mol (see Appendix C, Table C2).

19. For background theory on KIEs, see (a) Caldin, E. F. *Chem. Rev.* **1969**, 69, *135*. (b) Bell, R. P. *Chem. Soc. Rev.* **1974**, *3*, 513. (c) More O'Ferrall, R. A. *J. Phys. Org. Chem.* **2010**, *23*, 572. For examples of very large KIEs, see (d) Wang, J.-T.; Williams, F. *J. Am. Chem. Soc.* **1972**, 94, 2930. (e) Brunton, G.; Griller, D.; Barclay, L. R. C.; Ingold, K. U. *J. Am. Chem. Soc.* **1976**, *98*, 6803.

20. (a) For a recent, highly relevant and useful review of KIEs in organometallic chemistry, see Gómez-Gallego, M.; Sierra, M. A. *Chem. Rev.* **2011**, *111*, 4857 and references therein. (b) Pribich, D. C.; Rosenberg, E. *Organometallics* **1988**, *7*, 1741. (c) Hash, K. R.; Field, R. J.; Rosenberg, E. *Inorg. Chim. Acta*, **1997**, *259*, 329. (d) Hakanoglu, C.; Hawkins, J. M.; Asthagiri, A.; Weaver, J. F. *J. Phys. Chem. C* **2010**, *114*, 11485.

21. (a) Sherer, E. C.; Cramer, C. J. *Organometallics* **2003**, *22*, 1682. (b) Woodrum, N. L.; Cramer, C. J. *Organometallics* **2006**, *25*, 68. (c) Lewin, J. L.; Woodrum, N. L.; Cramer, C. J. *Organometallics* **2006**, *25*, 5906. (d) Barros, N.; Eisenstein, O.; Maron, L. *Dalton Trans.* **2006**, 3052. For a recent review of computational research on C-H activation by transition metal complexes, see (e) Balcells, D.; Clot, E.; Eisenstein, O. *Chem. Rev.* **2010**, *110*, 749.

22. See, for instance, (a) Mielke, Z.; Sobczyk, L. in "Isotope Effects in Chemistry and Biology", Kohen, A.; Limbach, H.-H., eds., Taylor & Francis, New York, 2006, p. 281. (b) Smedarchina, Z.; Siebrand, W.; Fernández-Ramos, A. in "Isotope Effects in Chemistry and Biology", Kohen, A.; Limbach, H.-H., eds., Taylor & Francis, New York, 2006, p. 521. (c) Kiefer, P. M.; Hynes, J. T. in "Isotope Effects in Chemistry and Biology", Kohen, A.; Limbach, H.-H.,

eds., Taylor & Francis, New York, 2006, p. 549. (d) Siebrand, W.; Smedarchina, Z. in "Isotope Effects in Chemistry and Biology", Kohen, A.; Limbach, H.-H., eds., Taylor & Francis, New York, 2006, p. 725. (e) Limbach, H.-H.; Lopez, J. M.; Kohen, A. *Phil. Trans. R. Soc. B* **2006**, *361*, 1399.

23. (a) Estimated on the basis of the standard expression $k = (k_BT/h)\exp(-\Delta G/RT)$.[22e] (b) Estimated by simulation of an exchange spectrum based on Figures 4.1 and 4.2 and using the expression $k = (k_BT/h)\exp(-\Delta G/RT)$. The error margin is probably ~1 kcal/mol. (c) Estimated by simulations utilizing the data of Figure 4.5 and the expression $k = (k_BT/h)\exp(-\Delta G/RT)$. The error margin is probably ~1 kcal/mol.

24. (a) Talarico, G.; Blok, A. N. J.; Woo, T. K.; Cavallo, L. *Organometallics* 2002, *21*, 4939 and references therein. (b) Busico, V.; Van Axel Castelli, V.; Aprea, P.; Cipullo, R.; Segre, A.; Talarico, G.; Vacatello, M. *J. Am. Chem. Soc.* **2003**, *125*, 5451.

25. (a) Rowland, R. S.; Taylor, R. *J. Phys. Chem.* **1996**, *100*, 7384. (b) Nag, S.; Banerjee, K.; Datta, D. *New J. Chem.* **2007**, *31*, 832. (c) Batsanov, S. S. *J. Molec. Struct.* **2011**, *990*, 63.

26. Kwart, H. *Acc. Chem. Res.* **1982**, *15*, 401.

27. (a) See, for exampole, Thewalt, U.; Woehrle, T. *J. Organomet. Chem.* **1994**, *464*, C17. (b) Chen, J.; Kai, Y.; Kasai, N.; Yasuda, H.; Yamamoto, H.; Nakamura, A. *J. Organomet. Chem.* **1991**, *407*, 191.

28. Kubas, G. J. "Metal Dihydrogen and σ-Bond Complexes", Kluwer Academic, New York, 2001, chap. 9.

Chapter 5

Mechanisms of random, reversible α-H(D), β-H(D) and γ-H(D) exchange in the titanocene(IV) complexes $[Cp_2TiCH_2CH(CH_3)(CMe_3)]^+$ and $[Cp_2TiCH_2CH(CD_3)(CMe_3)]^+$*

5.1 Abstract

*This chapter discusses a re-investigation of **II** to unravel some exchange processes that were not formerly seen in previous studies of **II** at lower temperatures (in chapter 3). EXSY and D-labeling (of β-Me: **II**-CD_3) experiments suggest that **II** undergoes a series of successive β-H elimination, 2,1-mingratory-insertion, β-H elimination and 1,2-migratory-insertion, a process (process A) which resembles chain-end epimerization. Olefin dissociation from $[Cp_2TiH(CH_2=CMeCMe_3)]^+$ is faster than process A and consequently, EXSY correlations are seen intermolecularly between **II** and 2,3,3-TMB, as well as intramolecularly in 2,3,3-TMB (fastest exchange) at 235 K. In **II**-CD_3, this rapid reversible olefin dissociation from the olefin-hydride complex following the slower process A leads to multiple isotopologuous rearrangements in 2,3,3-TMB before it can be re-incorporated in **II**, resulting in ~similar overall rates of deuterium incorporation at all α- and β- sites in **II**-d_x (x = 0-6, statistical distribution with an average x value of 3). The overall deuterium distribution at α-, β- and γ- sites in **II**-d_x tends to near randomness over time due to these numerous isotopologuous rearrangements, with slight preference for H at the α-site (a) that is agostic in the dominant α-agostic isomer, and accumulation of D at the β-site. This is consistent with DFT calculations that suggest the β-agostic conformation is the least favorable between α-a-, α-b-, β- and γ- agostomers of **II**, while the α-a-agostomer the preferred conformation. DFT calculations suggest that the $\Delta G^{\ddagger}$ for 1,2-insertion reaction is higher than that*

* The manuscript presented in chapter 5 will soon be submitted to: Dunlop-Brière, A. F.; Budzelaar, P. H. M.; Baird, M. C. *Organometallics*.

for 2,1-insertion in [$Cp_2TiH(CH_2=CMeCMe_3)$]$^+$, a complex which easily undergoes olefin dissociation.

5.2 Introduction

Coordination polymerization processes generally involve sequences of alkene coordination and migratory insertion steps, the latter being facilitated by α-agostic interactions as in **A** (P = polymeryl) with complementary β-agostic species (**B**) serving as resting states during propagation (Scheme 5.1).[1,2]

Scheme 5.1. α-agostic (A) and β-agostic (B) intermediates thought to be found in d^0 metallocene-catalyzed olefin-polymerization reactions

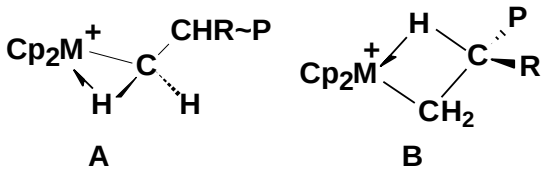

Agostic complexes are well known for late transition metal compounds,[2q,r] and a small number of β-agostic zirconocene complexes of the type $[Cp_2ZrRL]^+$ (R = Et, CH_2CH_2Ph, $CH_2CH_2CMe_3$, CH_2CHMe_2; L = PMe_3 MeCN) are also known.[3a,b,d] Zirconocene(IV) complexes containing α-agostic interactions of type **A** seem to be unknown and titanocene(IV) complexes containing α- or β-agostic complexes of types **A** and **B** have also until very recently[3e,f] not been characterized. Activation energies for migratory insertion processes involving readily polymerized alkenes such as ethylene, propylene and 1-alkenes are sufficiently low that lifetimes of species **A** and **B** are too short for them to be observed.

By way of contrast, we have investigated the reaction of $[Cp_2Ti(Me)(CD_2Cl_2)][B(C_6F_5)_4]$ (**I**) with the sterically hindered alkene, 3,3-dimethyl-1-butene ($CH_2=CHCMe_3$, 3,3-DMB). This alkene seems not to be known to undergo homo-polymerization via a coordination polymerization mechanism,[3f] and it therefore seemed likely that multiple insertion reactions would be difficult and that it might be possible to study normally unstable intermediates such as alkene and/or agostic

complexes. Reaction of **I** with 3,3-DMB proceeded readily in CD_2Cl_2 at 195-205 K and resulted in the formation of a single insertion α-agostic complex, $[Cp_2TiCH_2CHMe(CMe_3)]^+$ (**II**), of type **A**. Interestingly, although the diastereotopic α-CH_2 protons could not undergo mutual exchange, NMR spectral evidence and DFT calculations suggested that they alternated between agostic and non-agostic positions, i.e. that **II** equilibrated between structures **IIa** and **IIb** in a windshield wiper-like fashion (Scheme 5.2). [3f]

Scheme 5.2. Equilibrium between the two α-agostomers of **II.** Determination of which α-H is labeled H_a or H_b is dependent on chirality at C2. For a given chiral configuration (R or S) at C2, H_a is defined here as the α-H which spends the most time in the agostic configuration and H_b is the other proton, which is less agostic than the former.

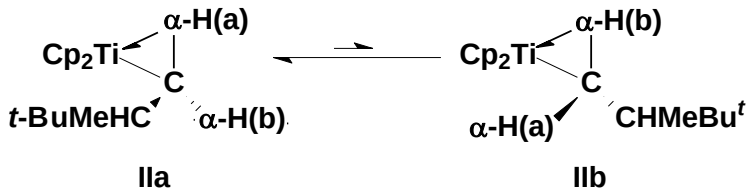

IIa **IIb**

The fact that α-H(a) and α-H(b) exhibited very different chemical shifts and $^1J_{CH}$ coupling constants suggested, moreover, that one of these conformations was strongly preferred.

Aside from its intrinsic novelty, the α-agostic structure observed for **II** is also unusual because most coordinatively unsaturated metal alkyl compounds bearing β-H atoms prefer β- over α-agostic structures.[1a-c,l,4] However, DFT calculations suggested that the β-agostic structure of **II** was significantly destabilized by steric factors arising from the presence of the methyl and *t*-Bu groups on the β-carbon atom.[3f]

Following our investigation of **II**, we carried out an analogous study of the reaction of **I** with trimethylvinylsilane (TMVS), another alkene which seems not to be readily polymerized via coordination polymerization processes.[3g] TMVS was found to undergo migratory-insertion into the Ti-Me bond to give the corresponding $[Cp_2TiCH_2CHMeSiMe_3]^+$ (**III**) which, in contrast to **II**, exists as equilibrating β- and γ-agostic isomers (agostomers) with, surprisingly, the latter being of

lower energy. In addition, while free rotation of the β-methyl group results as expected in a single, averaged γ-H resonance at higher temperatures, decoalescence occurs below ~200 K and the resonance of the γ-agostic hydrogen atom at δ ~–7.2 can be observed. Remarkably, EXSY studies showed that the β-H atom of **III** undergoes facile exchange with the three hydrogen atoms of the β-methyl group (β-H/γ-H exchange), but *not* with the two α-H atoms; on the basis of an unusually large kinetic isotope effect and other factors, it was proposed that quantum mechanical proton tunneling is involved during the β-H/γ-H exchange.

Finally, and most relevant to this paper, the deuterated analogue of **III**, $[Cp_2TiCH_2CH(CD_3)(SiMe_3)]^+$ (**III**-CD_3), was found to convert, via reversible β-elimination steps, to specifically the isotopomeric $[Cp_2TiCD_2CD(CH_3)(SiMe_3)]^+$ with which it was in equilibrium (Scheme 5.3, R = $SiMe_3$). No evidence was observed for CHD-, CHD_2- or CH_2D-containing intermediates or products.

Scheme 5.3. Exchange mechanism for the specific isotopic rearrangement of **III**-CD_3 to $[Cp_2TiCD_2CD(CH_3)(SiMe_3)]^+$

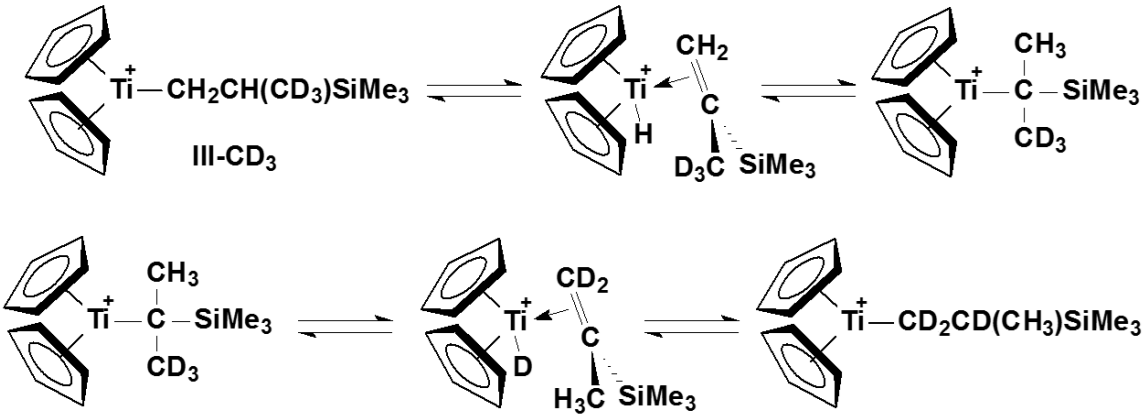

Interestingly, the two isotopomers of **III**-CD_3 exhibited subtle differences in their ^1H NMR spectra which were readily interpreted as indicating differences in the equilibrium constants for the γ-agostic/β-agostic interconversions. To understand this behavior, recall that, for chemical reactions involving equilibration of hydrogen and deuterium atoms

among chemically non-equivalent sites, the heavier isotope accumulates in those positions where the C-H(D) bonds are strongest.[5] In accord with this general phenomenon, computational and experimental evidence for **III** suggested that the isotopomer containing agostic CH_3 is preferred by ~0.1-0.3 kcal/mol over any containing agostic CD linkages. Thus a subtle but significant chemical shift difference of 0.07 ppm at 205 K between the Cp resonances of $[Cp_2TiCH_2CH(CD_3)(SiMe_3)]^+$ and $[Cp_2TiCD_2CD(CH_3)(SiMe_3)]^+$ provided evidence that conversion from $Cp_2TiCH_2CH(CD_3)(SiMe_3)]^+$ to $[Cp_2TiCD_2CD(CH_3)(SiMe_3)]^+$ involved in a shift of the equilibrium toward the γ-H agostomer, resulting in two different sets of NMR parameters for the averaged chemical shifts of each isotopomer.

In addition while deuteration of the β-methyl group resulted in essentially no change in the α-CH(a) and α-CH(b) chemical shifts ($\Delta\delta \leq 0.01$ ppm) relative to those of **III**, the β-H resonance shifted upfield by ~0.07 ppm at 225 K, indicating a greater contribution of the β-agostomer to the (averaged) β-H chemical shift. Similarly the γ-H resonance of $[Cp_2TiCD_2CD(CH_3)(SiMe_3)]^+$ at 250 K was shifted upfield by ~0.08 ppm relative to that of **III**, suggesting an analogous shift to the γ-H agostic structure. Furthermore, while $^1J_{CH}$ for the β-H atom of **III** was found to be 133 and 137 Hz at 225 K and 250 K, respectively, that of $[Cp_2TiCH_2CH(CD_3)(SiMe_3)]^+$ was 128 Hz at 225 K and 130 Hz at 250 K while $^1J_{CH}$ of the methyl resonances of **III** and $[Cp_2TiCD_2CD(CH_3)(SiMe_3)]^+$ at 250 K were ~133 Hz and 126 Hz, respectively. These differences were all attributable to the presence in solution of two sets of isotopomeric species involved in separate, independent equilibria and exhibiting slight but measureable differences in their NMR parameters.

Intrigued by these results, we decided to re-investigate $[Cp_2TiCH_2CH(CH_3)(CMe_3)]^+$ (**II**), assessing possibly undetected exchange phenomena in general and H-D exchange phenomena of $[Cp_2TiCH_2CH(CD_3)(CMe_3)]^+$ (henceforth **II**-CD_3) in particular in order to be able to make comparisons with $[Cp_2TiCH_2CH(CD_3)(SiMe_3)]^+$. To our surprise, the two homologues exhibit very different behaviour.

5.3 Experimental

All syntheses were carried out utilizing an MBraun Labmaster glovebox (under N_2) or standard Schlenk line techniques with argon deoxygenated by passage through a heated column of BASF copper catalyst and then dried by passing through a column of activated 4A molecular sieves. NMR spectra were recorded using a Bruker AV600 spectrometer, ^1H, ^2H, and ^{13}C NMR data being referenced to TMS via the residual proton signals of the solvent. Complex ^1H spectra with overlapping resonances were deconvoluted using sine bell processing, and activation parameters for exchange processes observed in EXSY experiments were obtained using EXSYCalc software and the Eyring equation. $[Ph_3C][B(C_6F_5)_4]$ was purchased from Asahi Glass Company and used as obtained, while CH_3Li, CD_3Li and 3,3-DMB were purchased from Aldrich while TMVS, was purchased from Alfa Aesar. Cp_2TiMe_2 was synthesized from Cp_2TiCl_2 and CH_3Li, as described previously,[3e,f] and was stored in ethyl ether solution (~40.5 mM) under argon at −30 °C. Dichloromethane-d_2 was dried by storage over activated 3A molecular sieves.

Solutions containing $[Cp_2Ti(Me)(CD_2Cl_2)][B(C_6F_5)_4]$ (**I**) for NMR studies were prepared as previously reported.[3g] After a spectrum of **I** was obtained at 205 K, the tube was removed from the probe to the dry ice/acetone bath, and aliquots of 3,3-DMB (molar ratio **I**:alkene ≈ 1:0.5 to 1:1.1) were added to the cold solution. The tube was carefully shaken at 195 K to induce homogeneous mixing and placed back in the probe still at 205 K and the temperature was then varied between ~175 K and ~270 K, and NMR spectra (Table 5.1) were obtained at various time intervals and

temperatures. Note that although solutions of **I** prepared as above always contained relatively small amounts of the contact ion pair $[Cp_2TiMe\{B(C_6F_5)_4\}]$,[3e,f] this did not react with alkenes under the experimental conditions used here.

The deuterium labelled compound **II**-CD_3 was prepared by the reaction of $[Cp_2Ti(CD_3)(CD_2Cl_2)][B(C_6F_5)_4]$ (**I**-CD_3)[3g] with 3,3-DMB. NMR solutions of **II**-CD_3 were prepared as described above for **II**, and typical ^1H NMR spectra are shown in Figure D1 of the Appendix C. Changes in the spectra were monitored at various temperatures and for various periods of time with results shown in Figure 5.1 and Table 5.1, and in the Appendix C, Figures D2-D5. NOESY experiments were typically performed with mixing times between 0.2 and 0.6 seconds, while measured t1 relaxation times were typically ranging between 0.1 s and 1 s. In NOESY spectra presented are phased to get the diagonal to be negative and thus, correlations that are of the same colour as the diagonal are also negative (EXSY correlations), and those that are of a different colour than the diagonal are positive (NOE).

Geometry optimizations were carried out with Turbomole[6a,b] using the TZVP basis[6c] and the b-p functional[6d-f] (without RI approximation) in combination with an external optimizer (PQS OPTIMIZE).[6j,k] Vibrational analyses were carried out for all stationary points to confirm their nature (1 imaginary frequency for transition states, none for minima). Final energies were obtained using the TZVPP basis[7a] and a COSMO solvent correction ($\varepsilon = 9.1$, CH_2Cl_2).[7b] These were combined with thermal corrections (enthalpy and entropy, 225 K, 1 bar) from the TZVP vibrational analyses to arrive at the final free energies. To account for the reduced freedom of movement in solution, entropy contributions to the free energies were scaled to 2/3 of their gas-phase values.[7c,d] To evaluate the sensitivity to method and basis sets, separate calculations were carried out (1) following the same procedure but with the b3-lyp[6f-i] functional used throughout and (2) by

recalculation at the b-p/TZVP geometries of improved single-point energies using Gaussian,[7e] the M06 functional, the (m)aug-cc-pVTZ basis set,[8,9] and a PCM(dichloromethane) solvent correction. The results of these test calculations did not differ dramatically from the b-p/TZVPP/COSMO//b-p/TZVP results, and therefore only the latter will be discussed in the text.

5.4 Results and Discussion

5.4.1 Synthesis and NMR properties of, and H-D exchange processes in II-CD_3.

Compound **II**-CD_3 was synthesized[3f,g] by combining solutions of $[Cp_2Ti(CD_3)(CD_2Cl_2)][B(C_6F_5)_4]$ (**I**-CD_3) with 3,3-DMB at 195 K followed by raising the temperature to 205 K; at this temperature the insertion reaction to give **II**-CD_3 takes ~1-2 h, depending on relative concentrations, to reach completion. The product formed was identified as **II**-CD_3 on the basis of comparisons with ^{1}H NMR data of **II**,[3f] the major difference being, of course, the absence of a β-Me resonance as a result of complete deuteration at this site (see the Appendix D, Figures D1, D2a) . The Cp:α-H(b):β-H:CMe_3:γ-Me:α-H(a) integrated intensity ratios were 10.00:0.98:1.02:9.02:0.02:1.00 for **II**-CD_3. NMR data (^{1}H, ^{13}C) for **II**, **II**-CD_3 and other species discussed in this paper are given in Table 5.1 and NMR spectra are shown in the Appendix D.

Table 5.1. ^{1}H and ^{13}C chemical shifts (δ) (and J-coupling constants expressed in Hz) at 225 K. The designations **a**, **b** and **c** are explained below.

Compound	**II**		**II**-CD_3		**a**		**b**		**c**	
	^{1}H	^{13}C ($^{1}J_{HC}$, Hz)	^{1}H	^{13}C ($^{1}J_{HC}$, Hz)	^{1}H	^{13}C ($^{1}J_{HC}$, Hz)	^{1}H	^{13}C ($^{1}J_{HC}$, Hz)	^{1}H	^{13}C ($^{1}J_{HC}$, Hz)
Cp	6.55	116.9 (178)	6.55	116.8 (180)	6.55	116.8 (180)	6.55	116.8 (180)	6.55	116.8 (180)
α-CH_a	−1.56	145.4 (102)	−1.55 ($^{3}J_{HH}$ 3.3)	145.1 (~106)	−1.57	145.1 (~105)	−1.66	144.8 (~105)	−1.68	144.8 (~103)
α-CH_b	5.94	145.4 (135)	5.94 ($^{3}J_{HH}$ 11.7, $^{2}J_{HH}$ 4.5)	145.1 (135)	~5.94	145.1 (~135)	n/a	n/a	n/a	n/a
β-CH	2.87	57.7 (134)	2.85	57.3 (~132)	~2.85	~57.3 (~132)	~2.85	~57.3 (~132)	~2.85	~57.3 (~132)
β-Me (γ-H)	0.43	16.6 (125)	n/a	n/a	n/a	n/a	n/a	n/a	n/a	n/a
$C(CH_3)_3$	0.76	26.4 (124)	0.76	26.4 (124)	0.76	26.4 (124)	0.76	26.4 (124)	0.76	26.4 (124)

Note that we describe **I**-CD_3 as containing a coordinated solvent molecule bound presumably via a chlorine lone pair; although we have no direct evidence for the presence of this ligand, there is considerable relevant circumstantial evidence.[3e-g] Solutions of $[Cp_2Ti(CH_3)(CD_2Cl_2)][B(C_6F_5)_4]$ (**I**), which we think of structurally as a solvent-separated ion pair,[3e-f] invariably also contain small amounts of the less reactive contact ion pair $[Cp_2Ti(CH_3)\{B(C_6F_5)_4\}]$, in which the $[B(C_6F_5)_4]^-$ is coordinated directly to the titanium.[3e-g] As we have previously pointed out,[3e-g] species of the type $[Cp_2TiR]^+$ (R = alkyl) contain two vacant receptor orbitals lying perpendicular to the Cp-Ti-Cp plane and in the plane containing the methyl ligand. These orbitals are used to form agostic bonds, of course, and are also positioned to interact with Lewis bases.[10] While it is possible that non-agostic alkyltitanocenium isomers of **II** and **III** exist, we have in fact successfully characterized

the *α-agostic* species $[Cp_2Ti(CH_2CHMeCMe_3)L]^+$ (L = Et_2O, MeCl).[3f,h] For sake of simplicity, however, we shall henceforth denote all species of the type $[Cp_2TiR]^+$ as unsolvated cations in the discussions to follow.

Except for the above mentioned lack of a γ-Me resonance in the deuterated compound, the ^1H NMR spectra of freshly prepared solutions of **II** and **II**-CD_3 were essentially identical with chemical shifts of most of the resonances of **II**-CD_3 within 0.01 ppm of those of **II** (Table 5.1), i.e. within experimental error given the natural line widths at the low temperatures used in this investigation ($\Delta\delta \approx 0.01$ ppm). In contrast, the resonance of the β-H of **II**-CD_3 was shifted upfield by 0.02 ppm relative to that of **II**, consistent with a three-bond deuterium isotope effect on a proton chemical shift.[11]

Interestingly, the loss of H-H spin-coupling from the β-Me group on going from **II** to **II**-CD_3 resulted in simplification of the resulting ^1H NMR spectrum. Although the resonances of α-H(a), α-H(b) and the β-H in the ^1H NMR spectrum of freshly prepared solutions of **II** all appeared as multiplets which were too broad for J values to be measured accurately,[3f] the resonances of α-H(b) and the β-H in the spectra of freshly prepared solutions of **II**-CD_3 appeared as near first order doublets of doublets. The geminal and vicinal coupling constants with α-H(a) (4.5 Hz and 3.3 Hz, respectively) could thus be measured directly on the spectrum of **II**-CD_3 at 205 K from the doublets of doublets of the β-H and α-H(b). Also, the vicinal coupling constant between α-H(b) and the β-H was found to be the same in both **II** and **II**-CD_3, 11.8 Hz. The resonance of α-H(a) of **II**-CD_3 remained featureless, but was found to be a triplet with geminal and vicinal coupling constants of ~4 Hz after deconvolution.

The ^1H NMR spectrum of **II** after 48 min at 225 K was very similar to that at 205 K although the chemical shifts were slightly different because of temperature effects. A NOESY experiment run on **II** at 225 K exhibited no negative cross-peaks, and thus there was no indication of intramolecular β-H/γ-H exchange of the type observed previously for **III**.[3g] Note that, as reported

previously,[3f] **II** did begin to undergo slow β-elimination as the temperature was raised to 225 K to give (undetected) $[Cp_2TiH]^+$ (**IV**) and 2,3,3-trimethyl-1-butene (2,3,3-TMB) (δ 4.66, 4.61, 1.71 and 1.00). Weak 2,3,3-TMB resonances had in fact appeared by the time the temperature had reached 225 K in addition to those of $[Cp_2TiCH_2CH_2CMe_3]^+$ (**V**; (δ 6.87, 4.28, 0.99, –0.62), the β-agostic product resulting from an insertion reaction of unreacted 3,3-DMB with the presumed but undetected $[Cp_2TiH]^+$ (**IV**) (Scheme 5.4).[3f] The amount of **V** which formed depended on the extent to which residual 3,3-DMB remained in solution; **V** is stable at 225 K, but slowly decomposes at 235 K. (Note that **IV** almost certainly does not exist as such but rather as the solvate, $[Cp_2TiH(CH_2Cl_2)]^+$, or contact ion pair, $[Cp_2TiH\{B(C_6F_5)_4\}]$, similar to **I**. However, we shall henceforth for simplicity designate **IV** as $[Cp_2TiH]^+$.)

Scheme 5.4. Mechanism of formation of 2,3,3-trimethyl-1-butene (2,3,3-TMB) and $[Cp_2TiCH_2CH_2CMe_3]^+$ (**V**) via the β-elimination product $[Cp_2TiH(CH_2{=}CMeCMe_3)]^+$ (**VI**)

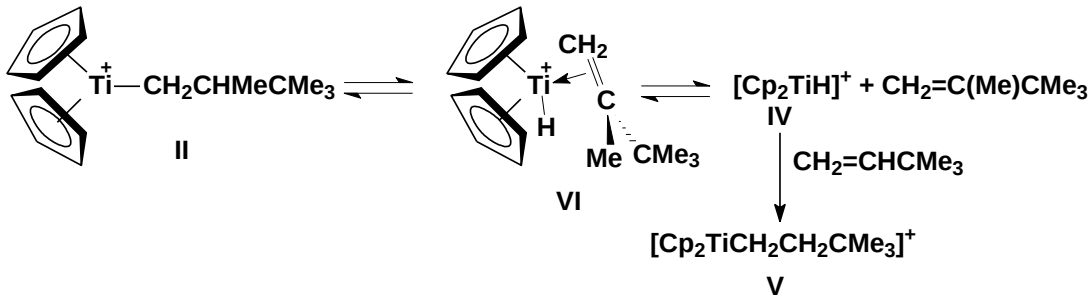

^{1}H NMR spectra of **II**-CD_3 changed little in the temperature range 195-205 K and the relative integrations did not change measurably over 45 min. Thus the compound appeared not to engage in slow H-D exchange processes between the β-CD_3 position and the α-H and β-H positions over this temperature range.

The temperature of a sample of **II**-CD_3 was therefore raised to 225 K, a temperature at which we had previously observed slow, selective H-D exchange in $[Cp_2TiCH_2CH(CD_3)(SiMe_3)]^+$ (**III**-CD_3) to give specifically $[Cp_2TiCD_2CD(CH_3)(SiMe_3)]^+$ (Scheme 5.3).[3g] Several ^{1}H NMR spectra were taken over 30 min, and changes were noted which seemed to indicate that H-D exchange of some kind was now occurring (see Appendix D, Figure D2a). For instance, the intensities of the α-

H(a), α-H(b) and β-H resonances decreased relative to those of the Cp and CMe_3 groups as a resonance of the γ-Me appeared and, after 27 min, the Cp:α-H(b):β-H:CMe_3:γ-Me:α-H(a) integrated intensity ratios had become approximately 10.0: 0.6: 0.8: 9.4: 0.9: 0.5, consistent with essentially random rather than the selective scrambling discussed above.

More importantly, there were pronounced changes in the overall shapes/multiplet patterns of the α-H(a), α-H(b) and β-H resonances and broad, new resonances appeared upfield of all three; the growing β-methyl resonance also evolved not as a doublet but as a variety of complex patterns extending over ~0.1 ppm. These changes are illustrated in detail in Figure 5.1 and in the Appendix D, Figures D2b-D2g; the spectra shown make it very clear that deuterium atoms were transferring from the γ- to both the two α- and the β-positions, conclusions verified by a ^{2}D NMR study which also showed that there was D-transfer from the γ-site to β- and α-H(a) sites although the α-H(b) site was obscured by the resonance of CD_2Cl_2 and could not be monitored.

Before discussing these changes in detail, we should note that the appearance of new ^{1}H resonances ~0.01-0.03 ppm upfield of the ^{1}H resonances of **II**-CD_3 is consistent with normal two- and three-bond deuterium isotope effects[11] and, where observed, can provide evidence for the structures of the deuterated products formed. That said however, as noted above, normal deuterium isotope effects are not the only phenomena which can induce changes of ^{1}H chemical shifts in isotopomers of **II**-CD_3.

In an instance where an agostic interaction can involve a CH or a CD bond, the CH bond is favored for donation to the metal center.[5] A slight increase in free energy (generally <1 kcal/mol) is expected upon deuteration of the agostic position in a given agostomer and, as a result, there is a shift of equilibrium between the agostomers which are significantly populated in favor of those in which the agostic atom is a proton. Thus when agostomeric exchange is rapid on the NMR time scale, as it is with **II**, deuteration of the sites of **II**-CD_3 which are involved in agostic interactions results in a shift in the weighted average of the exchanging species toward agostomers in which the

agostic site is a hydrogen. This can result in abnormal deuterium isotope effects which are different from the normal deuterium isotope effects discussed above and expected for a non-agostic species. This type of phenomenon was observed earlier, when the isotopomers $[Cp_2TiCH_2CH(CD_3)(SiMe_3)]^+$ (**III**-CD_3) and $[Cp_2TiCD_2CD(CH_3)(SiMe_3)]^+$ were found to exhibit different Cp chemical shifts.[3g]

We have previously shown that **II** is involved in rapid exchange between α-H(a) and α-H(b) agostomers (Scheme 5.2), resulting in a weighted averaged ^{1}H NMR spectrum that reflects the relative populations of each agostomeric rotamer at a given temperature.[3f] The calculated energy difference between α-H(a) and α-H(b) agostomers was ~0.8 kcal/mol, corresponding to a ratio of the two of ~6:1, while the calculated energies of the β-agostomer was ~4 kcal above the α-H(a) agostomer.

As shown in Figures 5.1 and D2a-g, a large number of isotopomers and possibly also isotopologues are formed during H-D exchanged in **II**-CD_3. In principle all such species should exhibit different NMR spectral parameters, a hypothesis which seems confirmed by the complexities developing in the spectra of deuterated **II**. We now discuss in turn, utilizing Figures 5.1 and D2b-D2g of the Appendix D, details of the NMR behavior of each site of **II**-CD_3 and its H-D exchange products. The Figures show details of the spectra of the various functional groups at (a) 205 K, (b) immediately after raising the temperature to 225 K and (c) after 27 min at 225 K. More significant changes were sometimes observed when solutions were held at 225 K for longer times or heated above 225 K. These will be discussed when useful, but **II** and **II**-CD_3 decompose slowly at 225 K and above and their resonances both weakened and broadened significantly because of the apparent formation of paramagnetic species.

5.4.2 Evolution and identification of the resonances of α-H(a)

The chemical shift of α-H(a) in the ^{1}H NMR spectrum of **II**-CD_3 is negative because its predominantly α-agostic nature exposes it to the ring current effects of the Cp π system.[3f] The α-

H(a) resonance is therefore well isolated from those of all other species in solution, and the changes it undergoes at 225 K are readily monitored without complications from overlap with other resonances. As H-D exchange between the γ- and α-/β-sites of **II**-CD_3 proceeded at 225 K, a shoulder appeared on the upfield side of the initial resonance of α-H(a) at δ −1.55 and two new resonances appeared at (δ ~−1.67 (see Appendix D, Figures D1, D2a).

An expanded view of these resonances, over a longer period of time (Figure 5.1), shows the shoulder more clearly; when deconvoluted, the resonance appeared as a doublet at δ −1.57 with J ~4.5 Hz, a coupling constant very close to that found above at 205 K for the geminal α-H(a)-α-H(b) coupling constant of **II**-CD_3. Thus it is likely that the shoulder is to be attributed to the β-deuterated species $[Cp_2TiCH_2CD(CD_2H)CMe_3]^+$ (henceforth denoted as **a**) although, as will be shown below, other β-methyl isotologues CH_mD_n (m, n = 0-3; m + n = 3) form as secondary products and would exhibit very similar spectra in the α-H(a) region. The chemical shift difference, ~0.02 ppm, is reasonable for a normal three-bond deuterium isotope effect.[11]

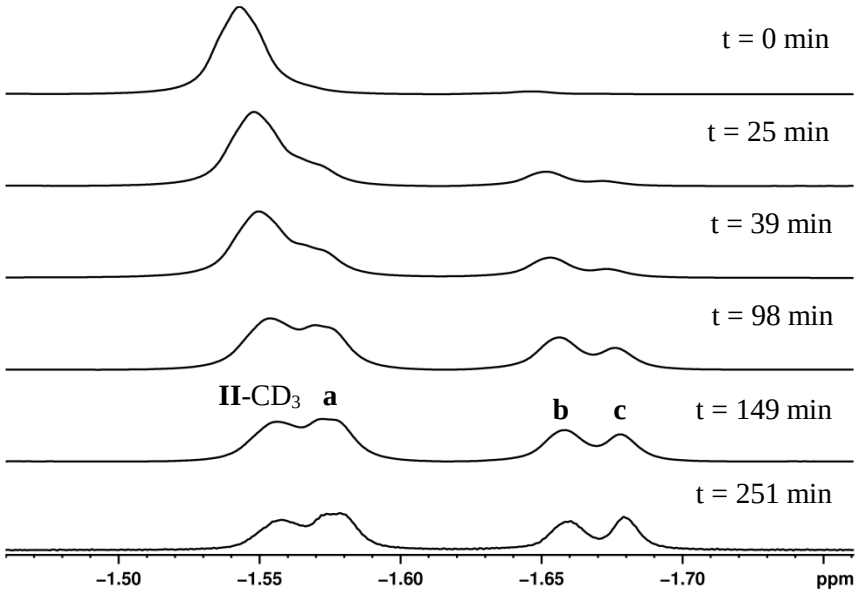

Figure 5.1. Development of the resonance of α-H(a) of **II**-CD_3 at 225 K. Species **a** has been identified above; for the **b** and **c** notations, see below. It is possible that the apparent drift to higher fields with time is to be attributed to the slow growth of paramagnetic species which also cause line broadening.

As can be seen, another resonance slowly appeared even further upfield, at δ −1.66; deconvolution showed it to be a doublet with J ~3.3 Hz. a coupling constant corresponding closely to the vicinal coupling constant of α-Ha with the β-H, identified above at 205 K for **II**-CD_3. The new resonance is therefore reasonably assigned to $[Cp_2Ti\{CH(a)D(b)\}CH(CD_2H)CMe_3]^+$ (henceforth denoted as **b**), in which the (a) and (b) labels indicate (predominantly) agostic and non-agostic positions, respectively. In addition a singlet also appeared at δ −1.68 and is reasonably attributed to α-H(a) in the species $[Cp_2Ti\{CH(a)D(b)\}CD(CH_2D)CMe_3]^+$ (henceforth denoted as **c**) since no H-H coupling could be resolved. As with **a**, species **b** and **c** may coexist with other β-methyl isotologues CH_mD_n ($m \geq 0$, $n \geq 0$ and $m + n = 3$) which would exhibit indistinguishable spectral parameters in this region of the NMR spectrum.

Notable is the fact that the new resonances at δ −1.66 and δ −1.68 lie 0.1-0.125 ppm upfield from the initial resonance, too far for their chemical shifts to be rationalized on the basis of normal deuterium isotope effects.[11] They must instead reflect equilibrium shift-induced abnormal deuterium isotope effects, consistent with identification of the two species as containing α-H(a)D(b) functionality. These observations suggest that deuteration of presumably the α-H(b) site induces a shift in equilibrium toward the α-H(a) agostomer which results in equilibrium shift-induced abnormal deuterium isotope effects in the averaged NMR spectra. Effects from deuteration of the β-H site are also possible but should be less important because of the low population of the β-agostomer.

Complementing Figure 5.1, the results of a NOESY experiment on a different NMR sample after the reaction had proceeded for 178 min at 225 K are shown in Appendix D, Figures D3a, D3b and D3d. After 178 min, all four α-H(a) resonances of Figure 5.1 appeared clearly as somewhat broadened singlets with those of **II**-CD_3 and **a** being of comparable intensity while those attributed to **b** and **c** were somewhat weaker but also of comparable intensities. As is apparent from the Appendix D, Figures D3a, D3b, all four α-H(a) resonances correlate to the Cp and the CMe_3

resonances, demonstrating as indicated above that all four are to attributed to **II**-type species and not to e.g. products of decomposition. Consistent with the assignments of **a** and **c** to species deuterated at the β-site, only the resonances of **II**-CD_3 and **b** were correlated to that of the β-H at δ 2.85. In addition, and consistent with **b** and **c** being species in which the α-(b) site is deuterated, only the resonances of **II**-CD_3 and **a** are correlated to that of α-H(b).

Interestingly, and as noted above in connection with **III**-CD_3 and its isotopomer $[Cp_2TiCD_2CD(CH_3)(SiMe_3)]^+$, the NOESY spectrum in Figure D3d of the Appendix D shows clearly the presence of two Cp resonances. The new resonance, downfield of the resonance of **III**-CD_3, is quite likely an indication of an abnormal deuterium isotope effect and is observed also in Figures D2f, D3d, D3e, D3f and D4g of the Appendix D.

An HSQC experiment was run in part to obtain carbon chemical shifts, which are reported in Table 5.1, in part to complement the NOESY experiments. The HSQC spectrum shown in the Appendix D, Figure D4a (inset in Figure D4b) shows that the α-H(a) resonances of **II**-CD_3 and **a** correlate with an α-carbon atom with a chemical shift of δ 145.1 while the α-H(a) resonances of **b** and **c** correlate with an α-carbon atom having a chemical shift of δ 144.8. The upfield shift of 0.3 ppm in the spectra of **b** and **c** relative to those of **II**-CD_3 and **a** is typical of a normal one bond deuterium isotope effect[11] while the lack of a three bond deuterium isotope effect in the spectra of **II**-CD_3 and **a** is also as anticipated for deuteration of the β-site.[11] As is observed, β-deuteration has little effect on the chemical shift of C(1) while deuteration at the non-agostic α-H(b) site results in a normal deuterium isotope effect on the chemical shift of C(1) (from δ 145.1 to δ 144.8).[11]

In addition to the above points, we note that the combined integrated intensity of the four resonances decreased smoothly over ~2 h with loss of nearly 50% of the initial intensity, relative to the Cp and CMe_3 groups, of the α-H(a) resonance of **II**-CD_3. Table D1 of Appendix D gives normalized percentage totals of the hydrogen atoms at each of the α-, β- and γ-positions, and Figures D6a-D6d of Appendix D illustrate evolution of the intensities of the four resonances.

5.4.3 Evolution and identification of the resonances of α-H(b)

The resonance of α-H(b) was observed at δ 5.96 at 205 K and is a multiplet in the NMR spectrum of **II**, a doublet of doublets with geminal and vicinal coupling constants of 4.5 Hz and 11.8 Hz, respectively, in the spectrum of **II**-CD_3 (see Appendix D, Figure D2c). On warming an NMR sample of **II**-CD_3 to 225 K, the resonance of α-H(b) now appeared at δ 5.94 and an additional new doublet at δ 5.78 (J ~11.8 Hz) was apparent in the first spectrum run. The new resonance increased in intensity over 4 h while becoming asymmetric, and deconvolution of this resonance in a spectrum run at 235 K revealed overlapping singlet and doublet resonances at δ ~5.78 (~5.75 at 235 K) as well as a change in multiplicity aspect of the resonance at δ ~5.94 (~5.92 at 235 K); the peaks are broad but their aspect is roughly compatible with the expected pattern for a doublet (~4.5 Hz, for species **a**) in overlap with the initial doublet of doublet (4.5 Hz and 11.8 Hz) of **II**-CD_3.

These observations paralleled to some extent those observed with α-H(a), discussed above. Thus the difference in chemical shift, ≤ ~0.02 ppm, between the α-H(b) resonances of **II**-CD_3 and **a** at δ ~5.94 corresponds to a normal three-bond deuterium isotope effect.[11] The species formed initially thus appears to be the β-deuterated species $[Cp_2TiCH_2CD(CH_2D)CMe_3]^+$, designated above as **a** following recognition of its α-H(a) resonance. To higher field, overlapping resonances at δ ~5.78, with apparently abnormal deuterium isotope effects of ~0.16 ppm, are reasonably attributed, by analogy with our conclusions for α-H(a) (see above), to species such as $[Cp_2Ti\{CD(a)H(b)\}CH(CD_2H)CMe_3]^+$ (henceforth **d**) and $[Cp_2Ti\{CD(a)H(b)\}CD(CH_2D)CMe_3]^+$ (henceforth **e**) plus other β-Me isotopologues. The fact that the relative intensities of components of the multiplet at δ ~5.78 changed drastically with time confirmed that more than one resonance was present and that the relative amounts of the species in solution were changing. As observed in the Appendix D, Figures D4a, D4c, deuteration of α-H(a) has a drastic effect on the chemical shift of C(1), shifting it upfield by ~2.0 ppm while vicinal deuteration has very little effect.

The ~11.8 Hz coupling constant corresponds to the above mentioned 11.8 Hz vicinal coupling constant measured for α-H(b) at 205 K. The NOESY spectrum mentioned above (see Appendix D, Figures D3a-c) exhibited correlations of the resonances at δ 5.94 and the new resonances at δ 5.78 with the Cp, CMe_3 and γ-Me resonances, but while the downfield α-H(b) resonances correlated with that of α-H(a), the resonances at δ 5.78 did not. Thus the overlapping doublet and singlet at δ 5.78 are readily attributed to D-agostic species of the type **d** and **e**, respectively (see above).

Another informative aspect of the NOESY inset presented in Appendix D, Figures D3c D3e, is the lack of significant NOE correlation between α-H(b) and the β-H resonances relative to that between α-H(a) and the β-H, a pattern noticed also in the d_0 system. Similarly no NOE is observed between the α-H(a) to γ-Me resonances for either **II** or **II**-CD_3 although an NOE is observed between α-H(b) and γ-Me resonances, it seems clear that the dominant conformation of **II** is that in which α-H(a) is anti to γ-Me and α-H(b) is anti to β-H. Two different NOE correlations of α-H(b) are observed in Figure D3e, consistent with the presence of an equilibrium between different agostomers resulting in different averaged chemical environment for the Cp groups. The difference between these two Cp resonances is 0.007 ppm.

As with the four α-H(a) resonances, the combined integrated intensity of the for α-H(b) resonances decreased smoothly over ~2 h, with loss of ~50 % of the initial intensity of the α-H(b) resonance of **II**-CD_3. See Table D1 of Appendix D for normalized percentage totals of the hydrogen atoms at each of the α-, β- and γ-positions, and Figures D6a-D6d of Appendix D for evolution of the intensities of the four resonances.

5.4.4 Evolution and identification of the resonances of the β-, γ-H and Cp sites

As shown in Appendix D, Figures D2a, D2d, the β-H resonance of **II**-CD_3 at δ 2.85 broadened somewhat and a new resonance appeared at higher field. No useful information could be gleaned from the change(s), which are presumably a result of both three-bond normal and equilibrium shift-

induced abnormal deuterium isotope effects. The NOESY spectrum shown in Appendix D, Figure D3f, shows clearly the presence of two Cp resonances, as discussed above, while a corresponding HSQC experiment indicates the presence of two different ^{13}C resonances at δ ~57.3 (see Appendix D, Figure D4d). Thus deuteration at α-H(a) results in a significant effect on the resonance of β-H and its ^{13}C resonance.

The pattern of emerging ^{1}H resonances of the γ-H (β-Me) group in the region δ 0.37-0.45 was extremely complex (see Appendix D, Figures D2a, D2e, D3g, D4e) and the spectra were not analyzed although they presumably contained resonances of CHD_2, CH_2D and CH_3 groups, some possibly experiencing shift-induced abnormal deuterium isotope effects. The rate of growth of the resonances of the γ-H site appeared to be comparable to the rates of diminution of those of the α-H(a) and α-H(b) sites, levelling off after 2-3 h. We note here that our finding that deuterium isotope effects were not observed when the β-Me group of **II** was deuterated to give **II**-CD_3 provides circumstantial support for our earlier conclusion[3f] that significant participation of a γ-agostomer does not occur with **II**, in contrast to the case for **III**.[3g] See Table D1 of Appendix D for normalized percentage totals of the hydrogen atoms at each of the α-, β- and γ-positions, and Figures D6a-D6d of Appendix D for evolution of the intensities of the four resonances.

5.4.5 Addenda concerning the isotopomers/isotopologues of partially deuterated II

A completely statistical redistribution of the hydrogen and deuterium atoms of **II**-CD_3 would, of course, result in diminution of each of the α-H(a), α-H(b) and β-H sites by ~50% although one anticipates a preference of hydrogen atoms for the agostic α-H(a) site at equilibrium.[5] Indeed, the total intensity of the four α-H(a) resonances at equilibrium does appear to be somewhat greater than 50 % of the initial α-H(a) intensity, unlike the resonances of the α-H(b) and β-H sites which both appear to be less than 50 % of original.

Table D1 in Appendix D presents normalized percentage totals of the hydrogen atoms at each of the α-, β- and γ-positions during evolution of the intensities of the four resonances, while Figures

D6a-D6d present the information graphically. The data clearly depict very complex processes, some of which may not have reached equilibrium and also undoubtedly involve significant kinetic isotope effects; we therefore hesitate to infer significant mechanistic conclusions. However, utilizing the Eyring equation one can estimate very approximate values of $\Delta G^{\ddagger}$ of ~16.6 kcal/mol for the overall H-D exchange processes; this information will be discussed below.

Interestingly, the methylene resonances of **V** at δ 4.28 and –0.61 exhibited no evidence of deuterium incorporation (see Appendix D, Figures D2a, D2b and D2g).

Evolution and identification of 2,3,3-TMB deuterated species

As mentioned above, slow thermal decomposition of **II** at 225 K resulted in β-elimination and release of 2,3,3-trimethyl-1-butene (2,3,3-TMB), as indicated by the appearance of vinyl resonances at δ 4.67 and 4.61 (doublets, $^2J_{HH}$ 2.1 Hz) and a 2-methyl resonance at δ 1.71 (see Appendix D, Figure D2a); the *t*-Bu resonance at δ 1.00 was obscured. The by-product of 2,3,3-TMB formation would be the undetected hydride $[Cp_2TiH]^+$ **IV** and, as described above, this apparently reacted rapidly with any residual 3,3-dimethyl-1-butene (3,3-DMB) to form the known β-agostic complex **V**.[3f] The resonances of **V** were observed at δ 6.87 (s, Cp), 4.12 (tr, α-CH_2), 0.99 (s, *t*-Bu) and –0.62 (t, β-CH_2) (see Appendix D, Figure D2a).

Analogous experiments with **II**-CD_3 resulted in the formation not specifically of 2,3,3-TMB-CD_3, but rather of 2,3,3-TMB partially deuterated in both vinyl sites and also in the 2-methyl position (see Appendix D, Figures D2a, g). Indeed, the first spectrum run when the temperature of an NMR sample of **II**-CD_3 was raised from 205 K to 225 K revealed weak resonances growing upfield of the vinyl resonances (δ 4.67, 4.61), which exhibited chemical shifts identical to those of undeuterated 2,3,3-TMB. The new resonances were both 0.014 ppm upfield of the original resonances, consistent with the normal two-bond deuterium isotope effect expected for the two geometric isomers of $CHD=C(CH_mD_n)(CMe_3)$. NOESY and HSQC experiments were consistent with these assignments, the HSQC spectrum (see Appendix D, Figure D4h) indicating that three

species were present, CH_2=CC(H_mD_n)CMe_3 (δ 106.5), CHaDb=CC(H/D)$_3CMe_3$ (δ ~106.2) and CHbDa=CC(H_mD_n)CMe_3 (δ ~106.2); the observed normal deuterium isotope effects on the ^{13}C resonances are ~0.3 ppm.

On warming the NMR sample to 225 K and monitoring it for 27 min, a weak resonance at δ 1.71 present at 205 K, attributable to the 2-CH_3 group of 2,3,3-TMB-d_z (z = 0, 1, or 2), increased in intensity as resonances at δ 1.69 and 1.67 also increased in intensity (see Appendix D, Figure D2h). The chemical shift differences between the two pairs of resonances are both ~0.02 ppm, consistent with the effects of normal two-bond deuterium isotope effects. Thus we assign the three resonances to compounds containing CH_3, CDH_2 and CHD_2 groups, respectively. Confirming these assignments, the central resonance was a 1:1:1 triplet ($^2J_{HD}$ 2.1 Hz). The assignments were also confirmed by HSQC experiments (see Appendix D, Figure D4f) which showed that the three resonances at δ 1.71, 1.69 and 1.67 correlated with ^{13}C-NMR resonances at δ 18.6, 18.4 and 18.2, respectively, matching closely the corresponding chemical shift of 2,3,3-TMB-d_0 and with chemical shift differences of ~0.3 ppm, a normal one-bond deuterium isotope effect on ^{13}C resonances.[11]

5.4.6 Possible Mechanism(s) for the H-H and H-D exchange process(es) of II, II-CD_3 and 2,3,3-TMB-CD_3

The mechanism most anticipated to rationalize the intermolecular exchange processes between **II** and free 2,3,3-TMB, evident in the NOESY (EXSY) experiments with **II**, would involve a sequence of reversible β-hydrogen elimination, insertion and/or dissociation reactions in which β-agostic **II** forms the the hydrido alkene complex **VI** which can in turn undergo competitively both reversible 2,1-insertion to give the sterically crowded, tertiary alkyl complex, $[Cp_2TiCMe_2(CMe_3)]^+$ (**VII**) and reversible dissociation to the hydride, $[Cp_2TiH]^+$ (**IV**) and free 2,3,3-TMB (Scheme 5.5). (As shown above, hydride **IV** also reacts with residual 3,3-DMB at 225 K to form the 1,2-insertion product **V**.)

Scheme 5.5. β-Hydrogen elimination from **II** followed by reversible 2,3,3-TMB dissociation and 2,1-re-insertion

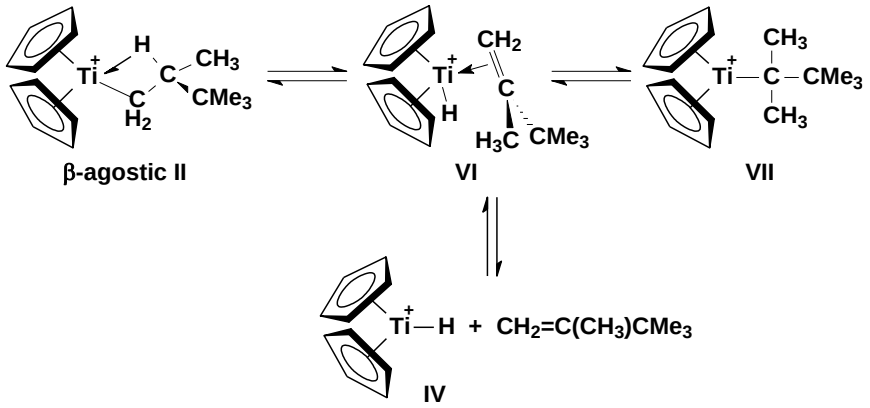

Since the two α-methyl groups of the intermediate tertiary alkyl complex **VII** are equivalent, any of the six β-H atoms could migrate to titanium to regenerate **VI** and, from this, free 2,3,3-TMB. Furthermore, as two of the hydrogen atoms of one of the methyl groups of **VII** are derived from the α-CH_2 group of **II** while the other one is derived from the β-H of **II**, this process would also result in intramolecular exchange of the β-H and α-H atoms with the γ-H atoms of **II**. Thus the process shown in Scheme 5.5 not only provides for random exchange of α-, β- and γ-hydrogen atoms of **II** if dissociative exchange of 2,3,3-TMB is competitive, but also for exchange of all three sites on **II** with the olefinic and 2-methyl hydrogen atoms of 2,3,3-TMB. Might the olefin dissociation from **VI** (to form 2,3,3-TMB and **IV**) be fast relative to the 1,2-migratory-insertion reaction, this process would also result in intramolecular exchange in 2,3,3-TMB.

As pointed out above, deuterium redistribution of **II**-CD_3 does occur slowly at 225 K but no EXSY exchange correlations were evident in NOESY experiments run at this temperature. We therefore carried out an NOESY experiment at 235 K utilizing a solution containing **II** and free 2,3,3-TMB (see Appendix D, Figures D5a-d). At this temperature, intermolecular exchange (EXSY) correlations were observed between the α-H(a) resonance of **II** with the olefinic resonance of 2,3,3-TMB at δ 4.68 (the hydrogen trans to the 2-methyl group) and between the α-H(b)

resonance of **II** with the olefinic resonance of 2,3,3-TMB at δ 4.62 (the hydrogen cis to the 2-methyl group). In addition, there were observed prominent EXSY correlations which indicated intermolecular exchange between both α-H(a) and α-H(b) of **II** with the hydrogens of the 2-methyl group of 2,3,3-TMB, between the β-hydrogen of **II** and the hydrogens of the 2-methyl group of 2,3,3-TMB, between the hydrogens of the β-methyl group of **II** and both the olefinic hydrogens and the hydrogens of the 2-methyl group of TMB, and intramolecularly between the olefinic and 2-methyl hydrogens of 2,3,3-TMB. Thus the hydrogens of the γ-Me group of 2,3,3-TMB undergo intermolecular exchange with all of the α-H(a), α-H(b), β-H and γ-H sites of **II** in addition to intramolecular exchange with the olefinic hydrogens of 2,3,3-TMB.

Complementary intramolecular exchange involving **II** was not observed, but such exchange cannot be ruled out as any such EXSY correlations may well be overwhelmed by stronger NOE correlations of opposite sign between the various pairs of exchanging hydrogen atoms of **II**. Indeed, it is difficult to reconcile the intermolecular exchange processes involved without an accompanying intramolecular exchange.

These conclusions stand in contrast to our previous findings for **III**, for which NOESY experiments provided no evidence for exchange with $CH_2=C(CH_3)SiMe_3$, and for **III**-CD_3 which forms a tertiary alkyl intermediate related to **VII**; the latter isomerizes selectively (apparently in the absence of detectable exchange with $CH_2=C(CD_3)SiMe_3$) to the isotopomeric $Cp_2TiCD_2CD(CH_3)(SiMe_3)]^+$ as in Scheme 5.3[3g] without any evidence for CHD and partially deuterated β-methyl groups. It is not clear at this point why **II** exchanges readily with 2,3,3-TMB while **III** does not exchange similarly with $CH_2=C(CH_3)SiMe_3$, but the larger size of the t-butyl group of 2,2,3-TMB and the lower electronegativity of silicon relative to carbon may well result in $CH_2=C(CH_3)SiMe_3$ being both less sterically demanding and a better electron donor. On this basis dissociative exchange of 2,3,3-TMB as in Scheme 5.5 may well be more facile, an hypothesis which will be considered computationally and discussed further below.

NOEs may also, via magnetization transfer, affect some or all of the intermolecular EXSY correlations observed, but we nonetheless determined approximate activation parameters from our data utilizing EXSYCalc software and the Eyring equation. A value of $\Delta G^{\ddagger}$ of ~16.1 kcal/mol was obtained for the β-H elimination reaction in **II**,[†] and this presumably represent an upper limit in view of the likelihood of NOE effects lessening intensities of cross peaks. Similarly, an upper value of ~15.5 kcal/mol was obtained for the intramolecular exchange seen in 2,3,3-TMB between $=CH_2$ and 2-Me that would effectively represent the barrier to formation of **VII** from 2,3,3-TMB in Scheme 5.5. Since the latter process is intramolecular and between hydrogens that are spatially close to each other, NOE effects almost certainly lessen intensities of the exchange cross peaks measured. These results are nonetheless in good agreement with the values of $\Delta G^{\ddagger}$, ~16.6 kcal/mol, determined above for H-D scrambling in **II**-CD_3, a result which suggests that the H-H and H-D exchange processes observed involve a common mechanism. Indeed, deuterium redistribution in **II**-CD_3 and 2,3,3-TMB-CD_3 appeared to be essentially synchronous, implying a common intermediate for this process also, as in Scheme 5.5.

While the processes of Scheme 5.5 seem to adequately rationalize our findings, an alternative process would involve isomerisation of **II**, via the hydrido-alkene complex **VI**, to the allylic dihydrogen species **VIII**, i.e. via allylic activation of the β-methyl group (Scheme 5.6).

Scheme 5.6. Allylic activation of the $CH_2CHMeCMe_3$ ligand of **II** to give the allylic dihydrogen species **VIII**

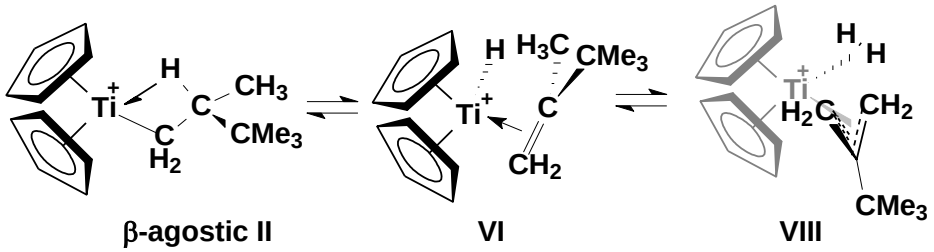

[†] The $\Delta G^{\ddagger}$ of β-H elimination presented here was obtained by measuring specific H exchange rate constants going from **II** to 2,3,3-TMB: α-Ha → Ha (=CH_2), α-Hb → Hb (=CH_2) and γ-H → 2-Me (see Tables D3-D4 for more data), and simply plugging in the rate constants obtained directly in the Eyring equation, $\Delta G^{\ddagger} = R \times T \times LN\left(\frac{hk}{k_B T}\right)$, where k is the averaged rate constant obtained, h is the Planck's constant, k_B is the Boltzmann's constant, R is the gas constant and T the temperature.

Allylic dihydrogen species analogous to that shown in Scheme 5.6 are believed to be involved in many metallocene-catalyzed propylene polymerization reactions, largely in order to rationalize the formation of dormant allylic species and the concomitant formation of H_2 as a by-product.[12] This type of isomerism has been postulated previously for the silyl analogue **III**, and could make random H-D exchange possible as shown in Scheme 5.7.[3g]

Scheme 5.7. Allylic dihydrogen mechanism for exchange between the β-H atom and the deuterium atoms of the β-methyl group of II-CD_3

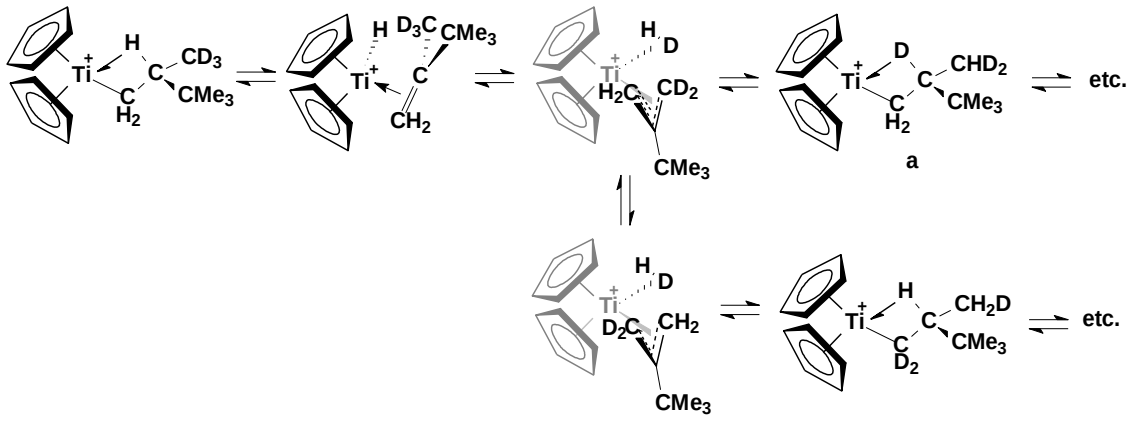

As shown in Scheme 5.7, rotation of the CD_3 group of the alkene hydride intermediate and of the HD ligand of the allylic dihydrogen species (**VIII**) would result in the H-D exchange process shown, forming in this case the isotopomer previously labelled **a**. This process only exchanges H/D atoms between the β and γ positions of the alkyl group, however, and an exchange of the two allyl termini is required for the allylic dihydrogen mechanism to also involve the α positions. This may not be a facile process given the nature of the metal-based orbitals involved (see below).[3g,10]

5.4.7 Computational study

To better understand the process(es) responsible for the exchange phenomena observed for **II** and **II**-CD_3, we have extended our earlier calculations[3e-g] to deal as best we can in totality with the mechanisms of the reactions involved. The resulting manifold of reactions is shown in Scheme 8 and the calculated total energies for all relevant species and transition states are summarized in

Table D2 of Appendix D. Since relative energies of the various species and transition states are of greatest interest here, the energies in Scheme 5.8 are all relative to **IIa**, the lowest energy agostomer of **II**.

Scheme 5.8. Energy minima and intervening transition state energies (kcal/mol relative to the α-agostic structure **IIa** at zero; "ti" = Cp_2Ti^+). Free energies of formation (225 K) are (black), transition state energies are in blue italics, and curved arrows indicate exchange between pairs of agostomers

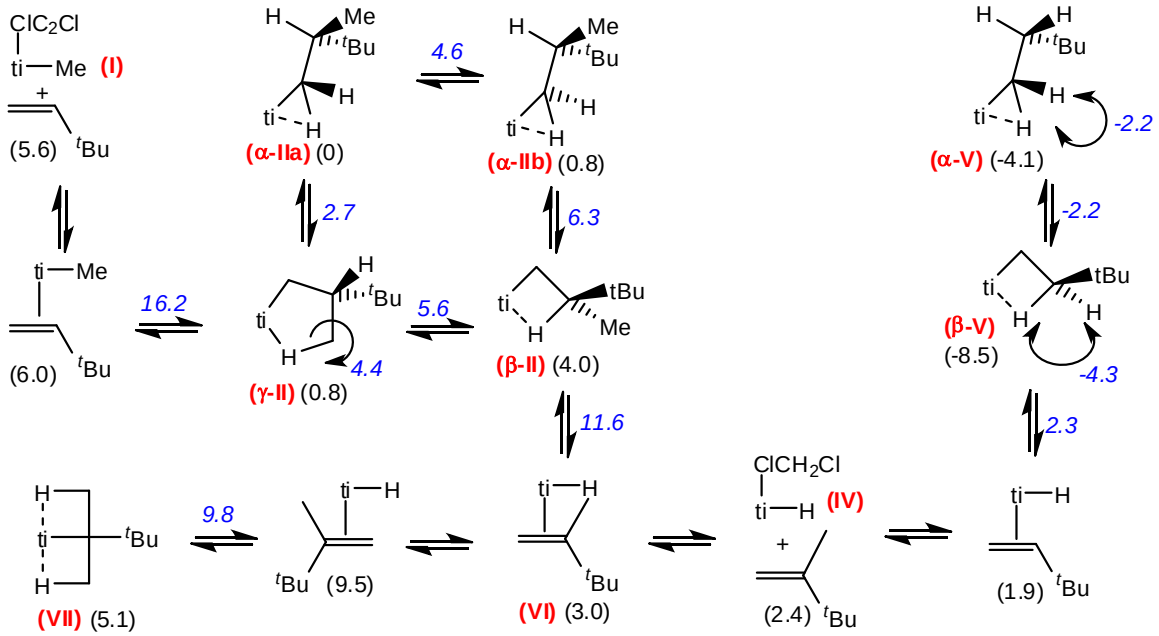

We note parenthetically that, where experimental data have been available, our previous utilizations of DFT methods to estimate the relative energies of both titanocene species and transition states for intramolecular conversion processes have generally resulted in excellent agreement between theory and experiment.[3e-g]

The reaction of **I** with 3,3-DMB to form γ-agostic **II** presumably passes through the alkene complex $[Cp_2TiMe(CH_2{=}CHCMe_3)]^+$ although this species was not observed. The transition state for alkene insertion is found at 16.2 kcal/mol above **IIa**, corresponding to an effective barrier for this step of 10.6 kcal/mol (16.2 – 5.6). The initial migratory insertion, with a reverse activation barrier of 16.2 kcal/mol, is not expected to be reversible since, as is shown below, all subsequent

processes under consideration here involve lower energy transition states and will occur preferentially. For much the same reason, since all interconversions between α, β and γ agostomers of **II** occur within a band of only 6.3 kcal/mol above **IIa**, the various agostic species should always exist at equilibrium.

All subsequent processes begin with β-hydrogen elimination from β-agostic **II**, the transition state of which is calculated to be 11.6 kcal/mol above **IIa**. The resulting hydrido alkene complex **VI** is only 3.0 kcal/mol above **IIa** and therefore its formation should also be reversible. When small amounts of free 3,3-DMB are still present, this alkene will quickly and virtually irreversibly trap the titanium hydride **IV** to form β-agostic **V**, which lies 8.5 kcal/mol below **IIa**. Interestingly, in view of the extensive H-D exchange which follows when **II**-CD_3 is utilized, no deuterium incorporation into **V** was detected. This suggests that β-hydrogen elimination of 2,3,3-TMB-CD_3 and interception of **IV** by 3,3-DMB must occur before significant amounts of the deuteride $[Cp_2TiD]^+$ are formed, and that the formation of **V** must indeed be essentially irreversible on the time scale of the investigation.

In the absence of free 3,3-DMB, **VI** can undergo alkene rotation and re-insertion as in Scheme 5.5 to give tertiary alkyl species **VII** which has two equivalent methyl groups and is found to be stabilized as doubly β-agostic; we note that the analogous silyl species, $[Cp_2TiCMe_2SiMe_3]^+$, was found to be similarly stabilized in a double β-agostic structure.[3g] Exchange between **VI** and **VII** rationalizes involvement of the α- and β-hydrogen atoms of **IIa** in the exchange processes detected in EXSY experiments as the highest transition state along the path from **VI** to **VII** is at 9.8 kcal/mol, well below the level of the original β-hydrogen elimination transition state of 11.6 kcal/mol. Furthermore, assuming that the barrier for alkene dissociation from **VI** to form **IV** and 2,3,3-TMB is not prohibitive, exchange of 2,3,3-TMB for CH_2Cl_2 can occur with virtually no change in free energy ($\Delta G \sim -0.6$ kcal/mol) and thus the EXSY-detected intermolecular exchange between **II** and 2,3,3-TMB is also rationalized.

The combination of intra- and intermolecular processes outlined in Scheme 5.5 also rationalizes the random H-D exchange processes exhibited by **II**-CD_3 and its isotopomers/isotopologues. These results stand in strong contrast with our previous finding for **III**-CD_3 (Scheme 5.3),[3g] where the coordinated CH_2=$CMeSiMe_3$ apparently does not take part in an exchange process involving dissociation from the intermediate hydrido alkene complex. What causes the differences in behaviour between **II** and **III**? While we do not have a complete explanation, the main issue seems to be that insertion of TMVS in a Ti-H or Ti-C bond is more exergonic, and hence less reversible, than insertion of 3,3-DMB. Thus de-insertion involving $[Cp_2TiCH_2CHMeSiMe_3]^+$ to give $[Cp_2TiH(CH_2=CMeSiMe_3)]^+$ costs 8.8 kcal/mol whereas, under the same conditions and calculated in the same way, de-insertion involving $[Cp_2TiCH_2CHMeCMe_3]^+$ to give $[Cp_2TiH(CH_2=CMeCMe_3)]^+$ costs only 3 kcal/mol.

A second rationale for the differing reactivities would involve weaker alkene-titanium bonding in $[Cp_2TiH(CH_2=CMeCMe_3)]^+$ than in $[Cp_2TiH(CH_2=CMeSiMe_3)]^+$, possibly because of greater steric hindrance in the former (larger *t*-butyl cone angle) and/or because the silyl alkene is a better electron donor. Consistent with this hypothesis, the calculated Ti-vinyl carbon bond lengths are calculated to be ~0.03 Å longer in **VI** than in $[Cp_2TiH(CH_2=CMeSiMe_3)]^+$; however, calculated bond strengths suggest that the alkene-titanium bonding is actually stronger in $[Cp_2TiH(CH_2=CMeCMe_3)]^+$ and thus the question remains unanswered.

We note at this point that there appears to be an incongruity between the experimental barriers for H-H and H-D exchange of 16-17 kcal/mol, deduced from rate data obtained from EXSY and deuterium scrambling experiments, and the calculated barrier for H-H exchange of 11.6 kcal/mol. However, as pointed out above, the EXSY-derived barriers almost certainly constitute an upper limit because of the unknown extent to which NOE effects may compromise intensities of the EXSY cross peaks. The barriers derived from the H-D exchange are also probably problematic

because they are subject to even greater uncertainties arising from unknown influences of kinetic isotope effects.

The barrier of 11.6 kcal/mol, on the other hand, may well be an unavoidable underestimation. Conversion of **VI** to **VII** involves an alkene rotation step analogous to that considered in our earlier investigation of the conversion of the silyl analogue of **VI** to the silyl analogue of **VII**, $[Cp_2TiCMe_2SiMe_3]^+$.[3g] In the latter case, the calculated barrier for alkene rotation seriously underestimated the barrier determined experimentally, apparently because rotation of the very bulky olefin was hindered in solution by ion pair formation with the very bulky $[B(C_6F_5)_4]^-$ counteranion. This unexpected impediment to alkene rotation could not be taken into account in the isolated cationic species which we used in our computational model, and we did not attempt a similar calculation for the conversion of **VI** to **VII**. Allowing also, however, for the intrinsic uncertainties involved in DFT calculations of highly complex species of the type of interest here, and the agreement between computational (11.6 kcal/mol) and experimental (16-17 kcal/mol) results is probably very good.

Finally, in our previous paper[3g] we discussed H-H exchange processes in **III** which involved an (allyl)(dihydrogen) intermediate analogous to **VIII**. For the present case, we see no need to invoke such intermediates as outlined in Schemes 5.6 and 5.7. The experimental observations can all be explained by a reversible β-hydrogen elimination pathway, and while additional contributions from an (allyl)(dihydrogen) mechanism cannot be ruled out, our calculations indicate that the transition state for formation of **VIII** to be significantly higher than any involved in the classical migratory insertion pathway discussed here.

5.5 Conclusion

We have previously shown that $[Cp_2TiCH_2CH(CH_3)(CMe_3)]^+$ (**II**) is α-agostic with the β-agostomer ~4 kcal/mol higher in energy; no exchange processes were noted other than alternation between agostic and non-agostic positions by the diastereomeric α-hydrogen atoms.[3f] More recently, however, we have investigated the analogous silyl compound $[Cp_2TiCH_2CH(CH_3)(SiMe_3)]^+$ (**III**) and the corresponding d_3 complex $[Cp_2TiCH_2CH(CD_3)(SiMe_3)]^+$ (**III**-CD_3),[3g] finding that **III** assumes a low energy γ-agostic structure with the β-agostomer sufficiently close in energy such that facile γ-agostomer-β-agostomer exchange occurs. In addition and quite independently, **III** undergoes very rapid, EXSY detected exchange of the β-H with the three hydrogen atoms of the β-methyl group (β-H/γ-H exchange) but *not* with the two α-H atoms, while **III**-CD_3 isomerizes specifically only to the isotopomeric $[Cp_2TiCD_2CD(CH_3)(SiMe_3)]^+$, with which it establishes an equilibrium (Scheme 5.3, R = $SiMe_3$).[3g]

Both exchange processes proceed via the hydrido alkene intermediate, $[Cp_2TiH(CH_2{=}CMeSiMe_3)]^+$ or its d_3 isotopologue, with the key step in the β-H/γ-H exchange of **III** involving tunneling between the 2-methyl hydrogen atoms and the hydride ligand via an allylic dihydrogen intermediate, $[Cp_2TiH_2(\eta^3\text{-}CH_2C(SiMe_3)CH_2]^+$. Because of an enormous kinetic isotope of >16000, **III**-CD_3 does not participate in a similarly rapid β-H/γ-D exchange, and thus the exchange between **III**-CD_3 and $[Cp_2TiCD_2CD(CH_3)(SiMe_3)]^+$ proceeds, much more slowly, via reversible β-elimination steps (Scheme 5.3) involving the doubly β-agostic tertiary alkyl intermediate $[Cp_2TiC(CH_3)(CD_3)(SiMe_3)]^+$.[3g]

In view of the strongly contrasting differences in behaviour between **II** and the rather exotic structural properties and exchange behavior of **III** and **III**-CD_3, we decided that a reinvestigation of **II** and its d_3 analogue, $[Cp_2TiCH_2CH(CD_3)(CMe_3)]^+$ (**II**-CD_3), would be appropriate in order to provide useful comparisons and to ascertain if we had missed something in our previous study.[3f]

We quickly ascertained that **II** indeed does not engage in an EXSY detected, hydrogen tunneling facilitated, β-H/γ-H exchange process. We also found, again in contrast with the **III**/**III**-CD_3 system, that while **II**-CD_3 does engage in H-D exchange, the exchange is not selective to e.g. $[Cp_2TiCD_2CD(CH_3)(CMe_3)]^+$ but rather seems to be essentially random such that a number of isotopomers and even isotopologues are formed. Concomitantly with the formation of variably deuterated **II**, isotopomers/isotopologues of $CH_2=C(CD_3)CMe_3$ also form. The mechanism for both exchange processes is believed to involve the hydrido alkene intermediate $[Cp_2TiH(CH_2=C(CD_3)CMe_3)]^+$, analogous to that posited above for **III**-CD_3 but with the difference that dissociative exchange of free and coordinated alkene occurs with **II**-CD_3 but not with **III**-CD_3. This is the key mechanistic difference between the H-D exchange chemistry of the **II**-CD_3 and **III**-CD_3 systems.

The major differences between **II** (studied here) and **III** (studied previously) can be ascribed to steric and electronic factors which result in dissociative exchange of $CH_2=CMeCMe_3$ from $[Cp_2TiH(CH_2=CMeCMe_3)]^+$ being much more facile than the analogous process involving $CH_2=CMeSiMe_3$ and $[Cp_2TiH(CH_2=CMeSiMe_3)]^+$.

5.6 Acknowledgements

MCB gratefully acknowledges the Natural Science and Engineering Research Council of Canada and Queen's University for funding of this research. PHMB thanks the Natural Science and Engineering Research Council of Canada, the Canada Foundation for Innovation, the Manitoba Research and Innovation Fund and SABIC Petrochemicals Europe for financial support. A.D.-B. thanks Queen's University for a Carrel Graduate Fellowship.

5.7 References

1. For useful reviews of metallocene polymerization catalysts, see (a) Resconi, L. ; Cavallo, L.; Fait, A. ; Piemontesi, F. *Chem. Rev*. **2000**, *100*, 1253. (b) Chen, E. Y.-X. ; Marks, T. J. *Chem. Rev*. **2000**, *100*, 1391. (c Rappé, A. K. ; Skiff, W. M. ; Casewit, C. J. *Chem. Rev*. **2000**, *100*, 1435. (d) Bochmann, M. *J. Organomet. Chem.* **2004**, *689*, 3982. (e) Fujita, T.; Makio, H. *Comp. Organomet. Chem.* III, chap. 11.20, *Crabtree, R. H.; Mingos, D. M. P. editors*, Elsevier, Amsterdam, 2007. (f) Froese, R. D. J. in Computational Modeling for Homogeneous and Enzymatic Catalysis, editors Morokuma, K.; Musaev, D. G. **2008**, 149. Wiley-VCH, Weinheim, Germany. (g) Busico, V. *Macromol. Chem. Phys.* **2007**, *208*, 26. (h) Wilson, P. A.; Hannant, M. H.; Wright, J. A.; Cannon, R. D.; Bochmann, M. *Macromol. Symp.* **2006**, *236* (Olefin Polymerization), 100. (i) Alt, H. G.; Licht, E. H.; Licht, A. I.; Schneider, K. J. *Coord. Chem. Rev.* **2006**, *250*, 2.

2. For reviews of agostic complexes, see (a) Brookhart, M.; Green, M. L. H. *J. Organomet. Chem.* **1983**, *250*, 395. (b) Brookhart, M.; Green, M. L. H.; Wong. L.-L. *Prog. Inorg. Chem.* **1988**, *36*. 1. (c) Grubbs, R. H.; Coates, G. W. *Acc. Chem. Res.* **1996**, *29*, 85. (d) Scherer, W.; McGrady, G. S. *Chem. Eur. J.* **2003**, *9*, 6057. (e) Clot, E.; Eisenstein, O. *Struct. Bonding (Berlin)* **2004**, *113*, 1. (f) Scherer, W.; McGrady, G. S. *Angew. Chem., Internat. Ed.* **2004**, *43*, 1782. (g) Brookhart, M.; Green, M. L. H.; Parkin, G. *Proc. Nat. Acad. Sci*. **2007**, *104*, 6908. (h) Lein, M. *Coord. Chem. Rev.* **2009**, *253*, 625. For computational papers discussing the importance of β-agostic structures during metallocene-induced alkene polymerization, see (i) Lohrenz, J. C. W.; Woo, T. K.; Ziegler, T. *J. Amer. Chem. Soc*. **1995**, *117*, 12793. (j) Jensen, V. R.; Koley, D.; Jagadeesh, M. N.; Thiel, W. *Macromolecules*, **2005**, *38*, 10266. (k) Mitoraj, M. P.; Michalak, A.; Ziegler, T. *Organometallics* **2009**, *28*, 3727. (l) Scherer, W.; Herz, V.; Hauf, C. *Struct. Bonding* **2012**, *146*, 159. (m) Laine, A.; Linnolahti, M.; Pakkanen, T. A.; Severn, J. R.; Kokko E.; Pakkanen, A. *Organometallics* **2010**, *29*, 1541. (n) Laine, A.; Linnolahti, M.; Pakkanen, T. A.; Severn, J. R.; Kokko E.; Pakkanen, A. *Organometallics* **2011**, *30*, 1350. (o) Dawoodi, Z.; Green, M. L. H.; Mtetwa, V.; Prout, K.; Schultz, A. J.; Williams, J. M.; Koetzle, T. F. *J. Chem. Soc., Dalt.* **1986**, 1629. (p) Scherer, W.; Priermeier, T.; Haaland, A.; Volden, H. V.; McGrady, G. S.; Downs, A. J.; Boese, R.; Bläser, D. *Organometallics* **1998**, *17*, 4406. For papers describing specifically late transition metal agostic complexes, see (q) Brookhart, M.; Lincoln, D. M.; Volpe. A. F.; Schmidt, G. F. *Organometallics* **1989**, *8*, 1212. (r) Shultz, L. H.; Brookhart, M. *Organometallics* **2001**, *20*, 3975.

3. (a) Jordan, R. F.; Bradley, P. K.; Baenziger, N. C.; Lapointe, R. E. *J. Am. Chem. Soc.* **1990**, *112*, 1289. (b) Alelyunas,Y. W.; Guo,Z.; Lapointe, R. E.; Jordan, R. F. *Organometallic* **1993**, *12*, 544. (c) Alelyunas, Y. W.; Baenziger, N. C.; Bradley, P. K.; Jordan, R. F. *Organometallics* **1994**, *13*, 148. (d) Guo, Z.; Swenson, D. C.; Jordan, R. F. *Organometallics* **1994**, *13*, 1424. (e) Sauriol, F.; Sonnenberg, J. F.; Chadder, S. J.; Dunlop-Brière, A. F.; Baird, M. C.; Budzelaar, P. H. M. *J. Am. Chem. Soc*. **2010**, *132*, 13357. (f) Dunlop-Brière, A. F.; Baird, M. C.; Budzelaar, P. H. M. *Organometallics*, **2012**, *31*, 1591. (g) Dunlop-Brière, A. F.; Baird, M. C.; Budzelaar, P. H. M. *J. Am. Chem. Soc*. **2014**, *135*, 17514. (h) Dunlop-Brière, A. F.; Baird, M. C., unpublished work.

4. A number of computational papers consider the interplay between α- and β-agostic species. See: (a) Nifant'ev, I. E.; Ustynyuk, L. Y.; Laikov, D. N. *Organometallics* **2001**, *20*, 5375. (b) Graf, M.; Angermund, K.; Fink, G.; Thiel, W.; Jensen, V. R. *J. Organomet. Chem.* **2006**, *691*,

4367. (c) Karttunen, V. A.; Linnolahti, M.; Pakkanen, T. A.; Severn, J. R.; Kokko, E.; Maaranen, J.; Pitkänen, P. *Organometallics* **2008**, *27*, 3390.

5. For relevant reviews on the influence of isotope effects on chemical equilibria, see (a) Jameson, C. J. *Isotopes in Physical and Biomedical Science, Vol. 2*, edited by Buncel, E.; Jones, J. R. Elsevier, 1991, p. 1. (b) Jameson, C. J. *Encycl. Nuc Mag. Res.* **1996**, *4*, 2638. (c) Jankowski, S. *Annual Reports on NMR Spectroscopy* **2009**, *68*, 149.

6. (a) Ahlrichs, R.; Armbruster, M. K.; Bachorz, R. A.; Bär, M.; Baron, H.-P.; Bauernschmitt, R.; Bischoff, F. A.; Böcker, S.; Crawford, N.; Deglmann, P.; Della Sala, F.; Diedenhofen, M.: Ehrig, M.; Eichkorn, K.; Elliott, S.; Friese, D.; Furche, F.; Glöss, A.; Haase, F.; Häser, M.; Hättig, C.; Hellweg, A.; Höfener, S.; Horn, H.; Huber, C.; Huniar, U.; Kattannek, M.; Klopper, W.; Köhn, A.; Kölmel, C.; Kollwitz, M.; May, K.; Nava, P.; Ochsenfeld, C.; Öhm, H.; Pabst, M.; Patzelt, H.; Rappoport, D.; Rubner, O.; Schäfer, A.; Schneider, U.; Sierka, M.; Tew, D. P.; Treutler, O.; Unterreiner, B.; von Arnim, M.; Weigend, F.; Weis, P.; Weiss, H.; Winter, N. *Turbomole* Version 5; Theoretical Chemistry Group, University of Karlsruhe, **2002**. (b) Treutler, O.; Ahlrichs, R. *J. Chem. Phys.* **1995**, *102*, 346. (c) Schäfer, A.; Huber, C.; Ahlrichs, R. *J. Chem. Phys.* **1994**, *100*, 5829. (d) Becke, A. D. *Phys. Rev. A* **1988**, *38*, 3098. (e) Perdew, J. P. *Phys. Rev. B* **1986**, *33*, 8822. (f) All Turbomole calculations were performed with the functionals "b-p" and "b3-lyp" of that package, which are similar (but not identical) to the Gaussian "BP86" and "B3LYP" functionals. (g) Lee, C.; Yang, W.; Parr, R. G. *Phys. Rev. B* **1988**, *37*, 785. (h) Becke, A. D. *J. Chem. Phys.* **1993**, *98*, 1372. (i) Becke, A. D. *J. Chem. Phys.* **1993**, *98*, 5648.

7. (a) Weigend, F.; Furche, F.; Ahlrichs, R. *J. Chem. Phys.* **2003**, *119*, 12753. (b) Klamt, A.; Schürmann, G. *J. Chem. Soc. Perkin Trans. 2* **1993**, *5*, 799. (c) Tobisch, S.; Ziegler, T. *J. Am. Chem. Soc.* **2004**, *126*, 9059. (d) Raucoules, R.; De Bruin, T.; Raybaud, P.; Adamo, C. *Organometallics* **2009**, *28*, 5358. (e) Gaussian 03, Revision C.02, Frisch, M. J.; Trucks, G. W.; Schlegel, H. B.; Scuseria, G. E.; Robb, M. A.; Cheeseman, J. R.; Montgomery, Jr., J. A.; Vreven, T.; Kudin, K. N.; Burant, J. C.; Millam, J. M.; Iyengar, S. S.; Tomasi, J.; Barone, V.; Mennucci, B.; Cossi, M.; Scalmani, G.; Rega, N.; Petersson, G. A.; Nakatsuji, H.; Hada, M.; Ehara, M.; Toyota, K.; Fukuda, R.; Hasegawa, J.; Ishida, M.; Nakajima, T.; Honda, Y.; Kitao, O.; Nakai, H.; Klene, M.; Li, X.; Knox, J. E.; Hratchian, H. P.; Cross, J. B.; Bakken, V.; Adamo, C.; Jaramillo, J.; Gomperts, R.; Stratmann, R. E.; Yazyev, O.; Austin, A. J.; Cammi, R.; Pomelli, C.; Ochterski, J. W.; Ayala, P. Y.; Morokuma, K.; Voth, G. A.; Salvador, P.; Dannenberg, J. J.; Zakrzewski, V. G.; Dapprich, S.; Daniels, A. D.; Strain, M. C.; Farkas, O.; Malick, D. K.; Rabuck, A. D.; Raghavachari, K.; Foresman, J. B.; Ortiz, J. V.; Cui, Q.; Baboul, A. G.; Clifford, S.; Cioslowski, J.; Stefanov, B. B.; Liu, G.; Liashenko, A.; Piskorz, P.; Komaromi, I.; Martin, R. L.; Fox, D. J.; Keith, T.; Al-Laham, M. A.; Peng, C. Y.; Nanayakkara, A.; Challacombe, M.; Gill, P. M. W.; Johnson, B.; Chen, W.; Wong, M. W.; Gonzalez, C.; and Pople, J. A. Gaussian, Inc., Wallingford C. T. **2004**. (f) Kutzelnigg, W.; Fleischer, U.; Schindler, M. "*The IGLO-Method: Ab Initio Calculation and Interpretation of NMR Chemical Shifts and Magnetic Susceptibilities*", in: Diehl, P.; Flück, E.; Günther, H.; Kosfeld, R.; Seelig, J. (eds) "*NMR basic principles and progress*", Springer-Verlag, Heidelberg, **1990**, vol. *23*.

8. (a) Papajak, E.; Leverentz, H. R.; Zheng, J.; Truhlar, D. G. *J. Chem. Theory Comput.* **2009**, *5*, 1197. (b) Papajak, E.; Truhlar, D. G. *J. Chem. Theory Comput.* **2010**, *6*, 597. (c) Dunning, T. H.; *J. Chem. Phys.* **1989**, *90*, 1007. (d) Kendall, R. A.; Dunning, T. H.; Harrison, R. J. *J. Chem. Phys.* **1992**, *96*, 6796. (e) Woon, D. E.; Dunning, T. H. *J. Chem. Phys. 98*, 1358 (**1993**). (f)

Dunning, T. H.; Peterson K. A.; Wilson, A. K. *J. Chem. Phys.* 2001, *114*, 9244. (g) Balabanov N. B.; Peterson K. A. *J. Chem. Phys*, **2005**, *123*, 064107

9. (a) Feller, D. *J. Comp. Chem.* **1996**, *17*, 1571. (b) Schuchardt, K. L.; Didier, B. T.; Elsethagen, T.; Sun, L.; Gurumoorthi, V.; Chase, J.; Li, J.; Windus, T. L. *J. Chem. Inf. Model.*, **2007**, *47*, 1045.

10. (a) Lauher, J. W.; Hoffmann, R. *J. Am. Chem. Soc.* **1976**, *98*, 1729. (b) Albright, T. A.; Burdett, J. K.; Whangbo, M.-H. "Orbital Interactions in Chemistry", Wiley, 1985, p. 393.

11. For relevant reviews on the influence of isotope effects on chemical shifts, see (a) Batiz-Hernandez, H.; Bernheim, R. A. *Prog. NMR Spectrosc.*, **1967**, *3*, 63. (b) Hansen, P. E. *Annual Reports on NMR Spectroscopy* **1983**, *15*, 105.

12. (a) Resconi, L.; Camurati, I.; Sudmeijrt, O. *Topics Catalysis* **1999**. *7*, 145. (b) Margl, P. M.; Woo, T. K.; Blöchl, P. E.; Ziegler, T. *J. Am. Chem. Soc.* **1998**, *120*, 2174. (b) Margl, P. M.; Woo, T. K.; Ziegler, T. *Organometallics* **1998**, *17*, 4997. (c) Resconi, L. *J. Molec. Catal., A* **1999**, *146*, 167. (d) Longo, P.; Grisi, F.; Guerra, G.; Cavallo, L. *Macromolecules*, **2000**, *33*, 4647. (e) Moscardi, M.; Resconi, L.; Cavallo, L. *Organometallics* **2001**, *20*, 1918. (f) Zhu, C.; Ziegler, T. *Inorg. Chim. Acta* **2003**, *345*, 1. (g) Pilme, J.; Busico, V.; Cossi, M.; Talarico, G. *J. Organomet. Chem.* **2007**, *692*, 4227.

Chapter 6

Concluding remarks and future work

6.1 Concluding remarks

In chapter 2, $[Cp_2TiCH_3(H_2O)]^+$ (**I**) was synthesized by addition of water to $[Cp_2TiMe]^+$ and its NMR characterization of was presented. **I** was initially not expected to exist and to be stable because it would have been expected instead to rapidly undergo hydrolysis, even at the low temperatures at which it was characterized, due to the oxaphilic nature of Ti and to the known prevalence of these catalyst to undergo hydrolysis at higher temperatures. In presence of excess water, the H_2O ligand was exchanging rapidly with free water molecules and engaging in H-bonding. At higher temperatures, **I** underwent hydrolysis and methane formation. One of the hydrogen atom of methane was confirmed to be from the water ligand by deuterium-labeling of water. The NMR data obtained for **I** was useful in other projects involving $[Cp_2TiMe]^+$ because it allowed a quick diagnosis of water infiltration in the sample. Water infiltration was sporadic, and the capability to detect such a process was useful for subsequent projects.

In chapter 3, formation of an α-agostic complex, $[Cp_2TiCH_2CHMeCMe_3]^+$ (**II**), via controlled (single 1,2-migratory insertion reaction of $[Cp_2TiMe]^+$ and 3,3-dimethyl-1-butene (3,3-DMB) at 205 K was presented. **II** exhibited an unusually low geminal HH coupling at α-CH_2, ~3-4 Hz, and exchanged between its two α-agostic isomers, with a marked preference for one isomer (α-a-agostomer, ground state) over the other (α-b-agostomer), as indicated by a difference in chemical shifts for the α- hydrogens of above 7 ppm, and a large difference in $^1J_{CH}$ (α-Ha 104 Hz; α-Hb 133 Hz). Surprisingly, **II** also remained α-agostic under coordination of Et_2O (**II-Et_2O**), although the α-agostic interaction is weakened in **II-Et_2O** relative to **II**. At 215 K and higher, $[Cp_2TiCH_2CHMeCMe_3]^+$ undergoes β-H transfer reaction with excess 3,3-DMB to form

$[Cp_2TiCH_2CH_2CMe_3]^+$, a degenerate β-agostic complex and 2,3,3-trimethyl-1-butene (2,3,3-TMB). DFT calculations were in good agreement with the experimental results and they also suggested an exchange between α-a- and α-b-agostomers, with preference for α-a-agostomer. The quantitative formation of **II** even in the presence of excess 3,3-DMB at 205 K seems surprising because it could be expected that **II** would undergo oligomerization with excess olefin, or be very prone to β-H elimination, even at that temperature. The stereoselectivity at the α-agostic interaction is an unprecedented feature for known group IV alkyl-metallocene complexes, and could have interesting implications in further understanding chain-end stereocontrol in polymerization of olefin using achiral catalysts.

In chapter 4, $[Cp_2TiCH_2CHMeSiMe_3]^+$ (**III**), a complex that exchanged between γ- (ground state) and β- agostomers, was prepared by reaction of $[Cp_2TiMe]^+$ with one equivalent of trimethylvinylsilane (TMVS) at 205 K. The γ-agostic interaction was strong enough to slow down the rotation of the β-Me around its C-C axis on the NMR time scale and achieve decoalescence of the three individual hydrogen resonances at ~180 K and below. At higher temperatures, β-Me only had one averaged resonance that was shifting downfield with increasing temperature, while that of β-H was shifting upfield, indicating that the exchange between β- and γ- agostomers was shifting toward the β-agostomer, with spectral properties of **III** reflecting a weighted average between those two conformations. It is interesting that changing only one atom from **II** results in a different agostic structure. The structural and reactivity differences was attributed to cone angle difference between CMe_3 and $SiMe_3$; the former having a larger cone angle, it was more hindering than $SiMe_3$.

There was H-exchange between β-H and γ-H from 215 K to 260 K but, despite crossing over each other, the ^1H resonances of these protons did not coalesce, even at 270 K: in fact they got sharper at higher temperatures, implying no or very little increase in rate of exchange. On the other hand, the isotopologous compound $[Cp_2TiCH_2CHCD_3SiMe_3]^+$ underwent a slow, reversible and exclusive isotopomeric rearrangement to form specifically $[Cp_2TiCD_2CDCH_3SiMe_3]^+$ through a

series of reversible β-H elimination, 2,1- and 1,2- migratory-insertion reactions resembling chain-end epimerization (process 1) only, with no sign of that β-/γ- exchange seen in **III**.

Process 1. Series of reversible β-H elimination, 2,1- and 1,2- migratory-insertion reactions leading to the specific isotopomeric reversible rearrangement of $[Cp_2TiCH_2CHCD_3SiMe_3]^+$ to $[Cp_2TiCD_2CDCH_3SiMe_3]^+$

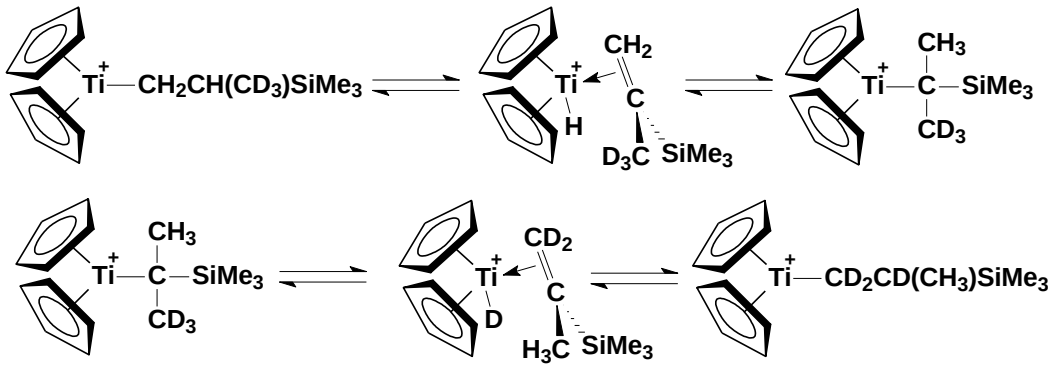

Deuteration of **III** at β- or γ- positions essentially shut down the β-H/γ-H exchange seen in **III**-d_0, with a k_H/k_D of at least 13000 since no intermediate of the type $[Cp_2TiCD_2CHCDH_2SiMe_3]^+$ or $[Cp_2TiCH_2CDCHD_2SiMe_3]^+$ were observed for 7 hours at 225 K. These results indicate that the β-H/γ-H exchange process is driven by H quantum mechanical tunneling (QMT). DFT calculations suggest this QMT process could take place from a $[Cp_2TiH(CH_2{=}CMeSiMe_3)]^+$ intermediate in which the hydride H-atom is 1.6 Å only from one of the H-atom on the olefinic methyl group. This QMT-driven β-H/γ-H exchange process was completely unprecedented. Meanwhile, the type of chemistry shown in process 1 above has rarely been directly characterized by NMR means and offers insight into chain-end epimerization mechanism. To our knowledge, **III** is the only characterized example of a γ-agostic group IV alkyl-metallocene complex that results from single insertion reaction.

Finally, chapter 5 presented a re-investigation of **II** to unravel some exchange processes that were not formerly seen in previous studies of **II** at lower temperatures (in chapter 3). While there is no sign in **II** of the β-H/γ-H exchange driven by QMT seen for **III**, EXSY and D-labeling (of β-Me: **II**-CD_3) experiments suggest that **II** also undergoes process 1. Unlike what was seen for **III**

however, olefin dissociation from $[Cp_2TiH(CH_2=CMeCMe_3)]^+$ is faster than process 1 and consequently, EXSY correlations are seen intermolecularly between **II** and 2,3,3-TMB, as well as intramolecularly in 2,3,3-TMB (fastest exchange) at 235 K. In **II**-CD_3, this rapid reversible olefin dissociation from the olefin-hydride complex following the slower process 1 leads to multiple isotopologuous rearrangements in 2,3,3-TMB before it can be re-incorporated in **II**. This in turn gives raise to ~similar overall rates of deuterium incorporation at all α- and β- sites in **II**-d_x (x = 0-6, statistical distribution with an average value of 3). The overall deuterium distribution at α-, β- and γ- sites in **II**-d_x tends to near randomness over time due to these numerous isotopologuous rearrangements, with slight preference for ^1H at the α-site (a) that is agostic in the dominant α-agostic isomer, and accumulation of deuterium at the β-site. This is consistent with DFT calculations that suggest the β-agostic conformation is the least favorable between α-a-, α-b-, β- and γ- agostomers of **II**, while the α-a-agostomer the preferred conformation.

6.2 Future work

Because **II** underwent β-H transfer to excess 3,3-DMB at 215 K and over, **II** was investigated for its capability to act as an effective source of $[Cp_2TiH]^+$ for reaction with di-substituted olefins of the type $CH_2=CMeR$ (R = $CHMe_2$ and $CH_2CHMeCH_2CH_2Me$ were investigated) was initiated. In the cases investigated thus far, β-agostic complexes of the type $[Cp_2TiCH_2CHMeR]^+$ were successfully characterized by NMR unraveling very interesting properties. In the β-agostic complex $[Cp_2TiCH_2CHMeCHMe_2]^+$, there was no exchange detected at 215 K, as opposed to what was seen for the β-agostic complex $[Cp_2TiCH_2CHMeCH_2CHMe_2]^+$.[1] On the other hand, $[Cp_2TiCH_2CHMeCH_2CHMeCH_2CH_2Me]^+$ (**IV**) and its diastereomer (**IV'**) behaved much like this formerly published complex and displayed intermolecular and intramolecular exchanges between α-, β- and γ- hydrogens. Because the latter pair is diastereomeric, they each have their own set of resonances and this allows following specific exchange rates to deduce mechanisms from relative

rates. This work is currently underway, with hope to extend the scope of olefins investigated for that project.

An investigation of reaction of triethylvinylsilane and triphenylvinylsilane with $[Cp_2TiMe]^+$ is also underway, with both olefin undergoing 1,2-migratory-insertion reaction, forming complexes of the type $[Cp_2TiCH_2CHMeSiR_3]^+$ (R = Et or Ph). The resulting complexes both have a negative β-Me δ_H, indicating γ-agostic character. Interestingly, in the case of $[Cp_2TiCH_2CHMeSiEt_2CH_2CH_3]^+$, the complex undergoes 1,5-σ bond metathesis via an ε-agostic interaction with one of the ethyl groups on Si at 235 K, to form $[Cp_2TiCH_2CH_2SiEt_2CHMe_2]^+$. Investigation of dynamic properties in these systems is hoped to be compared with what was seen in **III**.

Reaction of trimethoxyvinylsilane with $[Cp_2TiMe]^+$ produces, at low temperatures, a dative coordination complex bonded through the oxygen's electron lone pair, in which there is a rapid exchange between the three different O leading to an averaged methoxy resonance. As temperature is raised, a mixture of the 1,2- and the 2,1- insertion products is obtained, $[Cp_2TiCH_2CHMeSi(OMe)_3]^+$ and $Cp_2TiCH(CH_2Me)(Si(OMe)_3]^+$, respectively, with a slight preference for the latter. Both insertion complexes were chelated by one methoxy group at a time, although there is also exchange between the methoxy groups suggesting rotation around the C-Si bond. This chelation seems to provide stability to these complexes that survive a few hours at 250 K, unlike **III** or **II**. Interestingly, reaction of trimethoxyvinylsilane with the homologuous catalyst $[Cp_2ZrMe]^+$ resulted in a different chemistry that is currently under investigation.

In the late stage of the project presented in chapter 4, it was realized that TMVS (and triethylvinylsilane) undergoes controlled double insertion reaction, with the second migratory-insertion in a 2,1-fashion to give the diasteromeric pair of β-agostic $[Cp_2TiCH(SiMe_3)(CH_2CH_2CHMeSiMe_3)]^+$ (**V** and **V'**) with a diastereomeric ratio of 1:1.05-1:1.15. Unlike **IV** and **IV'**, **V** and **V**' did not exhibit noticeable exchanges by EXSY. At higher

temperatures, **V** and **V'** underwent allylic deactivation via H_2 loss, producing the internal allylic compound $[Cp_2Ti\text{-}\eta^3\text{-}\{CH(SiMe_3)(CHCHCHMeSiMe_3)\}]^+$, with allylic hydrogens all trans to each other according to their large $^3J_{HH}$ values. More interestingly, reaction of **II** with TMVS formed a similar double insertion diastereomeric pair ($[Cp_2TiCH(SiMe_3)(CH_2CH_2CHMeCMe_3)]^+$) but with a ratio of 4:1 this time. This could suggest that α-agostic do enhance chain-end stereocontrol on subsequent migratory-insertion reactions. **II** also underwent dative O-coordination to trimethoxyvinylsilane, followed by migratory-insertion at higher temperatures. It is hoped here that reaction of **III** with trimethoxysilane will result in a dative O-coordination complex that is α-agostic, and that this new agostic confirmation will enhance the diastereomeric ratio relative to what was obtained for **V** and **V'**.

In another preliminary investigation, **II**, **III** and $[Cp_2TiCH_2CHMeSiEt_3]^+$ (**VI**) were reacted with weak Lewis bases, such as ethylether, methylchloride, 2-chloropropane and 2-chlorobutane (2-CB). Interestingly, **III** and **VI** formed ethylether adduct, **III-Et_2O** and **VI-Et_2O** respectively, which had comparable α-agostic character to **II-Et_2O**, suggesting α-agostic interaction upon ligand coordination. Considering the parallel between a weak Lewis base ligand and olefins, this provides evidences that reorganization of β-agostic or γ-agostic polymeryl growing chains to α-agostic conformation upon olefin coordination can occur in polymerization systems. **VI-Et_2O** exchanges with **VI** at 225 K, but it was noticed that insertion of olefins into $[Cp_2TiMe(Et_2O)]^+$ was difficult and it was hoped that weaker Lewis bases would make it possible to study olefin double insertion at low temperatures to see if α-agostic conformation prior to olefin coordination could enhance diastereomeric ratios. Methylchloride, 2-chloropropane and 2-chlorobutane (CB) are all weak Lewis bases (L) that coordinated to **II** in a much dynamic fashion, exchanging rapidly between free- and coordinated- sites (eq. 6.1).

$$\textbf{II-L} + \underline{L} \rightleftharpoons \textbf{II-}\underline{\boldsymbol{L}} + \mathrm{L} \qquad (6.1)$$

CB is particularly interesting because it is chiral; **II-CB** is present as a mutually exchanging diastereomeric pair, with a diastereomeric ratio 1:1.17 at 205 K. Pre-orienting the growing polymeryl chain relative to the open coordination site could improve olefin-face selectivity and thus subsequent stereoselectivity at the migratory-insertion reaction, improving the tacticity of resulting polymers. Tests of double insertion of TMVS and triethylvinylsilane in presence of these Lewis bases have yet to be performed and are hoped to result in enhanced diastereomeric ratios.

Finally, if usage of a weak Lewis base to improve the diastereomeric ratio is shown to work, this could have useful implications in ligands design for improving the performances of olefin-polymerization catalysts. For example, addition of a weak Lewis base tether on the ancillary ligand(s) could induce α-agostic conformation in the growing polymeryl chain, which would potentially improve the tacticity of the polymer produced. Furthermore, the β-agostic conformation leads to undesirable side-reactions via β-H elimination (chain transfer, branching, stereoerror insertion through chain-end epimerization or to allylic deactivation) and favoring α-agostic over β-agostic conformations during polymerization reactions is thus also desirable from that perspective.

6.3 References

1. Sauriol, F.; Sonnenberg, J. F.; Chadder, S. J.; Dunlop-Briere, A. F.; Baird, M. C.; Budzelaar, P. H. M., *J. Am. Chem. Soc.* **2010,** *132* (38), 13357.

Appendix A

Supporting Information for Chapter 2:

The synthesis and properties of $[Cp_2Ti(Me)(H_2O)][B(C_6F_5)_4]$

Alexandre F. Dunlop-Brière and Michael C. Baird*

Department of Chemistry, Queen's University,
Kingston, ON K7L 3N6, Canada

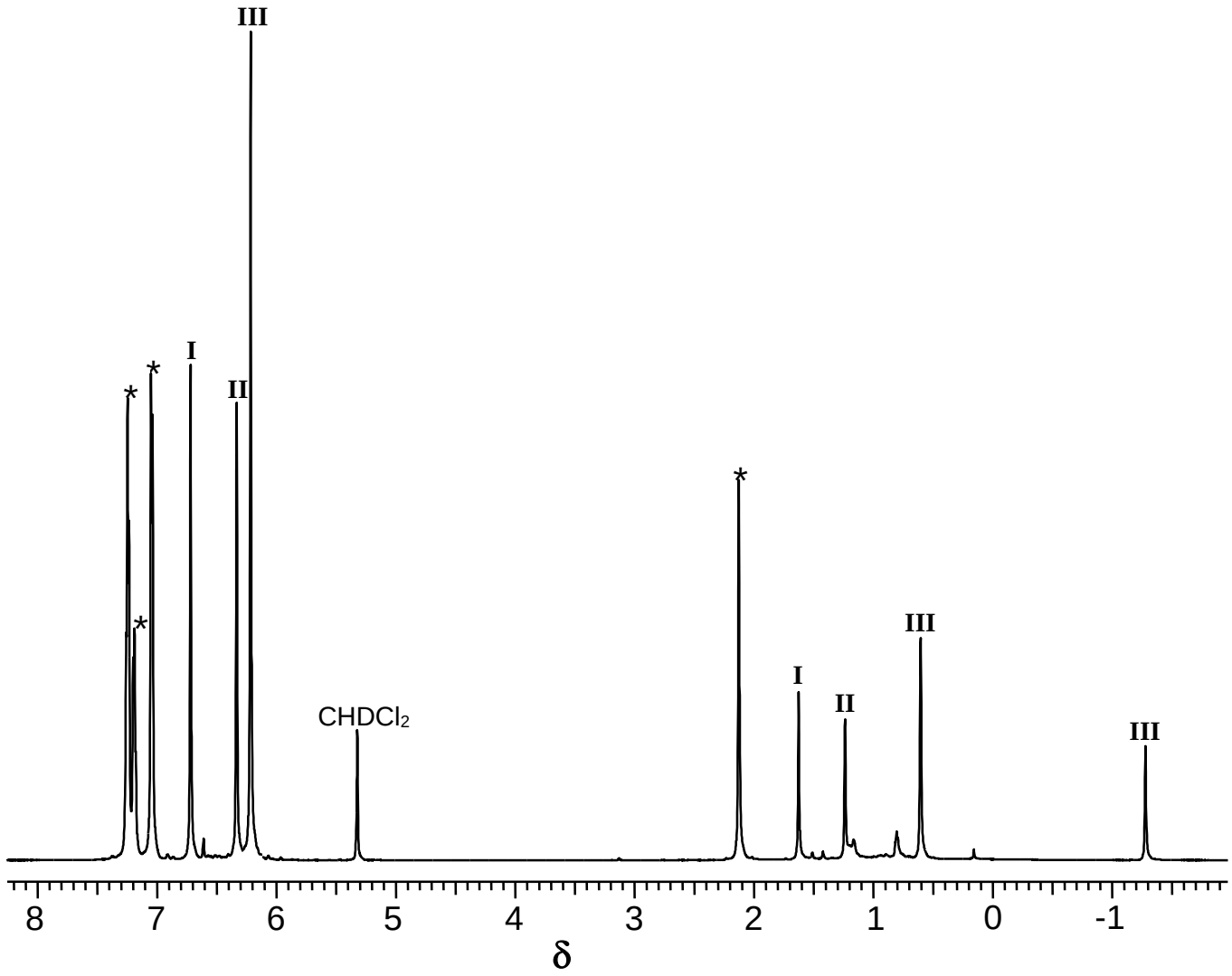

Figure A1. ^{1}H NMR spectrum (CD_2Cl_2, 205 K, from ref 3c) of a reaction mixture obtained from reaction of $[Ph_3C][B(C_6F_5)_4]$ with approximately two equivalents of Cp_2TiMe_2 and showing the presence of $[Cp_2TiMe(CD_2Cl_2)][B(C_6F_5)_4]$ (**I**), $[Cp_2TiMeB(C_6F_5)_4]$ (**II**) and $\{[Cp_2TiMe]_2(\mu\text{-}Me)\}[B(C_6F_5)_4]$ (**III**); * denotes the resonances of $MeCPh_3$.

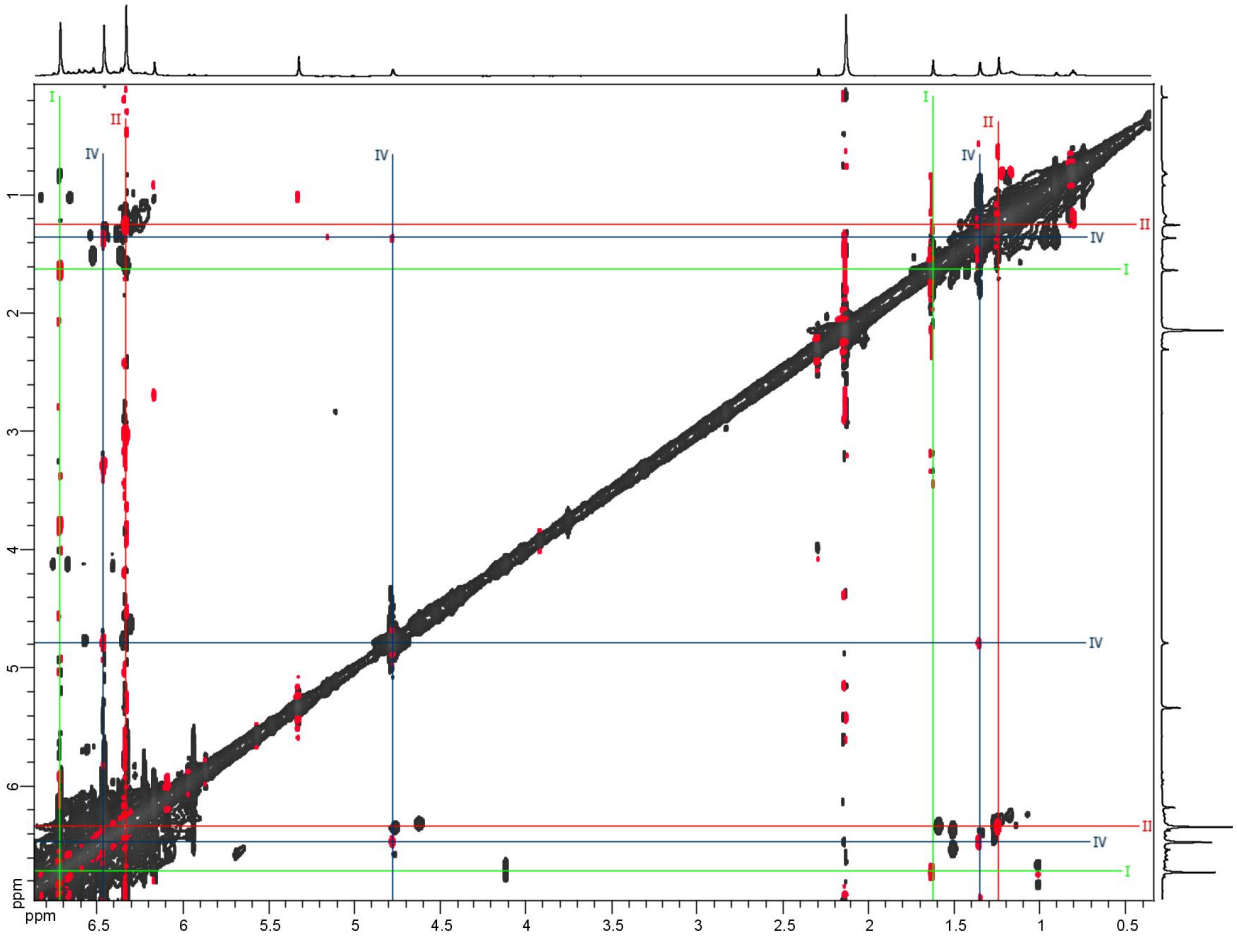

Figure A2. NOESY spectrum (CD_2Cl_2, 205 K) of a Cp_2TiMe_2/$[Ph_3C][B(C_6F_5)_4]$ reaction mixture containing significant amounts of **I** (green lines), **II** (red lines) and **IV** (blue lines) in order to make clear the NOE correlations. The NOE correlations between the Cp and Me resonances of each compound **I**, **II** and **IV** are apparent, as are the correlations of the Cp and Me resonances of **IV** with the resonance of the aqua ligand.

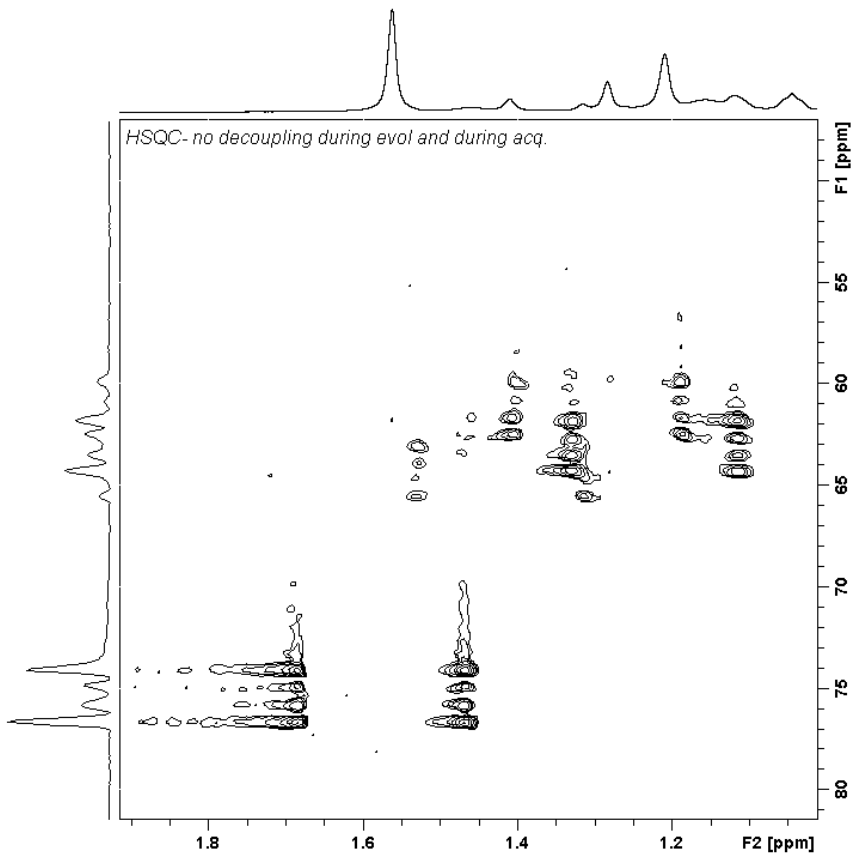

Figure A3. HSQC experiment (CD_2Cl_2, 205 K) on a Cp_2TiMe_2/$[Ph_3C][B(C_6F_5)_4]$ reaction mixture contaminated with a small amount of what appears to be $[Cp_2TiMe(Et_2O)][B(C_6F_5)_4]$. The proton and carbon decouplers were turned off during the evolution and the acquisition, respectively.

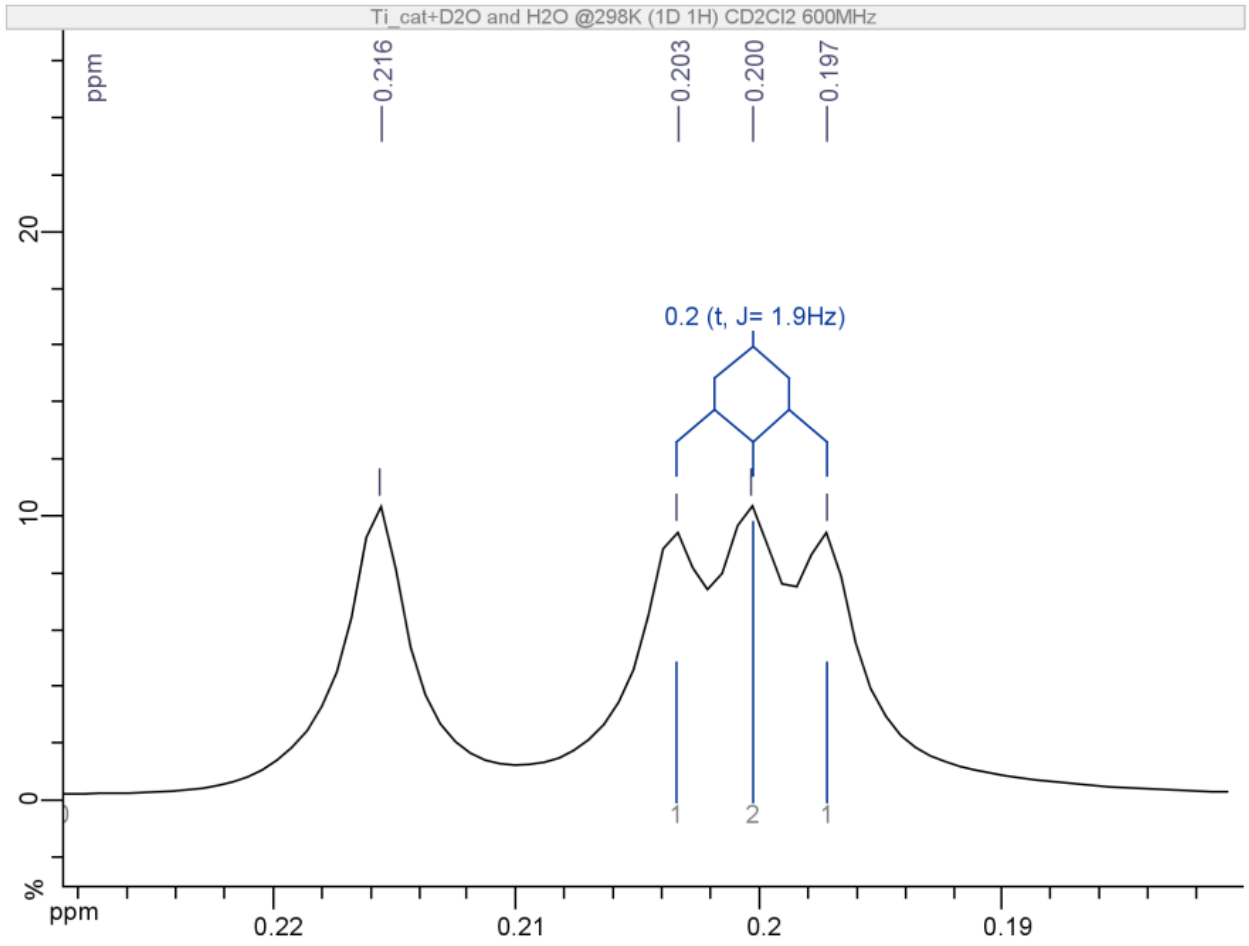

Figure A4. Resonance of CH_3D (CD_2Cl_2, 298 K).

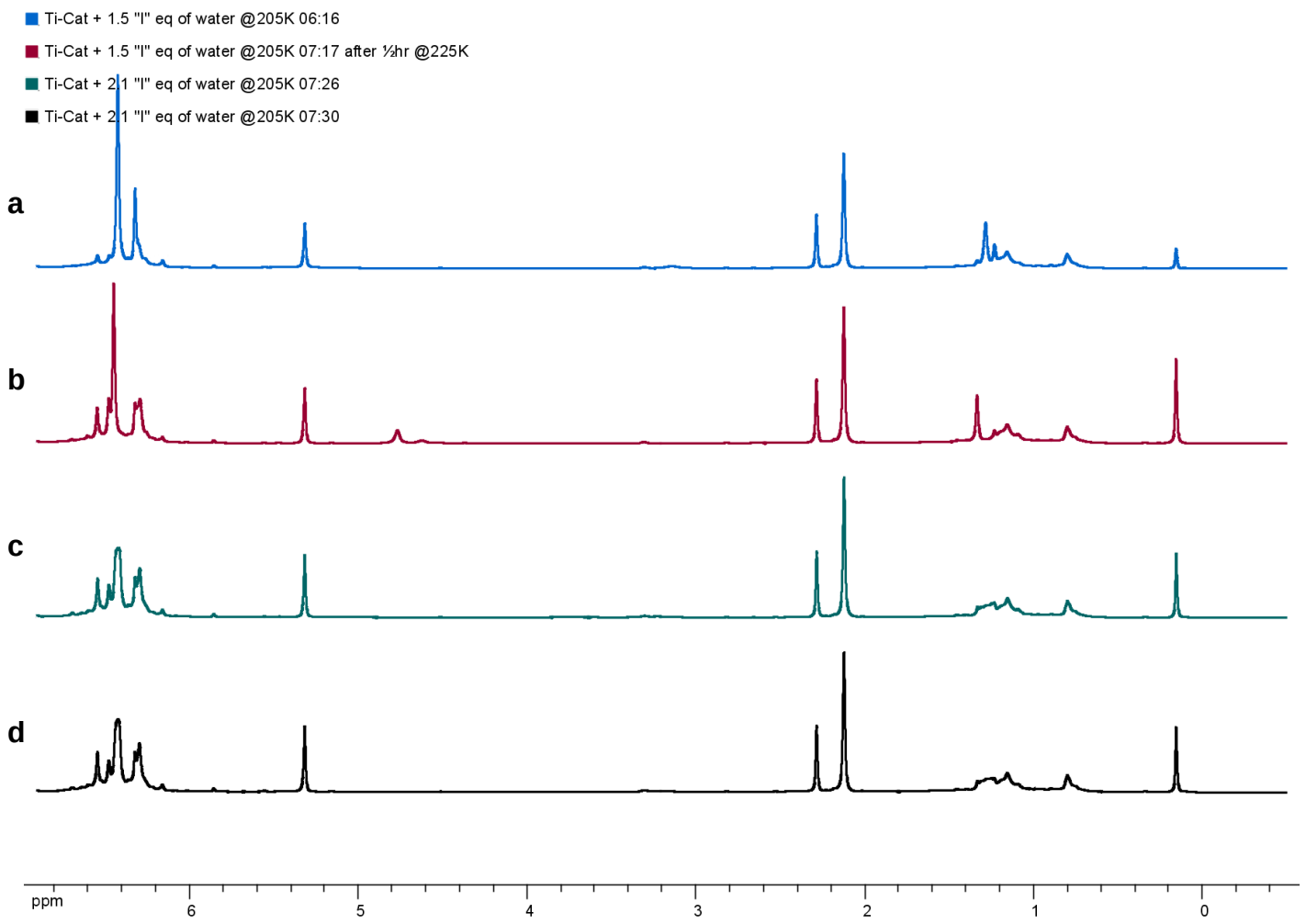

Figure A5. ^{1}H NMR spectra (CD_2Cl_2) (a) of a mixture of **II** and **IV** in the presence of excess of water at 205 K, (b) of the same mixture after being at 225 K for 30 min, (c,d) at 205 K after the addition of more water.

Appendix B

Supporting Information for Chapter 3:

α- and β-Agostic Alkyl-Titanocene Complexes

A. F. Dunlop-Brière and M. C. Baird*
Department of Chemistry, Queen's University,
Kingston, ON K7L 3N6, Canada
Email: bairdmc@chem.queensu.ca

P. H. M. Budzelaar*

Department of Chemistry, University of Manitoba,
Winnipeg, MB R3T 2N2, Canada

Experimental Procedures

All syntheses were carried out under dry, deoxygenated argon using standard Schlenk line techniques. Argon was deoxygenated by passage through a heated column of BASF copper catalyst and then dried by passing through a column of activated 4 Å molecular sieves. Handling of Cp_2TiMe_2 was done in an MBraun Labmaster glovebox, and the compound was stored in ethylether under argon in a freezer. NMR spectra were recorded using a Bruker AV600 spectrometer, ^1H, ^2H, and ^{13}C NMR data being referenced to TMS via the residual proton signals of the deuterated solvent. $[Ph_3C][B(C_6F_5)_4]$ was purchased from Asahi Glass Company and used as obtained, and CH_3Li was purchased from Aldrich. Cp_2TiMe_2 was synthesized from Cp_2TiCl_2 and methyllithium, as described elsewhere,[1] and was stored in diethyl-ether solution under Ar, at -30 °C. Dichloromethane-d2 was dried by storage over activated 3 Å molecular sieves. The olefin used in this study, tertbutylethylene or 3,3-dimethyl-1-butene (3,3-DMB) was purchased from Aldrich and dried by storage with activated 4Å molecular sieves.

Solutions containing $[Cp_2Ti(Me)(CD_2Cl_2)][B(C_6F5)_4]$ (**I**) for NMR studies were prepared by dissolving 35-45 mg (~0.04 mmol) of triphenylcarbenium tetrakis(pentafluorophenyl)borate ($[(C_6H_5)_3C][B(C_6F_5)_4]$) in 0.6 mL of CD_2Cl_2, in the glovebox. The solutions were subsequently added to 0.5-1 equivalent of Cp_2TiMe_2 residue (solvent pre-evaporated) to ensure complete reaction of the later. The mixture was then syringed into a rubber septum sealed NMR tube (under Ar), which was taken quickly out of the glovebox and immersed within 2-4 min in a dry ice/acetone bath (195 K). The NMR tube was placed in the pre-cooled (185-205 K) probe of the NMR spectrometer, and a ^1H-NMR spectrum was run. The tube was then removed from the probe to the dry ice/acetone bath, and several aliquots of the 3,3-dimethyl-1-butene (DMB) (molar ratio **I**:olefin ≈ 1:0.5-1:6) were added to the cold solution. The tube was shaken vigorously at 195 K to induce mixing and placed back in the probe at 185-215 K, and NMR spectra were obtained at various time intervals and temperatures. Note that although solutions of **I** prepared as above always contained some $[Cp_2TiMe\{B(C_6F_5)_4\}]$ (**II**),[6] reaction of the latter with DMB was extremely slow. NOESY experiments were typically performed with mixing times between 0.2 and 0.6 seconds, while measured t1 relaxation times were typically ranging between 0.1 s and 1 s. In NOESY spectra presented are phased to get the diagonal to be

negative and thus, correlations that are of the same colour as the diagonal are also negative (EXSY correlations), and those that are of a different colour than the diagonal are positive (NOE).

References

(a) Alt, H. G.; Di Sanzo, F. P.; Rausch, M. D.; Uden, P. C. *J. Organomet. Chem.* **1976**, *107*, p.257. (b) Clauss, K.; Bestian, H. *Justus Liebigs Ann. Chem.* **1962**, *654*, p.8. (c) Erskine, G. J.; Wilson, D. A.; McCowan, J. D. *J. Organomet. Chem*. **1976**, *114*, p.119. (d) Erskine, G. J.; Hartgerink, J.; Weinberg, E. L.; McCowan, J. D. *J. Organomet. Chem.* **1979**, *170*, p.51. (e) Razuvaev, G. A.; Mar'in,V. P.; Andrianov,Y. A. *J. Organomet. Chem.* **1979**, *174*, p.67. (f) Razuvaev, G. A.; Mar'in, V. P.; Drushkov, O. N.; Vyshinskaya, L. I. *J. Organomet. Chem.* **1982**, *231*, p.125. (g) Li, H.; Neckers, D. C. *Can. J. Chem.* **2003**, *81*, p.758. (h) Dollinger, L. M.; Ndakala, A. J.; Hashemzadeh, M.; Wang, G.;Wang,Y.; Martinez, I.; Arcari, J. T.; Galluzzo, D. J.; Howell, A. R.; Rheingold, A. L.; Figuero, J. S. J. *Org. Chem.* **1999**, *64*, p.7074.

NMR data at 215 K (CD_2Cl_2):

[$Cp_2Ti(Me)(CD_2Cl_2)]^+$ (I). ^{1}H NMR: δ 1.63 (Me), 6.72 (Cp); ^{13}C-NMR: δ 128.1 (Cp, $^1J_{CH}$ 176 Hz), 75.7 (Me, $^1J_{CH}$ 129 Hz)).

[$Cp_2TiCH_2CHMe^tBu]^+$ (III). ^{1}H NMR: δ –1.66 (br m, $^2J_{HH} \approx {}^3J_{HH} \approx$ 3-4 Hz, α-H(a)), 0.41 (d, $^3J_{HH}$ = 6.3 Hz, β-Me), 0.73 (s, *t*-Bu), 2.85 (m, β-H), 5.97 (dd, $^2J_{HH}$ = 3.7, $^3J_{HH}$ = 11.4 Hz, α-H(b)), 6.53 (s, Cp). ^{13}C-NMR: δ 16.6 (β-Me, $^1J_{CH}$ 126 Hz), 26.2 (Me of *t*-Bu, $^1J_{CH}$ 124 Hz), 35.9 (*C*Me_3), 57.5 (β-C, $^1J_{CH}$ 129 Hz), 116.6 (Cp, $^1J_{CH}$ 178 Hz), 144.9 (α-C, $^1J_{CH}$ = 104, 133 Hz).

2,3,3-trimethyl-1-butene. ^{1}H NMR: δ 4.64 and 4.60 (CH_2); 1.69 (Me), 0.98 (t-Bu). ^{13}C-NMR: δ 106.5 (C-1, $^1J_{CH}$ 155, 154 Hz); 18.8 (Me, $^1J_{CH}$ 126 Hz); 28.7 (Me, $^1J_{CH}$ 128 Hz); 34.8 (quaternary C); 153.9 (C-2). This set of spectral data are very similar to those of TMB: ^{1}H NMR: δ 4.86 and 4.78 (CH_2, $^3J_{HH}$ 17.4 Hz, $^3J_{HH}$ 10.7 Hz, respectively); 5.81 (CH); 0.93 (Me), ^{13}C-NMR: δ 107.9 (CH_2, $^1J_{CH}$ 155, 157 Hz), 148.9 (CH, $^1J_{CH}$ 151 Hz), 27.8 (Me, $^1J_{CH}$ 125 Hz), 33.0 (quaternary C). *A combination of HSQC and HMBC allowed a full characterization of the 1,2,2-trimethyl-1-butene: δ_H 4.64 and 4.60 (CH_2); 1.69 (Me);*

0.98 (^{t}Bu), δ_C 106.5 (CH_2, $^1J_{CH}$ 155 Hz and 154 Hz, respectively); 18.8 (Me, $^1J_{CH}$ 126 Hz); 28.7 (Me of ^{t}Bu, $^1J_{CH}$ 128 Hz); 34.8 (quaternary C of ^{t}Bu); 153.9 (internal olefinic C).

[Cp$_2$TiCH$_2$CH$_2$^{t}Bu]$^+$ (IV). ^{1}H NMR: δ –0.61 (t, $^3J_{HH}$ 7.7 Hz, 2H, β-H), 0.97 (s, 9H, CMe_3), 4.18 (t, $^3J_{HH}$ 7.7 Hz, 2H, α-H), 6.88 (s, 10H, Cp). ^{13}C-NMR: δ 94.7 (α-C, $^1J_{CH}$ 145 Hz), 55.7 (β-C, $^1J_{CH}$ 117 Hz), 28.2 (Me, $^1J_{CH}$ 126 Hz), 35.9 (quaternary C), 120.5 (Cp, $^1J_{CH}$ 178 Hz).

[Cp$_2$TiCH$_2$CHMe^{t}Bu(Et$_2$O)]$^+$ (V). m the α-a (δ_H -0.31, triplet, ~3.2Hz), upfield in the ^{1}H-NMR (see fig. 2.2), the n-α (δ_H 4.78, doublet of doublet, 3.5 Hz and 11.3 Hz), the β-H (δ_H 2.54, multiplet) and γ-Me (δ_H 0.48, doublet, 6.6 Hz) were easily linked together by a COSY experiment (see fig. B10). NOESY (see fig. B11) was useful to link this segment to its corresponding ^{t}Bu (δ_H 0.75), Cp's (δ_H 6.43, 6.39) and Et_2O portions (δ_H(CH_2) 3.06 and 3.45 (diastereotopic), multiplets; δ_H(CH_3) 1.10). A HSQC experiment (see fig. B12) was performed to obtain the ^{13}C chemical shift and the $^1J_{CH}$ coupling constants (see fig. B12, δ_C 119.5 (α-CH_2, $^1J_{CH}$ 107 Hz and 132 Hz); 55.2 (β-CH, $^1J_{CH}$ 124 Hz); 16.6 (γ-Me, $^1J_{CH}$ 124 Hz); 26.3 (Me of ^{t}Bu, $^1J_{CH}$ 124 Hz); 68.9 (CH_2 of Et_2O, $^1J_{CH}$ 148 Hz and 149 Hz); 11.8 (CH_3 of Et_2O, $^1J_{CH}$ 130 Hz); 116.5 (Cp, $^1J_{CH}$ 176 Hz); 116.7 (Cp, $^1J_{CH}$ 176 Hz)). Finally, a HMBC (see fig. B13) was performed to find the chemical shift of the quaternary C of tBu (35.9) and to confirm the connectivity of the alkyl backbone.

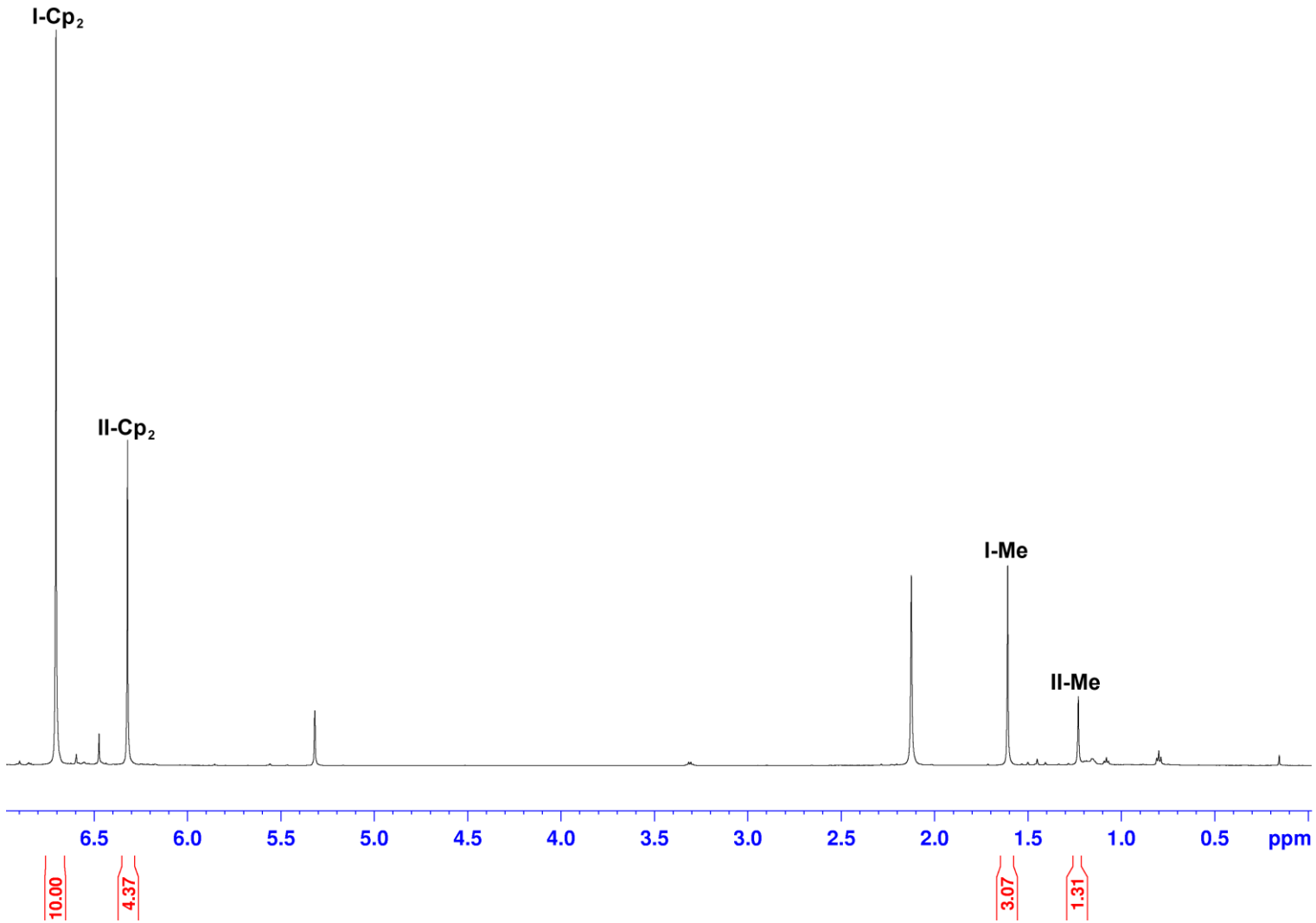

Figure B1. ^{1}H-NMR spectrum of a typical mixture of **I** and **II** in CD_2Cl_2 205 K. The methyl resonance of 2,2,2-triphenylethane (2.13 ppm, singlet) is also present on this portion of the spectrum but the aryl region of the spectrum is not shown.

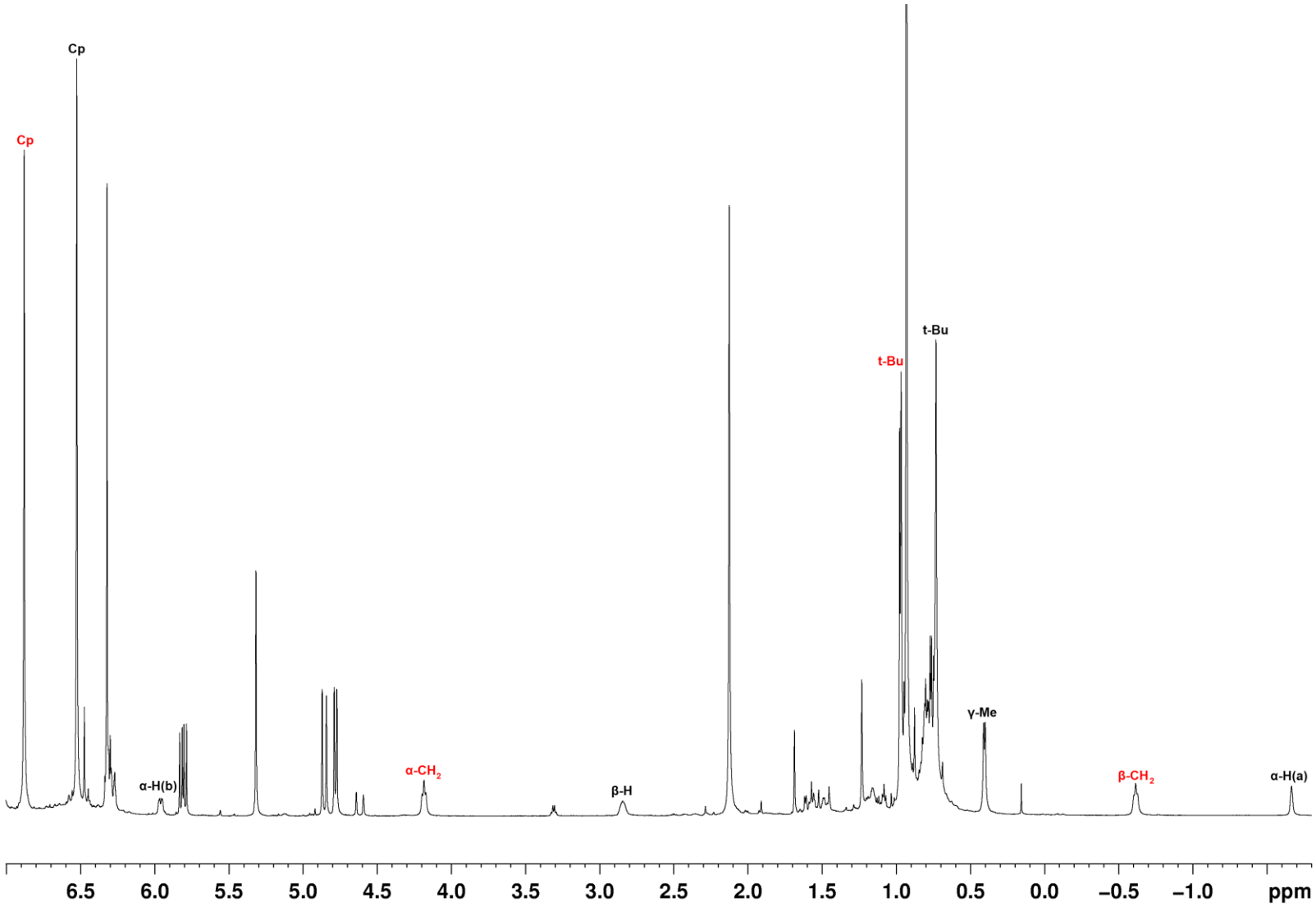

Figure B2. ^{1}H-NMR spectrum of **III** (black) and **IV** (red) in CD_2Cl_2 at 205 K. Resonances of excess 3,3-dimethyl-1-butene are also observed at δ 0.93 (t-Bu), 4.78 (olefinic methylene H, cis to methyne), 4.86 (olefinic methylene H, trans to methyne), 5.81 (methyne).

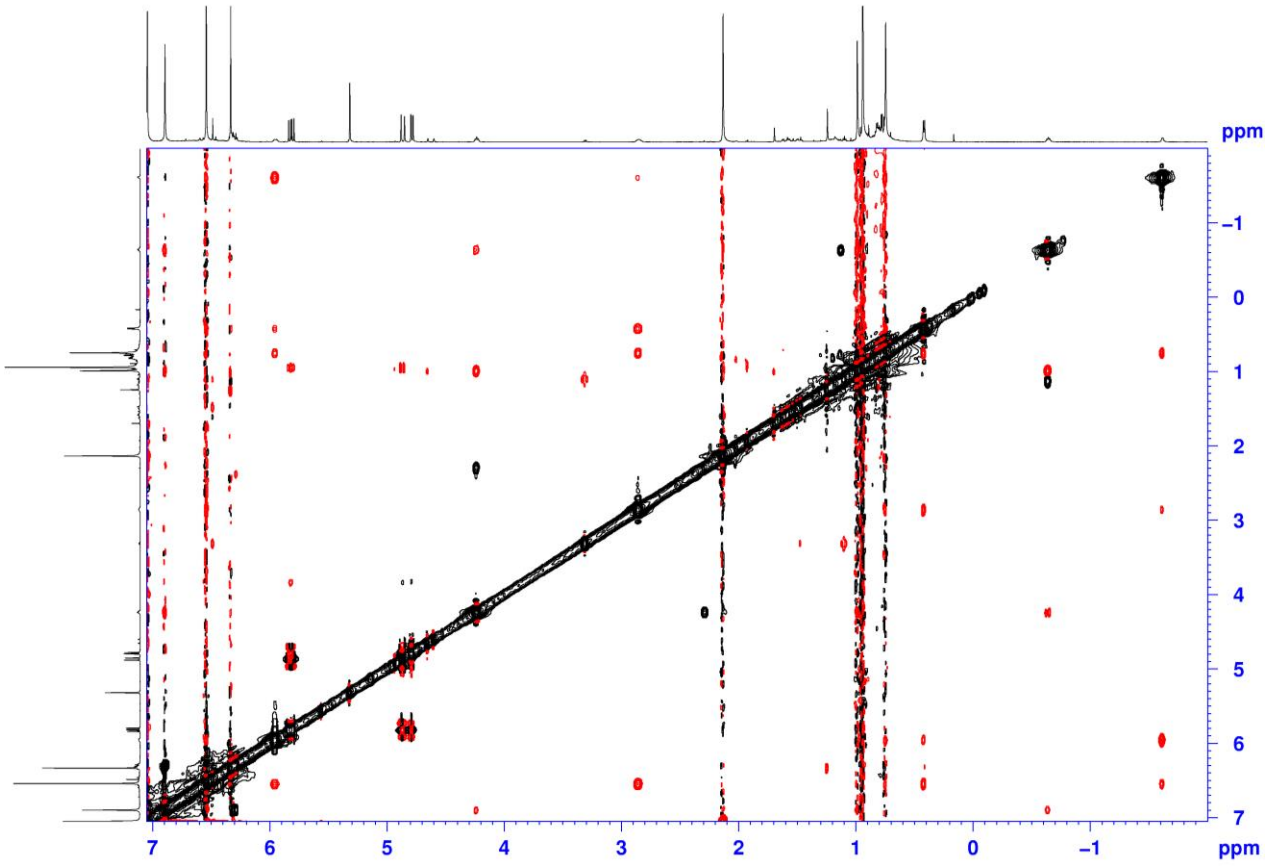

Figure B3. NOESY spectrum of **III** and **IV** and 3,3-dimethyl-1-butene in CD_2Cl_2 at 215 K; 3,3-dimethyl-1-butene was present in large excess in this sample. This sample contained predominantly the kinetic product **III** and exhibits NOE correlations between what is clearly the Cp resonance of **III**, at δ 6.53, with the single proton resonances at δ −1.66, 2.85 and 5.97 and with the three proton methyl resonance at δ 0.41, while the apparent *t*-Bu resonance (9H) at δ 0.73 exhibited NOEs to the resonances at δ −1.66, 0.41, 2.85 and 5.97. Also apparent are correlations of the resonances of of **IV**: between the Cp resonance at δ 6.88 and the triplet at δ 4.18, between the t-Bu resonance at δ 0.97 and the triplet at δ −0.61, and between the triplets at δ 4.18 and −0.61.

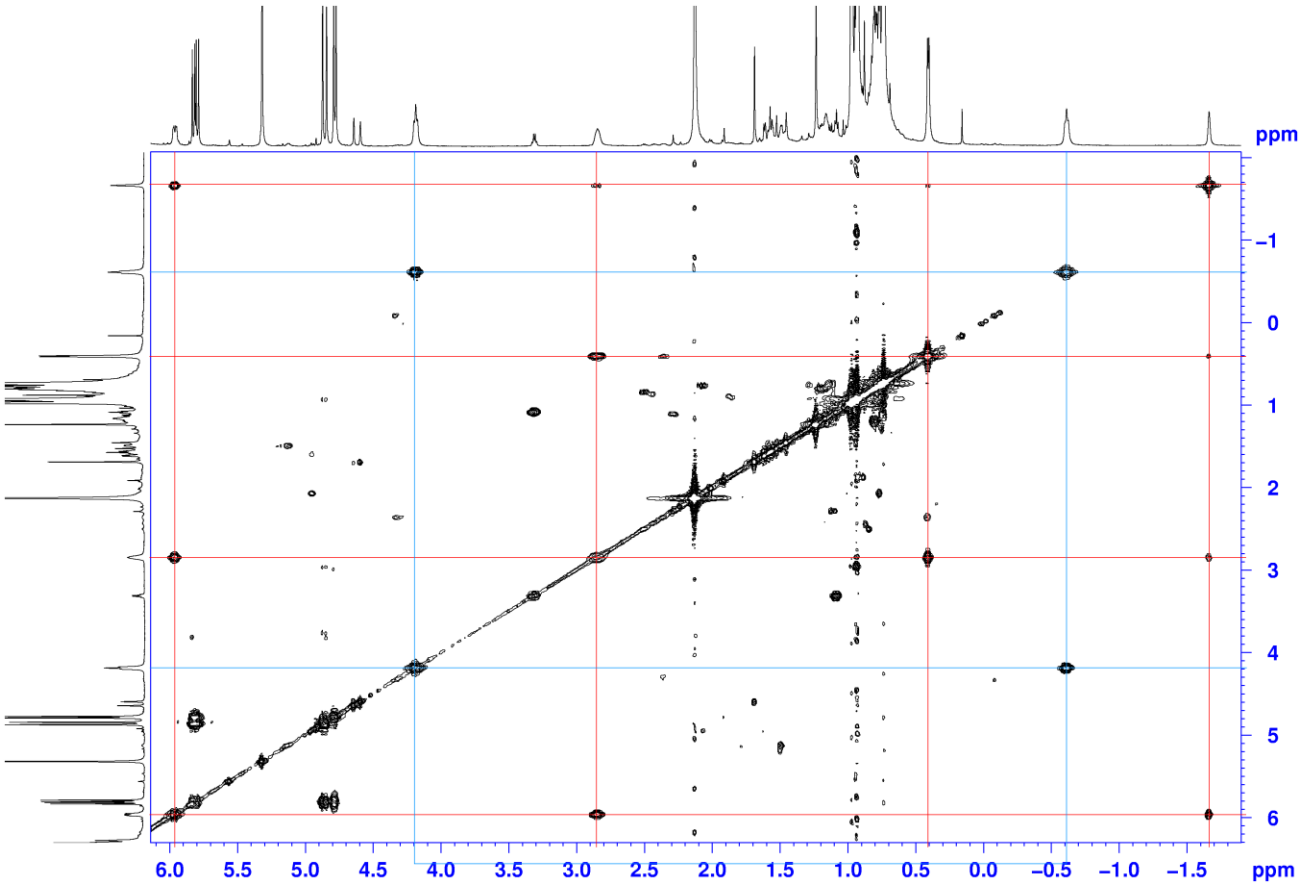

Figure B4. COSY spectrum of **III** (red lines) and **IV** (blue lines) in CD_2Cl_2 at 205 K. This spectrum exhibits correlations between the resonance at δ −1.66 with those at δ 0.41, 2.85 and 5.97, between the resonance at δ 0.41 with that at δ 2.85, and between the resonance at δ 2.85 with that at δ 5.97. Thus all of these resonances are to be attributed to $[Cp_2TiCH_2CHMe^tBu]^+$ (**III**). The two hydrogen atoms on the α-C atom are diastereotopic because the β-C atom is a stereogenic centre. Also apparent are correlations of the two types of CH_2 resonances of **IV**, the triplets at δ 4.18 and −0.61.

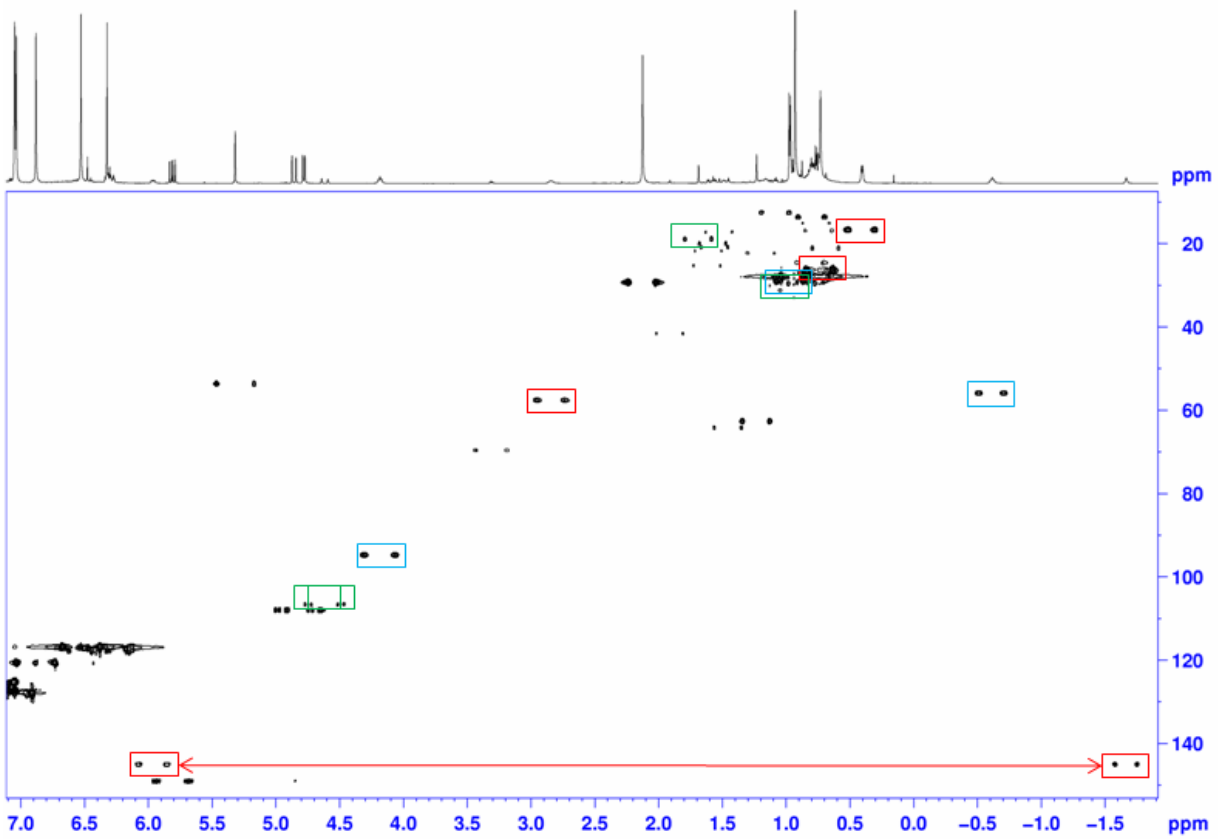

Figure B5. HSQC spectrum of **III** (red squares)**, IV** (blue squares) and 3,3-dimethyl-1-butene (green squares) in CD_2Cl_2 at 205 K. The ^{13}C-decoupler was turned off during acquisition leading to the splitting of signals in the H-axis and allowing measurement of $^1J_{CH}$ using the row trace of interest for higher accuracy. 3,3-dimethyl-1-butene was present in excess. This spectrum exhibits correlations between the ^1H resonances at δ 0.41 (γ-Me), 0.73 (*t*-Bu), 2.85 (β-H) and 6.53 (Cp) with ^{13}C resonances at δ 16.6 (γ-Me, $^1J_{CH}$ 126 Hz), 26.2 (Me of *t*-Bu, $^1J_{CH}$ 124 Hz), 57.5 (β-C, $^1J_{CH}$ 129 Hz) and 116.6 (Cp, $^1J_{CH}$ 178 Hz). Of great interest and significance, the ^1H resonances at δ −1.66 and 5.97 both correlated with the same ^{13}C resonance, at δ 144.9 (α-C, $^1J_{CH}$ = 104, 133 Hz, respectively), and therefore are to be assigned to the α-H atoms, designated α-H(a) and α-H(b), respectively

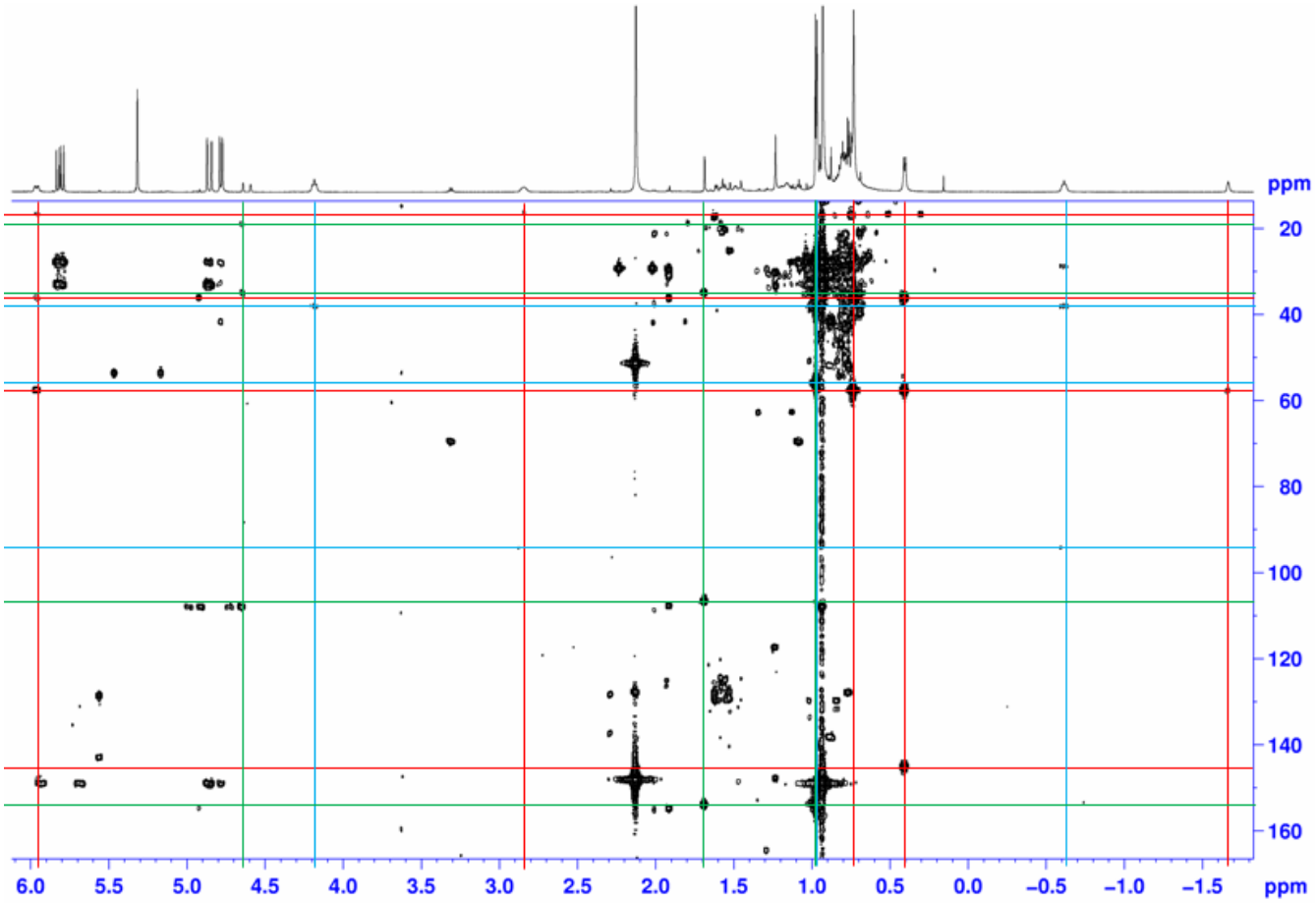

Figure B6. HMBC spectrum of **IV** (red lines) and **V** (blue lines) and 3,3-dimethyl-1-butene (green lines) in CD_2Cl_2 at 205 K. 3,3-dimethyl-1-butene was present in large excess in this sample. This spectrum exhibits long range couplings between the α-H resonances at δ −1.66 and 5.97 and the ^{13}C resonance of the β-C atom at δ 57.5, between the γ-Me resonance at δ 0.41 and the ^{13}C resonances at δ 35.9 (*t*-Bu tertiary C), 57.5 (β-C) and 144 (α-C).

DFT Methods

Geometries of all minima and transition states were optimized at the b-p[1,2]/TZVP[3] level using the Turbomole program[4] coupled to an external optimizer.[5] Final geometries were checked by a vibrational analysis (0 imaginary frequencies for minima, 1 for transition states), which was also used to calculate thermal corrections (enthalpy and entropy). Single-point calculations were then carried out with a larger basis set (TZVPP[6]) and inclusion of an electronic correction for solvent effects using COSMO[7] ($\varepsilon = 9.1$, CH_2Cl_2). These improved energies were combined with the above thermal corrections (entropy scaled by 0.67 to account for reduced freedom of motion in solution[8]) to obtain the final free energies mentioned in the text. We previously found[9] that prediction of NMR parameters is more accurate with the hybrid functional B3LYP. Therefore, relevant structures were re-optimized at the b3-lyp[10]/TZVP level and chemical shifts and coupling constants were then calculated using Gaussian 03[11] with the B3LYP functional[10a,10c,12] and the IGLO-III[13] basisset (TZVP basis on Ti).

Table B1. Important calculated bond lengths, bond angles and torsional angles of conformations **IVa** and **IVb**.

Structural parameter	Bond lengths (Å)	
	IVa	**IVb**
Ti-(α-C)	2.099	2.093
(α-C)-(β-C)	1.520	1.525
(β-C)-(β-Me)	1.541	1.545
(β-C)-(γ-C)	1.581	1.574
(β-C)-(β-H)	1.093	1.093
(α-C)-α-H(a)	1.143	1.146
(α-C)-α-H(b)	1.087	1.086
Ti-α-H(a)	2.041	2.030
Ti-α-H(b)	2.696	2.700

	Bond angles (°)	
Ti-(α-C)-(β-C)	135.24	136.23
Ti-(α-C)-α-H(a)	71.20	70.82
Ti-(α-C)-α-H(b)	111.65	112.33
(α-C)-(β-C)-(β-Me)	107.29	108.86
(α-C)-(β-C)-(γ-C)	114.12	112.21

	Dihedral angles (°)	
Ti-(α-C)-(β-C)-(β-Me)	89.01	-125.11
Ti-(α-C)-(β-C)-(β-H)	–27.56	-8.65
Ti-(α-C)-(β-C)-(γ-C)	–144.51	108-25
α-H(a)-(α-C)-(β-C)-(β-H)	58.35	58.35
α-H(b)-(α-C)-(β-C)-(β-H)	176.75	70.06

Table B2. Comparison of calculated and observed NMR parameters for **IV**.

	α1	α2	β	γ	Obs'd
δ(Hα1)	-2.82	11.05	5.02	3.34	-1.66
^{1}J(C-Hα1)	80	137	143	139	105
δ(Hα2)	10.86	-3.78	5.67	5.75	5.96
^{1}J(C-Hα2)	138	79	145	133	133
δ (Cα)	211.0	216.9	105.5	97.1	144.9
δ(Hβ)	4.44	4.42	-3.40	2.16	2.85
^{1}J(C-Hβ)	124	125	90	125	130
δ(Cβ)	75.5	76.8	71.6	43.0	57.5
δ(Hγ) av	0.86	1.32	1.82	-0.94	0.41
^{1}J(C-Hγ) av	124	124	125	120	125
δ(Cγ)	16.9	22.0	27.1	16.0	16.6

References

1. (a) Becke, A. D., *Phys Rev A* **1988,** *38* (6), 3098;(b) Perdew, J. P., *Phys Rev B* **1986,** *33* (12), 8822.
2. All Turbomole calculations were performed with the functionals "b-p" and "b3-lyp" of that package, which are similar (but not identical) to the Gaussian "BP86" and "B3LYP" functionals.
3. Schafer, A.; Huber, C.; Ahlrichs, R., *J Chem Phys* **1994,** *100* (8), 5829.
4. (a) Treutler, O.; Ahlrichs, R., *J Chem Phys* **1995,** *102* (1), 346;(b) Ahlrichs, R.; Bär, M.; Baron, H.-P.; Bauernschmitt, R.; Böcker, S.; Ehrig, M.; Eichkorn, K.; Elliott, S.; Furche, F.; Haase, F.; Häser, M.; Hättig, C.; Horn, H.; Huber, C.; Huniar, U.; Kattannek, M.; Köhn, A.; Kölmel, C.; Kollwitz, M.; May, K.; Ochsenfeld, C.; Ohm, H.; Schäfer, A.; Schneider, U.; Treutler, O.; Tsereteli, K.; Unterreiner, B.; Von Arnim, M.; Weigend, F.; Weis, P.; Weiss, H. *Turbomole*, 5; Theoretical Chemistry Group, University of Karlsruhe: 2002.

5. (a) Baker, J., *J Comput Chem* **1986,** *7* (4), 385;(b) Baker, J. *PQS*, 2.4; Parallel Quantum Solutions: Fayetteville, AR, 2001.
6. Weigend, F.; Furche, F.; Ahlrichs, R., *J Chem Phys* **2003,** *119* (24), 12753.
7. Klamt, A.; Schuurmann, G., *J Chem Soc Perk T 2* **1993,** (5), 799.
8. (a) Tobisch, S.; Ziegler, T., *J Am Chem Soc* **2004,** *126* (29), 9059;(b) Raucoules, R.; de Bruin, T.; Raybaud, P.; Adamo, C., *Organometallics* **2009,** *28* (18), 5358.
9. Sauriol, F.; Sonnenberg, J. F.; Chadder, S. J.; Dunlop-Briere, A. F.; Baird, M. C.; Budzelaar, P. H. M., *J Am Chem Soc* **2010,** *132* (38), 13357.
10. (a) Becke, A. D., *J Chem Phys* **1993,** *98* (7), 5648;(b) Becke, A. D., *J Chem Phys* **1993,** *98* (2), 1372;(c) Lee, C. T.; Yang, W. T.; Parr, R. G., *Phys Rev B* **1988,** *37* (2), 785.
11. Frisch, M. J.; Trucks, G. W.; Schlegel, H. B.; Scuseria, G. E.; Robb, M. A.; Cheeseman, J. R.; Montgomery Jr., J. A.; Vreven, T.; Kudin, K. N.; Burant, J. C.; Millam, J. M.; Iyengar, S. S.; Tomasi, J.; Barone, V.; Mennucci, B.; Cossi, M.; Scalmani, G.; Rega, N.; Petersson, G. A.; Nakatsuji, H.; Hada, M.; Ehara, M.; Toyota, K.; Fukuda, R.; Hasegawa, J.; Ishida, M.; Nakajima, T.; Honda, Y.; Kitao, O.; Nakai, H.; Klene, M.; Li, X.; Knox, J. E.; Hratchian, H. P.; Cross, J. B.; Bakken, V.; Adamo, C.; Jaramillo, J.; Gomperts, R.; Stratmann, R. E.; Yazyev, O.; Austin, A. J.; Cammi, R.; Pomelli, C.; Ochterski, J. W.; Ayala, P. Y.; Morokuma, K.; Voth, G. A.; Salvador, P.; Dannenberg, J. J.; Zakrzewski, V. G.; Dapprich, S.; Daniels, A. D.; Strain, M. C.; Farkas, O.; Malick, D. K.; Rabuck, A. D.; Raghavachari, K.; Foresman, J. B.; Ortiz, J. V.; Cui, Q.; Baboul, A. G.; Clifford, S.; Cioslowski, J.; Stefanov, B. B.; Liu, G.; Liashenko, A.; Piskorz, P.; Komaromi, I.; Martin, R. L.; Fox, D. J.; Keith, T.; Al-Laham, M. A.; Peng, C. Y.; Nanayakkara, A.; Challacombe, M.; Gill, P. M. W.; Johnson, B.; Chen, W.; Wong, M. W.; Gonzalez, C.; Pople, J. A. *Gaussian 03*, C.02; Gaussian, Inc.: Wallingford CT, 2004.
12. Stephens, P. J.; Devlin, F. J.; Chabalowski, C. F.; Frisch, M. J., *J Phys Chem-Us* **1994,** *98* (45), 11623.
13. Kutzelnigg, W.; Fleischer, U.; Schindler, M., The IGLO-Method: Ab Initio Calculation and Interpretation of NMR Chemical Shifts and Magnetic Susceptibilities. In *NMR basic principles and progress*, Diehl, P.; Flück, E.; Günther, H.; Kosfeld, R.; Seelig, J., Eds. Springer-Verlag: Heidelberg, 1990; Vol. 23.

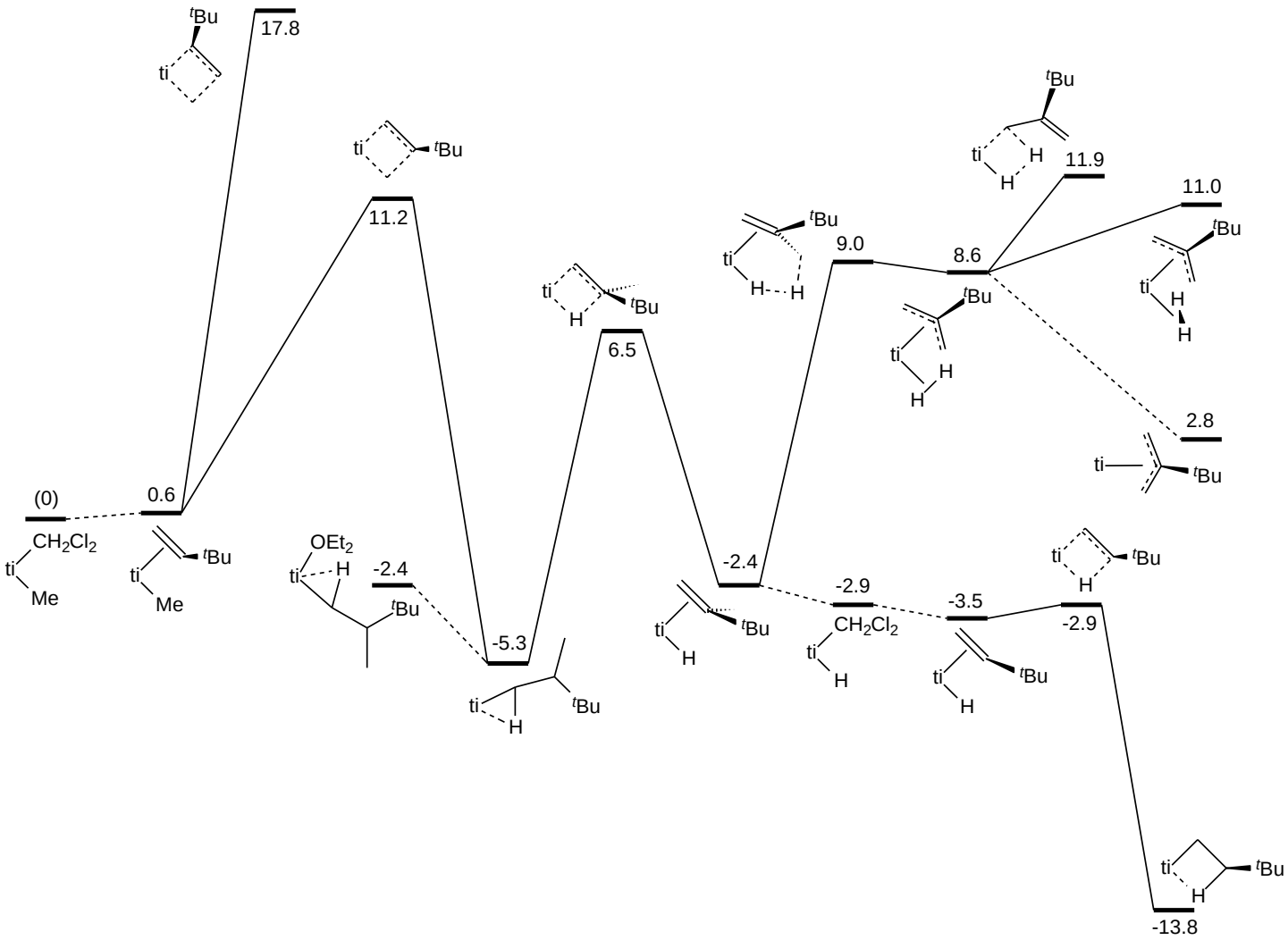

Figure B7. Free energy profile (kcal/mol) for the insertion reaction of $[Cp_2TiMe(CH_2Cl_2)]^+$ with $Me_3CCH{=}CH_2$ and subsequent rearrangements. Dotted lines indicate steps that might involve a separate ligand displacement barrier.

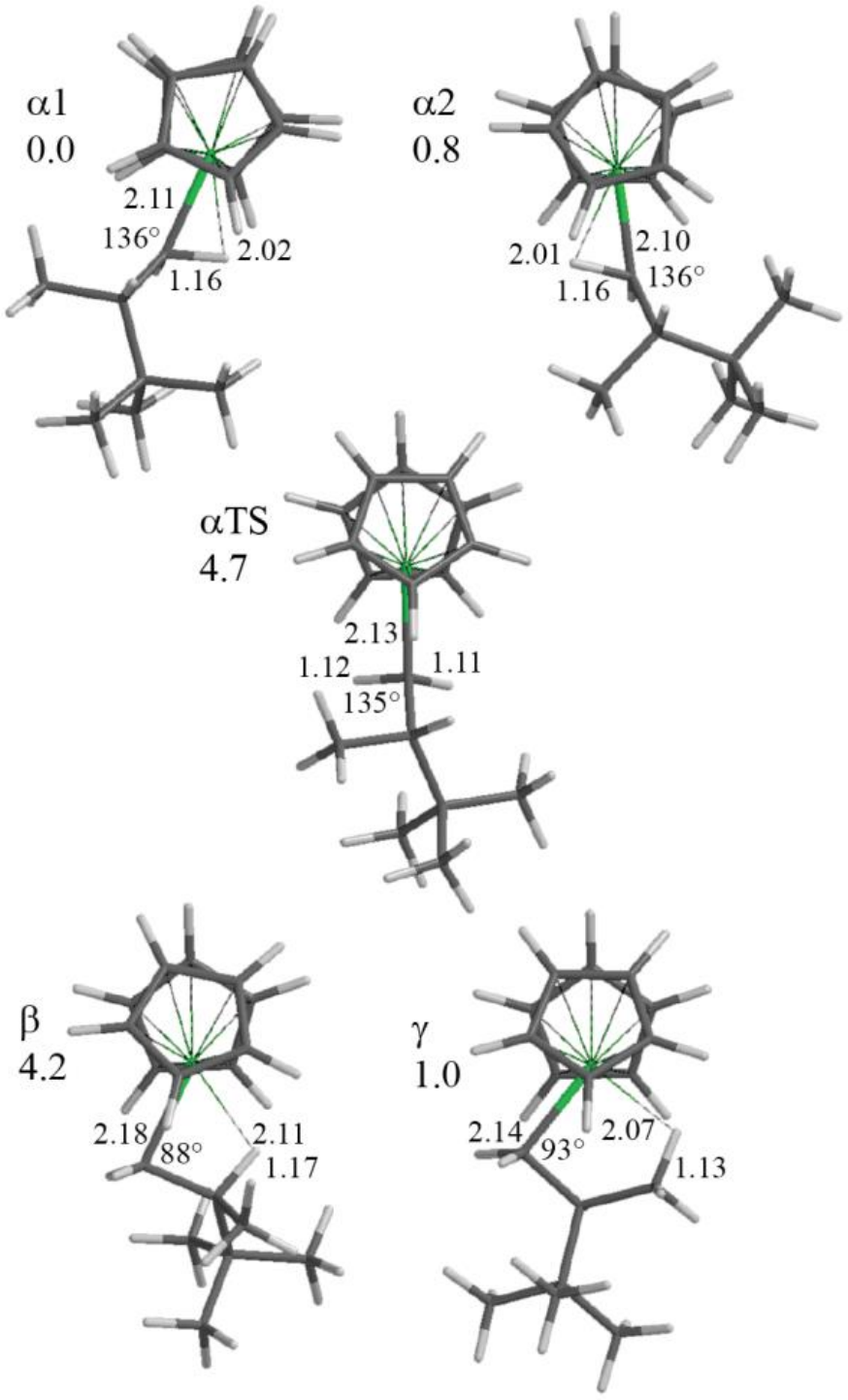

Figure B8. Structures of α, β and γ agostic isomers of $Cp_2TiCH_2CH(Me)(t\text{-}Bu)^+$. Bond lengths in Å, angles in degrees (all non-agostic aliphatic C-H bonds are 1.10 Å). Energies relative to α1.

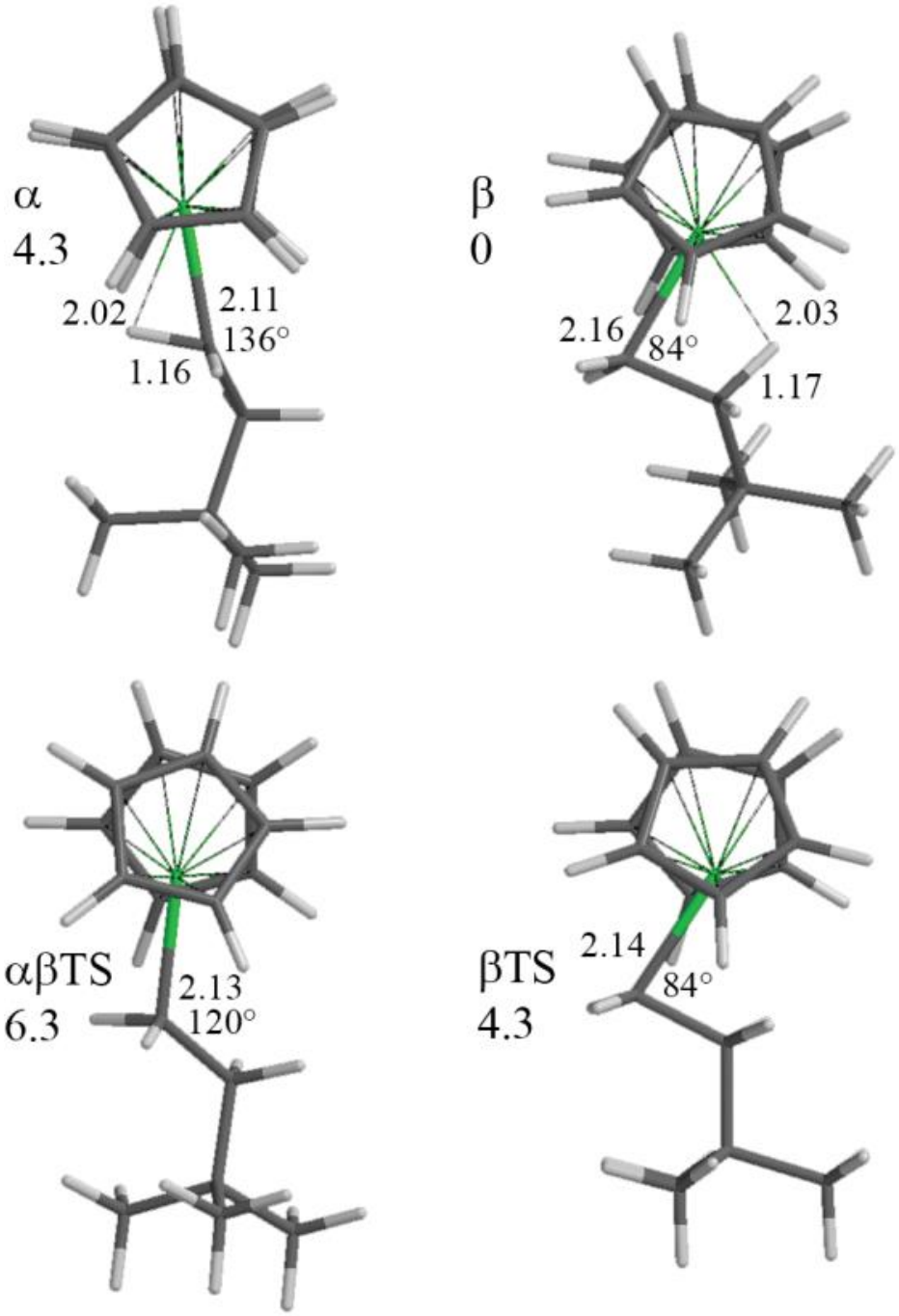

Figure B9. Structures of α and β agostic isomers of $Cp_2TiCH_2CH_2(t\text{-}Bu)^+$, and interconversion transition states. Bond lengths in Å, angles in degrees (all non-agostic aliphatic C-H bonds are 1.10 Å). Energies relative to β.

Appendix C

Supporting Information for Chapter 4:

$[Cp_2TiCH_2CHMe(SiMe_3)]^+$, an Alkyl—Titanium Complex Which (a) Exists in Equilibrium between a β-Agostic and a Lower Energy γ-Agostic Isomer and (b) Undergoes Hydrogen Atom Exchange between α-, β-, and γ- Sites via a Combination of Conventional β-Hydrogen Elimination-Reinsertion and a Nonconventional CH Bond Activation Process Which Involves Proton Tunneling

A. F. Dunlop-Brière and M. C. Baird*
Department of Chemistry, Queen's University,
Kingston, ON K7L 3N6, Canada
Email: bairdmc@chem.queensu.ca

Peter H. M. Budzelaar*
Department of Chemistry, University of Manitoba,
Winnipeg, MB R3T 2N2, Canada

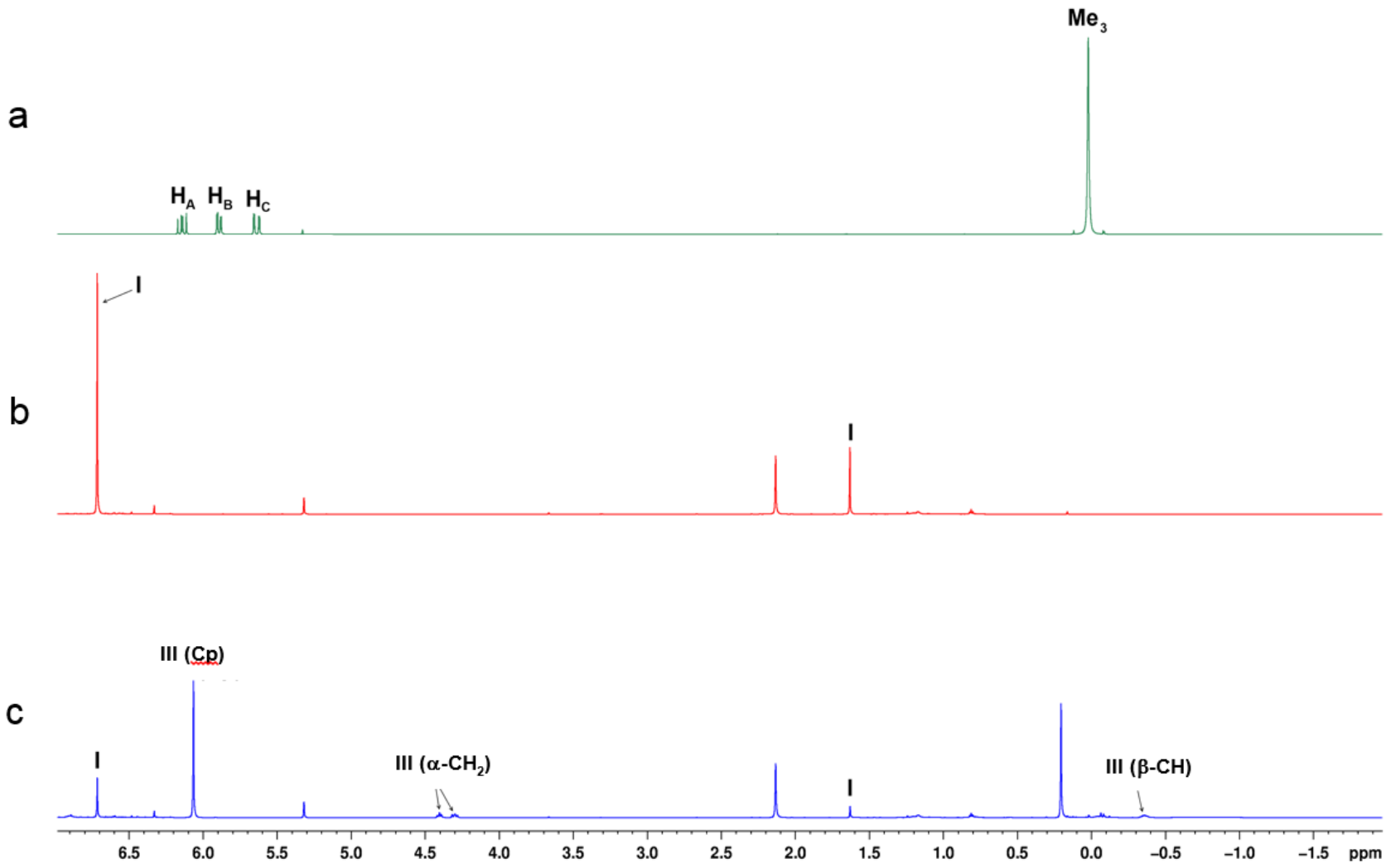

Figure C1. ^{1}H NMR spectra at 215 K in CD_2Cl_2 of (a) TMVS, (b) a mixture of **I** and $Cp_2TiMeB(C_6F_5)_4$, (c) a reaction mixture containing **III**, immediately after the addition of TMVS at 215 K. The methyl resonance of 2,2,2-triphenylethane is observed in (b) and (c) at δ 2.13 (s) but the aryl region of the spectrum is not shown.

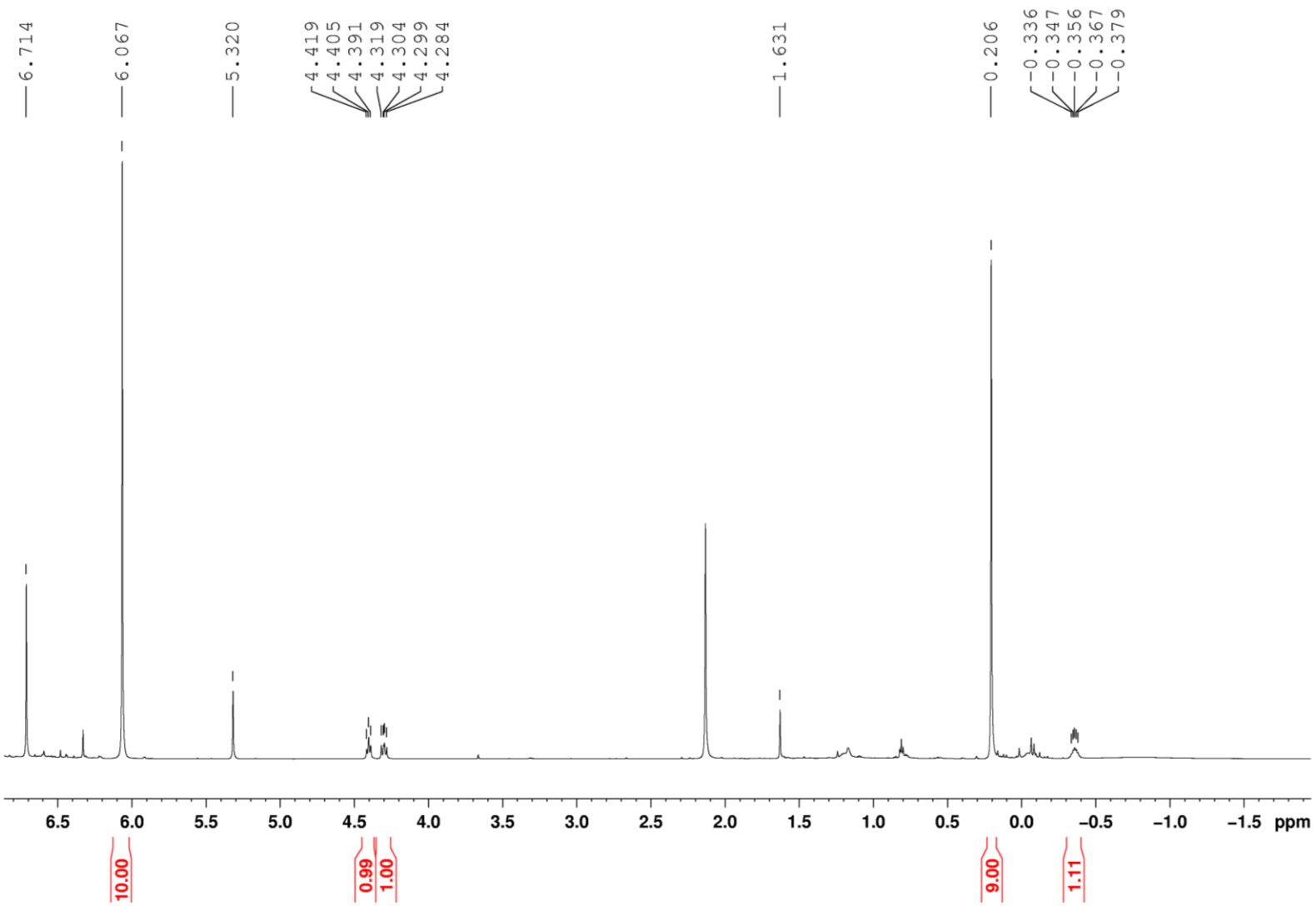

Figure C2. An expansion of spectrum (c) shown on the previous page.

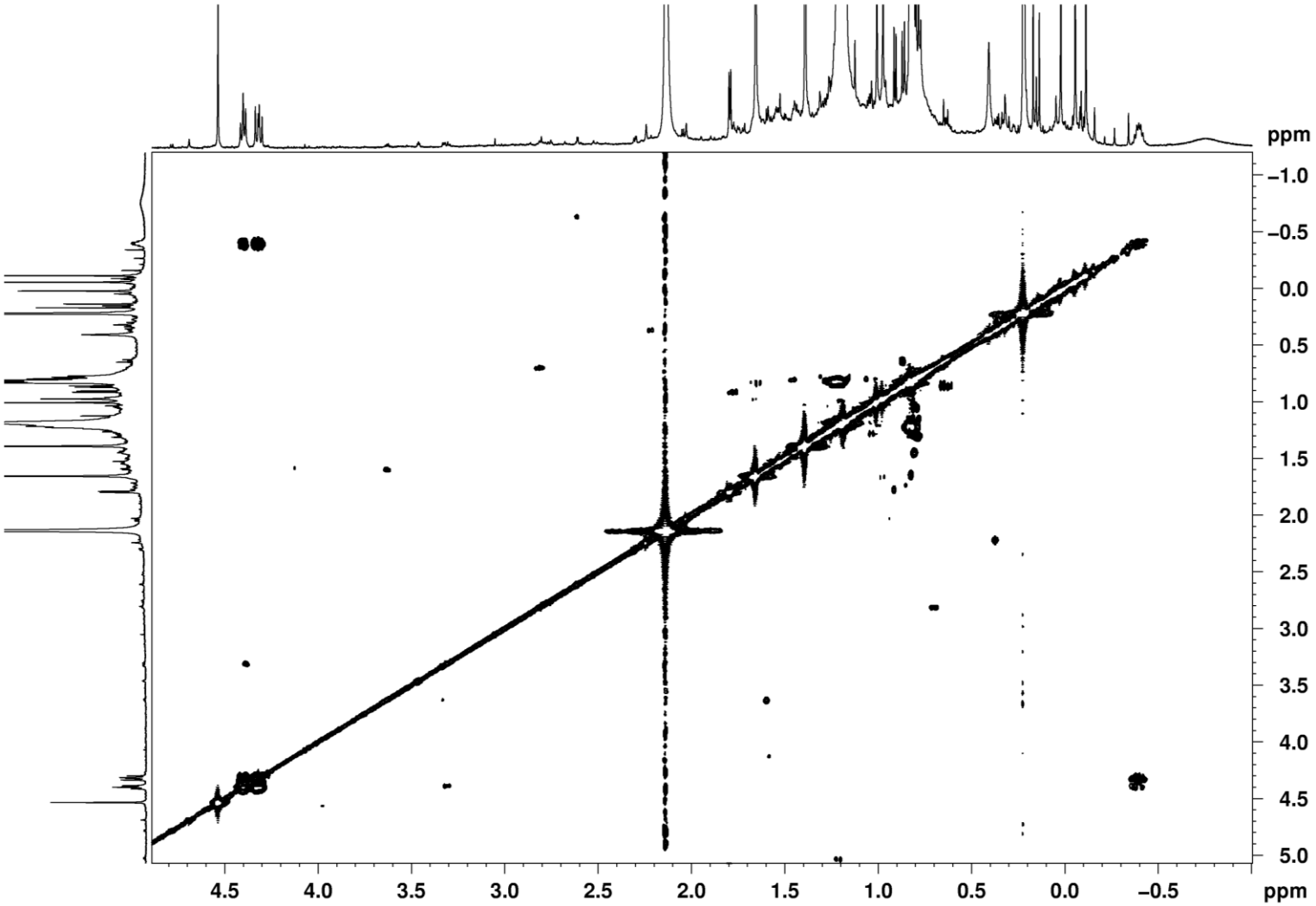

Figure C3. COSY spectrum of **III** in CD_2Cl_2 at 225 K showing geminal correlations between α-H, as well as the vicinal coupling of these to H_β. The mutual vicinal correlations of H_β and Me_γ are not apparent at that temperature, because Me_γ is too broad (half height width >> $^3J_{HH}$) to observe a COSY correlation.

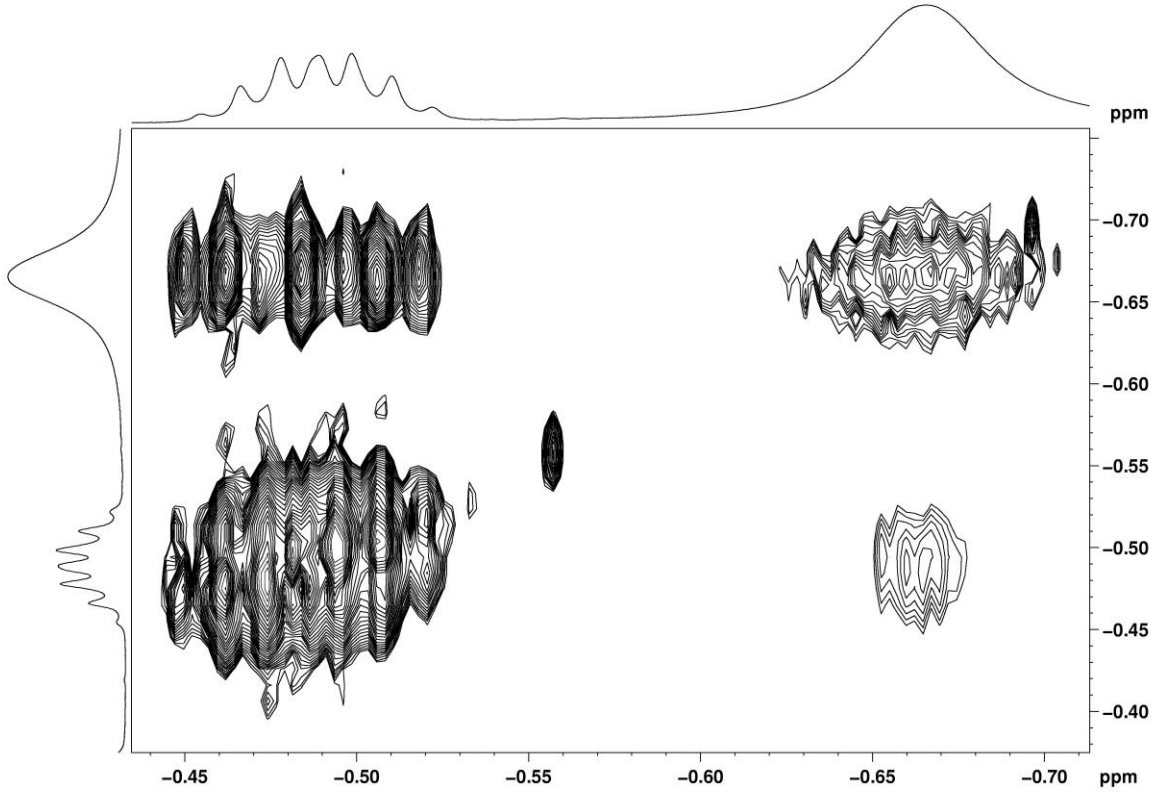

Figure C4. COSY spectrum of **III** in CD_2Cl_2 at 245 K in the high field region, showing the correlation between the β-H atom and the H atoms of the β-methyl group.

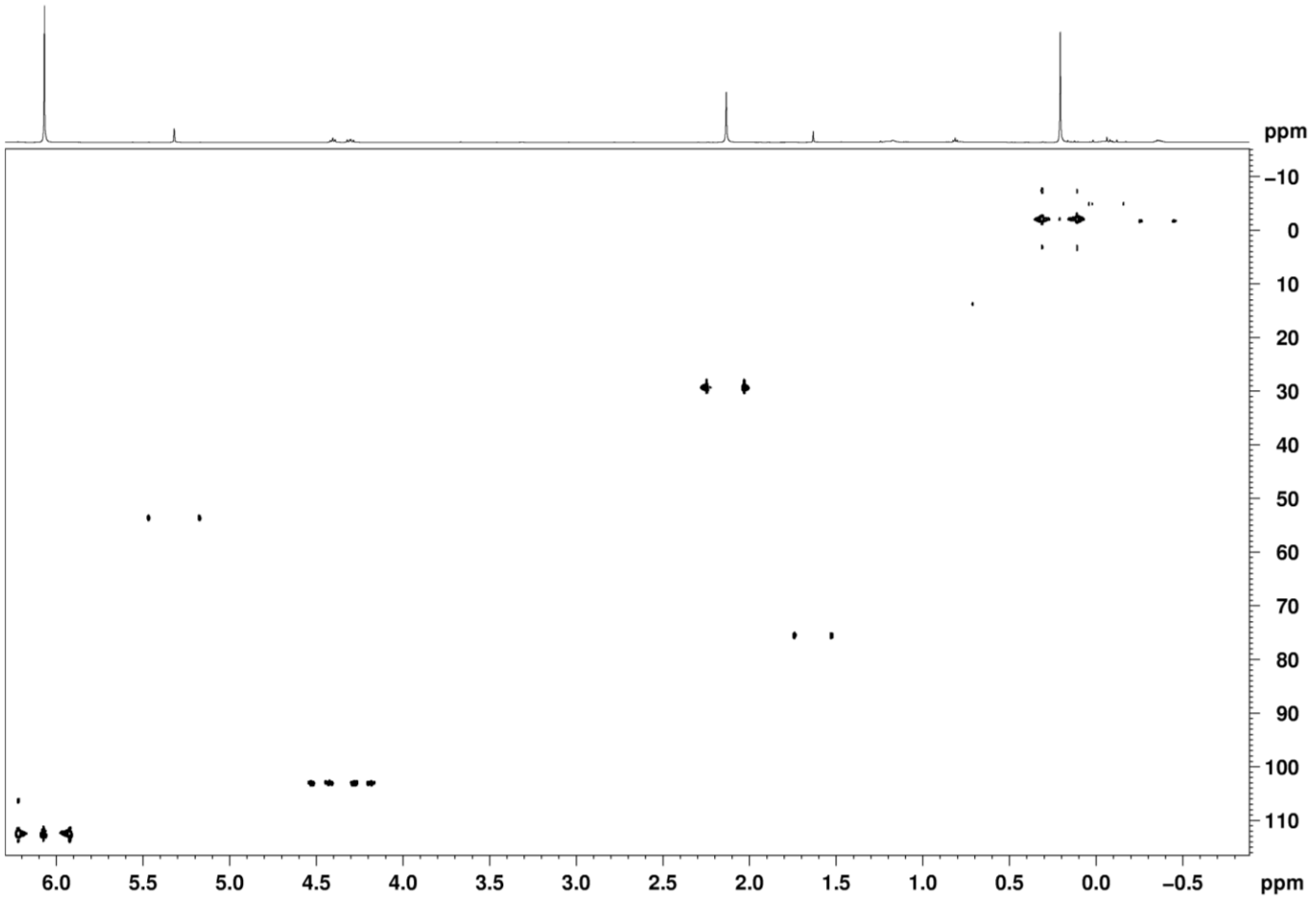

Figure C5. ^{13}C-^{1}H HSQC spectrum of **III** in CD_2Cl_2 at 215 K. The ^{13}C decoupler was not used during data acquisition and the correlation peaks shown are the projections of ^{13}C satellites in the horizontal (^{1}H) axis. Hence the difference between those satellite projections corresponds to the $^{1}J_{CH}$ coupling constants. Correlations of γ-Me were not observed at this temperature because of exchange broadening.

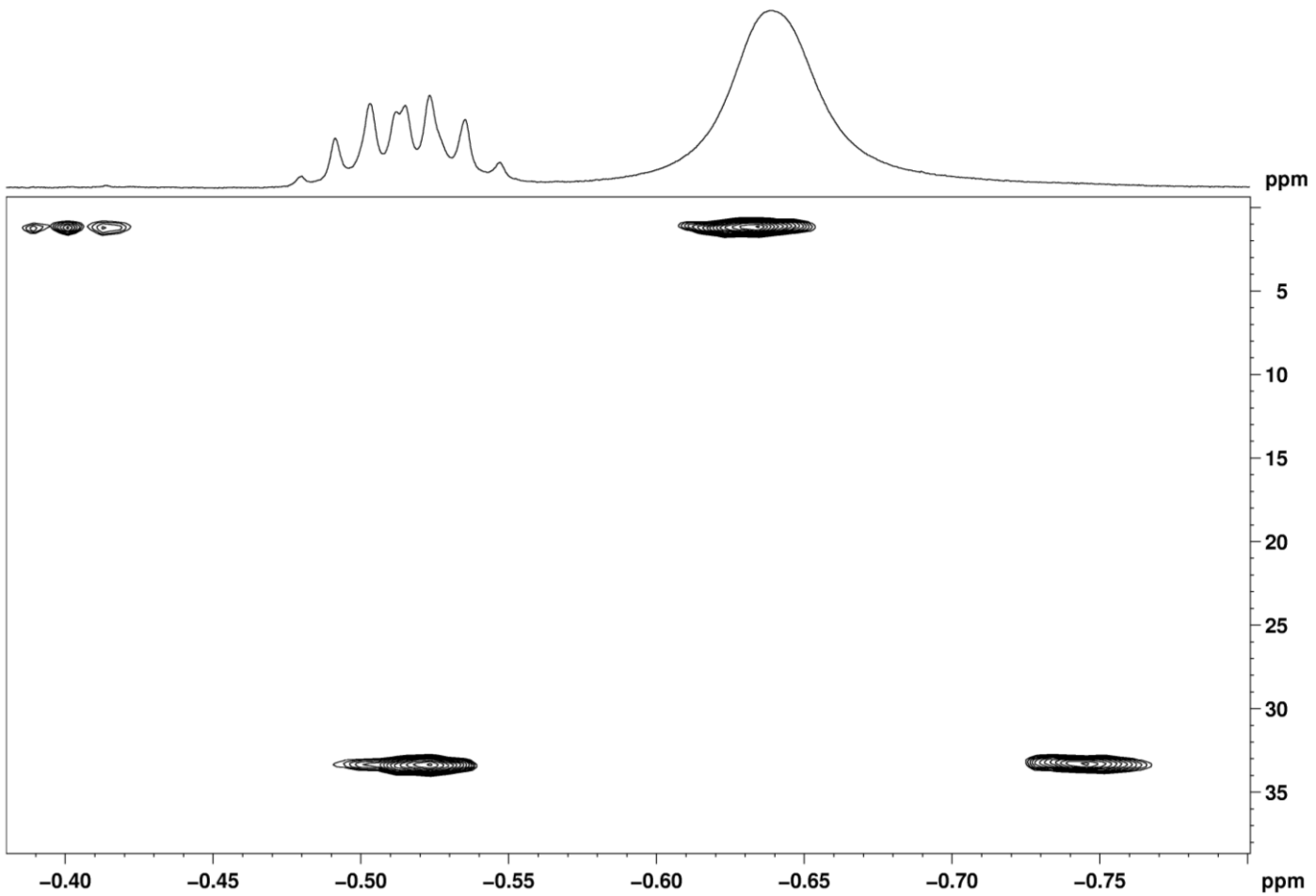

Figure C6. ^{13}C-^{1}H HSQC spectrum of **III** in CD_2Cl_2 at 250K in the high field region. The ^{13}C decoupler was not used during data acquisition and the correlation peaks shown are the projections of ^{13}C satellites in the horizontal (^{1}H) axis. Hence, the difference between those satellite projections corresponds to the $^{1}J_{CH}$ coupling constants.

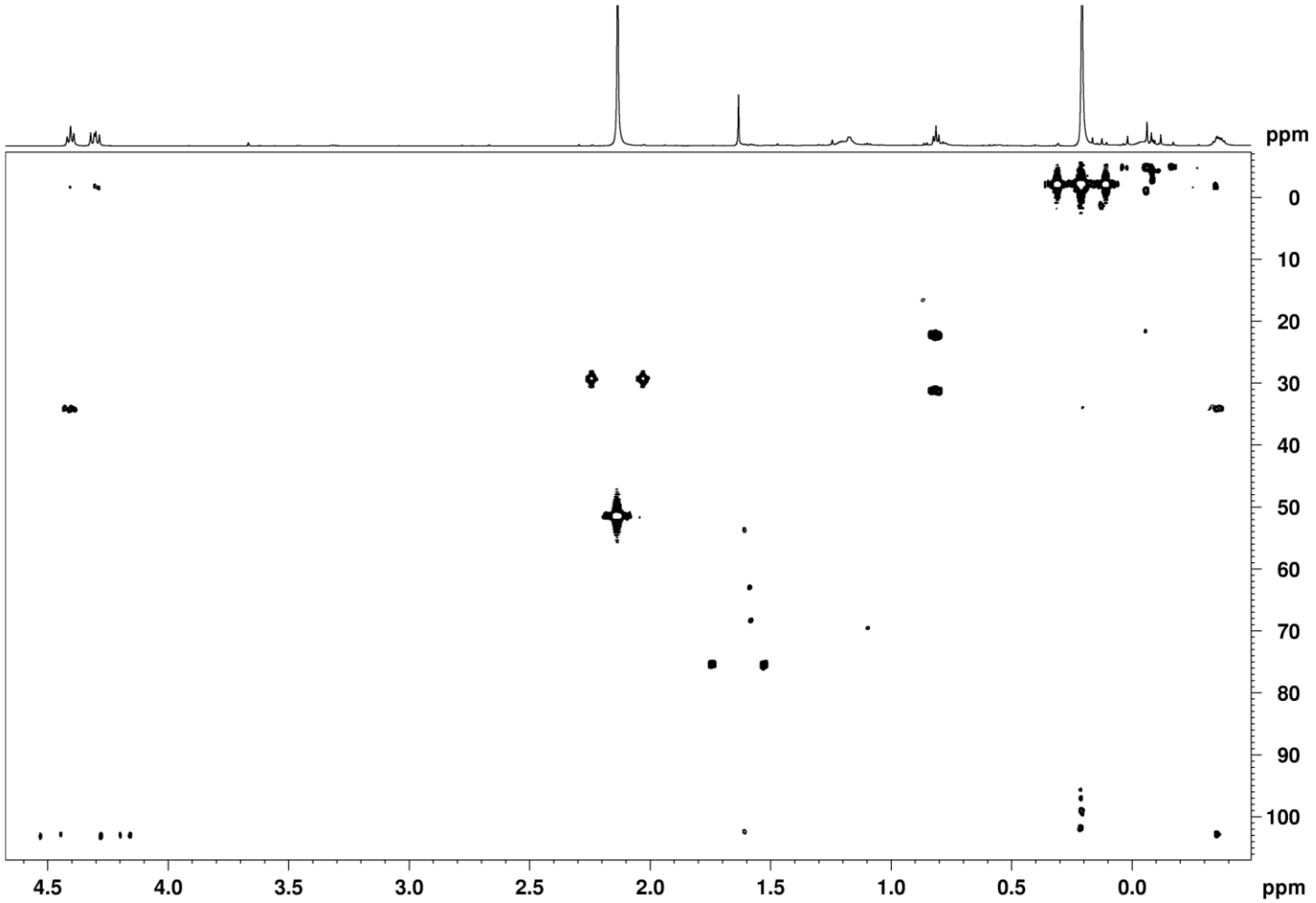

Figure C7. ^{13}C-^{1}H HMBC spectrum of **III** in CD_2Cl_2 at 215 K. Correlations of $H_{\alpha 1}$ and H_{β} to C of Me_{γ} establish connectivity between the methyl and the silylalkyl backbone.

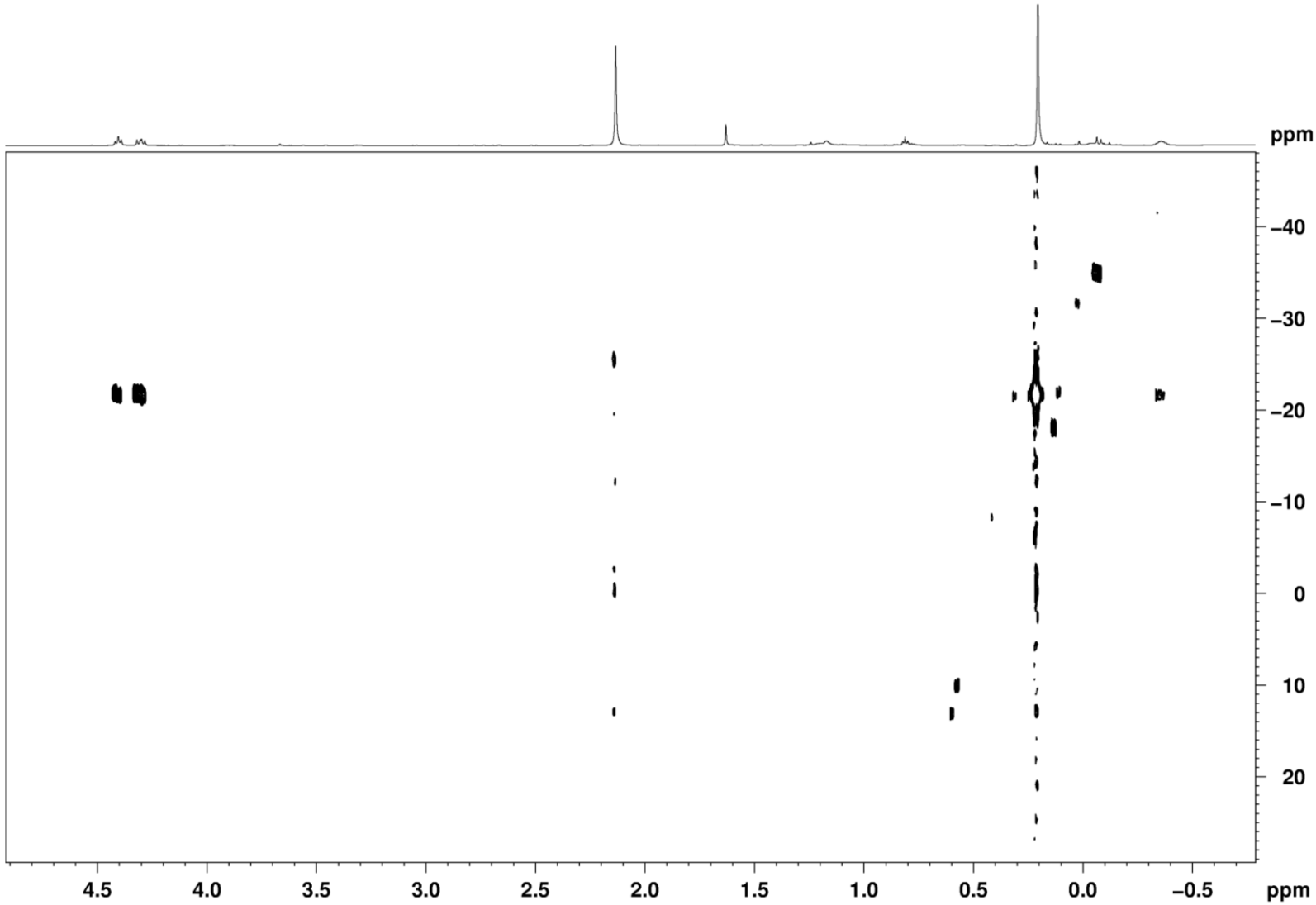

Figure C8. ^{29}Si-^{1}H HMBC spectrum of **III** in CD_2Cl_2 at 215 K.

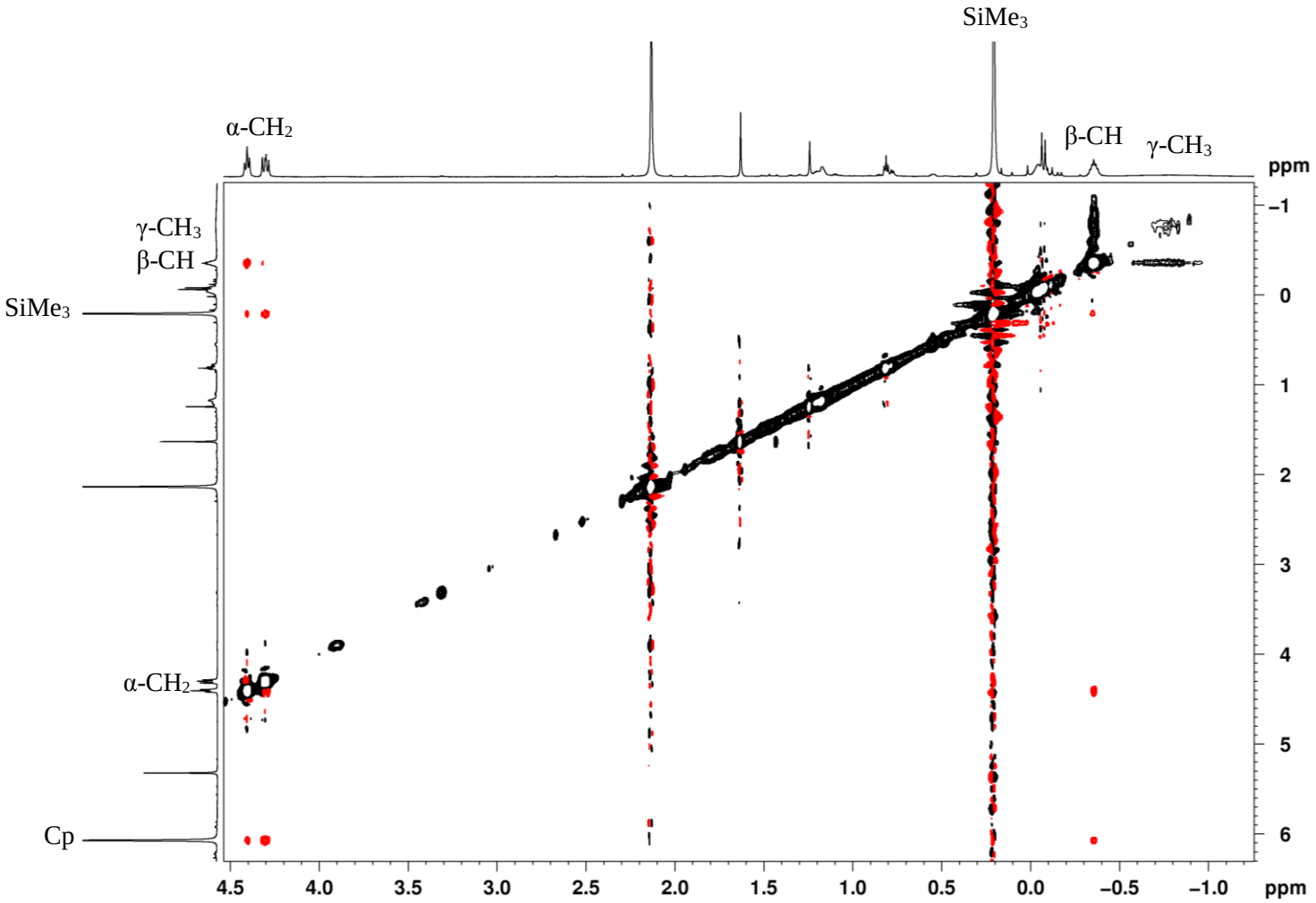

Figure C9. NOESY spectrum of **III** in CD_2Cl_2 at 215 K; Cp region omitted in the horizontal axis for clarity. Note that the correlations between the β-H and the γ-H of the β-Me are negative (black), indicating an exchange between these sites.

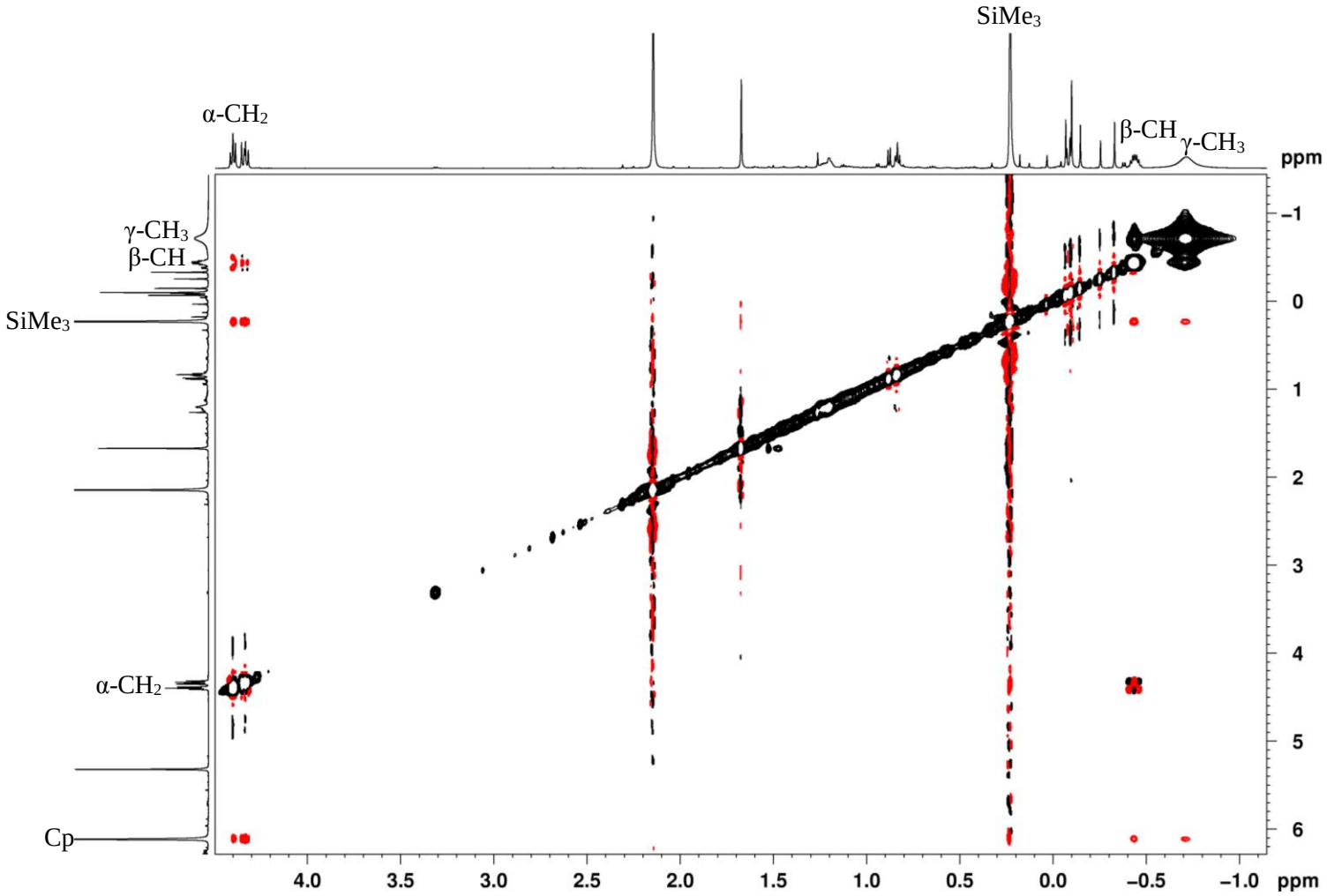

Figure C10. NOESY spectrum of **III** in CD_2Cl_2 at 235 K; Cp region omitted in the horizontal axis for clarity. Note that the correlations between the β-H and the γ-H of the β-Me are negative (black), indicating an exchange between these sites.

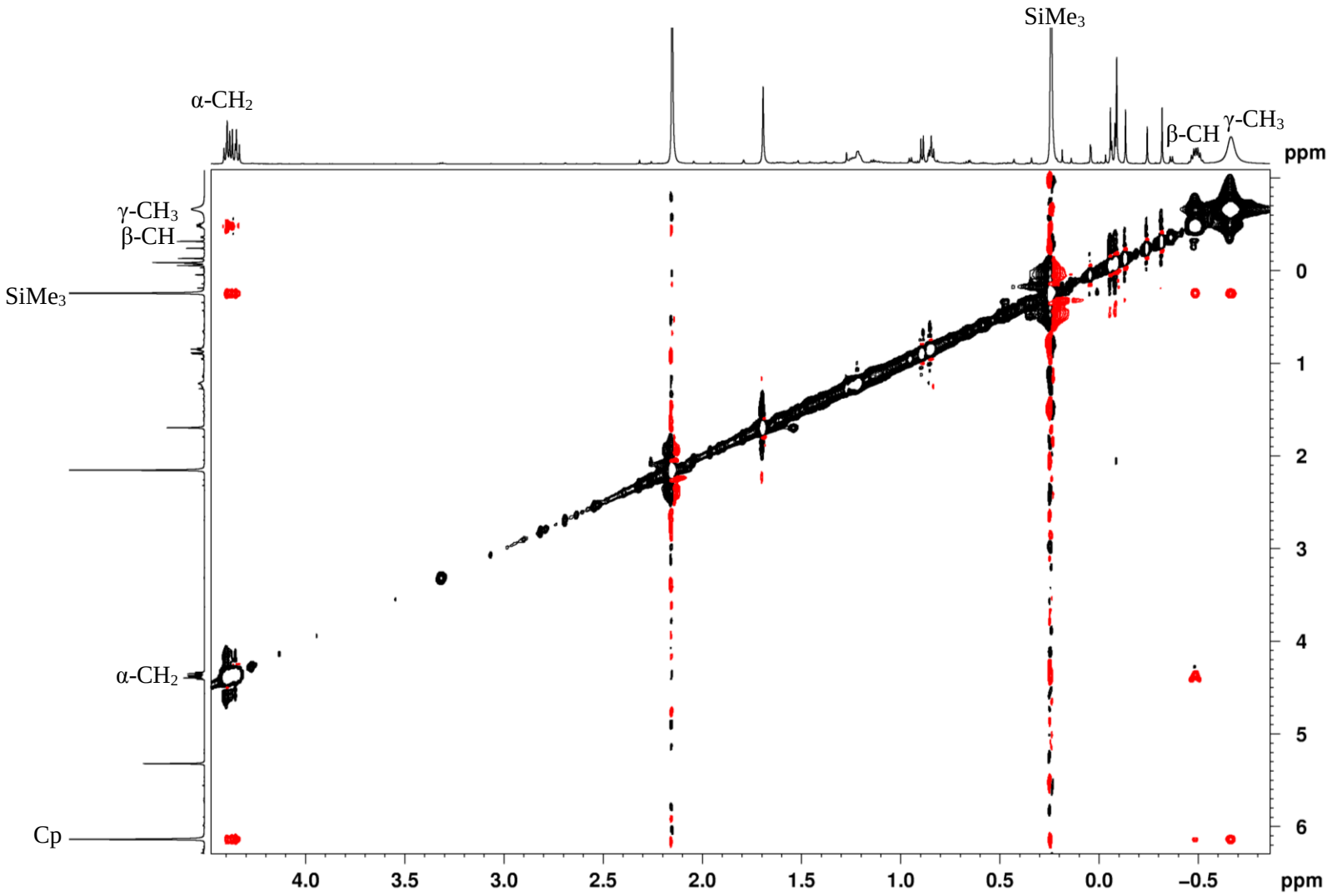

Figure C11. NOESY spectrum of **III** in CD_2Cl_2 at 245 K; Cp region omitted in the horizontal axis for clarity. Note that the correlations between the β-H and the γ-H of the β-Me are negative (black), indicating an exchange between these sites.

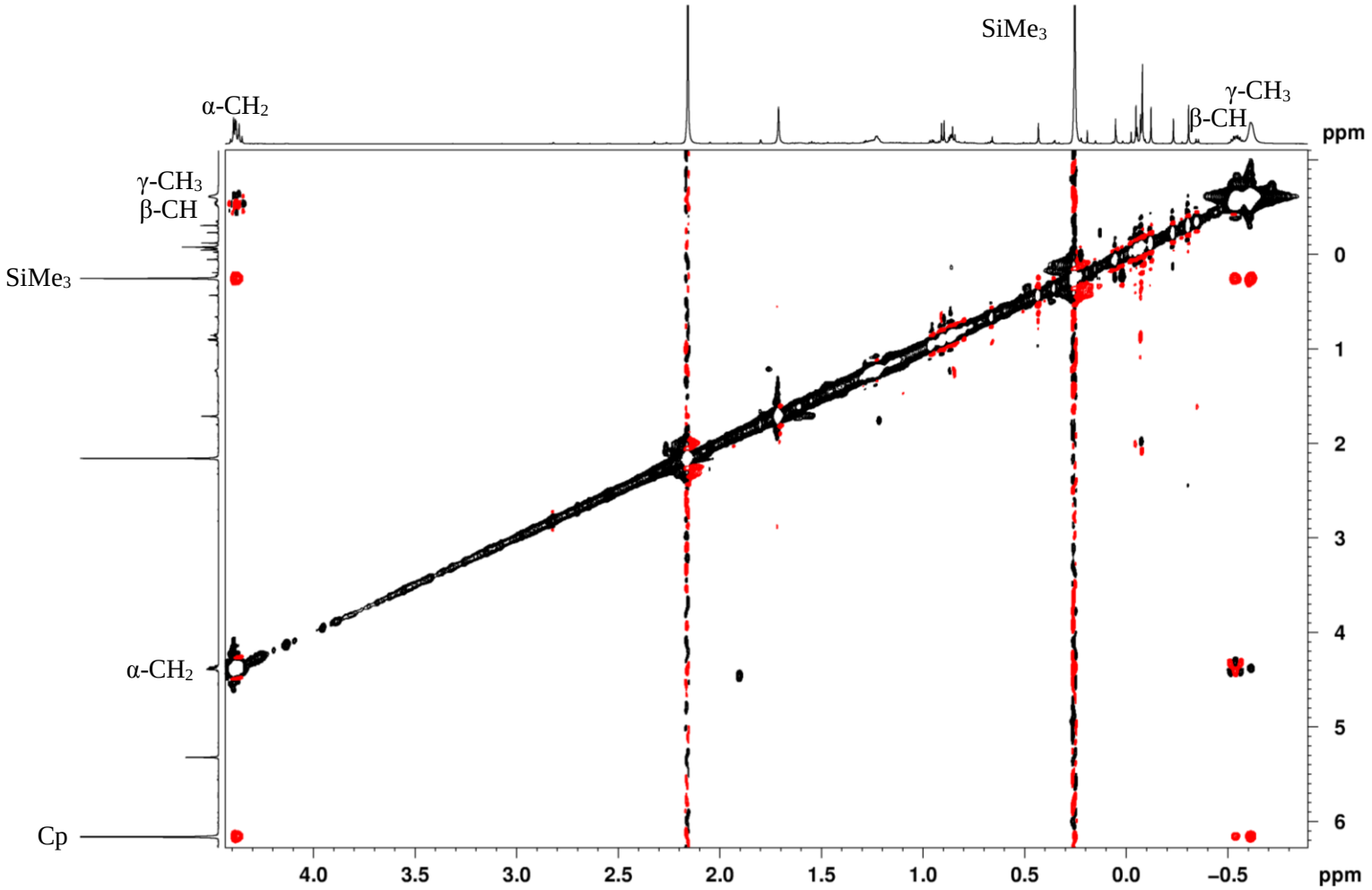

Figure C12. NOESY spectrum of **III** in CD_2Cl_2 at 255 K; Cp region omitted in the horizontal axis for clarity. Note that the correlations between the β-H and the γ-H of the β-Me are negative (black), indicating an exchange between these sites. Note also the exchange correlation between α-H_a and α-H_b with the γ-H of the β-methyl group, not observed at lower temperatures (Figures C7-C9).

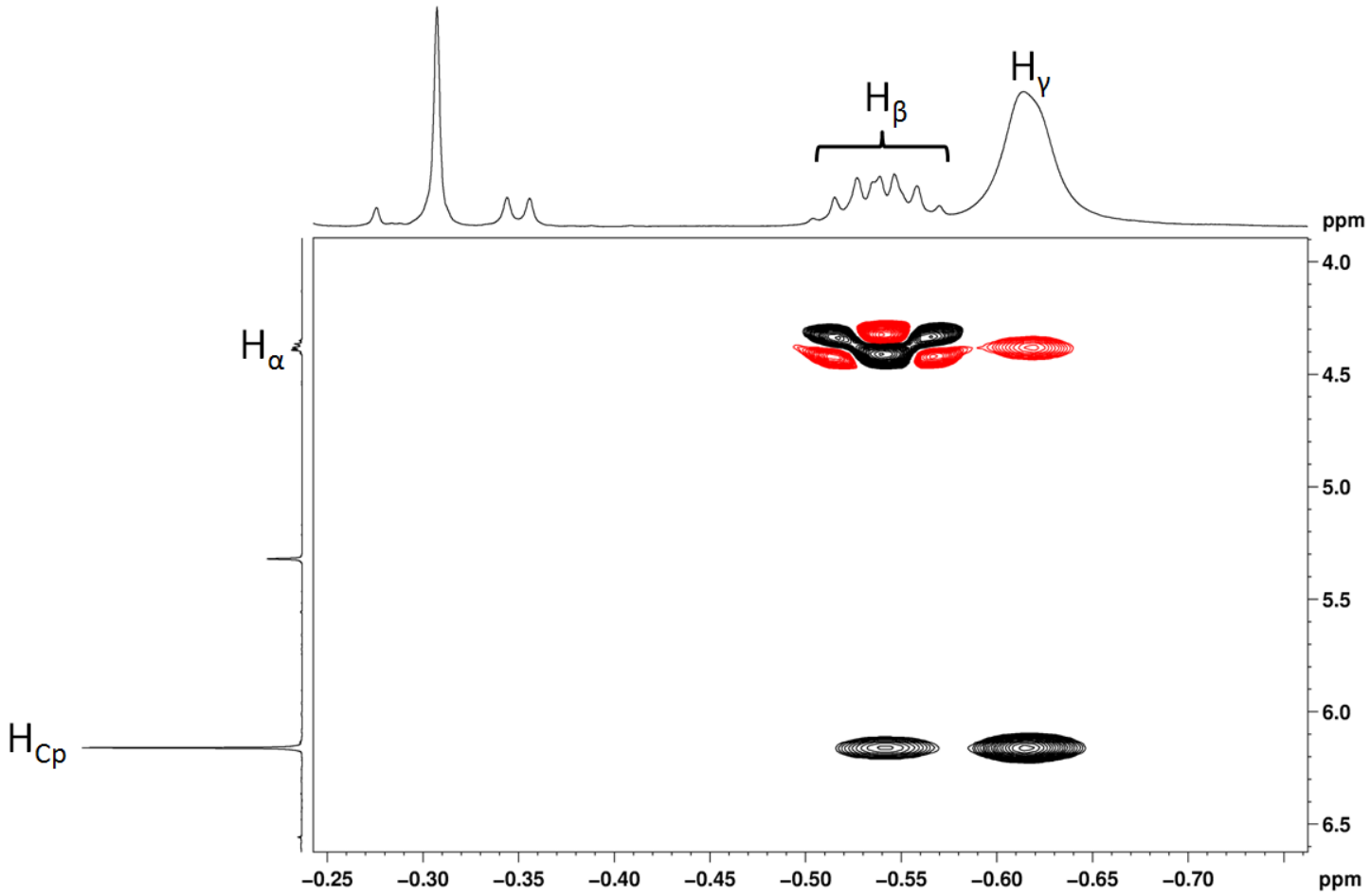

Figure C13. NOESY, referenced to $CHDCl_2$ (5.32 ppm), in CD_2Cl_2 at 255 K, high intensity scale in the α-H to β- and γ- H region. Notice that the correlation of H_α to Me_γ (broad) is negative (red here), indicating an exchange between these protons despite scalar coupling still present. This implies that the exchange rate must be roughly in the same order as the $[\text{mixing time}]^{-1}$ (1/0.3s, or 3.3Hz) and the smallest measured coupling constant (here the averaged $^3J_{HH}$ (H_β-Me_γ)~6.4Hz). The H_α to H_β correlation is a typical COSY artifact, with an overall integration near zero because of the alternating negative-positive pattern.

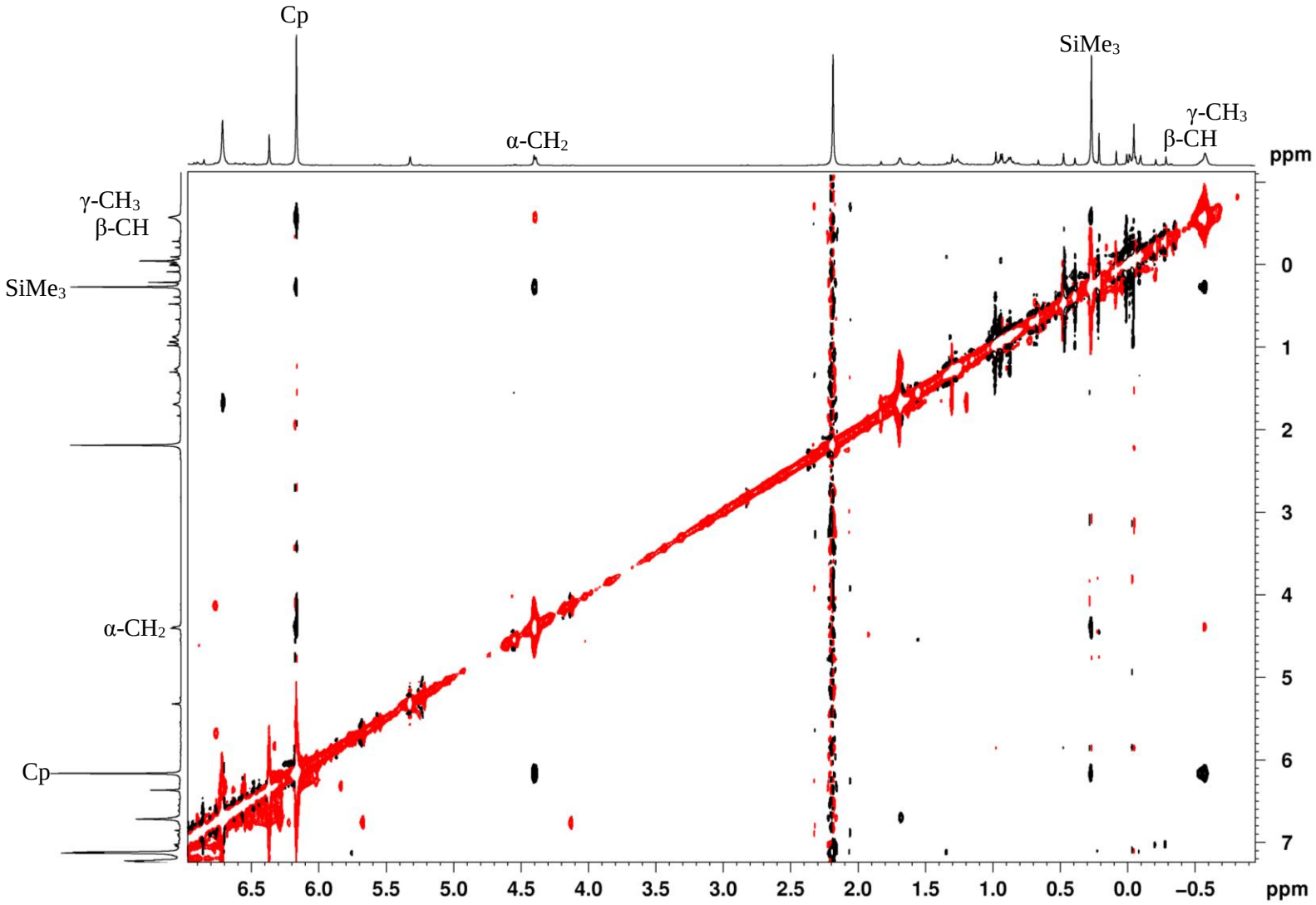

Figure C14. NOESY, referenced to $CHDCl_2$ (5.32 ppm), in CD_2Cl_2 at 260 K. Notice that the correlations of H_β to Me_γ are negative (red here), indicating an exchange between these protons despite scalar coupling still present, but the two are now in partial overlap.

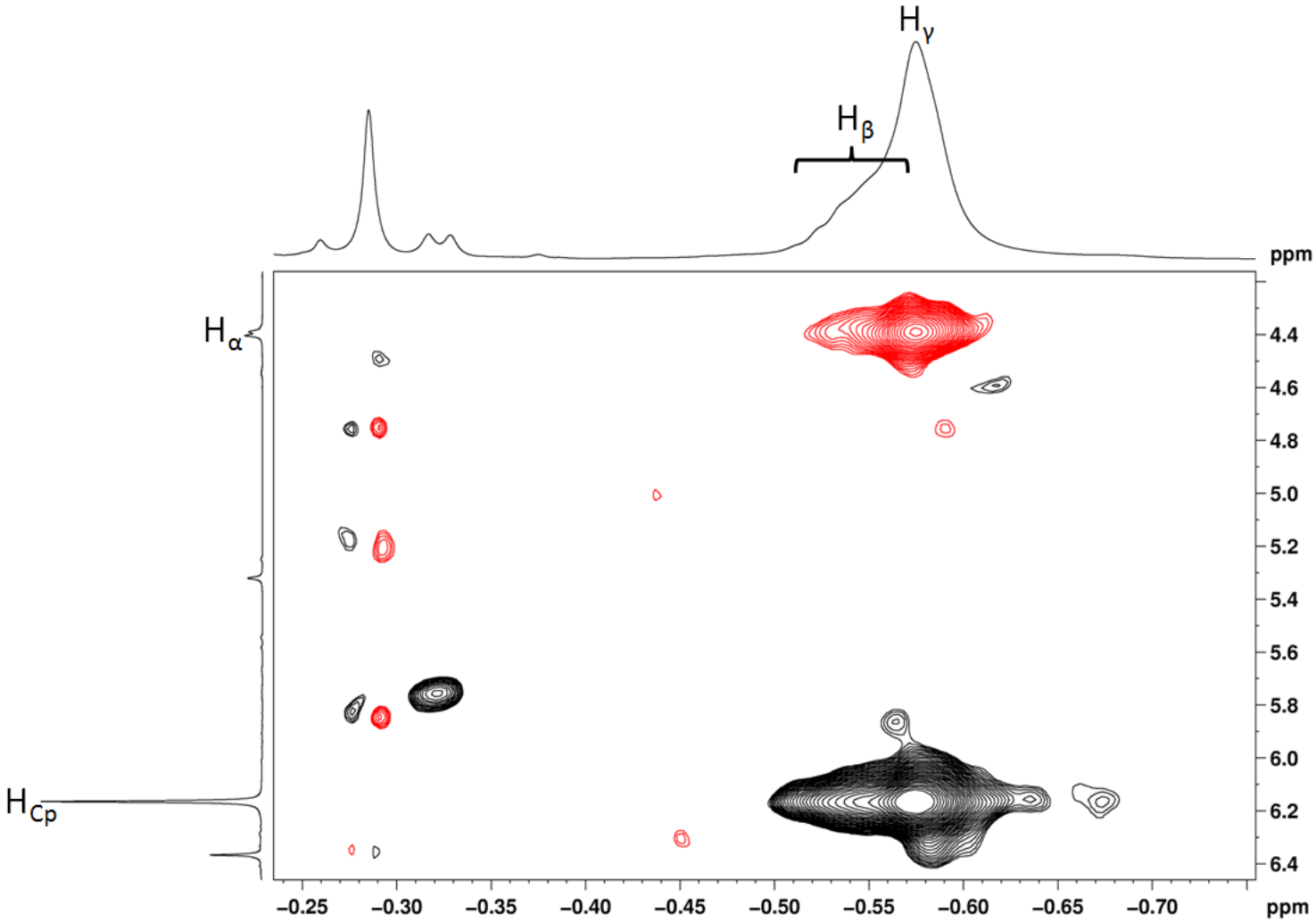

Figure C15. NOESY, referenced to $CHDCl_2$ (5.32 ppm), in CD_2Cl_2 at 260 K, high intensity scale in the α-H to β- and γ- H region. The H_α to H_β correlation now seem to be negative (red) too, though the interpretation is subject to debate because of the overlap between β-H and γ-H signals.

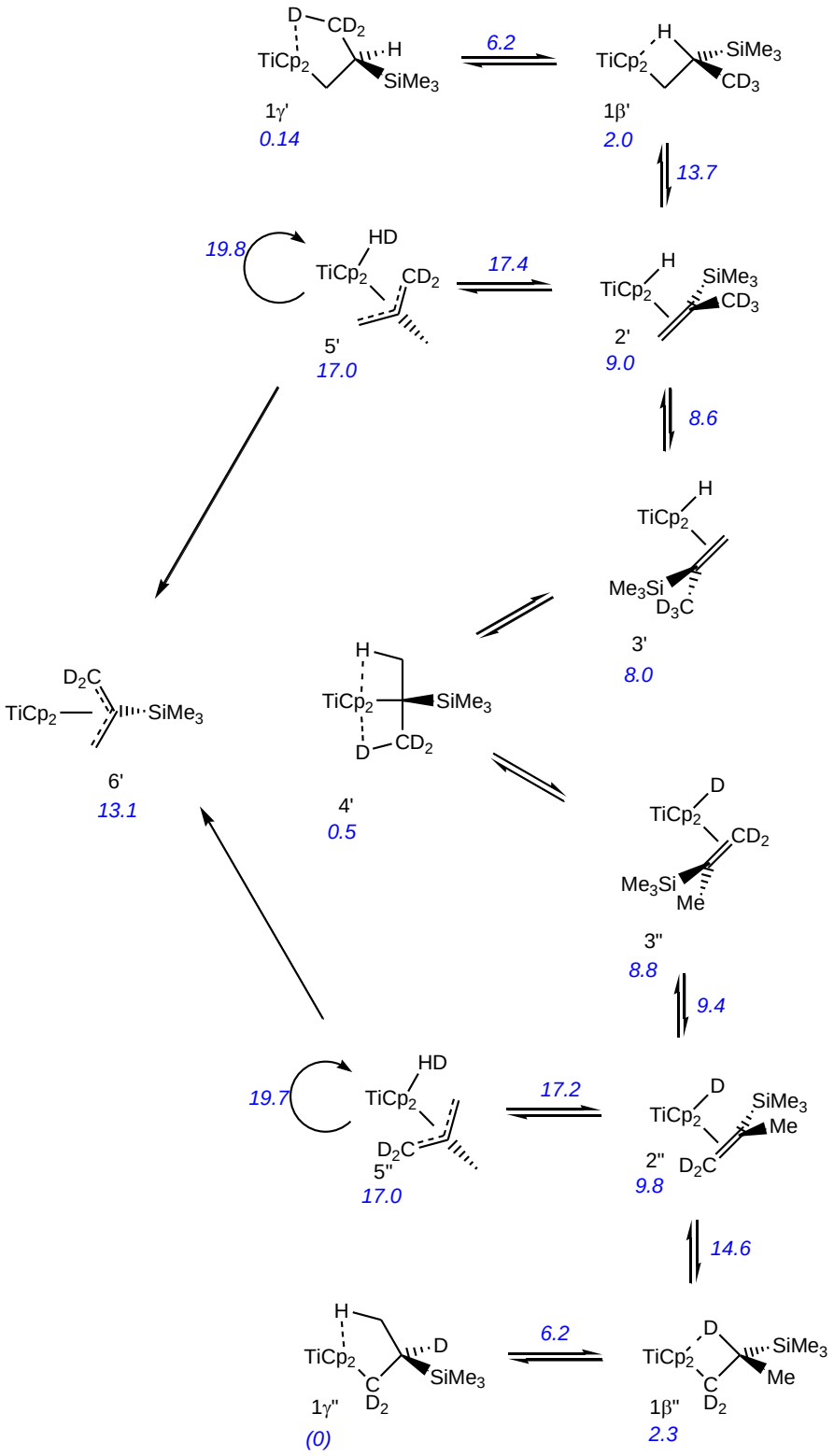

Figure C16. Relative free energies and barriers (kcal/mol) for H exchange in **III** (H_3/D_3). All transition state energies are relative to zero.

Table C1. Calculated energies for the $Cp_2TiCH_3^+$+VTMS system.[a]

Species	E_{tot} (h)	*H* corr (h)	*TS* corr (h)	*G* (225K) (h)	on scale (h)	G_{rel} (kcal/mol)
H_2	-1.17803	0.01275	0.01103	-1.17267		
CH_2Cl_2	-959.85681	0.03242	0.02287	-959.83971		
VTMS	-487.38688	0.15830	0.03335	-487.25092		
$Cp_2TiMe(CH_2Cl_2)^+$	-2236.49693	0.24402	0.04746	-2236.28470	-1763.69592	12.21
$Cp_2TiMe(VTMS)^+$	-1764.02668	0.37009	0.05553	-1763.69379	-1763.69379	13.55
insertion TS	-1764.02024	0.36957	0.05162	-1763.68525	-1763.68525	18.91
$1\alpha_1$	-1764.04491	0.37154	0.05548	-1763.71054	-1763.71054	3.03
$1\alpha_2$	-1764.04318	0.37120	0.05482	-1763.70871	-1763.70871	4.19
1β	-1764.04905	0.37195	0.05252	-1763.71229	-1763.71229	1.94
1γ	-1764.05354	0.37290	0.05185	-1763.71538	-1763.71538	0.00
$TS1\alpha_1_1\alpha_2$_a	-1764.03645	0.37046	0.05503	-1763.70286	-1763.70286	7.85
$TS1\alpha_1_1\alpha_2$_b	-1764.03521	0.36977	0.05456	-1763.70200	-1763.70200	8.40
$TS1\alpha_1\_1\beta$	-1764.03926	0.37055	0.05463	-1763.70531	-1763.70531	6.32
$TS1\alpha_2\_1\beta$	-1764.03634	0.37047	0.05488	-1763.70264	-1763.70264	7.99
$TS1\alpha_1\_1\gamma$	-1764.03925	0.37058	0.05421	-1763.70499	-1763.70499	6.52
$TS1\beta\_1\gamma$	-1764.04246	0.37183	0.05223	-1763.70562	-1763.70562	6.12
$TS1\gamma\_1\gamma$	-1764.04143	0.37181	0.05249	-1763.70479	-1763.70479	6.65
TS1β_2	-1764.02703	0.36797	0.05178	-1763.69376	-1763.69376	13.57
2	-1764.03186	0.36841	0.05654	-1763.70134	-1763.70134	8.81
2'	-1764.03154	0.36911	0.05243	-1763.69756	-1763.69756	11.18
TS_2_5	-1764.02044	0.36570	0.05133	-1763.68914	-1763.68914	16.47
5	-1764.02296	0.36799	0.05138	-1763.68939	-1763.68939	16.31
TS_5_5	-1764.01711	0.36650	0.05155	-1763.68515	-1763.68515	18.97
6	-1762.83875	0.35013	0.05177	-1762.52331	-1763.69597	12.18
TS_2_3	-1764.03355	0.36789	0.05412	-1763.70193	-1763.70193	8.44
3	-1764.03443	0.36896	0.05579	-1763.70285	-1763.70285	7.86
TS_3_4	-1764.03565	0.36911	0.05209	-1763.70144	-1763.70144	8.75
4	-1764.05173	0.37098	0.05129	-1763.71511	-1763.71511	0.17

[a] Total energies at COSMO/b-p/TZVPP//b-p/TZVP, thermal corrections from b-p/TZVP frequencies, entropies scaled by 0.67. For numbering of compounds, see Figure C16.

Table C2. Calculated energies for the $Cp_2TiCD_3^+$+VTMS system.[a]

Species	E_{tot} (h)	*H* corr (h)	*TS* corr (h)	*G* (225K) (h)	on scale (h)	G_{rel} (kcal/mol)
H_2	-1.17803	0.01146	0.01215	-1.17470		
$1\alpha_1$'	-1764.04491	0.36246	0.05609	-1763.72002	-1763.72002	3.12
$1\alpha_2$'	-1764.04318	0.36214	0.05543	-1763.71818	-1763.71818	4.27
1β'	-1764.04905	0.36280	0.05312	-1763.72184	-1763.72184	1.98
1γ'	-1764.05354	0.36386	0.05239	-1763.72477	-1763.72477	0.14
TS$1\alpha_1$_$1\alpha_2$_a'	-1764.03645	0.36140	0.05563	-1763.71233	-1763.71233	7.95
TS$1\alpha_1$_$1\alpha_2$_b'	-1764.03521	0.36071	0.05517	-1763.71146	-1763.71146	8.49
TS$1\alpha_1$_1β'	-1764.03926	0.36149	0.05522	-1763.71476	-1763.71476	6.42
TS$1\alpha_2$_1β'	-1764.03634	0.36140	0.05547	-1763.71210	-1763.71210	8.09
TS$1\alpha_1$_1γ'	-1764.03925	0.36152	0.05480	-1763.71445	-1763.71445	6.62
TS1β_1γ'	-1764.04246	0.36276	0.05278	-1763.71506	-1763.71506	6.24
TS1γ_1γ'	-1764.04143	0.36284	0.05287	-1763.71402	-1763.71402	6.89
TS1β_2'	-1764.02703	0.35890	0.05237	-1763.70322	-1763.70322	13.66
2'	-1764.03186	0.35948	0.05717	-1763.71069	-1763.71069	8.97
TS_2_5'	-1764.02044	0.35786	0.05181	-1763.69729	-1763.69729	17.38
5'	-1764.02296	0.35989	0.05204	-1763.69794	-1763.69794	16.98
TS_5_5'	-1764.01711	0.35862	0.05218	-1763.69345	-1763.69345	19.79
6'	-1762.83875	0.34423	0.05218	-1762.52948	-1763.70419	13.06
TS_2_3'	-1764.03355	0.35894	0.05473	-1763.71128	-1763.71128	8.60
3'	-1764.03443	0.36000	0.05641	-1763.71222	-1763.71222	8.01
TS_3_4'	-1764.03565	0.36021	0.05266	-1763.71072	-1763.71072	8.96
4'	-1764.05173	0.36216	0.05180	-1763.72427	-1763.72427	0.45
TS_3_4"	-1764.03565	0.36125	0.05273	-1763.70973	-1763.70973	9.58
3"	-1764.03443	0.36129	0.05645	-1763.71097	-1763.71097	8.80
TS_2_3"	-1764.03355	0.36024	0.05479	-1763.71003	-1763.71003	9.39
TS_5_5"	-1764.01711	0.35852	0.05218	-1763.69356	-1763.69356	19.73
5"	-1764.02296	0.35985	0.05205	-1763.69798	-1763.69798	16.95
TS_2_5"	-1764.02044	0.35755	0.05190	-1763.69767	-1763.69767	17.15
2"	-1764.03186	0.36089	0.05722	-1763.70931	-1763.70931	9.84
TS1β_2"	-1764.02703	0.36044	0.05238	-1763.70169	-1763.70169	14.62
TS1γ_1γ"	-1764.04143	0.36254	0.05298	-1763.71439	-1763.71439	6.65
TS1β_1γ"	-1764.04246	0.36268	0.05272	-1763.71511	-1763.71511	6.20
TS$1\alpha_1$_1γ"	-1764.03925	0.36167	0.05473	-1763.71424	-1763.71424	6.75
TS$1\alpha_2$_1β"	-1764.03634	0.36166	0.05538	-1763.71178	-1763.71178	8.29
TS$1\alpha_1$_1β"	-1764.03926	0.36164	0.05515	-1763.71456	-1763.71456	6.55
TS$1\alpha_1$_$1\alpha_2$_b"	-1764.03521	0.36125	0.05500	-1763.71081	-1763.71081	8.90
TS$1\alpha_1$_$1\alpha_2$_a"	-1764.03645	0.36166	0.05554	-1763.71200	-1763.71200	8.15
1γ"	-1764.05354	0.36361	0.05234	-1763.72499	-1763.72499	0.00
1β"	-1764.04905	0.36321	0.05305	-1763.72138	-1763.72138	2.27
$1\alpha_2$"	-1764.04318	0.36245	0.05531	-1763.71779	-1763.71779	4.52
$1\alpha_1$"	-1764.04491	0.36271	0.05597	-1763.71970	-1763.71970	3.32

[a] Total energies at COSMO/b-p/TZVPP//b-p/TZVP, thermal corrections from b-p/TZVP frequencies, entropies scaled by 0.67. For numbering of compounds, see Figure C17.

Table C3. Calculated NMR parameters (ppm and Hz) for the various possible agostic structures of $[Cp_2TiCH_2CHMe(SiMe_3)]^+$.[a]

1α₁	H	α_1	α_2	β	γ_1	γ_2	γ_3	δ_1	δ_2	δ_3	δ_4	δ_5	δ_6	δ_7	δ_8	δ_9
	δ	-4.26	10.40	4.66	1.57	1.21	0.73	0.55	0.36	0.46	0.05	0.42	0.30	-0.29	0.45	0.26
							1.17									0.28
	H	Cp_{1a}	Cp_{1b}	Cp_{1c}	Cp_{1d}	Cp_{1e}	Cp_{2a}	Cp_{2b}	Cp_{2c}	Cp_{2d}	Cp_{2e}					
	δ	7.68	7.82	5.45	8.87	5.78	7.70	5.50	5.52	8.55	8.33					
						7.12					7.12					
											7.12					
	H-H	α_1-α_2	α_1-β	α_2-β	β-γ_1	β-γ_2	β-γ_3	γ_1-γ_2	γ_1-γ_3	γ_2-γ_3						
	J	-3.87	-0.19	13.63	2.88	13.29	3.76	-12.54	-11.71	-11.66						
							6.64			-11.97						
	C	α	β	γ	Si	δ_1	δ_2	δ_3								
	δ	213.05	69.90	18.49	28.60	-1.40	-5.35	-0.79								
								-2.51								
	C	Cp_{1a}	Cp_{1b}	Cp_{1c}	Cp_{1d}	Cp_{1e}	Cp_{2a}	Cp_{2b}	Cp_{2c}	Cp_{2d}	Cp_{2e}					
	δ	125.20	132.22	131.16	138.72	139.73	129.50	126.80	139.47	137.94	131.21					
						133.41					132.98					
											133.20					
	H-C	α_1-α	α_2-α	β-β	γ_1-γ	γ_2-γ	γ_3-γ									
	J	76.4	138.9	121.0	127.5	123.9	123.8									
							125.1									

1α$_2$	H:	α_1	α_2	β	γ_1	γ_2	γ_3	δ_1	δ_2	δ_3	δ_4	δ_5	δ_6	δ_7	δ_8	δ_9
	δ	10.65	-3.91	4.46	1.23	1.33	1.81	0.31	0.58	0.37	0.05	0.30	0.56	-1.80	-0.11	0.19
							1.46									0.05
	H:	Cp_{1a}	Cp_{1b}	Cp_{1c}	Cp_{1d}	Cp_{1e}	Cp_{2a}	Cp_{2b}	Cp_{2c}	Cp_{2d}	Cp_{2e}					
	δ	7.99	5.51	5.50	8.81	7.70	7.85	8.15	5.20	8.52	5.78					
						7.10					7.10					
											7.10					
	H-H	α_1-α_2	α_1-β	α_2-β	β-γ_1	β-γ_2	β-γ_3	γ_1-γ_2	γ_1-γ_3	γ_2-γ_3						
	J	-4.60	13.58	3.42	4.15	13.05	2.63	-11.58	-11.83	-12.21						
							6.6			-11.87						
	C	α	β	γ	Si	δ_1	δ_2	δ_3								
	δ	219.25	64.92	23.77	28.89	-0.58	2.17	-4.84								
								-1.08								
	C	Cp_{1a}	Cp_{1b}	Cp_{1c}	Cp_{1d}	Cp_{1e}	Cp_{2a}	Cp_{2b}	Cp_{2c}	Cp_{2d}	Cp_{2e}					
	δ	129.84	128.62	138.77	136.50	127.84	124.74	133.79	126.77	138.77	137.40					
						132.31					132.29					
											132.30					
	H-C	α_1-α	α_2-α	β-β	γ_1-γ	γ_2-γ	γ_3-γ									
	J	139.0	71.0	120.9	125.9	125.0	126.0									
							125.6									

1β	H	α_1	α_2	β	γ_1	γ_2	γ_3	δ_1	δ_2	δ_3	δ_4	δ_5	δ_6	δ_7	δ_8	δ_9
	δ	4.71	5.61	-4.34	1.41	1.76	2.10	0.11	0.57	0.42	0.54	0.36	0.29	0.94	0.99	0.77
							1.76									0.55

H	Cp_{1a}	Cp_{1b}	Cp_{1c}	Cp_{1d}	Cp_{1e}	Cp_{2a}	Cp_{2b}	Cp_{2c}	Cp_{2d}	Cp_{2e}
δ	5.37	8.30	7.26	5.27	8.33	6.35	6.71	6.32	9.24	6.23
					6.90					6.97
										6.94

H-H	α_1-α_2	α_1-β	α_2-β	β-γ_1	β-γ_2	β-γ_3	γ_1-γ_2	γ_1-γ_3	γ_2-γ_3
	24-23	24-30	23-30	30-27	30-28	30-29	27-28	27-29	28-29
J	-5.81	0.54	7.14	2.78	8.94	1.10	-12.65	-12.47	-12.79
						4.3			-12.64

C	α	β	γ	Si	δ_1	δ_2	δ_3
δ	108.42	56.99	24.36	43.09	-1.82	0.55	1.00
							-0.09

C	Cp_{1a}	Cp_{1b}	Cp_{1c}	Cp_{1d}	Cp_{1e}	Cp_{2a}	Cp_{2b}	Cp_{2c}	Cp_{2d}	Cp_{2e}
δ	121.10	131.63	127.01	135.64	133.40	126.68	132.23	142.28	134.28	124.30
					129.76					131.95
										130.85

H-C	α_1-α	α_2-α	β-β	γ_1-γ	γ_2-γ	γ_3-γ
J	146.3	145.7	93.7	123.97	127.6	124.7
						125.4

1γ	H	α_1	α_2	β	γ_1	γ_2	γ_3	δ_1	δ_2	δ_3	δ_4	δ_5	δ_6	δ_7	δ_8	δ_9
	δ	4.78	4.77	0.03	2.91	1.44	-7.16	0.44	0.35	0.64	0.55	0.43	0.54	0.07	0.42	0.31
							-0.94									0.42
	H	Cp_{1a}	Cp_{1b}	Cp_{1c}	Cp_{1d}	Cp_{1e}	Cp_{2a}	Cp_{2b}	Cp_{2c}	Cp_{2d}	Cp_{2e}					
	δ	5.95	6.07	6.33	5.69	6.72	6.56	6.32	5.88	5.76	6.99					
						6.15					6.30					
											6.23					
	H-H	α_1-α_2	α_1-β	α_2-β	β-γ_1	β-γ_2	β-γ_3	γ_1-γ_2	γ_1-γ_3	γ_2-γ_3						
	J	-9.48	7.29	13.10	5.55	14.12	1.19	-11.92	-17.71	-9.30						
							6.95			-12.97						
	C	α	β	γ	Si	δ_1	δ_2	δ_3								
	δ	107.47	7.65	34.19	39.45	0.68	1.34	-4.49								
								-0.82								
	C	Cp_{1a}	Cp_{1b}	Cp_{1c}	Cp_{1d}	Cp_{1e}	Cp_{2a}	Cp_{2b}	Cp_{2c}	Cp_{2d}	Cp_{2e}					
	δ	115.41	120.32	119.69	136.58	126.02	118.88	127.58	127.85	128.34	122.83					
						123.60					125.10					
											124.35					
	H-C	α_1-α	α_2-α	β-β	γ_1-γ	γ_2-γ	γ_3-γ									
	J	148.3	142.7	124.8	137.7	137.1	93.0									
							122.6									

[a] GIAO, B3LYP/IGLO-III,TZVP//b3-lyp/TZVP.

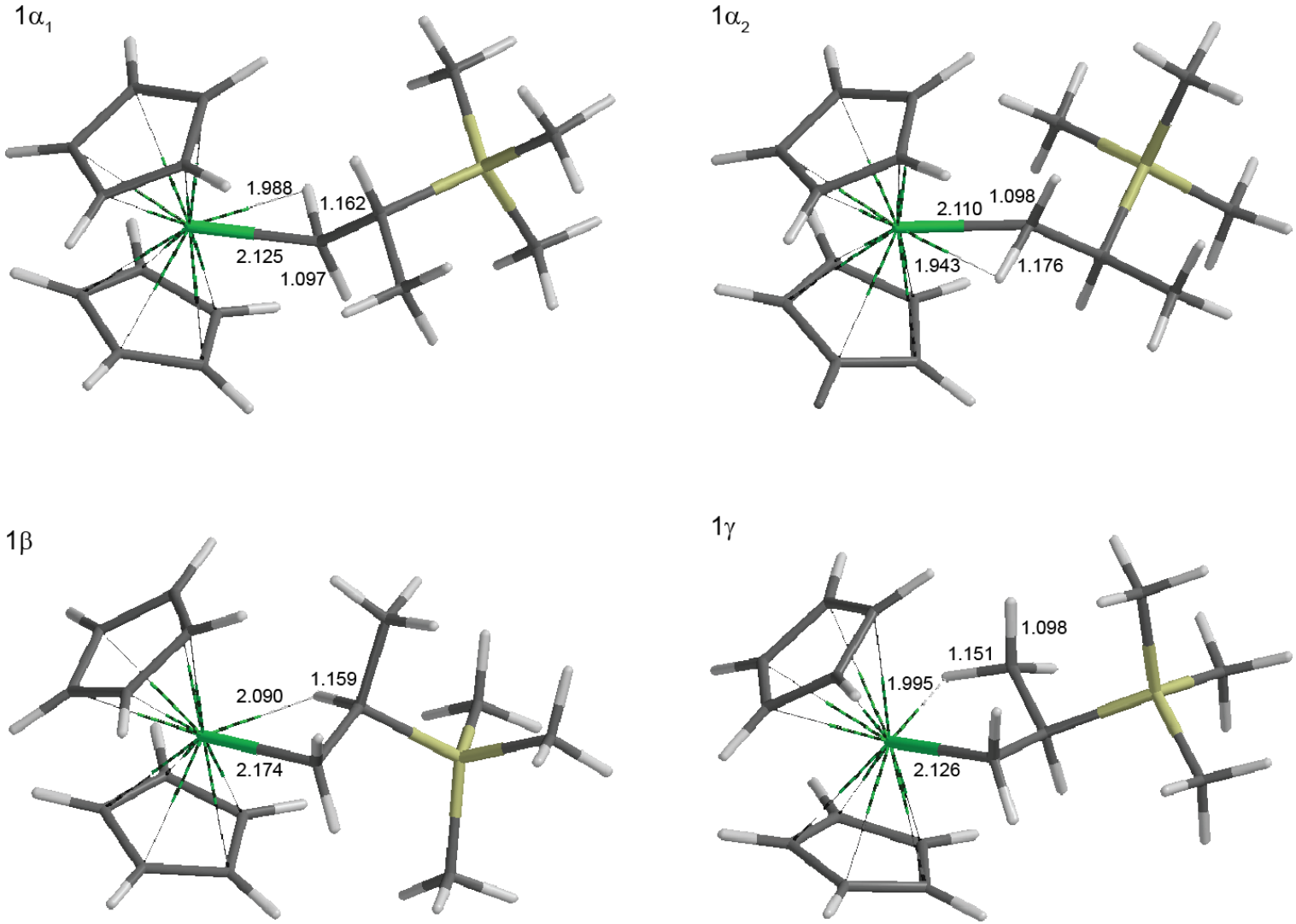

Figure C18. Calculated structures (b-p/TZVP). Distances in Å. For structure numbering, see Figure C16.

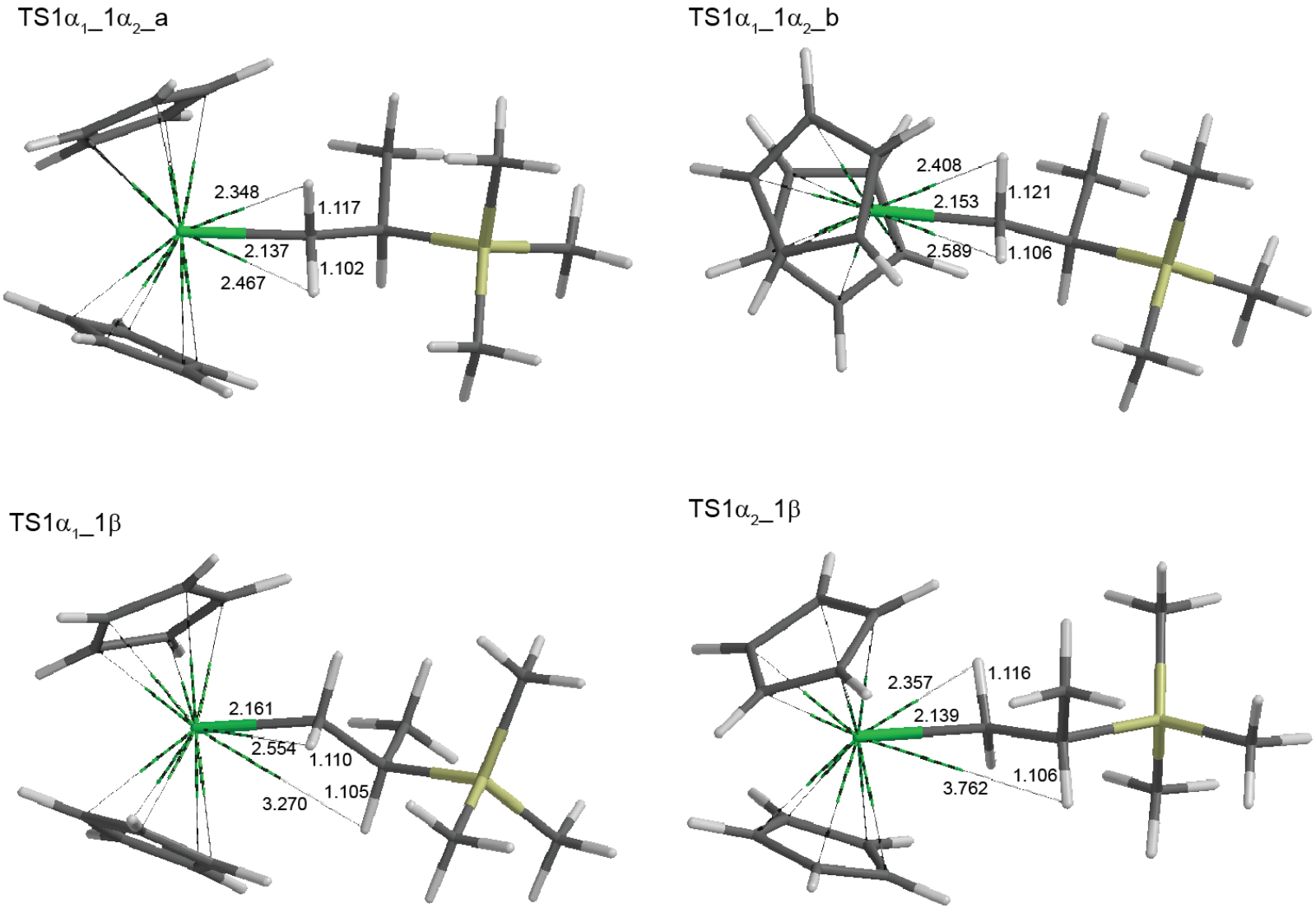

Figure C18 (cont). Calculated structures (b-p/TZVP). Distances in Å. For structure numbering, see Figure C16.

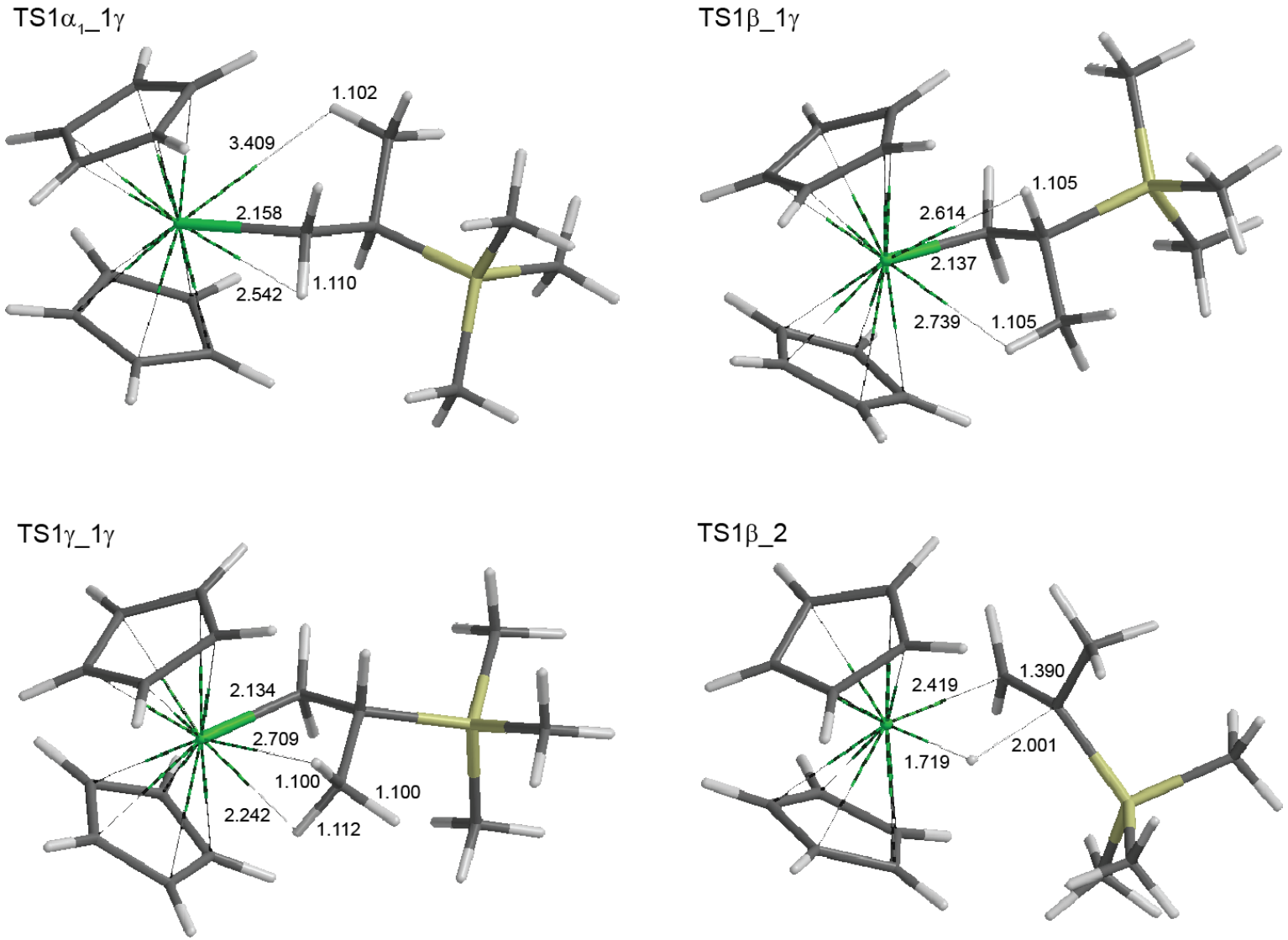

Figure C18 (cont). Calculated structures (b-p/TZVP). Distances in Å. For structure numbering, see Figure C16.

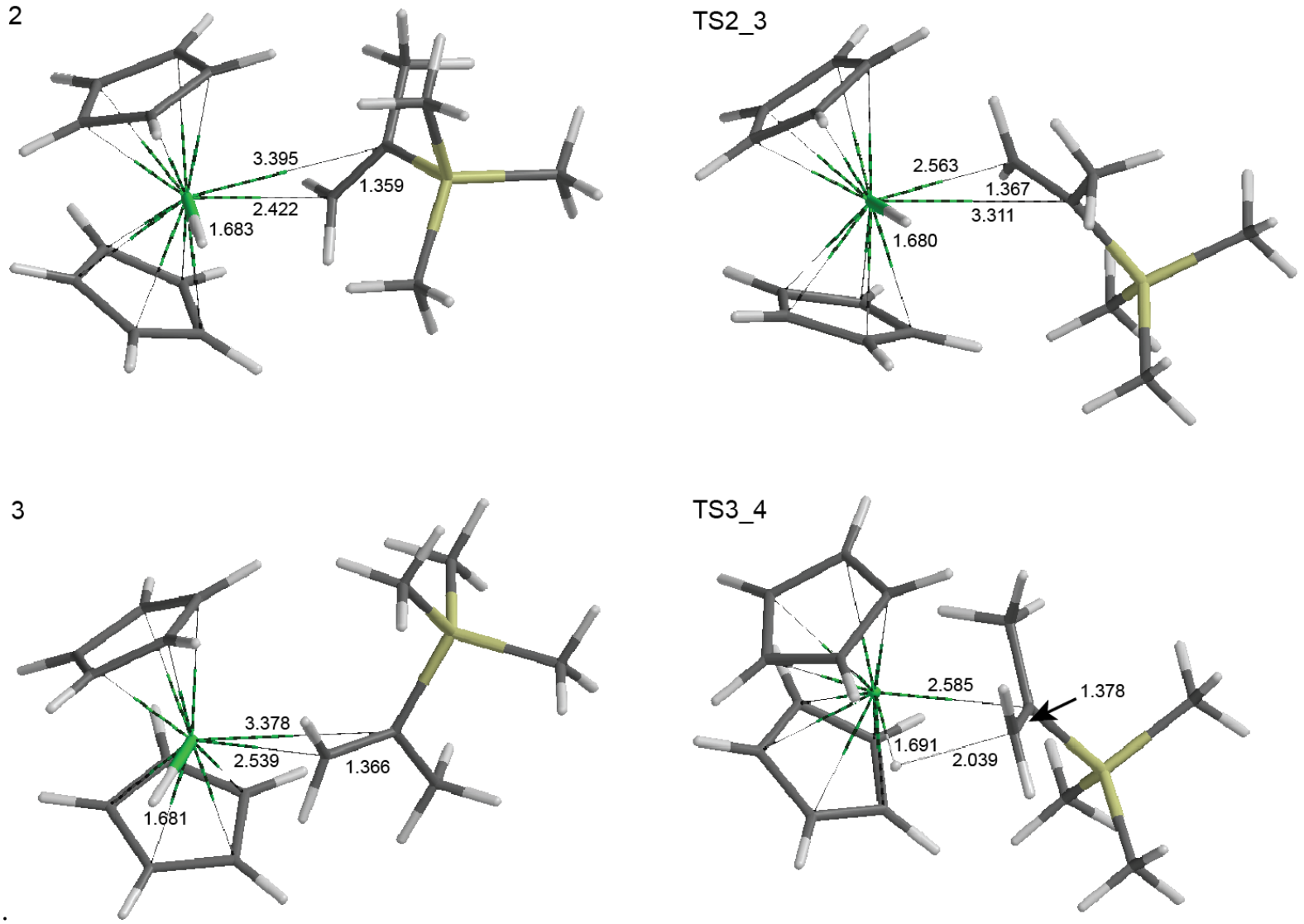

Figure C18 (cont). Calculated structures (b-p/TZVP). Distances in Å. For structure numbering, see Figure C16.

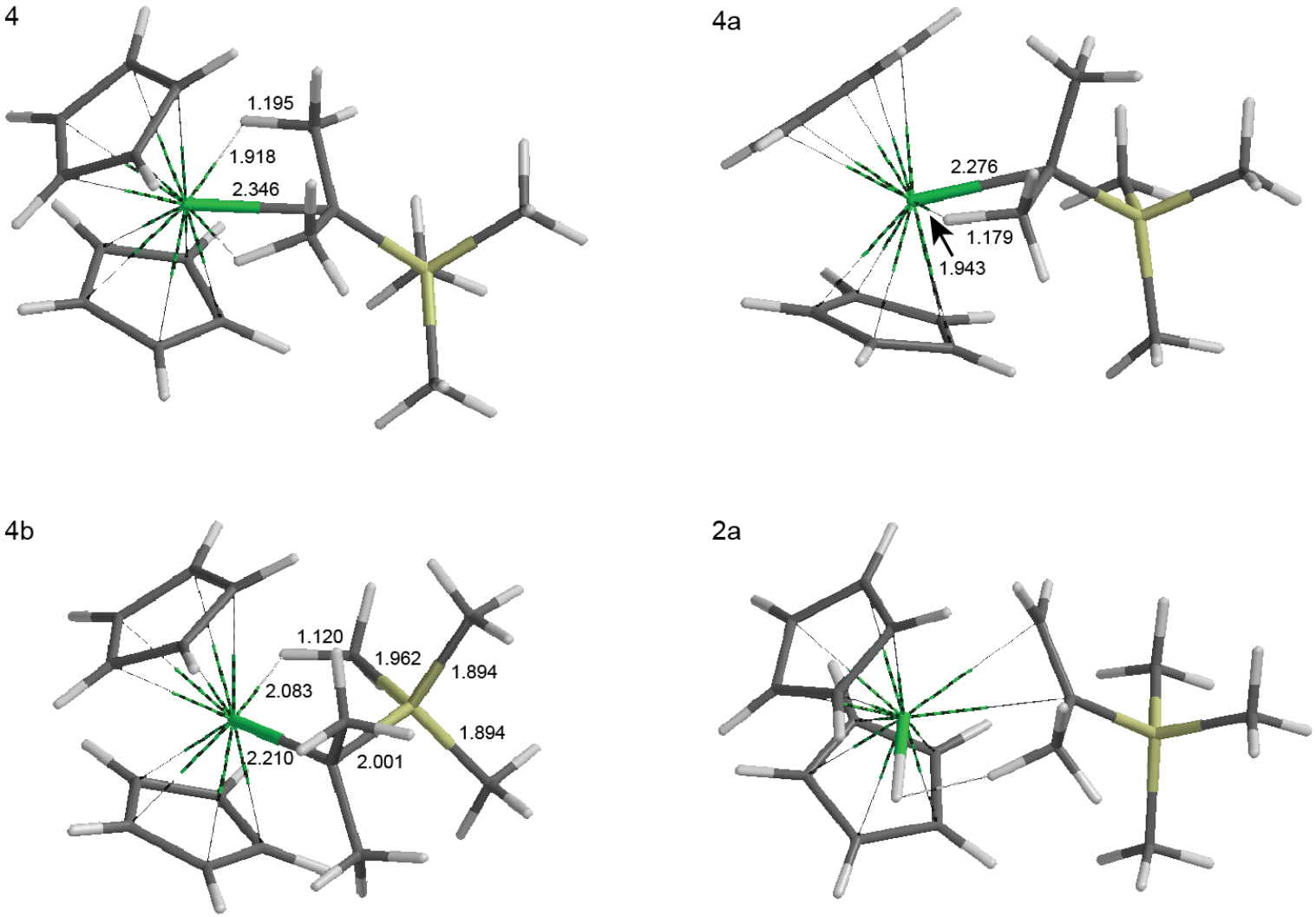

Figure C18 (cont). Calculated structures (b-p/TZVP). Distances in Å. For structure numbering, see Figure C16.

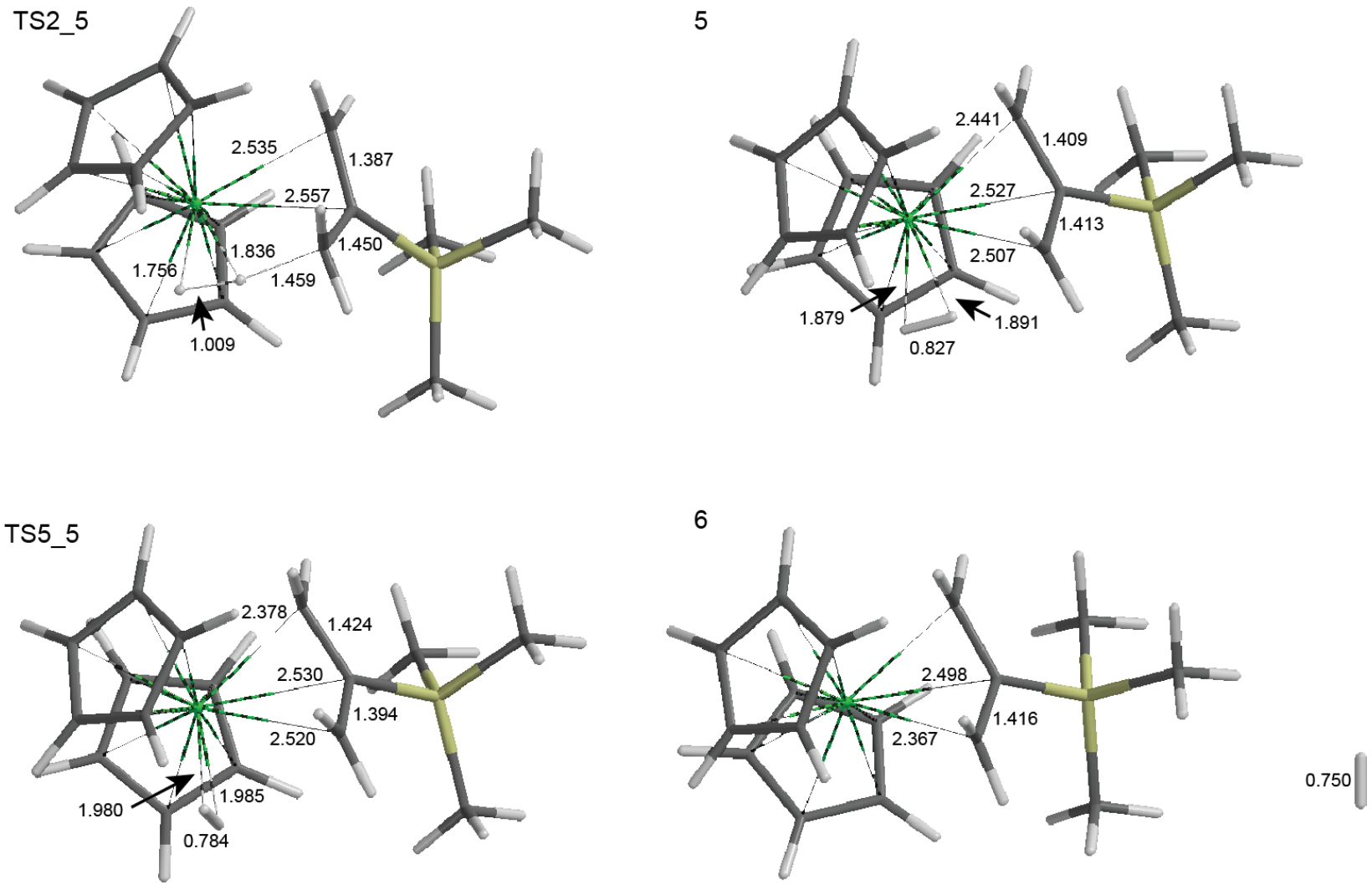

Figure C18 (cont). Calculated structures (b-p/TZVP). Distances in Å. For structure numbering, see Figure C16.

Table C4. b-p geometries

==========

2

H2.xyz

H 0.0000000 0.0000000 -0.0054347

H 0.0000000 0.0000000 0.7454351

==========

5

CH2Cl2.xyz

Cl 0.0931660 0.1612433 -1.7113661

C 0.0619101 0.1073058 0.0875946

H 1.0951748 0.0846494 0.4389721

Cl -0.7754346 -1.3437667 0.7459365

H -0.4748162 0.9905682 0.4388629

==========

30

Cp2TiMe+_CH2Cl2.xyz

Ti -0.2988467 0.1228341 -0.0028763

H 0.3179986 -1.9483073 2.2302561

C -0.5535370 -1.5158528 1.7447743

C -1.1802973 -2.0069941 0.5742094

H -1.0046793 0.2647218 3.0285293

H -0.9013623 -2.9054060 0.0324152

C -2.2758045 -1.1405525 0.2690310

H -2.9841960 -1.2704502 -0.5438859

C -2.3209712 -0.1245858 1.2632474

H -3.0464811 0.6812777 1.3218763

C -1.2485185 -0.3474022 2.1644566

H 1.9244391 1.5996676 -1.5840511

C 1.1141495 0.9024724 -1.7808998

C -0.2168264 1.2622593 -2.1043817

H 2.0859647 -1.1186489 -1.5657699
H -0.5973684 2.2722596 -2.2145958
C -0.9647058 0.0625011 -2.2721768
H -2.0116091 0.0007806 -2.5556690
C -0.0775508 -1.0398414 -2.0881069
H -0.3346055 -2.0895619 -2.1876179
C 1.1992919 -0.5226303 -1.7712620
C 3.4759111 -0.1428382 1.1024689
Cl 1.8781109 0.7120911 1.4845645
C -0.7475415 2.1734432 0.5114211
H 3.7654015 0.1775214 0.0999110
Cl 3.3679669 -1.9078797 1.1695533
H 4.1560050 0.2189731 1.8770363
H 0.0211526 2.8527269 0.1184005
H -0.8268522 2.2984101 1.6001808
H -1.7146383 2.4790116 0.0789611
==========
43
Cp2TiMe+_CH2CHSiMe3_endo.xyz
Ti -0.5510323 -0.7480999 -1.2372130
C -1.9121703 0.4257688 -0.0301167
H 0.9465211 -3.0947436 0.2288974
C -0.0037599 -2.9087624 -0.2670411
C -0.2614436 -3.0709997 -1.6537060
H -1.3341760 -2.2698039 1.4174324
H 0.4470391 -3.4234279 -2.3977005
C -1.6373491 -2.7645915 -1.8756682
H -2.1628022 -2.8472568 -2.8217763
C -2.2132836 -2.3935708 -0.6314499
H -3.2472818 -2.1070463 -0.4643399
C -1.2026865 -2.4812905 0.3603697

H	1.9154081	0.0184045	-3.0041278
C	0.8373045	0.1603130	-3.0030628
C	0.1314408	1.2474314	-2.4049869
H	0.1140461	-1.6055572	-4.1579576
H	0.5736232	2.0882327	-1.8777865
C	-1.2509721	1.0627499	-2.6524951
H	-2.0490312	1.7365775	-2.3602610
C	-1.4069128	-0.1525537	-3.3729338
H	-2.3469518	-0.5570431	-3.7368924
C	-0.1079286	-0.6976467	-3.6054291
H	-1.5231823	1.4529436	0.0241095
H	-1.9741745	-0.0005523	0.9791958
H	-2.9346028	0.4752788	-0.4331969
C	1.6194239	-0.1214740	-0.0289732
H	2.0618552	0.7653702	-0.4830693
H	1.8033788	-1.0701810	-0.5667404
C	1.1282653	-0.1030310	1.2333761
H	0.7984673	-1.0611945	1.6545533
Si	1.1643098	1.3960692	2.4453184
C	1.4334939	2.9928280	1.4657152
H	2.3586858	2.9679381	0.8714731
H	1.5228216	3.8399221	2.1620684
H	0.5904702	3.2142674	0.7950769
C	2.6381595	1.0180208	3.5781687
H	3.5823067	0.9738585	3.0174607
H	2.5099749	0.0656322	4.1120881
H	2.7306701	1.8131594	4.3335961
C	-0.4490009	1.4289857	3.4328720
H	-0.3902439	2.2094938	4.2061340
H	-0.6285555	0.4734693	3.9471542
H	-1.3201242	1.6521117	2.8018648

==========

43

Cp2TiMe+_CH2CHSiMe3_insTS.xyz

Ti	-0.5510050	-0.8134472	-1.0837994
C	-1.4559855	0.5617492	0.2915168
H	0.2832948	-3.1386987	0.8712320
C	-0.4647407	-2.9310688	0.1108056
C	-0.3426514	-3.2091537	-1.2763787
H	-2.1467436	-2.0584670	1.2995132
H	0.5173847	-3.6591225	-1.7661109
C	-1.5673935	-2.8432845	-1.9022623
H	-1.8092466	-2.9673248	-2.9534363
C	-2.4263893	-2.3054747	-0.9110364
H	-3.4389268	-1.9426495	-1.0723723
C	-1.7417803	-2.3595184	0.3381839
H	2.1475590	-0.3032820	-2.5747882
C	1.0925529	-0.0682439	-2.6773564
C	0.4363599	1.1068230	-2.1981016
H	0.3325851	-1.7882571	-3.8796701
H	0.8976002	1.9091677	-1.6300056
C	-0.9129484	1.0524115	-2.6123349
H	-1.6750478	1.8016472	-2.4132834
C	-1.1166236	-0.1701647	-3.3091919
H	-2.0465349	-0.4947615	-3.7676600
C	0.1380909	-0.8477664	-3.3727730
H	-1.2652730	1.6341528	0.2000533
H	-1.9386446	0.3289619	1.2431587
H	-2.2036982	0.2856841	-0.5224459
C	1.4782202	-0.6076788	0.1753536
H	2.1930932	0.0634998	-0.2995507
H	1.7530031	-1.6640377	0.1482471

C 0.6363587 -0.1154454 1.1699572
H 0.1279798 -0.8715519 1.7784147
Si 0.9818975 1.5318403 2.1342030
C 2.4300850 1.0190749 3.2471431
H 3.3158651 0.7390651 2.6598593
H 2.1675681 0.1705727 3.8952405
H 2.7086039 1.8603760 3.8998892
C 1.5040950 2.9349201 0.9739200
H 2.3500113 2.6552500 0.3291514
H 1.8383620 3.7884542 1.5832053
H 0.6804549 3.2973604 0.3424720
C -0.5025502 2.0206877 3.2011339
H -0.1921475 2.8034767 3.9096067
H -0.8680038 1.1724608 3.7989667
H -1.3446905 2.4217627 2.6213304
==========
==========
43
1a1.xyz
Ti 1.8491123 -0.3874717 -0.3364366
C 2.0853954 -2.1976816 -1.7928273
C 2.8714029 -1.1414290 -2.3463378
H -0.1335995 -2.3870328 -1.5123629
H 3.9474407 -1.1518860 -2.4883416
C 1.9966771 -0.0852794 -2.7074308
H 2.2892460 0.8655833 -3.1488511
C 0.6673436 -0.4908354 -2.3991406
H -0.2294289 0.0999061 -2.5655897
C 0.7180685 -1.7973399 -1.8380901
H 4.9428788 -0.7206320 -0.3599617
C 4.1444168 -0.4573478 0.3266437

C	3.3947967	-1.3690874	1.1287805
H	4.0366177	1.7697263	0.1327425
H	3.5326526	-2.4468377	1.1680968
C	2.4838158	-0.6107133	1.9220865
H	1.8022448	-1.0092198	2.6674544
C	2.6511210	0.7611452	1.5820509
H	2.1018421	1.5978834	2.0069401
C	3.6745097	0.8530479	0.5946033
C	-0.0699579	-0.0990155	0.5293373
H	0.0056437	0.1409346	1.5972089
H	0.3068404	0.8353915	-0.0496657
H	2.4610103	-3.1562817	-1.4439243
C	-1.4849824	-0.4525839	0.1939541
C	-1.9840204	-1.5965839	1.1032121
H	-3.0176704	-1.8751853	0.8597784
H	-1.9558317	-1.3117889	2.1656593
H	-1.3617998	-2.4986298	0.9901870
H	-1.5907864	-0.7593422	-0.8604471
Si	-2.6842996	1.1053043	0.3476966
C	-4.4307383	0.5233081	-0.1002761
H	-4.8371806	-0.1773976	0.6421557
H	-4.4598382	0.0339839	-1.0848188
H	-5.1094863	1.3885662	-0.1412847
C	-2.6227291	1.7904516	2.1142812
H	-1.6272131	2.1757629	2.3792638
H	-2.9070614	1.0352657	2.8609900
H	-3.3312612	2.6266326	2.2122058
C	-2.1098575	2.4260379	-0.8923041
H	-1.0915847	2.7912215	-0.6895173
H	-2.7765686	3.2998824	-0.8383530
H	-2.1471805	2.0595670	-1.9293678

==========

43

1a2.xyz

Ti	1.8495958	-0.4532337	-0.2846154
C	2.1283260	-2.2053390	-1.8110295
C	2.9506277	-1.1441905	-2.2883410
H	-0.1033375	-2.3713120	-1.6380959
H	4.0319919	-1.1647277	-2.3813116
C	2.1090482	-0.0534259	-2.6321427
H	2.4340581	0.9085513	-3.0230388
C	0.7593514	-0.4541620	-2.4091079
H	-0.1234413	0.1540989	-2.5910349
C	0.7681006	-1.7797988	-1.9002279
H	4.9331564	-0.9302980	-0.1859273
C	4.1403324	-0.5096231	0.4247988
C	3.3490010	-1.2238593	1.3659759
H	4.1257877	1.6474295	-0.1823201
H	3.4337842	-2.2836182	1.5976595
C	2.4545367	-0.2992289	1.9832800
H	1.7543365	-0.5264634	2.7807349
C	2.6828610	0.9807373	1.4012515
H	2.1641850	1.9016212	1.6569380
C	3.7171165	0.8469010	0.4306248
C	-0.0654075	-0.0578256	0.5071772
H	-0.0308831	0.3771479	1.5149351
H	0.3555902	0.7858093	-0.1955575
H	2.4738730	-3.1826446	-1.4810672
C	-1.4751830	-0.4255425	0.1675586
Si	-2.0569675	-1.9288244	1.2953500
H	-1.5591769	-0.7949512	-0.8678398
C	-2.4574177	0.7598650	0.3482985

H -2.1904993 1.5967036 -0.3162622
H -2.4474391 1.1428841 1.3792304
H -3.4877505 0.4644030 0.1068863
C -3.8141955 -2.3903430 0.7600922
C -0.9018601 -3.4183388 1.0410158
C -2.0200342 -1.4006343 3.1164788
H -3.8715744 -2.6056308 -0.3170993
H -4.5399642 -1.5976358 0.9888719
H -4.1373421 -3.2957990 1.2956775
H -1.0048593 -1.1627058 3.4670959
H -2.3956009 -2.2215296 3.7458633
H -2.6591093 -0.5268595 3.3077476
H 0.1502953 -3.1711262 1.2505103
H -0.9672131 -3.8308740 0.0233306
H -1.1867243 -4.2276616 1.7303028
==========

43

1b.xyz

Ti 0.5569315 -0.3743251 -1.4296994
H 2.5660714 -2.5334498 -0.4372620
C 1.5396108 -2.4689888 -0.7912398
C 1.1067281 -2.6186274 -2.1322171
H 0.3838435 -2.1627716 1.1002678
H 1.7461439 -2.8176454 -2.9866696
C -0.3071823 -2.4565423 -2.1628317
H -0.9370099 -2.5123899 -3.0482678
C -0.7576502 -2.2547990 -0.8268369
H -1.7898656 -2.1613876 -0.5092197
C 0.3855140 -2.2611843 0.0188563
H 3.4125795 -0.4494494 -2.4854294
C 2.5145235 0.1482354 -2.6165515

C	2.1599014	1.3042841	-1.8662086
H	1.4889436	-0.8443465	-4.3518499
H	2.7395493	1.7430108	-1.0570737
C	0.9306434	1.8017535	-2.3866201
H	0.4017888	2.6877005	-2.0531883
C	0.5227288	0.9549190	-3.4471260
H	-0.3841402	1.0655390	-4.0376919
C	1.5015388	-0.0623847	-3.5986949
C	-1.1241165	0.7020686	-0.5681987
H	-1.4053449	1.6320409	-1.0697112
H	-2.0039862	0.0735566	-0.4107393
C	-0.2263960	0.8909463	0.6279917
C	0.3374927	2.3102229	0.8417470
H	0.9948158	2.3517895	1.7221597
H	-0.4917874	3.0082463	1.0156400
H	0.9118273	2.6974739	-0.0061220
H	0.6713465	0.1581362	0.5882850
Si	-1.0510311	0.3341570	2.3518882
C	0.3490602	-0.0784490	3.5626046
H	0.9414732	-0.9509380	3.2490346
H	-0.0734154	-0.3129090	4.5512236
H	1.0398712	0.7663041	3.6983738
C	-2.0619649	1.8171001	2.9554555
H	-1.4363142	2.6763045	3.2313781
H	-2.6269951	1.5194385	3.8517571
H	-2.7915270	2.1473603	2.2016571
C	-2.2318872	-1.1412161	2.1772996
H	-1.7463956	-2.0943929	1.9309064
H	-3.0342528	-0.9539361	1.4490407
H	-2.7216645	-1.2804551	3.1538828

==========

43

1g.xyz

Ti	0.6807982	-1.0480467	-0.8954134
H	2.4500160	-3.3568785	0.1043850
C	1.4096281	-3.1919960	-0.1646475
C	0.8374854	-3.3787481	-1.4486882
H	0.4709273	-2.6105446	1.7855278
H	1.3645121	-3.7136892	-2.3363986
C	-0.5506107	-3.0692802	-1.3690692
H	-1.2648128	-3.1077202	-2.1876136
C	-0.8434504	-2.7281026	-0.0266572
H	-1.8233524	-2.4695293	0.3624475
C	0.3646363	-2.7944226	0.7191383
H	3.2142851	-1.8574781	-2.4852204
C	2.4840169	-1.0535230	-2.4731160
C	2.5989458	0.1621948	-1.7596729
H	0.8901046	-1.7834904	-3.8800983
H	3.4295612	0.4437904	-1.1162797
C	1.4404493	0.9418878	-2.0254725
H	1.2317776	1.9320780	-1.6295336
C	0.6140629	0.2179145	-2.9283846
H	-0.3260862	0.5551071	-3.3532923
C	1.2544890	-1.0170742	-3.2023018
C	-1.0588965	0.1262876	-0.5586027
H	-1.0876182	1.0601557	-1.1257114
H	-2.0593074	-0.3101793	-0.5171233
C	-0.4620573	0.2626074	0.8577017
C	1.0694794	0.3517162	1.0907626
H	1.2647998	0.2347037	2.1648238
H	1.5206763	1.2902831	0.7512982
H	1.7579695	-0.4751133	0.6843792

H -0.8472655 -0.5429999 1.4975518
Si -1.2768556 1.8850320 1.6791527
C -0.6759415 1.9520894 3.4749229
H 0.3995234 2.1643140 3.5572229
H -0.8889286 1.0192135 4.0174530
H -1.2056257 2.7608785 4.0015331
C -3.1471421 1.6380264 1.6032206
H -3.6453423 2.4569852 2.1439554
H -3.4547429 0.6964269 2.0811765
H -3.5266517 1.6430321 0.5723845
C -0.7271190 3.4226344 0.7226568
H 0.3609200 3.5790583 0.7559938
H -1.1894488 4.3087795 1.1839517
H -1.0478087 3.4036200 -0.3283425
==========
43
2.xyz
Ti -0.8031871 1.0607162 -1.1314678
H 1.4481662 3.1803401 -1.6810916
C 0.7127637 2.5960633 -2.2304308
C -0.6241924 2.9861382 -2.4985101
H 1.8508768 0.7476787 -2.7822760
H -1.0778347 3.9343279 -2.2262558
C -1.2335804 1.9465089 -3.2650897
H -2.2353167 1.9685572 -3.6814988
C -0.2794878 0.9070826 -3.4475576
H -0.4193040 -0.0008706 -4.0250503
C 0.9235406 1.3143459 -2.8035223
H -2.9876466 3.2179414 -0.6765901
C -2.7785205 2.1855072 -0.4130136
C -2.1114403 1.7433663 0.7539053

H	-3.7225757	1.0303766	-2.0897300
H	-1.6968538	2.3839152	1.5293355
C	-2.0808760	0.3200174	0.7327506
H	-1.6577385	-0.3214154	1.4980256
C	-2.7325113	-0.1247718	-0.4501507
H	-2.9283756	-1.1546125	-0.7288864
C	-3.1580071	1.0328654	-1.1627257
C	1.1157731	0.5183819	0.2427719
H	1.1133932	1.6296330	0.2510058
H	1.4725342	0.0429155	-0.6785170
C	1.0774764	-0.1739436	1.4120419
H	-0.8506646	-0.5218675	-1.6997332
C	0.8593715	0.5298254	2.7164433
H	0.0642893	0.0495530	3.3092462
H	0.6292145	1.5990033	2.6011759
H	1.7704459	0.4465654	3.3327788
Si	1.4409304	-2.0852755	1.4502402
C	1.7728717	-2.6878224	-0.3106899
H	2.6771199	-2.2314383	-0.7396101
H	0.9255507	-2.4881561	-0.9830333
H	1.9346226	-3.7761424	-0.3014211
C	-0.0723835	-2.9503546	2.1979378
H	0.1462045	-4.0231182	2.3096622
H	-0.9599031	-2.8651882	1.5550314
H	-0.3253722	-2.5662785	3.1964843
C	2.9615353	-2.3043656	2.5583257
H	3.8223903	-1.7292605	2.1885270
H	3.2528810	-3.3653006	2.5748141
H	2.7638201	-2.0014436	3.5963483

==========

43

3.xyz

Ti	-1.6594577	-0.6820265	-0.4771792
H	0.3874790	-0.8597626	-2.7966328
C	-0.5730315	-1.2887801	-2.5211304
C	-1.8414609	-0.7542325	-2.8488998
H	-0.0054351	-3.1422971	-1.3891016
H	-2.0255046	0.1364141	-3.4422234
C	-2.8355845	-1.6154954	-2.2949011
H	-3.9097939	-1.5076729	-2.4054593
C	-2.1784747	-2.6870290	-1.6263221
H	-2.6563109	-3.5408762	-1.1576820
C	-0.7774750	-2.4781017	-1.7665672
H	-0.7840152	2.1321563	0.4778366
C	-1.7026593	1.5610736	0.3689926
C	-2.2921356	0.7308578	1.3566183
H	-2.3359073	2.0518137	-1.7193729
H	-1.9184618	0.5588651	2.3624411
C	-3.4758580	0.1579418	0.8118243
H	-4.1743324	-0.4848655	1.3379936
C	-3.6086977	0.6374869	-0.5204090
H	-4.4364903	0.4298616	-1.1904953
C	-2.5019408	1.4964833	-0.8011568
C	0.4225981	-1.0243333	0.9363511
H	0.0978085	-2.0441778	0.6680326
H	-0.0217187	-0.5983865	1.8361644
C	1.5872251	-0.5081901	0.4423270
H	-2.3655730	-1.8624317	0.4899690
C	2.3869325	-1.2112506	-0.6144301
H	2.6539309	-0.5344011	-1.4419763
H	1.8994657	-2.1063752	-1.0205986
H	3.3491761	-1.5279305	-0.1780766

Si 2.4097280 1.0753839 1.2180908
C 2.4740724 2.4211185 -0.1192058
H 2.9402899 3.3275715 0.2949957
H 1.4785111 2.7038611 -0.4898268
H 3.0808104 2.1082576 -0.9811543
C 1.4313731 1.6400963 2.7377658
H 1.9543159 2.4888745 3.2037510
H 1.3658014 0.8466814 3.4967187
H 0.4131588 1.9826327 2.5065005
C 4.1605571 0.5625333 1.7280372
H 4.6537669 1.4033267 2.2385227
H 4.7838437 0.2924973 0.8639993
H 4.1494744 -0.2871728 2.4258688
==========
43
4.xyz
Ti -0.6161806 1.4938810 -0.7069684
H 1.2643852 2.5362821 -2.9543189
C 0.4738393 1.8057113 -2.8052737
C -0.9105019 2.0144324 -3.0314985
H 1.5949314 -0.0598337 -2.2731635
H -1.3624370 2.9443700 -3.3645206
C -1.5929332 0.7984663 -2.7627774
H -2.6592119 0.6308052 -2.8727249
C -0.6349305 -0.1735418 -2.3588213
H -0.8341548 -1.2187894 -2.1383894
C 0.6492823 0.4459862 -2.4100038
H -1.2941208 4.3709280 0.2959838
C -1.7358931 3.3776562 0.2981649
C -1.5779105 2.3852541 1.3131572
H -2.9654317 3.3852139 -1.5644837

H -1.0209524 2.5010363 2.2379155
C -2.3811263 1.2669117 0.9607755
H -2.5076634 0.3576200 1.5430167
C -3.0064861 1.5457973 -0.2760844
H -3.7089335 0.8970909 -0.7901474
C -2.6164228 2.8611878 -0.6800208
C 1.4652607 1.0090824 0.2613421
C 0.5236739 0.0937198 0.9318991
H -0.4712372 -0.1273357 0.3011124
H 0.9007099 -0.9361530 0.9876861
H 0.1328356 0.4053550 1.9088392
C 1.3438947 2.4763705 0.3653201
H 2.2564528 3.0002613 0.0495166
H 0.9937815 2.8832297 1.3219355
H 0.5895385 2.9587373 -0.4257501
Si 3.2133312 0.3335973 -0.2011686
C 3.1721319 -1.5271034 -0.5762580
H 4.2038834 -1.8619781 -0.7631729
H 2.5815738 -1.8077575 -1.4594383
H 2.8028340 -2.1135335 0.2778039
C 4.2419922 0.6164724 1.3706021
H 5.2684037 0.2502486 1.2170090
H 3.8224589 0.0804893 2.2341046
H 4.3065185 1.6827569 1.6320705
C 4.0053383 1.3025950 -1.6296906
H 3.5378022 1.1217866 -2.6072549
H 5.0580078 0.9924976 -1.7153779
H 4.0124593 2.3877385 -1.4491304
==========
43
5.xyz

Ti	-1.2858094	0.5263790	-0.2865874
H	1.2425318	0.4524569	-2.1101848
C	0.2139671	0.1128875	-2.1201635
C	-0.8904184	0.8376915	-2.6247758
H	0.3420203	-1.9500566	-1.2457799
H	-0.8498718	1.8299826	-3.0650362
C	-2.0506017	0.0119625	-2.5098711
H	-3.0521569	0.2646692	-2.8442732
C	-1.6588762	-1.2136262	-1.9243261
H	-2.3037267	-2.0696995	-1.7419854
C	-0.2600310	-1.1457503	-1.6538801
H	-1.0428582	3.6355506	-0.1569102
C	-1.7772358	2.8653219	0.0608058
C	-1.9966715	2.2423353	1.3242596
H	-2.8769207	2.6697611	-1.8720557
H	-1.4501900	2.4482315	2.2404879
C	-3.0728850	1.3382443	1.1926848
H	-3.4874018	0.7150838	1.9816008
C	-3.5229634	1.3814657	-0.1584715
H	-4.3615990	0.8249909	-0.5679604
C	-2.7419858	2.3541325	-0.8426439
C	0.8606035	1.3565260	0.5235742
H	0.4536976	2.1390634	1.1603472
H	1.6417941	1.7018643	-0.1553465
C	0.8537641	0.0163274	0.9571546
H	-2.3810724	-0.9080604	0.2363887
C	-0.2126448	-0.4427223	1.7606851
H	-1.7758795	-0.9415120	0.7993714
H	-0.7399957	0.2363215	2.4342274
H	-0.2322264	-1.4892763	2.0747210
Si	2.3893428	-1.1566785	0.6921380

C 1.9123564 -2.9829104 0.8826027
H 2.8328145 -3.5852502 0.8372518
H 1.2436395 -3.3667910 0.0991361
H 1.4478206 -3.1888369 1.8578341
C 3.3156168 -0.8583881 -0.9344980
H 4.2909839 -1.3641569 -0.8638320
H 3.5276002 0.2063474 -1.1115599
H 2.8070076 -1.2687830 -1.8173683
C 3.4861849 -0.6352728 2.1483137
H 4.3995106 -1.2488259 2.1652927
H 2.9733006 -0.7691606 3.1112699
H 3.7894653 0.4181608 2.0673624
==========
41
6.xyz
Ti -1.2928924 0.6321344 -0.3162306
H 1.1590187 -0.3412510 -1.9451799
C 0.0765720 -0.3836062 -1.9848272
C -0.7614474 0.5542458 -2.6486599
H -0.4158018 -2.2654729 -0.8704831
H -0.4307529 1.4456876 -3.1773975
C -2.1020411 0.1117677 -2.5175560
H -2.9770008 0.5939825 -2.9423131
C -2.1021137 -1.0771616 -1.7340880
H -2.9770138 -1.6607644 -1.4579597
C -0.7518707 -1.3951518 -1.4225013
H -1.3361133 3.7205625 0.1837891
C -2.0034081 2.8686497 0.2900080
C -2.1774690 2.0814140 1.4581050
H -2.9985011 2.7712631 -1.7089005
H -1.6629462 2.2257803 2.4045387

C -3.1454253 1.0804783 1.1832644
H -3.4999468 0.3238217 1.8791435
C -3.5776376 1.2485892 -0.1580432
H -4.3448087 0.6643238 -0.6574722
C -2.8669974 2.3569714 -0.7136720
C 0.8066672 1.3699694 0.5636531
H 0.3405206 2.1122631 1.2119535
H 1.6162055 1.7616032 -0.0559555
C 0.7907247 0.0037481 0.9098844
C -0.3670577 -0.5246407 1.5296301
H -0.9007914 0.0609174 2.2790520
H -0.4554347 -1.6042108 1.6710255
Si 2.3786485 -1.0967602 0.6546518
C 3.1156902 -1.0342132 2.4011394
H 4.0654660 -1.5895253 2.4219108
H 2.4414094 -1.4897136 3.1399373
H 3.3217798 -0.0018537 2.7167888
C 3.5886395 -0.3106341 -0.5749391
H 4.5411113 -0.8599076 -0.5151560
H 3.8098566 0.7374201 -0.3272139
H 3.2667206 -0.3561322 -1.6251468
C 1.9952260 -2.8919644 0.1810200
H 2.9015130 -3.4922361 0.3546342
H 1.7311136 -3.0140793 -0.8785496
H 1.2005888 -3.3363141 0.7981157

==========

43

TS1a1_1a2.xyz

Ti 1.8301854 -0.4009557 -0.4252648
C 2.0579541 -2.5844285 -1.2520906
C 3.0362268 -1.8047218 -1.9374857

H	-0.1854901	-2.5386010	-1.3366406
H	4.1131359	-1.9224069	-1.8653169
C	2.3574781	-0.8441018	-2.7279843
H	2.8231370	-0.0942257	-3.3647738
C	0.9576391	-1.0496155	-2.5613515
H	0.1717595	-0.4764198	-3.0483327
C	0.7677212	-2.1269114	-1.6546810
H	4.6878807	0.6264499	-0.6413219
C	3.9621983	0.4089107	0.1383656
C	3.8127058	-0.8310475	0.8242590
H	2.8771355	2.3590311	0.3782972
H	4.4059775	-1.7265956	0.6663094
C	2.7744103	-0.6812324	1.7849487
H	2.4198647	-1.4519322	2.4653676
C	2.2847908	0.6445168	1.7032608
H	1.5021434	1.0716500	2.3206639
C	3.0097280	1.3204187	0.6770334
C	-0.1862630	-0.0049945	0.1632280
H	0.1627624	1.0270229	0.4089557
H	-0.5646204	-0.0133709	-0.8718361
H	2.2608638	-3.4131895	-0.5777419
C	-1.2683411	-0.4716379	1.1050241
C	-0.8806217	-0.5071142	2.5901711
H	-1.6988466	-0.9145753	3.1992976
H	-0.6586753	0.4967307	2.9835599
H	0.0005759	-1.1424426	2.7687536
H	-1.5689426	-1.4882016	0.7884329
Si	-2.9261683	0.5580776	0.8370990
C	-4.2711691	-0.2097138	1.9297674
H	-4.0588027	-0.0854320	3.0009877
H	-4.3966913	-1.2838295	1.7281950

H -5.2366073 0.2784195 1.7286014
C -2.6226296 2.3707872 1.3090636
H -1.8522445 2.8409171 0.6797077
H -2.3206458 2.4789912 2.3609936
H -3.5478772 2.9512310 1.1764940
C -3.4209391 0.4235863 -0.9917463
H -2.7067062 0.9279246 -1.6595699
H -4.3997405 0.9001258 -1.1507143
H -3.5156016 -0.6244896 -1.3139526
==========
43
TS1a1_b.xyz
Ti 1.8486610 0.3862798 -0.2988413
C 2.9271554 -0.8926721 -2.0026625
C 3.1080765 0.4838453 -2.3291723
H 1.0750863 -2.1448942 -1.8835373
H 4.0574104 1.0091671 -2.3845678
C 1.8282518 1.0485637 -2.5706589
H 1.6288055 2.0845568 -2.8395395
C 0.8514551 0.0174921 -2.4183372
H -0.2183345 0.1239351 -2.5662664
C 1.5354491 -1.1779753 -2.0765984
H 4.8975231 0.1474731 0.0708200
C 4.0278008 0.4721099 0.6340550
C 3.2207709 -0.3488950 1.4694024
H 3.8935948 2.6564823 0.1390445
H 3.3700666 -1.4098589 1.6600443
C 2.2076561 0.4744225 2.0479019
H 1.4408182 0.1485907 2.7438608
C 2.3791892 1.7916340 1.5515976
H 1.7516272 2.6482591 1.7883529

C 3.4963510 1.7925453 0.6668037
C -0.2241262 0.5535095 0.2859654
H -0.2915897 1.0465529 1.2645199
H -0.5318822 1.2915214 -0.4836959
H 3.7144584 -1.6070957 -1.7764139
C -1.0738851 -0.7098461 0.2665170
C -0.7637336 -1.6697683 1.4345577
H -1.4166762 -2.5526531 1.4080472
H -0.9187890 -1.1782399 2.4070199
H 0.2726609 -2.0449364 1.4187406
H -0.9525503 -1.2549017 -0.6866606
Si -2.9880641 -0.2383619 0.2568211
C -3.9830804 -1.8516414 0.1824252
H -3.8743955 -2.4517843 1.0967667
H -3.6890924 -2.4756308 -0.6744570
H -5.0530590 -1.6192438 0.0691021
C -3.4045661 0.7426384 1.8248771
H -2.8569582 1.6946917 1.8767257
H -3.1891403 0.1713584 2.7393549
H -4.4785094 0.9823914 1.8373563
C -3.3365762 0.8018343 -1.2930923
H -2.7829634 1.7523089 -1.2994766
H -4.4066052 1.0547343 -1.3375302
H -3.0982911 0.2535008 -2.2171716
==========
43
TS1a1_g.xyz
Ti 1.6779943 0.2854410 -0.8684645
C 1.9516137 -0.7804774 -2.9875365
C 2.1700468 0.6153195 -3.1841847
H 0.1188199 -1.9106495 -2.3753135

H	3.0981729	1.0788169	-3.5068157
C	0.9599815	1.2942063	-2.8849233
H	0.8033368	2.3704051	-2.9353783
C	-0.0196420	0.3187725	-2.5247853
H	-1.0553966	0.5177364	-2.2690131
C	0.5951059	-0.9579641	-2.5981851
H	4.6139746	-0.2346970	-1.6396612
C	4.0359950	0.0587146	-0.7683931
C	3.4644067	-0.8239492	0.1898226
H	4.0188633	2.2983422	-0.9063630
H	3.5344594	-1.9099964	0.1809690
C	2.8213774	-0.0313180	1.1885480
H	2.3033621	-0.4066612	2.0657967
C	2.9792734	1.3323880	0.8320579
H	2.5838226	2.1842877	1.3814857
C	3.7195460	1.3925359	-0.3840491
C	-0.0313848	0.5049316	0.4318251
H	0.2983362	0.8491929	1.4206319
H	-0.4843371	1.3728466	-0.0924285
H	2.6795519	-1.5719971	-3.1449060
C	-0.9878999	-0.6711767	0.5701911
C	-0.4404748	-1.7944650	1.4749925
H	-1.1647609	-2.6142963	1.5740754
H	-0.2274775	-1.4222096	2.4889626
H	0.4899715	-2.2408003	1.0877815
H	-1.2406808	-1.0975569	-0.4175321
Si	-2.7382480	-0.0476527	1.2303277
C	-3.8770062	-1.5572270	1.3780720
H	-3.5496515	-2.2504910	2.1654251
H	-3.9415529	-2.1168467	0.4331814
H	-4.8949647	-1.2265264	1.6350021

C -2.5134220 0.8010275 2.9103503
H -1.8785904 1.6962228 2.8407597
H -2.0751313 0.1258914 3.6594298
H -3.4922178 1.1230760 3.2966112
C -3.4502888 1.1693361 -0.0415622
H -2.8210111 2.0619053 -0.1745180
H -4.4372157 1.5218819 0.2939119
H -3.5966570 0.6956804 -1.0241976
==========
43
TS1a2_b.xyz
Ti 1.7748073 -0.3750698 -0.7735774
C 2.0549744 -0.5785063 -3.1323559
C 2.0840635 0.8031601 -2.7850898
H 0.4154690 -2.0994619 -3.0013895
H 2.9304251 1.4754637 -2.9019144
C 0.7977360 1.1520500 -2.2834761
H 0.4884481 2.1401340 -1.9460824
C -0.0258040 -0.0121578 -2.3344728
H -1.0685066 -0.0714842 -2.0422568
C 0.7533246 -1.0768994 -2.8487677
H 4.6727135 -0.5769985 -1.8480130
C 4.1269881 -0.7634831 -0.9281333
C 3.4732570 -1.9797759 -0.5712205
H 4.3073660 1.1867555 0.1553610
H 3.4491722 -2.8894234 -1.1669339
C 2.9111985 -1.8132264 0.7300416
H 2.3761163 -2.5684909 1.2979918
C 3.1956458 -0.4877992 1.1543995
H 2.8990788 -0.0411038 2.1009342
C 3.9363310 0.1640039 0.1267840

C 0.1375598 -0.7993609 0.5360648
H 0.7128125 -0.5761699 1.4493158
H -0.3244389 0.1464366 0.1642124
H 2.8714069 -1.1482106 -3.5662102
C -0.9013346 -1.8530907 0.8326957
Si -1.9938922 -1.3384641 2.3893711
H -0.3704022 -2.7502297 1.2033536
C -1.7914370 -2.2555278 -0.3518150
H -1.1988830 -2.6178396 -1.2062394
H -2.4147495 -1.4189277 -0.7036431
H -2.4762608 -3.0667440 -0.0697199
C -3.1723921 -2.7716471 2.7756782
C -0.8287968 -1.0424730 3.8597070
C -2.9607861 0.2426809 1.9823711
H -2.6304561 -3.7172915 2.9239980
H -3.9163587 -2.9247971 1.9812473
H -3.7237126 -2.5584468 3.7038934
H -2.2957086 1.0931516 1.7708107
H -3.5890095 0.5277049 2.8395882
H -3.6309097 0.1075283 1.1208652
H -0.1735734 -0.1715043 3.7095858
H -0.1966278 -1.9199613 4.0632665
H -1.4158497 -0.8485228 4.7697806
==========
43
TS1b_1g.xyz
Ti 1.0231086 -0.5087577 -1.2014356
H 3.1592342 -2.6825850 -0.9943909
C 2.0758815 -2.6149518 -1.0538319
C 1.2971483 -2.6422442 -2.2437548
H 1.4586869 -2.5335290 1.0980463

H	1.6844953	-2.7396397	-3.2526641
C	-0.0766716	-2.5621032	-1.8795873
H	-0.9213101	-2.5494982	-2.5641275
C	-0.1507374	-2.5109178	-0.4683120
H	-1.0628708	-2.4572117	0.1180444
C	1.1771137	-2.5360997	0.0470138
H	3.5380684	-0.6609167	-2.9651831
C	2.7166050	0.0238638	-2.7758361
C	2.7156858	1.0908690	-1.8434067
H	1.1596300	-0.6146667	-4.2684684
H	3.5315708	1.3450331	-1.1690639
C	1.4658445	1.7575118	-1.9344287
H	1.1575252	2.6164870	-1.3472742
C	0.6886947	1.1149461	-2.9358830
H	-0.3050344	1.4054082	-3.2626705
C	1.4587765	0.0431939	-3.4581827
C	-0.8093865	0.3597836	-0.5247578
H	-1.0282287	1.3621266	-0.9032139
H	-1.7089402	-0.2584057	-0.5887551
C	-0.2001240	0.3896039	0.8822769
C	0.9313755	1.3916443	1.2216360
H	1.1124955	1.3942237	2.3049356
H	0.6671908	2.4152825	0.9232403
H	1.9147676	1.1700677	0.7698516
H	0.0881457	-0.6158752	1.2380069
Si	-1.7297596	0.7226015	2.1232455
C	-1.0335504	0.7214882	3.8866129
H	-0.4592880	-0.1900291	4.1078301
H	-1.8733805	0.7580481	4.5974800
H	-0.3963487	1.5917156	4.0956355
C	-2.4999198	2.3946562	1.6918088

H -1.7717212 3.2163473 1.7518591
H -3.3020176 2.6193005 2.4111797
H -2.9465179 2.3999745 0.6877573
C -2.9782330 -0.6889907 1.9324839
H -2.5391375 -1.6672824 2.1792376
H -3.4213258 -0.7442335 0.9283430
H -3.8065407 -0.5252392 2.6387026
==========
43
TS1b_2.xyz
Ti -0.5438108 1.2847535 -0.7414572
H 1.4582169 2.2147958 -2.9234144
C 0.6723991 1.4721203 -2.7980950
C -0.6965484 1.6506494 -3.1098937
H 1.7838695 -0.3028075 -2.0183879
H -1.1348991 2.5434165 -3.5441352
C -1.3846176 0.4460416 -2.7831276
H -2.4460703 0.2600109 -2.9206359
C -0.4310286 -0.4894995 -2.2894773
H -0.6301047 -1.5218639 -2.0223310
C 0.8415167 0.1524349 -2.2979516
H -0.5994335 4.3432191 -0.3854586
C -1.2253812 3.4832285 -0.1559873
C -1.1715111 2.6973099 1.0330799
H -2.5802402 3.3676367 -1.9285668
H -0.5247180 2.8901136 1.8829816
C -2.1668023 1.6836553 0.9390830
H -2.4161000 0.9501110 1.6978008
C -2.8289293 1.8436530 -0.3101932
H -3.6458984 1.2281195 -0.6771490
C -2.2654356 2.9695570 -0.9693550

C 1.3819849 0.8538145 0.6575600
H 1.4331968 1.8077732 1.1949411
H 2.1671753 0.6886194 -0.0805849
C 0.7225342 -0.2237682 1.2381760
H -0.8959056 -0.1935385 0.0618227
C 0.0373204 -0.0377431 2.5720738
H -0.8645255 -0.6555883 2.6783708
H -0.2039312 1.0053211 2.8063857
H 0.7407394 -0.3800556 3.3487660
Si 1.1557156 -2.1106641 0.9257048
C -0.4414196 -3.1246921 0.8457847
H -0.1941704 -4.1890562 0.7163948
H -1.0898642 -2.8285181 0.0095548
H -1.0261034 -3.0381665 1.7728371
C 2.1546417 -2.5848209 2.4707119
H 3.0145480 -1.9171835 2.6265922
H 2.5484675 -3.6039975 2.3393098
H 1.5455590 -2.5850491 3.3850002
C 2.2524321 -2.4334017 -0.5861939
H 3.1044359 -1.7409401 -0.6539140
H 1.7134647 -2.4339146 -1.5419803
H 2.6792309 -3.4410855 -0.4646418
==========
43
TS1g_1g.xyz
Ti 0.7225989 -1.0591496 -0.9248713
H 2.4609627 -3.2863330 0.3197513
C 1.4477444 -3.1647528 -0.0570264
C 1.0181410 -3.4052832 -1.3845696
H 0.2923868 -2.5746789 1.7710779
H 1.6442194 -3.7419359 -2.2049116

C	-0.3773592	-3.1298862	-1.4573116
H	-1.0027591	-3.2162336	-2.3420308
C	-0.8200025	-2.7592285	-0.1620051
H	-1.8427168	-2.5340071	0.1209723
C	0.3058396	-2.7764151	0.7035158
H	3.1807868	-1.7979685	-2.6508633
C	2.4122879	-1.0316781	-2.6135376
C	2.5214153	0.2238001	-1.9679914
H	0.7682413	-1.8837336	-3.8848895
H	3.3830936	0.5705899	-1.4006234
C	1.3161880	0.9426504	-2.1878734
H	1.0901142	1.9364086	-1.8100787
C	0.4604271	0.1414312	-2.9900781
H	-0.5247354	0.4173800	-3.3533694
C	1.1374220	-1.0763261	-3.2597815
C	-1.0102919	0.0925120	-0.4521225
H	-1.0452207	1.0278297	-1.0191717
H	-2.0099124	-0.3475416	-0.4378110
C	-0.4578999	0.2673043	0.9798660
C	1.0975026	0.3043868	1.1890586
H	1.4106892	1.1050073	1.8752467
H	1.6918601	0.5614680	0.2854788
H	1.5002240	-0.6187070	1.6330790
H	-0.8506476	-0.5378548	1.6169145
Si	-1.2720464	1.8972891	1.7396286
C	-0.7849191	1.9490946	3.5719255
H	0.2982882	2.0463632	3.7328346
H	-1.1319328	1.0543676	4.1087020
H	-1.2592010	2.8214329	4.0470532
C	-3.1472393	1.7506719	1.5548870
H	-3.6359239	2.6021640	2.0517058

H -3.5317705 0.8336847 2.0251323
H -3.4638823 1.7565354 0.5028239
C -0.5961365 3.4097692 0.8191962
H 0.4985070 3.4921607 0.8892089
H -1.0149313 4.3240154 1.2660536
H -0.8794113 3.4133965 -0.2431947
==========
43
TS2_3.xyz
Ti -1.0343091 1.4230474 -0.6674783
H 1.0095939 1.0409784 -2.9545575
C 0.0261139 0.6721887 -2.6692618
C -1.2122291 1.2453655 -3.0429558
H 0.4983177 -1.1267820 -1.4217568
H -1.3474163 2.1116914 -3.6837390
C -2.2513207 0.4686417 -2.4501015
H -3.3181832 0.6277700 -2.5732664
C -1.6527793 -0.5969251 -1.7187580
H -2.1783741 -1.3976334 -1.2094835
C -0.2425642 -0.4625616 -1.8516195
H 0.1014442 4.2235396 0.0970925
C -0.8648248 3.7285342 0.0181536
C -1.5348395 3.0298779 1.0568314
H -1.4407475 4.1234857 -2.1049603
H -1.1867029 2.9088888 2.0794678
C -2.7623425 2.5271430 0.5407721
H -3.5213421 1.9933784 1.1034117
C -2.8431535 2.9186865 -0.8246190
H -3.6820048 2.7366212 -1.4886368
C -1.6619703 3.6528888 -1.1516705
C 1.1192091 1.0955880 0.6838566

H 0.7076022 1.9514952 1.2278293
H 1.8008814 1.3223821 -0.1446347
C 1.1377767 -0.1282609 1.2925879
H -1.8758199 0.3745781 0.3396045
C 0.3272318 -0.3712529 2.5315384
H -0.3316470 -1.2445299 2.4012997
H -0.2908111 0.4905389 2.8194786
H 0.9912588 -0.6215576 3.3751280
Si 2.3920438 -1.5293532 0.7915465
C 1.4653487 -3.1650494 0.5416936
H 2.1940052 -3.9649109 0.3416652
H 0.7619353 -3.1475856 -0.3027020
H 0.9056743 -3.4515614 1.4435149
C 3.3761427 -1.0241221 -0.7471963
H 4.1437676 -1.7886879 -0.9406223
H 3.9042298 -0.0708469 -0.5975920
H 2.7712089 -0.9450339 -1.6611784
C 3.5614005 -1.6626417 2.2790951
H 4.3662974 -2.3751164 2.0435391
H 3.0480463 -2.0309712 3.1782794
H 4.0301540 -0.6976166 2.5184706
==========
43
TS2_5.xyz
Ti -1.3294176 0.5252117 -0.2645433
H 1.1110566 0.3434480 -2.1965976
C 0.0833245 0.0025995 -2.1445347
C -1.0415794 0.7014135 -2.6346807
H 0.2496663 -1.9970365 -1.1405823
H -1.0203092 1.6623808 -3.1406034
C -2.1992216 -0.1024320 -2.3955834

H	-3.2144171	0.1375889	-2.6952389
C	-1.7847290	-1.2914764	-1.7479590
H	-2.4208829	-2.1304027	-1.4806849
C	-0.3705618	-1.2186266	-1.5711263
H	-1.0213095	3.6176700	-0.0634479
C	-1.7738507	2.8560902	0.1196164
C	-2.0174293	2.1839389	1.3551134
H	-2.8476150	2.7527044	-1.8345859
H	-1.4835088	2.3473276	2.2871918
C	-3.1241494	1.3189401	1.1783812
H	-3.5729006	0.6839428	1.9377267
C	-3.5595119	1.4355139	-0.1698300
H	-4.4010495	0.9083834	-0.6096364
C	-2.7400822	2.4049205	-0.8118575
C	0.9204414	1.3728864	0.5410029
H	0.4228351	2.1376420	1.1327896
H	1.6981175	1.7455896	-0.1281196
C	0.8902756	0.0357207	0.9075461
H	-2.2555333	-0.7967240	0.4260040
C	-0.2023432	-0.4619830	1.7215451
H	-1.4401479	-0.7819919	1.0198537
H	-0.5943299	0.1911640	2.5074095
H	-0.1198293	-1.5017236	2.0568264
Si	2.4406866	-1.1113110	0.6050601
C	3.5386819	-0.6037894	2.0660414
H	4.4602308	-1.2052129	2.0640813
H	3.0366565	-0.7645184	3.0308339
H	3.8255401	0.4554290	2.0037142
C	2.0114457	-2.9524796	0.7627889
H	2.9565476	-3.5173569	0.7796657
H	1.4170353	-3.3609379	-0.0664298

H 1.4913974 -3.1840322 1.7038021
C 3.3326842 -0.7555097 -1.0277011
H 4.3276419 -1.2243366 -0.9814626
H 3.4987261 0.3183290 -1.1976887
H 2.8217180 -1.1769537 -1.9041007
==========
43
TS3_4.xyz
Ti -0.7464308 1.3995632 -0.6860115
H 1.6205652 2.2412373 -2.5400868
C 0.6663054 1.7278554 -2.6111214
C -0.5915660 2.3387819 -2.8525993
H 1.2247738 -0.4174761 -2.2846581
H -0.7636285 3.3968336 -3.0303776
C -1.5715733 1.3041381 -2.8982641
H -2.6232906 1.4383762 -3.1283010
C -0.9257083 0.0637549 -2.6428029
H -1.3914294 -0.9169476 -2.6394436
C 0.4622483 0.3303884 -2.4732515
H -1.3863130 4.1147330 0.7374796
C -1.8550241 3.1525556 0.5457227
C -1.7808131 1.9991479 1.3816884
H -2.9446739 3.5134922 -1.3664073
H -1.2782908 1.9459869 2.3434647
C -2.5715979 0.9720564 0.7946030
H -2.7748175 -0.0080773 1.2150110
C -3.1178980 1.4898236 -0.4108655
H -3.7864235 0.9549836 -1.0787504
C -2.6811139 2.8389350 -0.5569248
C 1.5765315 0.9484062 0.3535549
C 0.6905891 0.0491491 0.9063704

H -0.9423822 -0.2297152 -0.2823065
H 0.8624163 -1.0232644 0.8093273
H -0.0172895 0.3328495 1.6866294
C 1.3440086 2.4242099 0.5281260
H 2.2367421 3.0203146 0.2958284
H 0.9739575 2.7033803 1.5231008
H 0.5929956 2.8799534 -0.2083451
Si 3.3409746 0.3367491 -0.2075812
C 3.4188021 -1.5404035 0.0166341
H 4.4325193 -1.8878270 -0.2334453
H 2.7208508 -2.0911582 -0.6308379
H 3.2243951 -1.8326212 1.0588031
C 4.4839242 1.2041163 1.0367992
H 5.5077938 0.8199545 0.9116188
H 4.1848198 1.0228391 2.0786153
H 4.5265369 2.2914055 0.8748884
C 3.9047111 0.8270731 -1.9523350
H 3.3406859 0.3480785 -2.7632276
H 4.9514006 0.4997319 -2.0556053
H 3.9005164 1.9146299 -2.1154353
==========
43
TS5_5.xyz
Ti -1.2026230 0.4448951 -0.3129276
H 1.3038314 0.3761353 -2.1625312
C 0.2833027 0.0139212 -2.1514872
C -0.8474129 0.7039110 -2.6523861
H 0.4740712 -2.0347004 -1.2571527
H -0.8329949 1.6845494 -3.1183665
C -1.9852349 -0.1484238 -2.5123580
H -2.9957720 0.0724219 -2.8416810

C	-1.5517609	-1.3575992	-1.9225583
H	-2.1707896	-2.2312710	-1.7307676
C	-0.1517186	-1.2512285	-1.6697830
H	-0.8971610	3.5518840	-0.1495172
C	-1.6571246	2.7986951	0.0363285
C	-1.9292649	2.1691076	1.2840911
H	-2.6957781	2.6467016	-1.9353406
H	-1.4067997	2.3526774	2.2186448
C	-3.0263908	1.2946283	1.1086806
H	-3.5062594	0.7068819	1.8891729
C	-3.4311789	1.3628613	-0.2585893
H	-4.2703845	0.8324565	-0.6997297
C	-2.6028029	2.3185799	-0.9052666
C	0.8974853	1.2660616	0.4435286
H	0.5579331	2.0502855	1.1185866
H	1.6683455	1.6064083	-0.2498181
C	0.9409054	-0.0733068	0.9264445
H	-2.4113038	-0.7729120	0.6761364
Si	2.4950099	-1.2188940	0.6738480
C	-0.1001012	-0.5214414	1.7366129
H	-2.0023252	-1.2839120	0.2450242
H	-0.6961714	0.1655346	2.3414396
H	-0.1633399	-1.5688798	2.0366848
C	2.0495547	-3.0477571	0.9100651
C	3.3952851	-0.9445731	-0.9727419
C	3.6070038	-0.6422093	2.0969134
H	2.9764197	-3.6401677	0.8707766
H	1.3789493	-3.4558952	0.1403450
H	1.5936295	-3.2357984	1.8927058
H	4.3747259	-1.4430337	-0.9086563
H	3.5976580	0.1186283	-1.1690710

H 2.8775026 -1.3713327 -1.8423985
H 4.5371184 -1.2299182 2.1070640
H 3.1155195 -0.7712887 3.0713782
H 3.8799128 0.4172167 1.9906210
==========
43
Cp2TiH+_CH2CMeSiMe3_beforeH2.xyz
Ti -1.4663588 0.4878601 -0.2587104
H 0.9530963 -0.4290794 -2.0036204
C -0.1216713 -0.5693798 -1.9558403
C -1.0867192 0.2583855 -2.5798065
H -0.3470667 -2.3723195 -0.6458700
H -0.8793202 1.1106491 -3.2201912
C -2.3762995 -0.2902561 -2.2917427
H -3.3200477 0.0729757 -2.6844818
C -2.2037663 -1.4229778 -1.4557176
H -2.9859944 -2.0850751 -1.0983026
C -0.8036815 -1.5861846 -1.2384978
H -0.8738950 3.5551804 -0.1592630
C -1.7002755 2.8666348 -0.0087574
C -2.0705202 2.2335134 1.2187773
H -2.6267105 2.7954782 -2.0345810
H -1.5858802 2.3684127 2.1820765
C -3.2440018 1.4658747 0.9856242
H -3.8176989 0.9224390 1.7295711
C -3.5776390 1.6022082 -0.3906336
H -4.4349890 1.1463508 -0.8759472
C -2.6294330 2.4756980 -0.9964329
C 0.9856666 1.4125487 0.5203031
H 0.4274624 2.1689299 1.0694053
H 1.6969387 1.7926020 -0.2158794

C	0.9895354	0.1011004	0.8989893
H	-2.4471650	-0.5747687	0.6055106
C	-0.0309175	-0.3765266	1.8926716
H	-1.0760568	-0.5890792	1.4424457
H	-0.2131442	0.3330521	2.7107718
H	0.2056094	-1.3619971	2.3165159
Si	2.5505037	-1.0043047	0.5345663
C	3.4565296	-0.9156950	2.2002271
H	4.4023888	-1.4740484	2.1288928
H	2.8721399	-1.3617657	3.0174774
H	3.6970738	0.1203077	2.4765499
C	2.1573789	-2.8152712	0.1366667
H	3.0888388	-3.3930229	0.2405292
H	1.8007717	-2.9674299	-0.8911337
H	1.4315672	-3.2610372	0.8327086
C	3.6133482	-0.2225473	-0.8233540
H	4.5417595	-0.8066939	-0.9165358
H	3.9070005	0.8082126	-0.5783493
H	3.1416431	-0.2189542	-1.8166316

==========

Appendix D

Supporting Information for Chapter 5:

Mechanism(s) of random, reversible α-H(D), β-H(D) and γ-H(D) exchange in the isotopologous titanocene(IV) complexes $[Cp_2TiCH_2CH(CH_3)(CMe_3)]^+$ and $[Cp_2TiCH_2CH(CD_3)(CMe_3)]^+$

Alexandre F. Dunlop-Brière and Michael C. Baird*
Department of Chemistry, Queen's University,
Kingston, ON K7L 3N6, Canada
Email: bairdmc@chem.queensu.ca

Peter H. M. Budzelaar*
Department of Chemistry, University of Manitoba,
Winnipeg, MB R3T 2N2, Canada

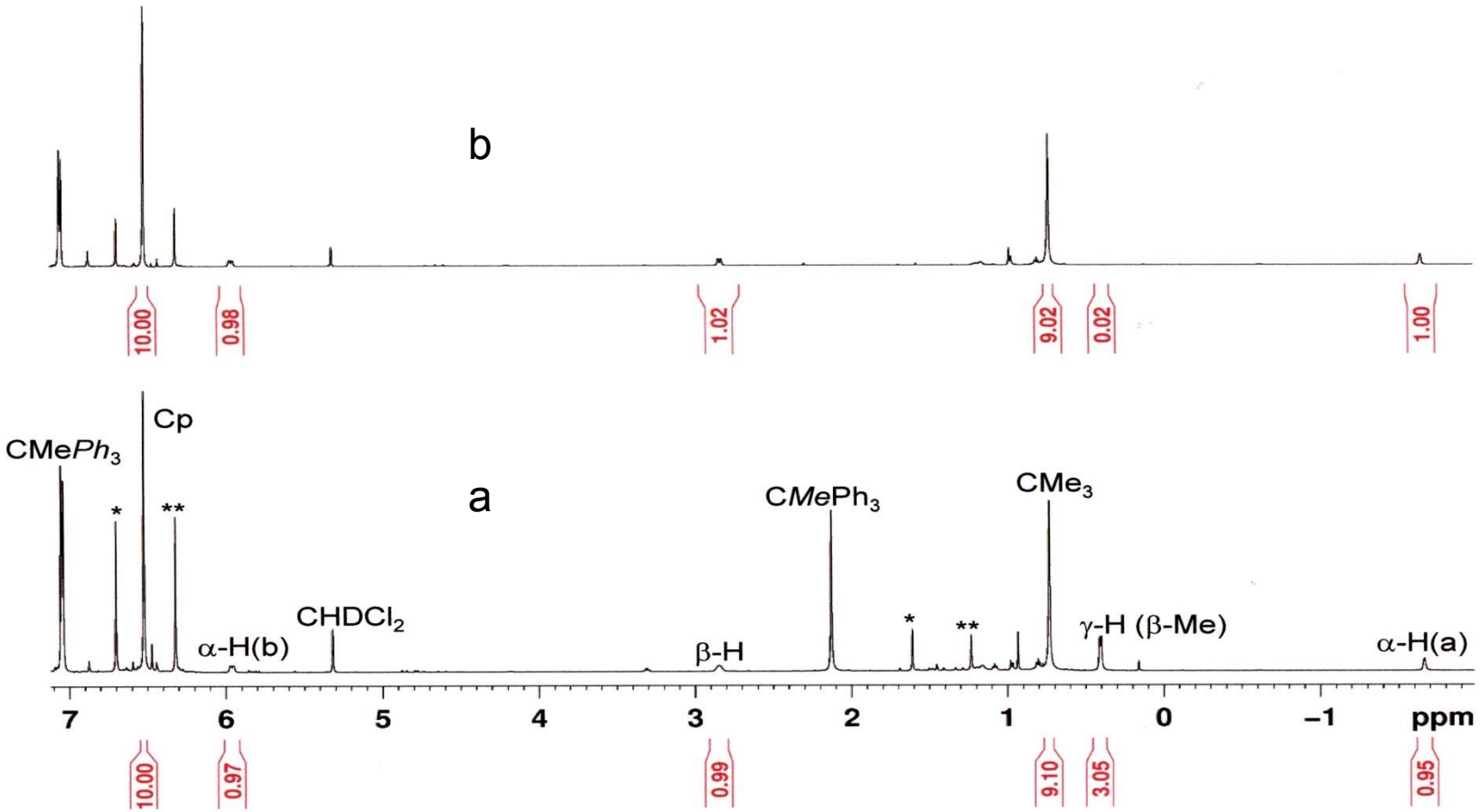

Figure D1. ^{1}H NMR spectra (205 K, CD_2Cl_2) of $[Cp_2TiCH_2CHCH_3CMe_3]^+$ (**II**) (**a**) and $[Cp_2TiCH_2CHCD_3CMe_3]^+$ (**II**-CD_3) (**b**). In (**a**), the Cp, α-H(a), α-H(b), β-H, CMe_3 and γ-Me resonances of **II** are noted (δ 6.526, 5.964, 2.849, 0.735, 0.483, -1.663); the methyl and Cp resonances of **I** and the contact ion pair $[Cp_2TiMe\{B(C_6F_5)_4\}]$,[3e,f] are noted by * and **, respectively. Note that the γ-Me resonance of **II**-CD_3 is absent (**b**) because of the deuteration.

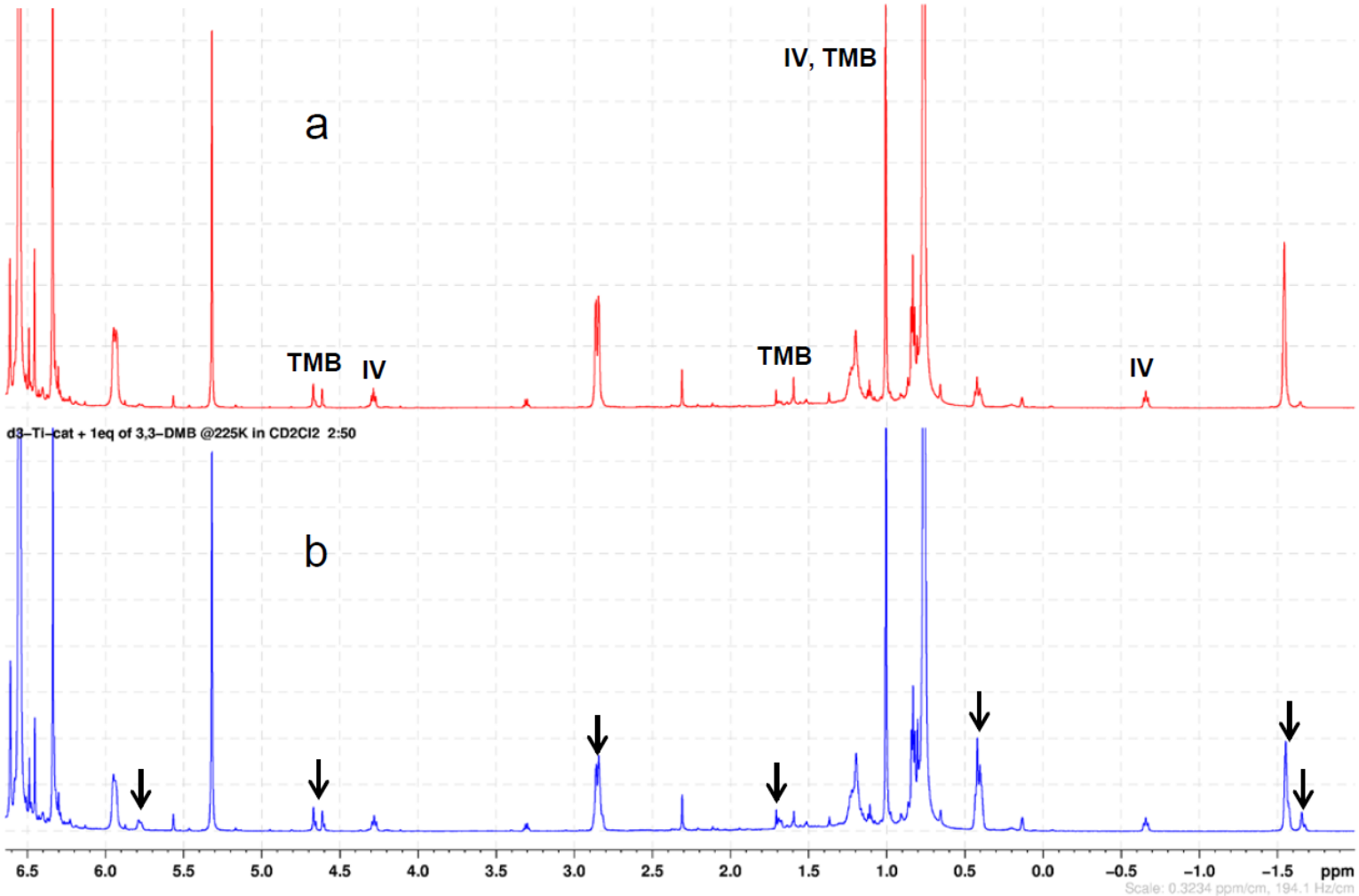

Figure D2a. ^{1}H NMR spectra at in CD_2Cl_2 of **II-CD$_3$** and its thermolysis products (**a**) immediately after warming to 225 K, (**b**) at 27 min. Assignments are as in Figure D1; note the resonances of $[Cp_2TiCH_2CH_2CMe_3]^+$ (**V**) and 2,3,3-TMB, which have begun to grow inintensity. The vertical arrows indicate the new peaks which are growing in as new isotopomers/isotopologues of **II**-CD_3 form and deuterium appears in the 2,3,3-TMB. Notice that the CMe_3 resonances of **V** and 2,3,3-TMB overlap and cannot be distinguished.

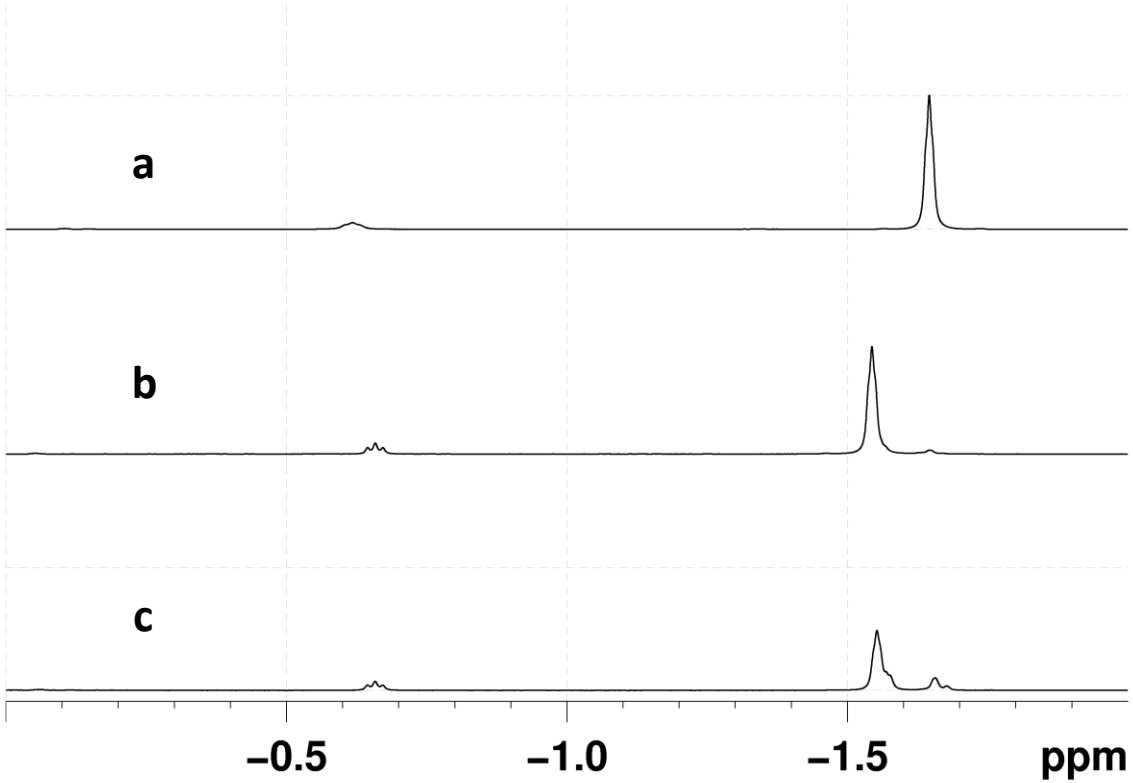

Figure D2b. Inset of the negative region of the spectrum at 205 K (a), immediately after warming to 225 K (b) and after 27 min at 225 K (c). The Figure shows the resonances of both α-H(a) at δ ~–1.55-1.65, and also of the (agostic) β-CH_2 resonance of **V** at δ –0.65.

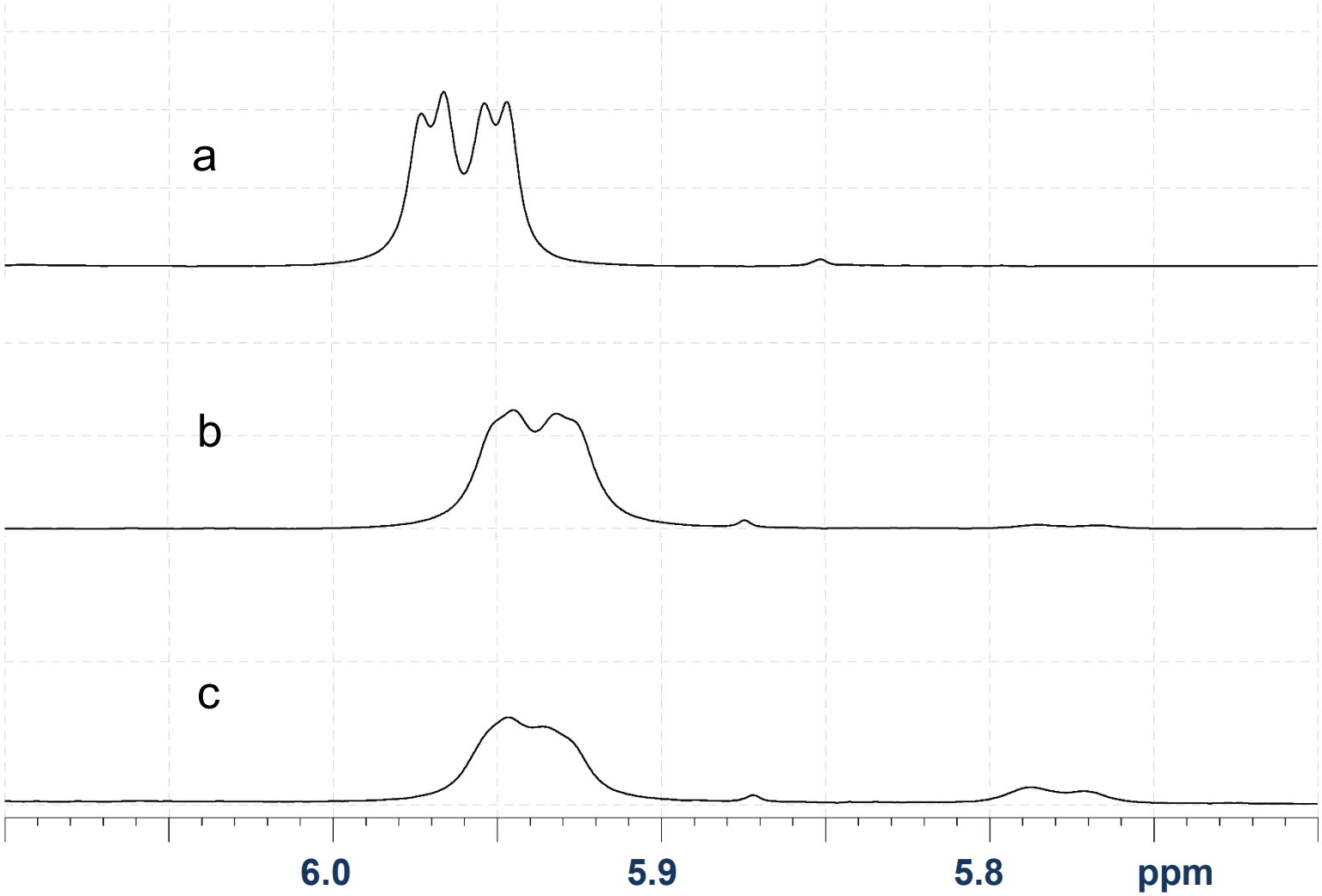

Figure D2c. Inset of the α-H(b) region at 205 K (a), immediately after warming to 225 K (b) and after 27 min at 225 K (c).

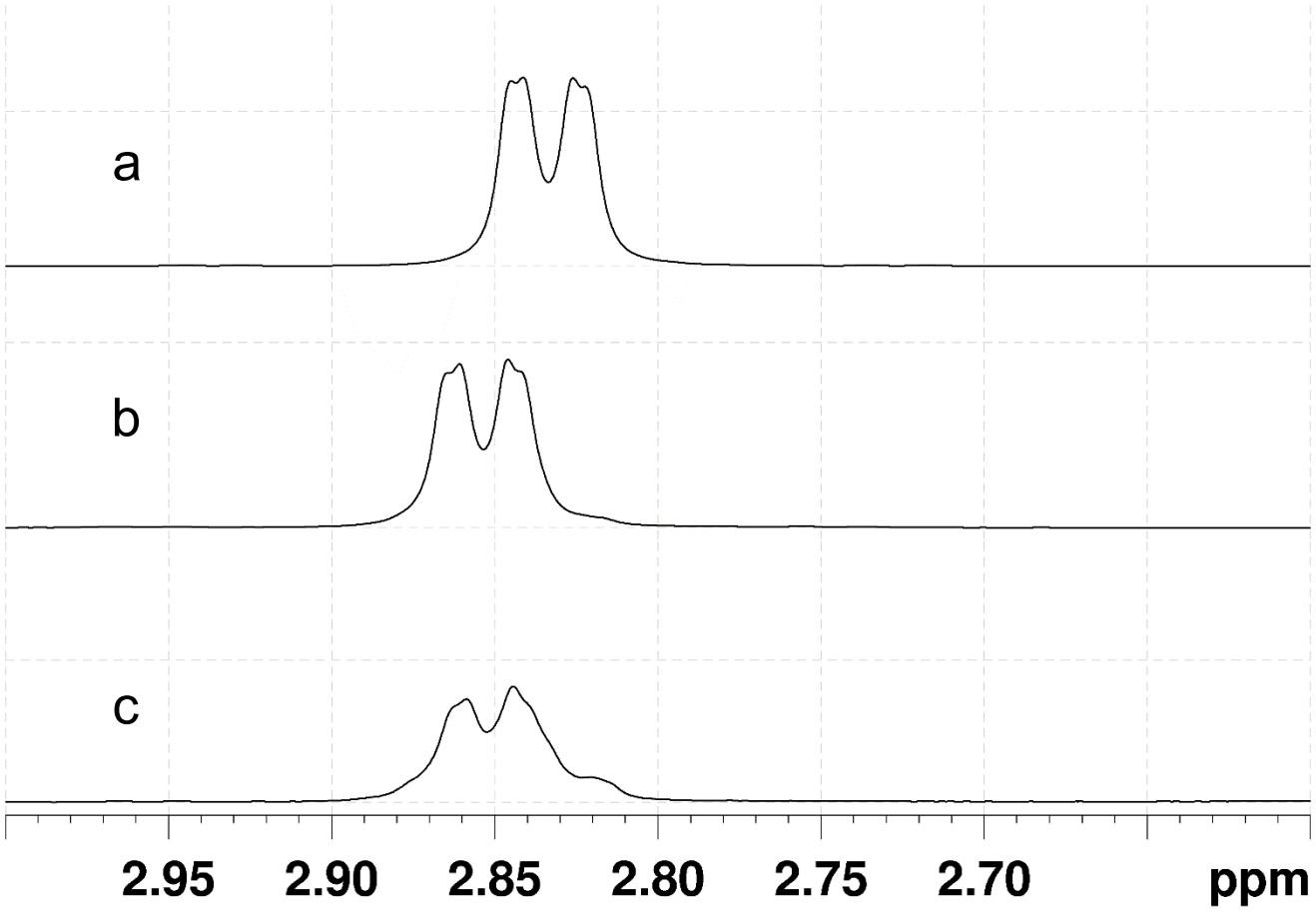

Figure D2d. Inset of the β-H region at 205 K (a), immediately after warming to 225 K (b) and after 27 min at 225 K (c).

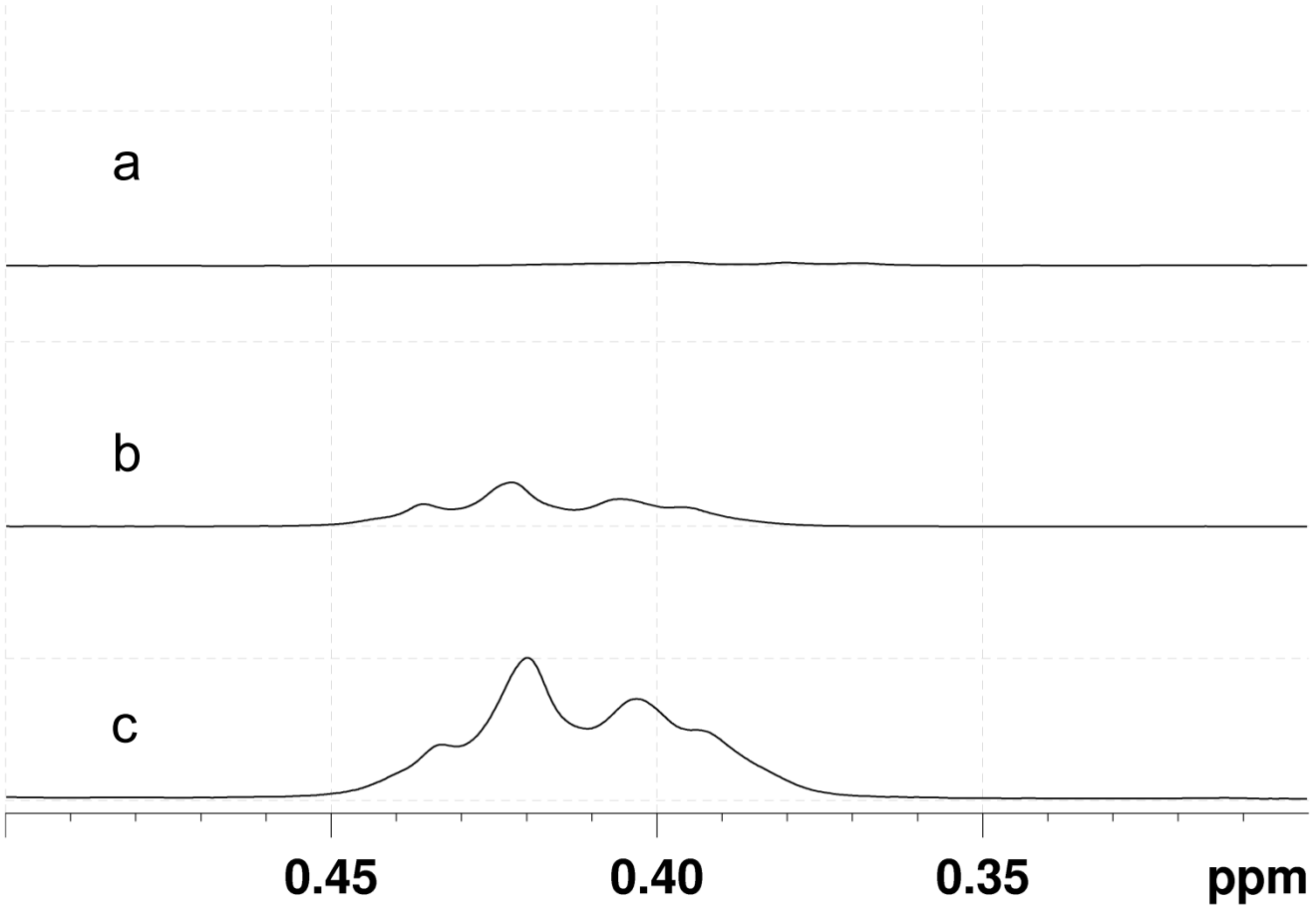

Figure D2e. Inset of the γ-Me region at 205 K (a), immediately after warming to 225 K (b) and after 27 min at 225 K (c).

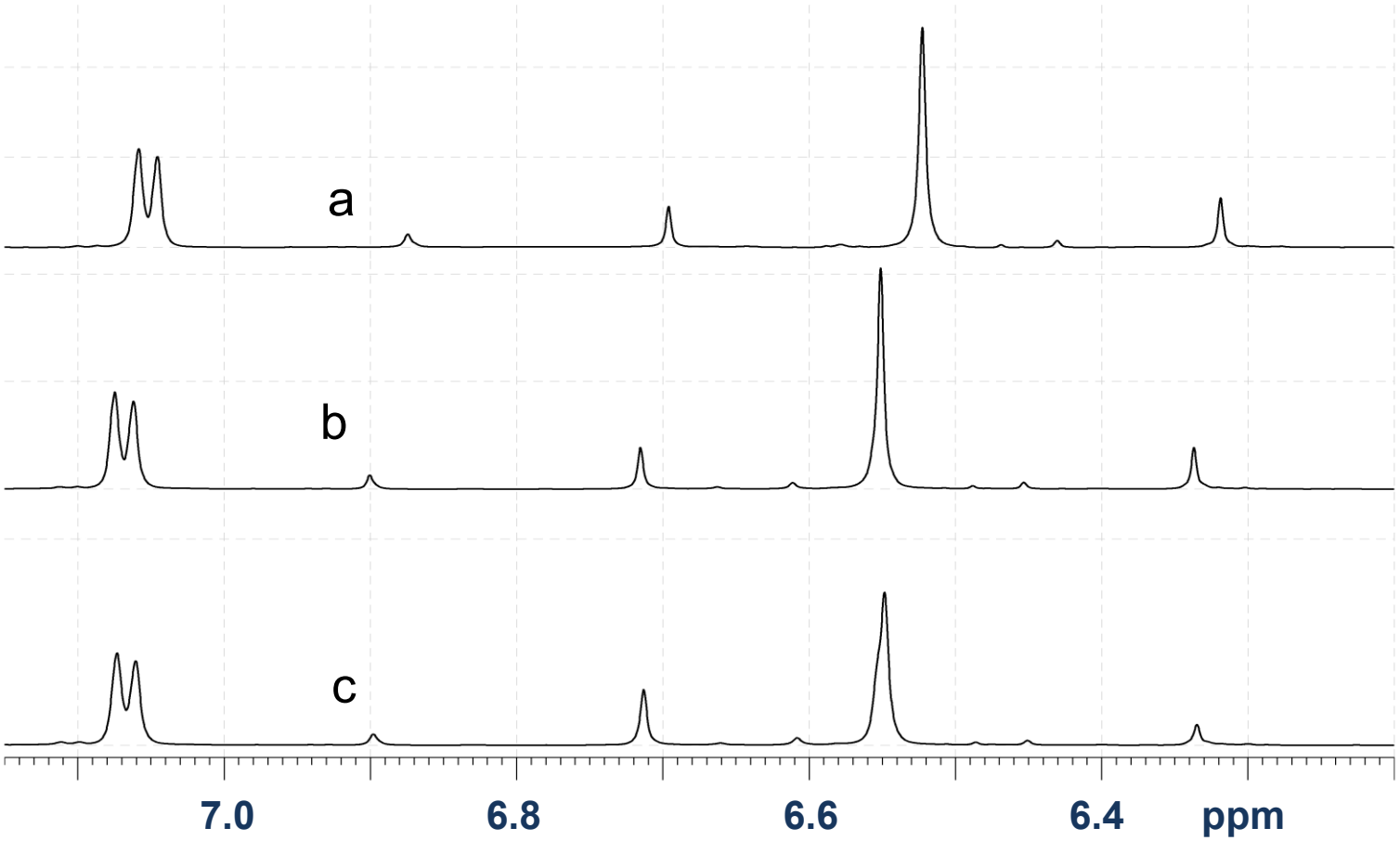

Figure D2f. Inset of the Cp region at 205 K (a), immediately after warming to 225 K (b) and after 27 min at 225 K (c). Also shown are a phenyl resonance of Ph_3CMe at δ 7.08 and Cp resonances of **I** and the contact ion pair $[Cp_2TiMe\{B(C_6F_5)_4\}]$at δ 6.71 and 6.34 respectively.

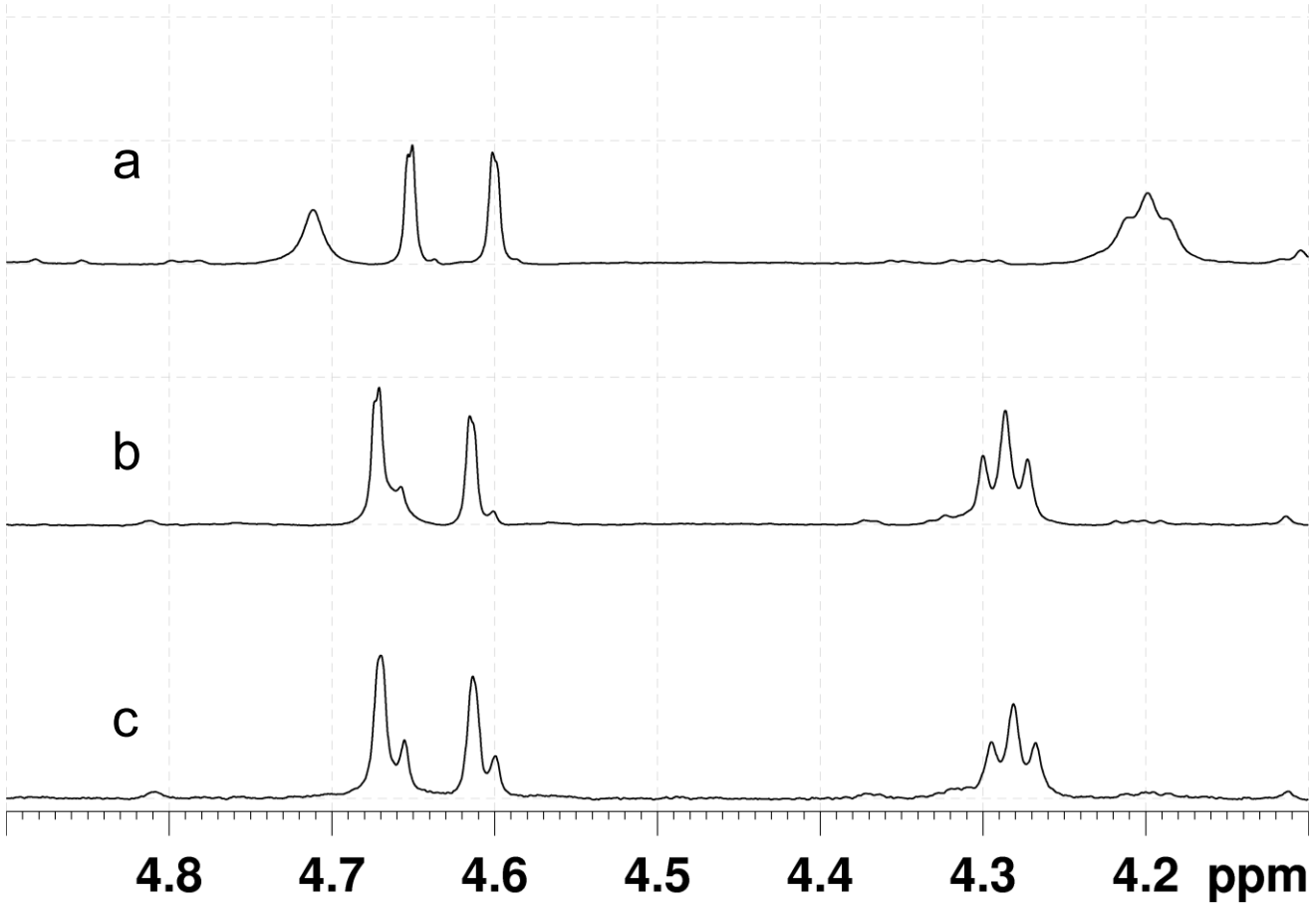

Figure D2g. Inset of the 2,3,3-TMB olefinic region region at 205 K (a), immediately after warming to at 225 K (b) and after 27 min at 225 K (c). After 251 min at 225 K, the four resonances are of nearly identical intensities.

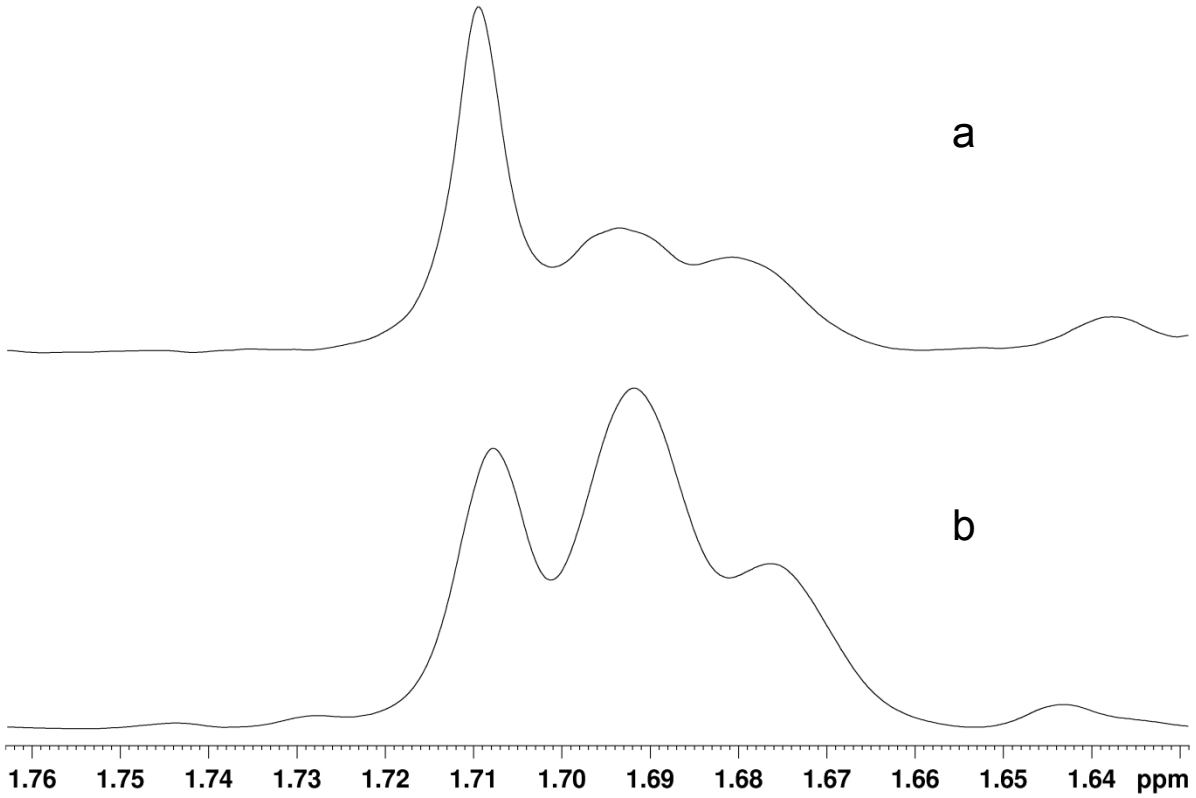

Figure D2h. Methyl region of partially deuterated 2,3,3-TMB immediately after raising the temperature to 225 K (a) and after 251 min at 225 K (b).

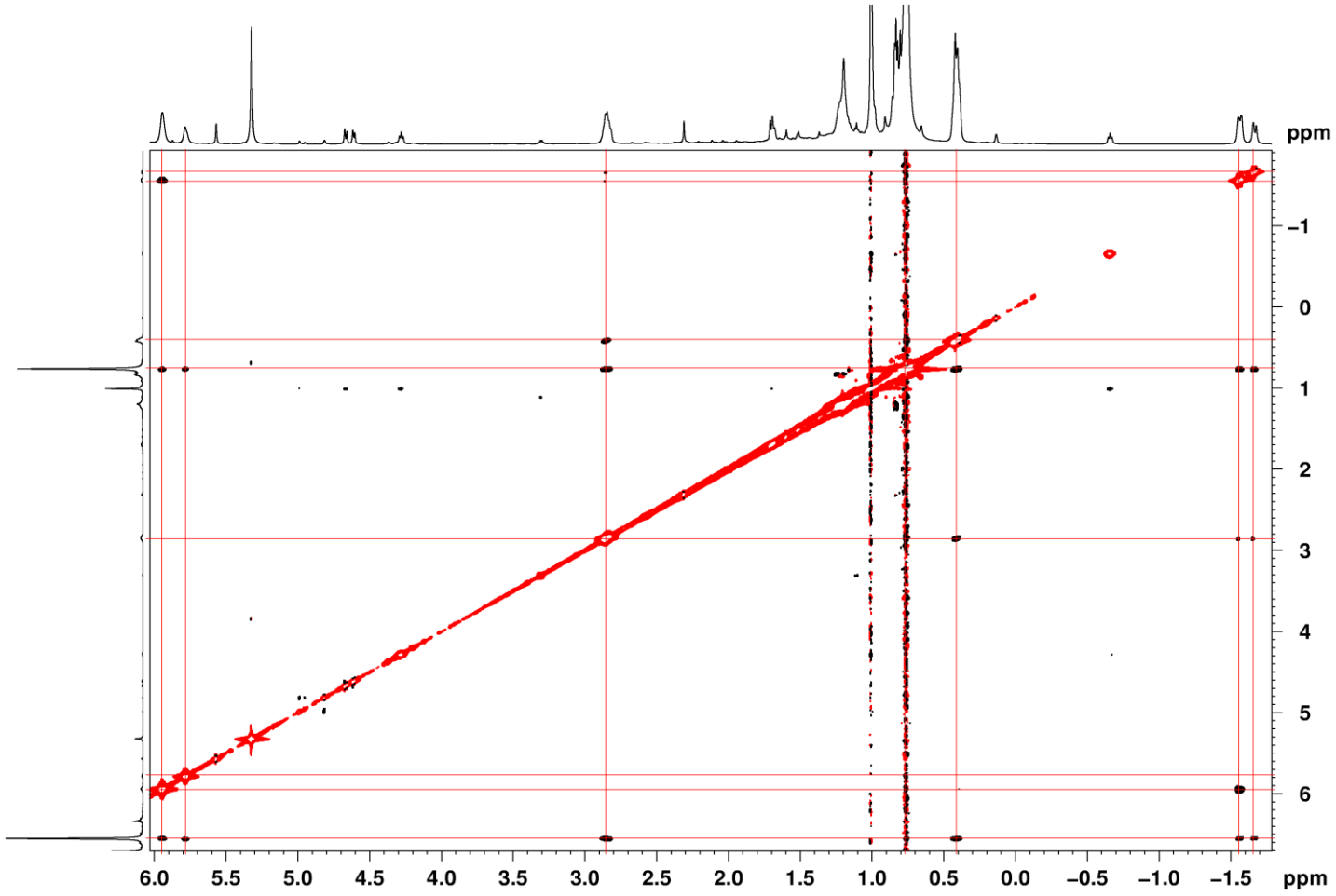

Figure D3a. NOESY spectrum in CD_2Cl_2 of **II**-CD_3 and its thermolysis products after 178 min at 225 K.

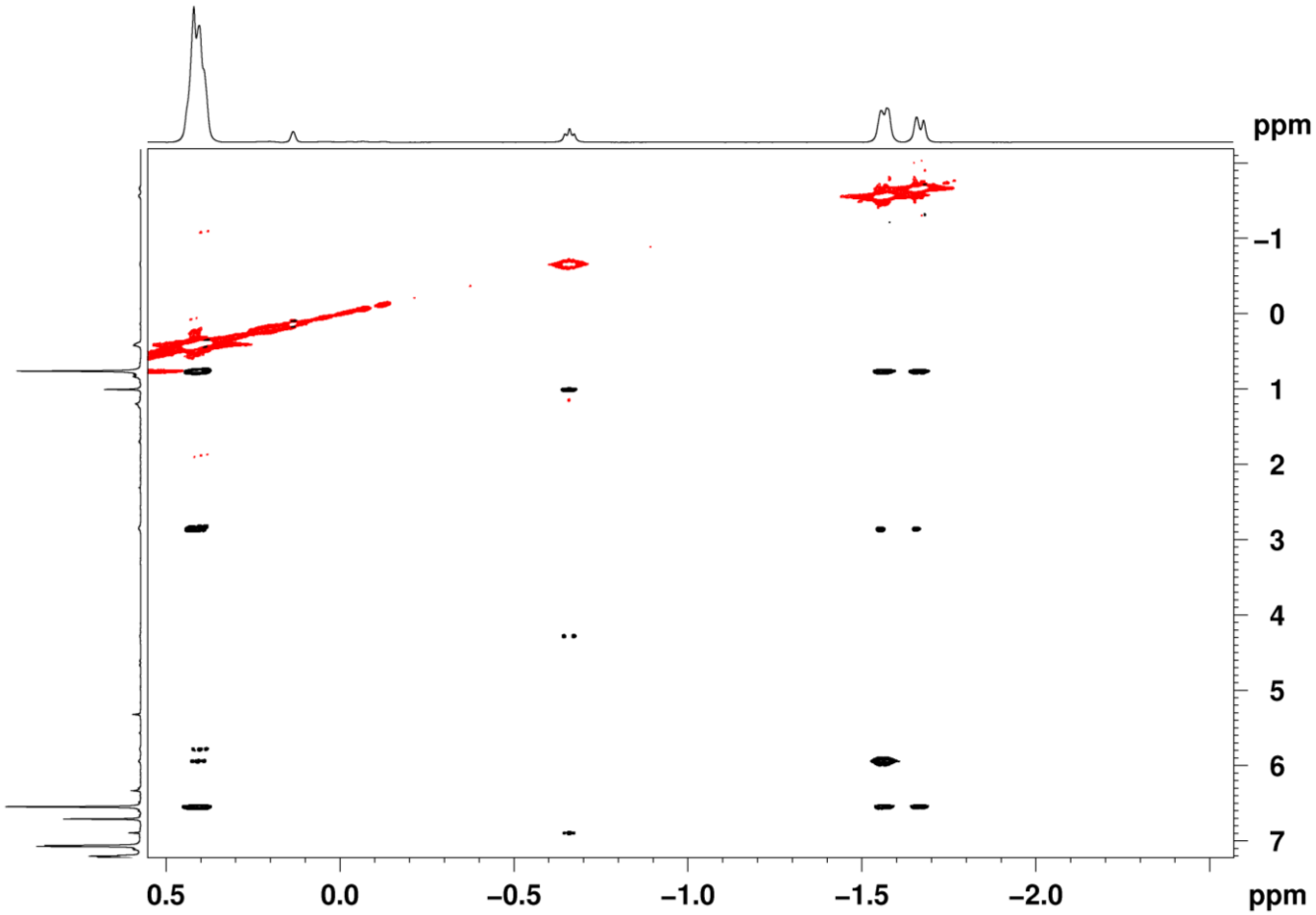

Figure D3b. Inset of Figure D3a: NOESY spectrum of **II**-CD_3 and its thermolysis products after 178 min at 225 K in the α-H(a) and Me region. Note that all α-Ha isotopomers shown exhibit a NOE to the same Cp and to the same CMe_3, indicating that they are part of a different isotopologue of **II**-CD_3. In addition, only α-Ha of **II**-CD_3 and **II-b** exhibit a NOE to β-H, and only **II**-CD_3 and **II-a** exhibit a NOE to α-Hb. Finally, the growing peak attributed to the γ-Me is also connected to the same Cp and CMe_3, thus proving that γ-Me is getting protonated as the reaction evolves at 225 K.

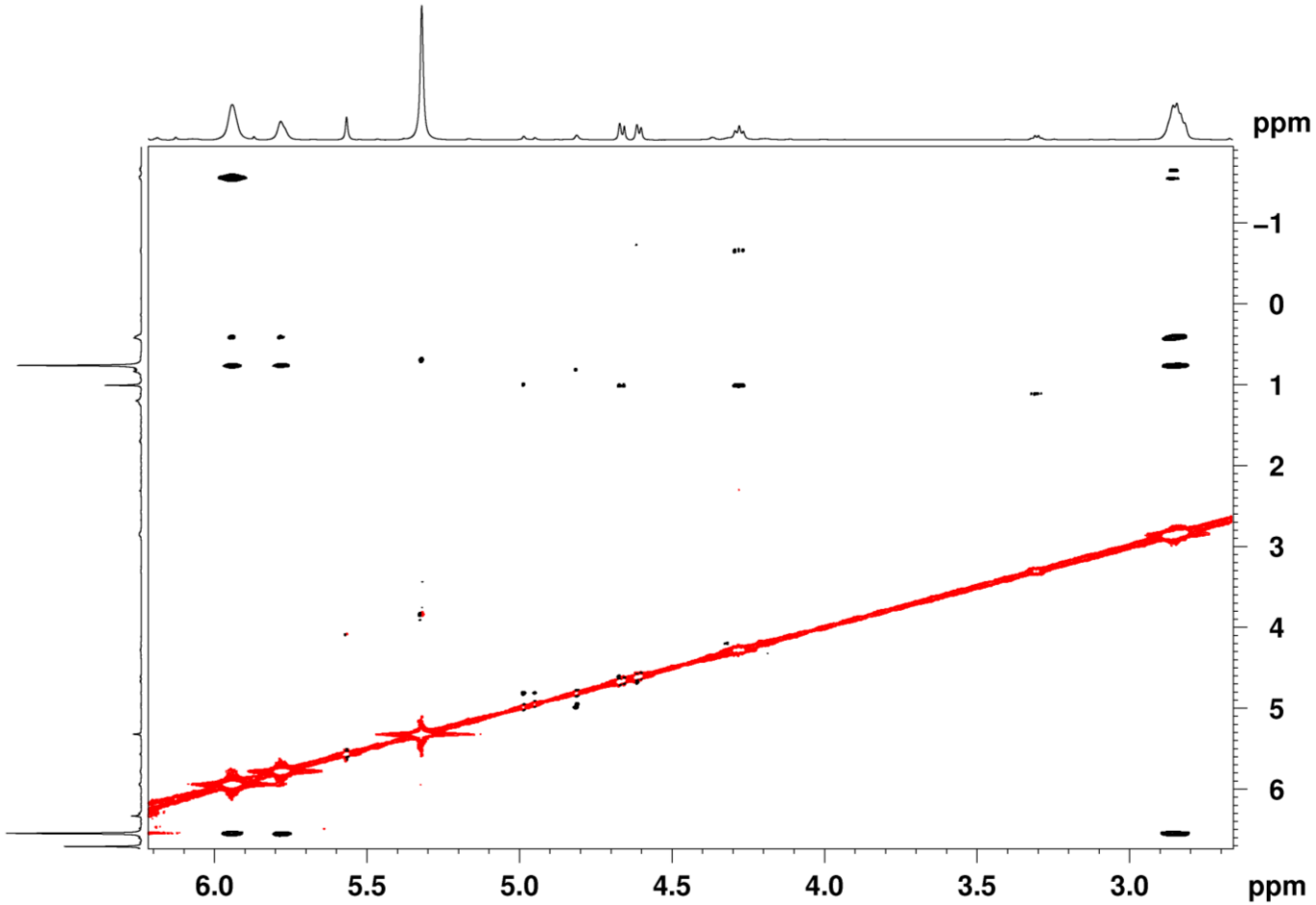

FigureD3c. Inset of Figure D3a: NOESY spectrum of **II**-CD_3 and its thermolysis products after 178 min at 225 K in the α-(b) and β-H region. Note that all α-Hb isotopomers shown exhibit an NOE to the same Cp and to the same CMe_3, as well as to the same γ-Me, indicating that they are attributed to isotopologues of **II**-CD_3. In addition, only **II**-CD_3 and **II**-a but not **II-d**,**e** exhibit a NOE correlation from α-Hb to α-Ha, providing evidence that **II-d**,**e** are deuterated at α-Ha.

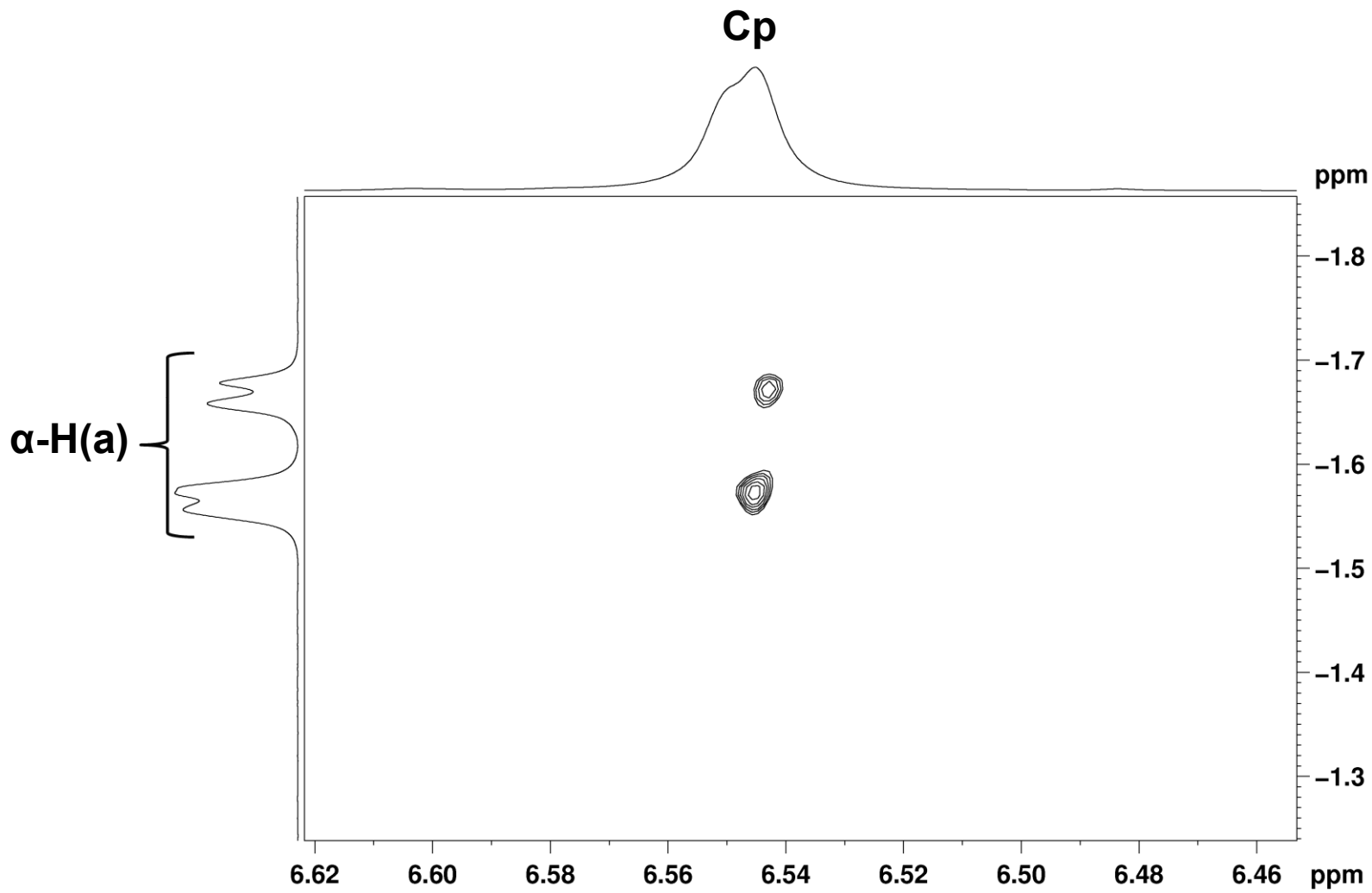

Figure D3d. NOESY spectrum of **II**-CD_3 after 178 min at 225 K showing correlations of the Cp and α-H(a) resonances.

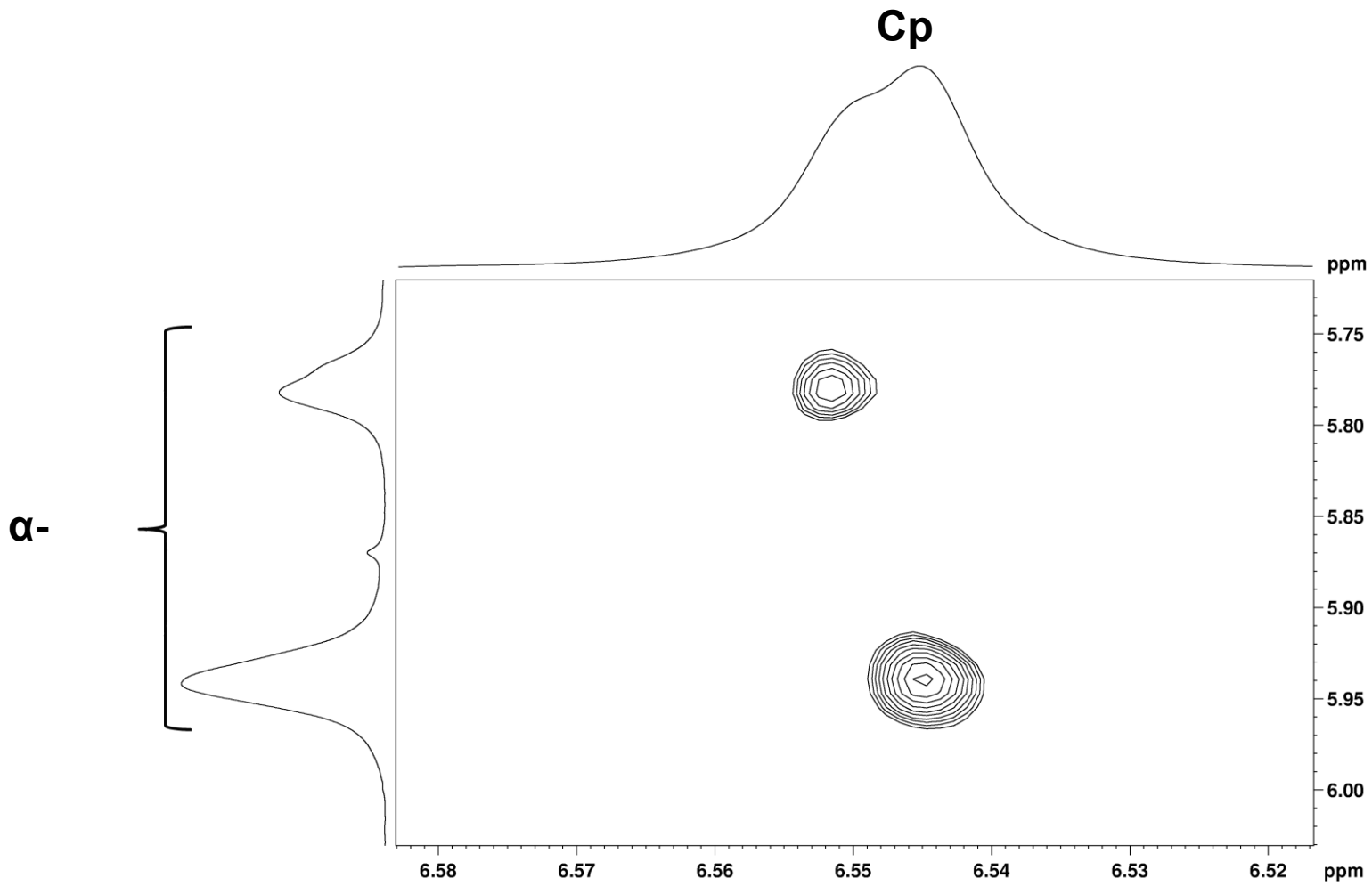

Figure D3e. NOESY spectrum of **II**-CD_3 and its thermolysis products after 178 min at 225 K, showing correlations between the Cp with α-H(b) resonances.

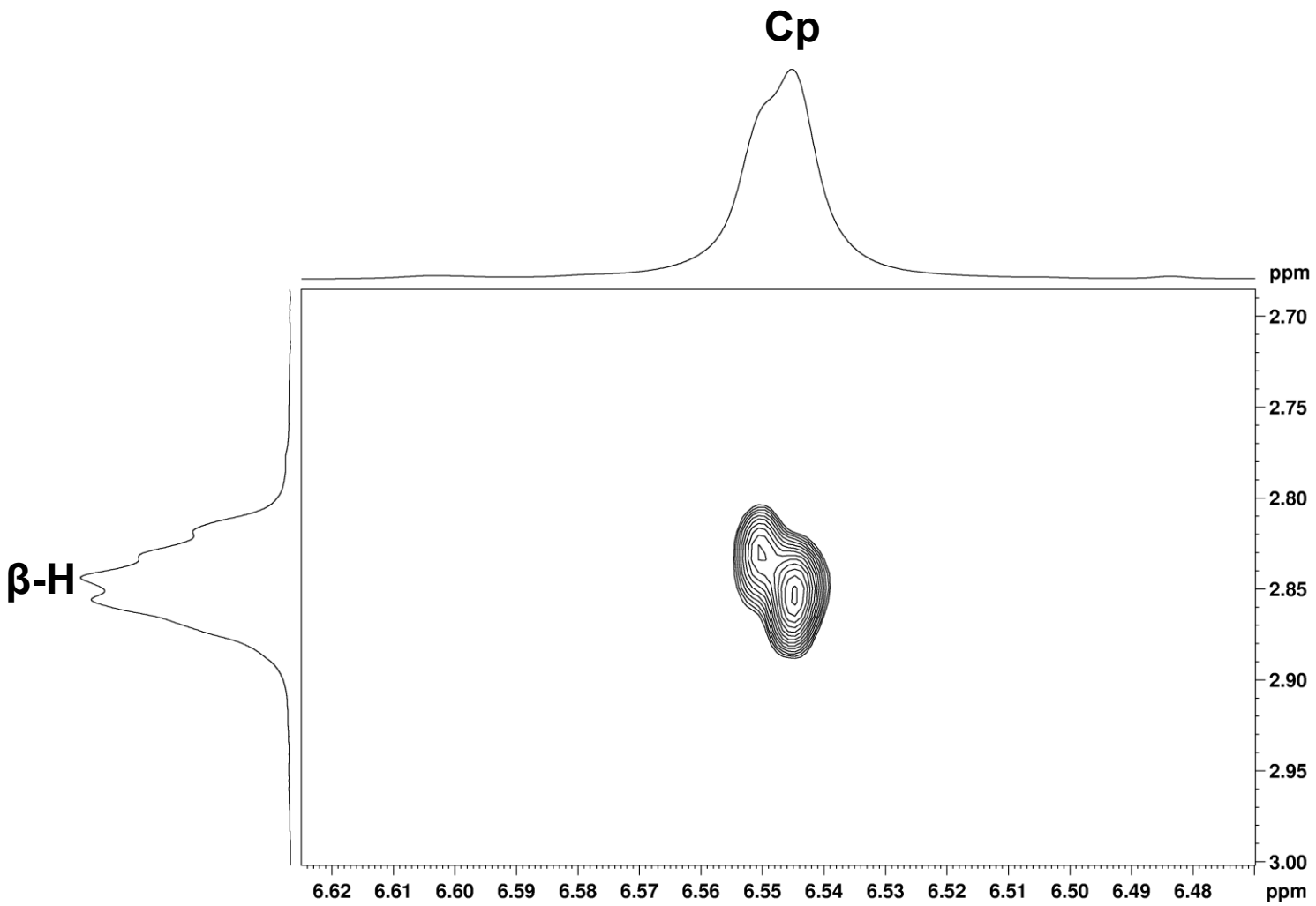

Figure D3f. NOESY spectrum of **II**-CD_3 and its thermolysis products after 178 min at 225 K, showing correlations between the Cp and the β-hydrogen resonances.

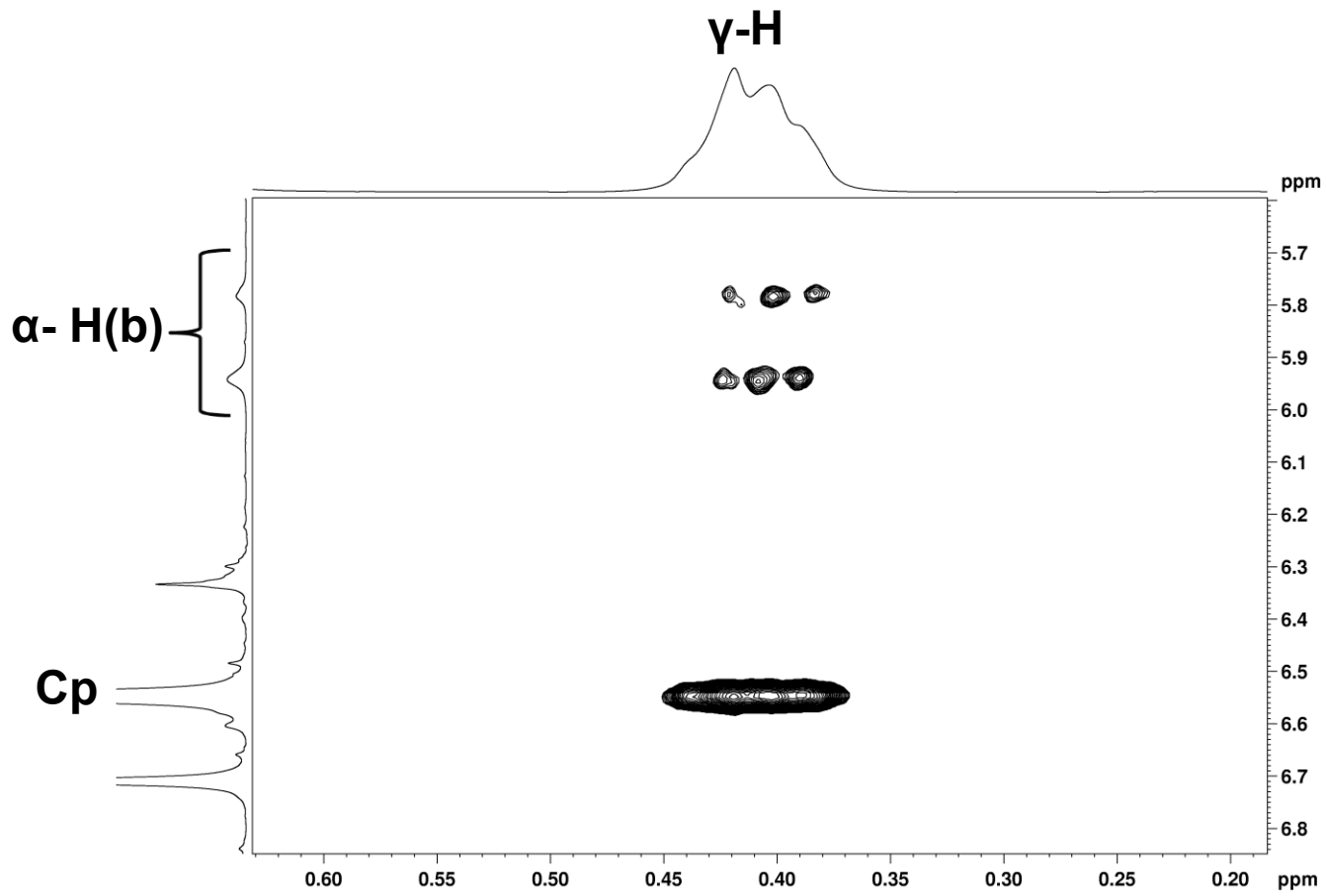

Figure D3g. NOESY spectrum of **II**-CD_3 and its thermolysis products after 178 min at 225 K showing correlations between the γ-H with resonances of α-H(b) and the Cp group.

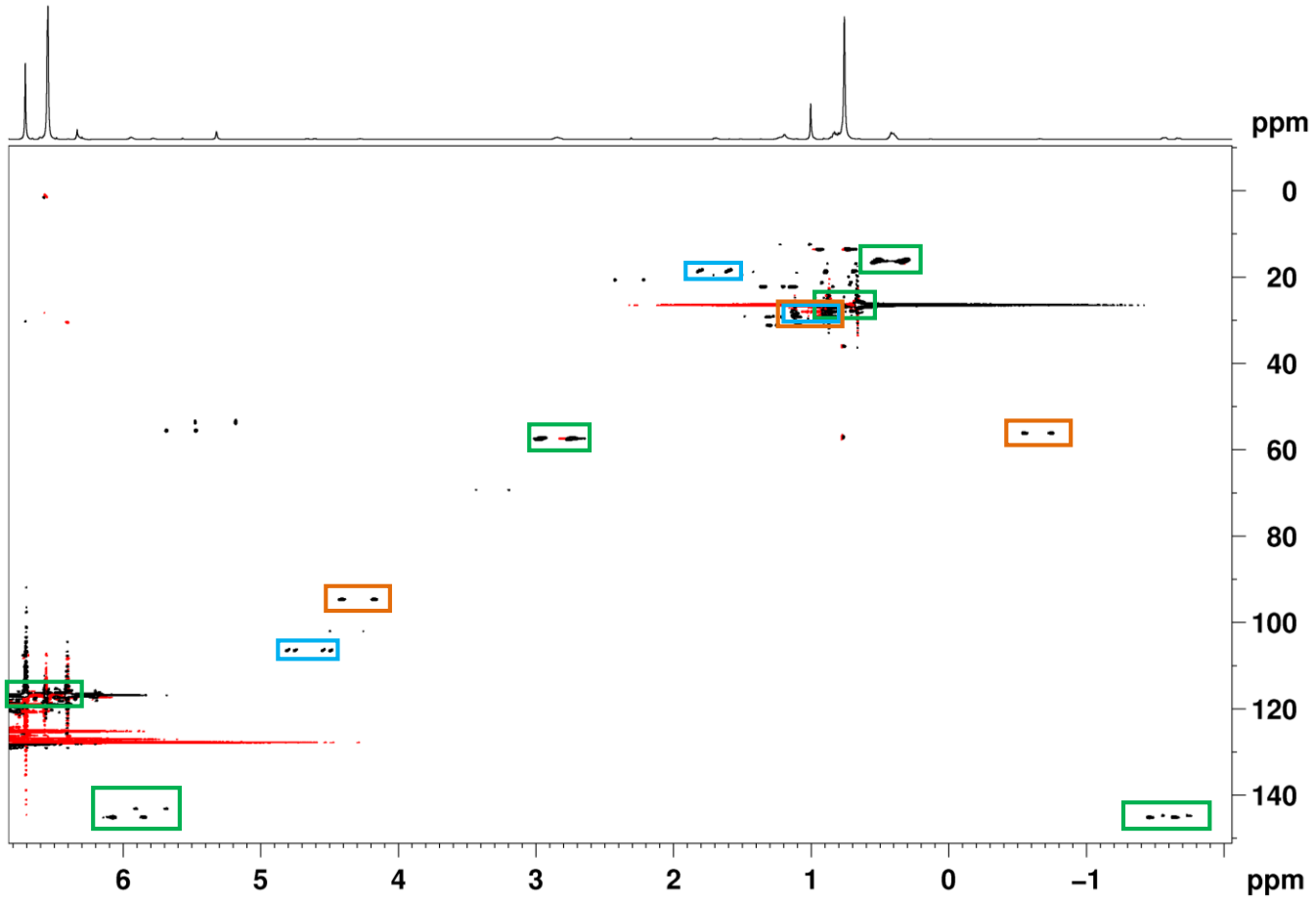

Figure D4a. ^{13}C-^{1}H HSQC spectrum of **II**-CD_3 and its thermolysis products after 178 min at 225 K: **II**-CD_3**, II-a-e,** 2,3,3-TMB and $[Cp_2TiCH_2CH_2CMe_3]^+$.

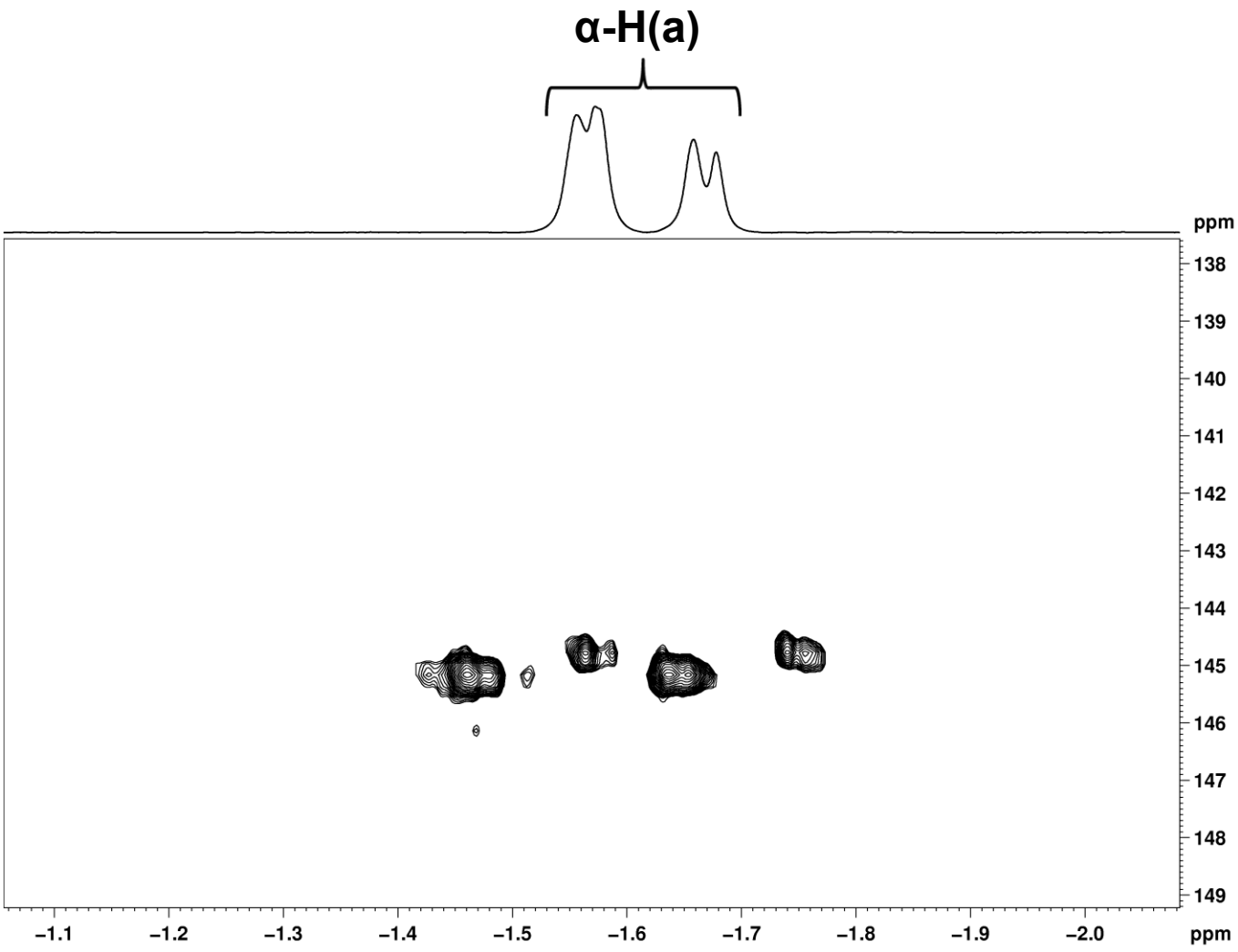

Figure D4b. ^{13}C-^{1}H HSQC spectrum of **II**-CD_3 and its thermolysis products after 178 min at 225 K with no decoupling during acquisition. The correlations shown correspond to the ^{13}C satellite projections of the α-H(a) region at 225K.

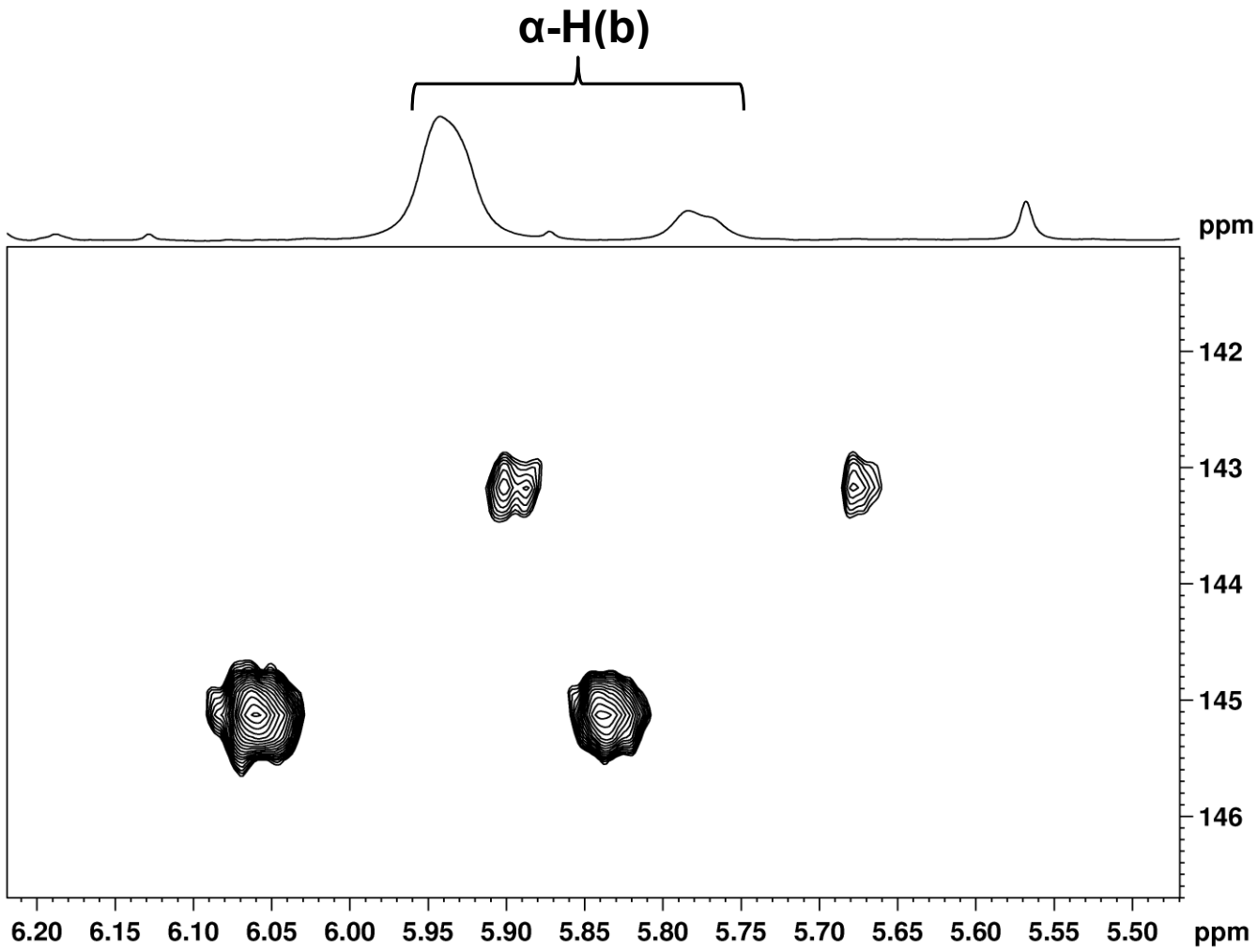

Figure D4c. ^{13}C-^{1}H HSQC spectrum of **II**-CD_3 and its thermolysis products after 178 min at 225 K with no decoupling during acquisition. The correlations shown correspond to the ^{13}C satellite projections of the α-H(b) region.

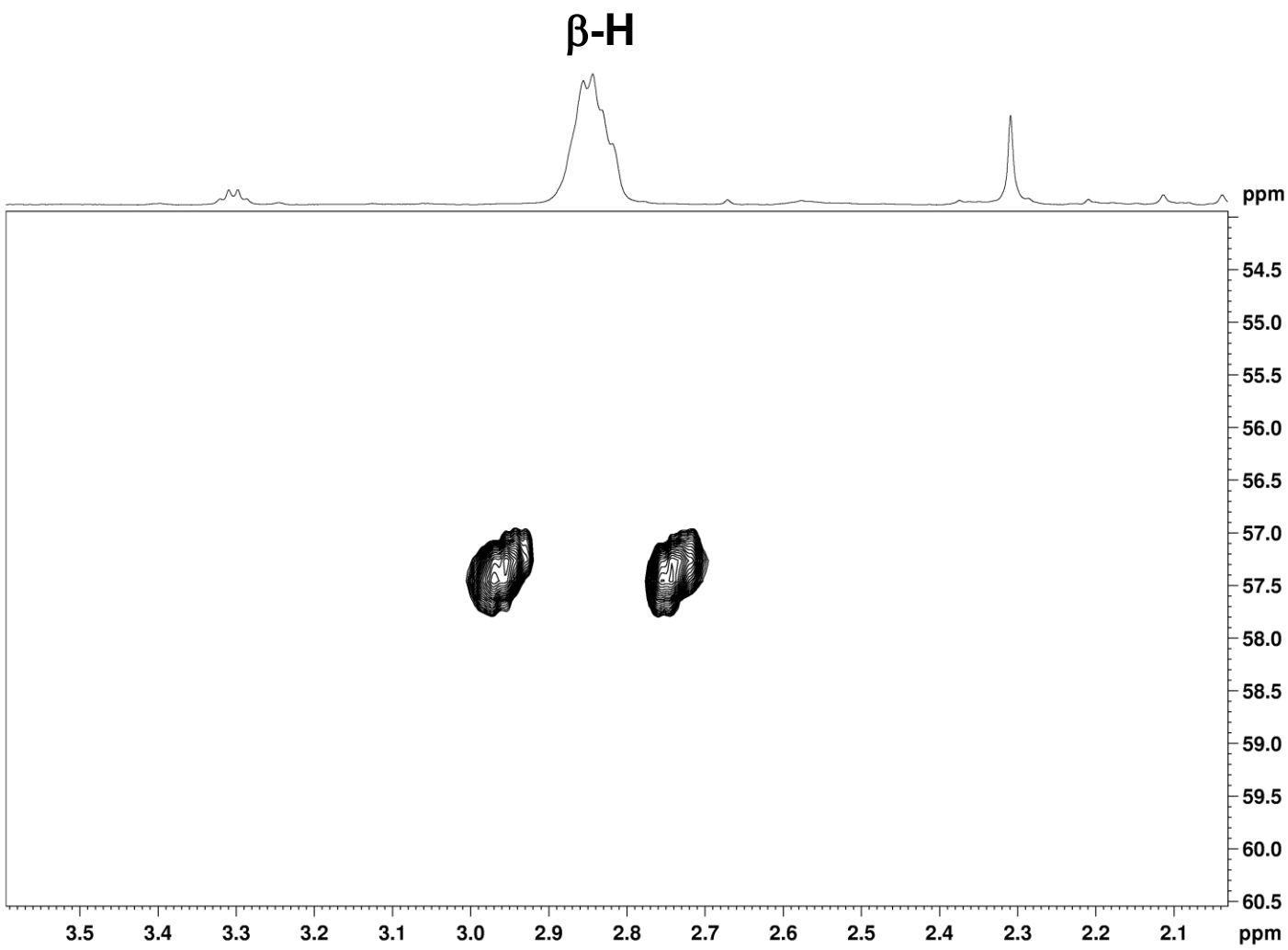

Figure D4d. ^{13}C-^{1}H HSQC spectrum of **II**-CD_3 and its thermolysis products after 178 min at 225 K with no decoupling during acquisition. The correlations shown correspond to the ^{13}C satellite projections of the β-H region.

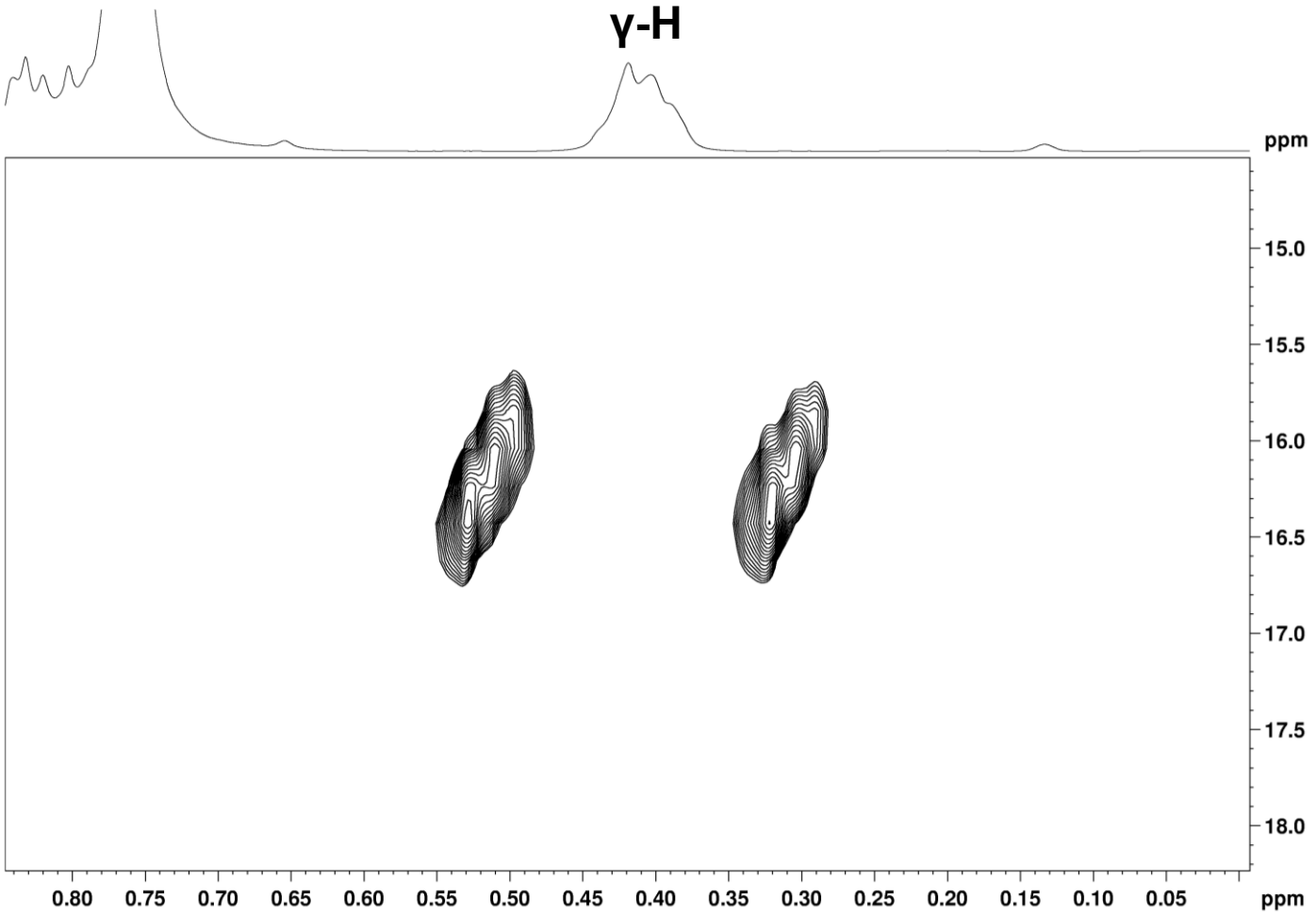

Figure D4e. ^{13}C-^{1}H HSQC spectrum of **II**-CD_3 and its thermolysis products after 178 min at 225 K with no decoupling during acquisition. The correlations correspond to the ^{13}C satellite projections of the γ-H region. The three apparent main correlations are attributed, from bottom-left to top-right, to CH_3, CH_2D and CHD_2.

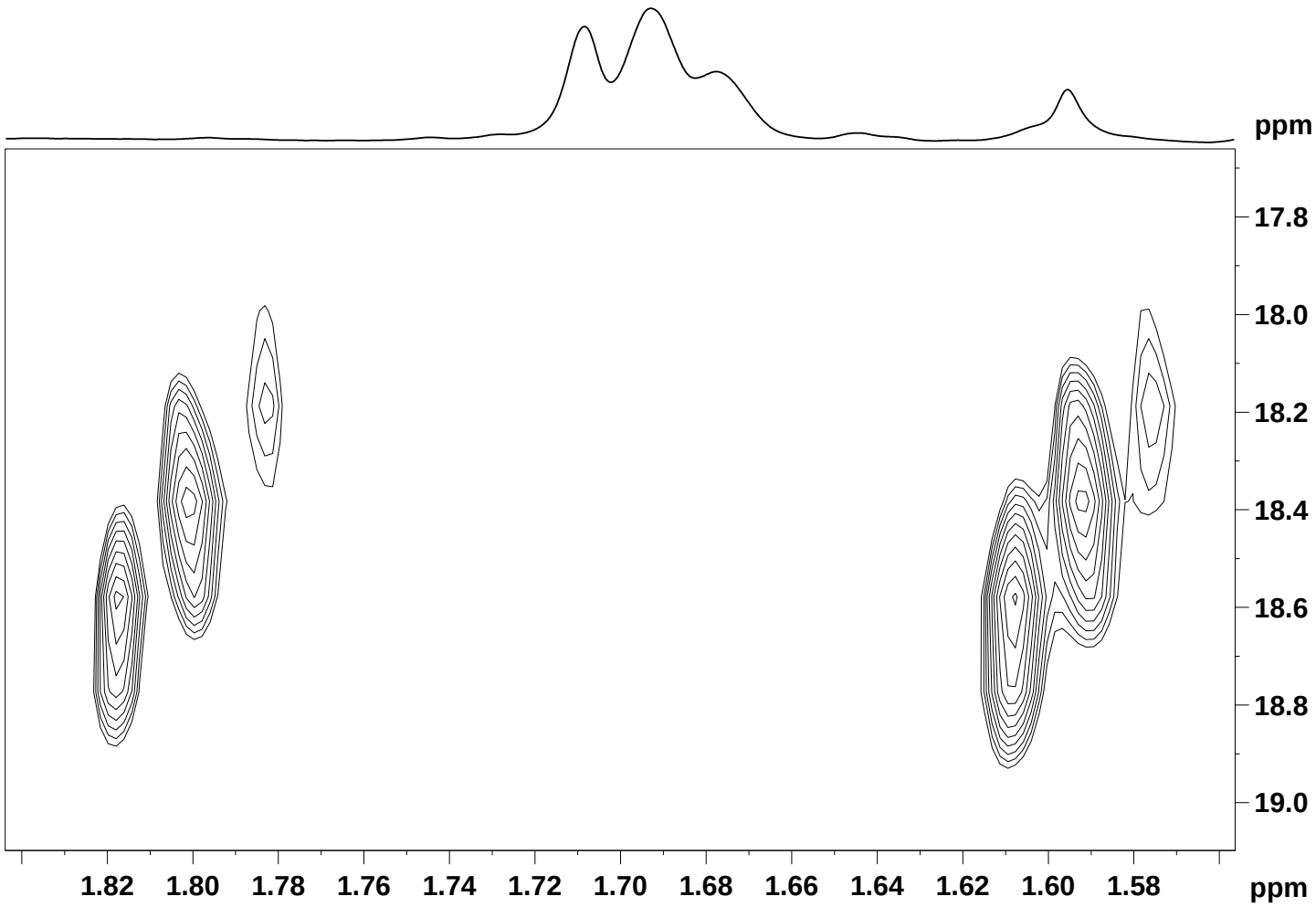

Figure D4f. ^{13}C-^{1}H HSQC spectrum of **II**-CD_3 and its thermolysis products after 178 min at 225 K with no decoupling during acquisition. The correlations shown correspond to the ^{13}C satellite projections of the γ-Me region of TMB. The three apparent main correlations are attributed, from bottom-left to top-right, to CH_3, CH_2D and CHD_2.

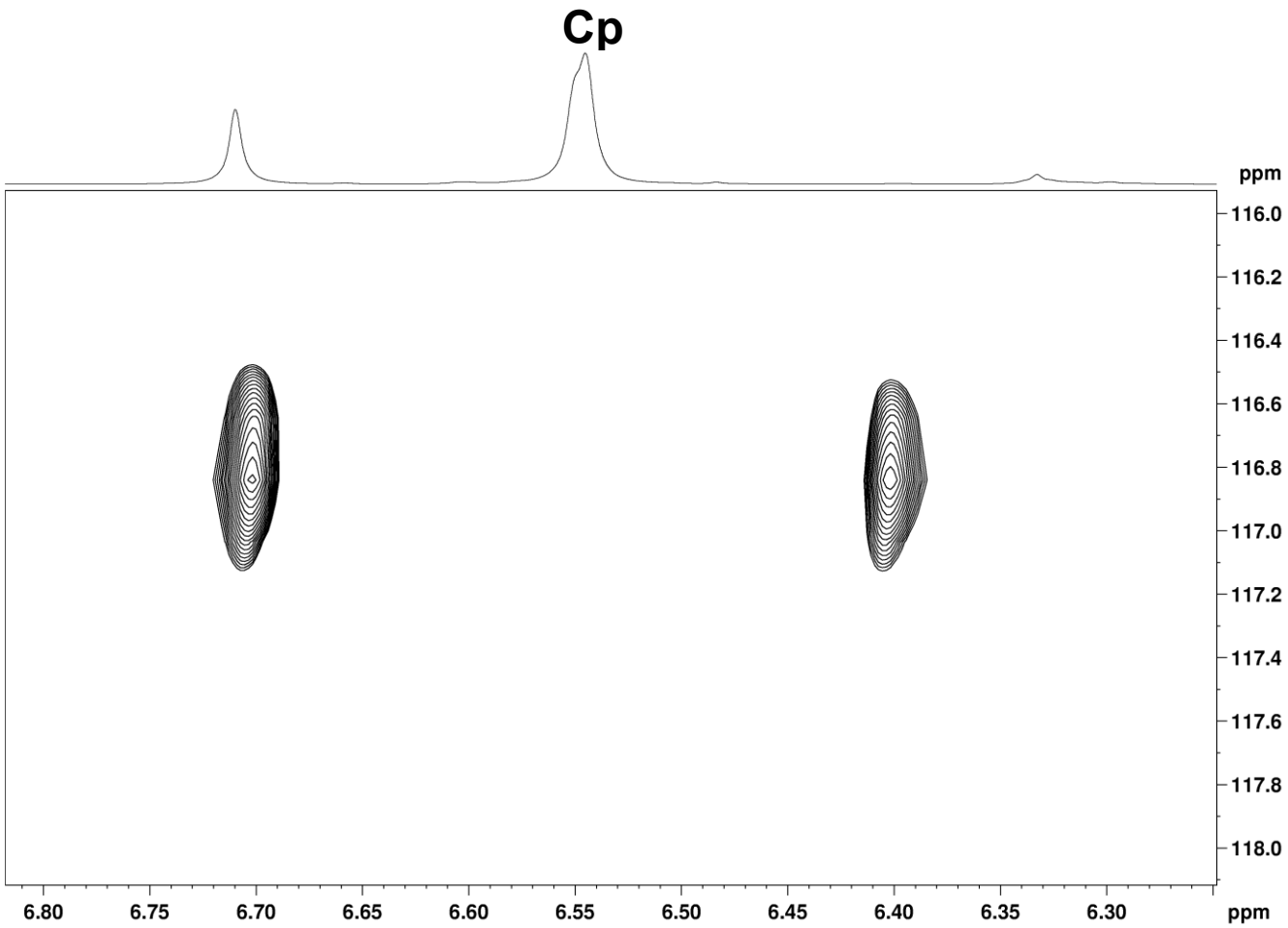

Figure D4g. ^{13}C-^{1}H HSQC spectrum of **II**-CD_3 and its thermolysis products after 178 min at 225 K with no decoupling during acquisition. The correlations shown correspond to the ^{13}C satellite projections of the Cp region. As seen above, even if there are two Cp peaks partly resolved in the ^{1}H NMR spectrum, they are not resolved in the HSQC spectrum shown here.

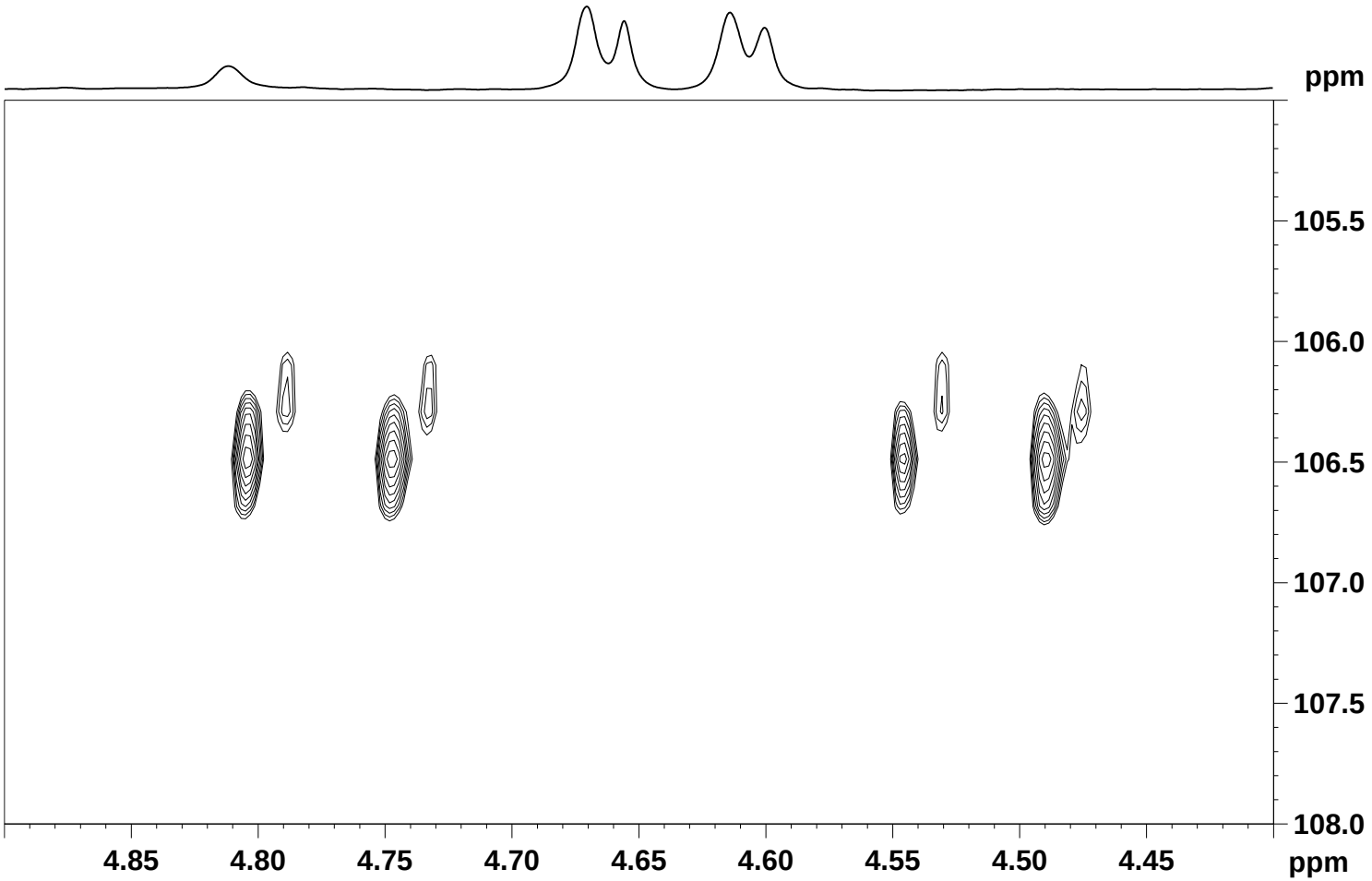

Figure D4h. ^{13}C-^{1}H HSQC spectrum of **II**-CD_3 and its thermolysis products after 178 min at 225 K with no decoupling during acquisition. The correlations shown correspond to the ^{13}C satellite projections of the α-CH_2 region of TMB, at 225 K, and the three species are attributed to CH_2=$CC(H/D)_3CMe_3$ (δ 106.5), CHaDb=$CC(H/D)_3CMe_3$ (δ 106.2) and CHbDa=$CC(H/D)_3CMe_3$ (δ 106.2), respectively.

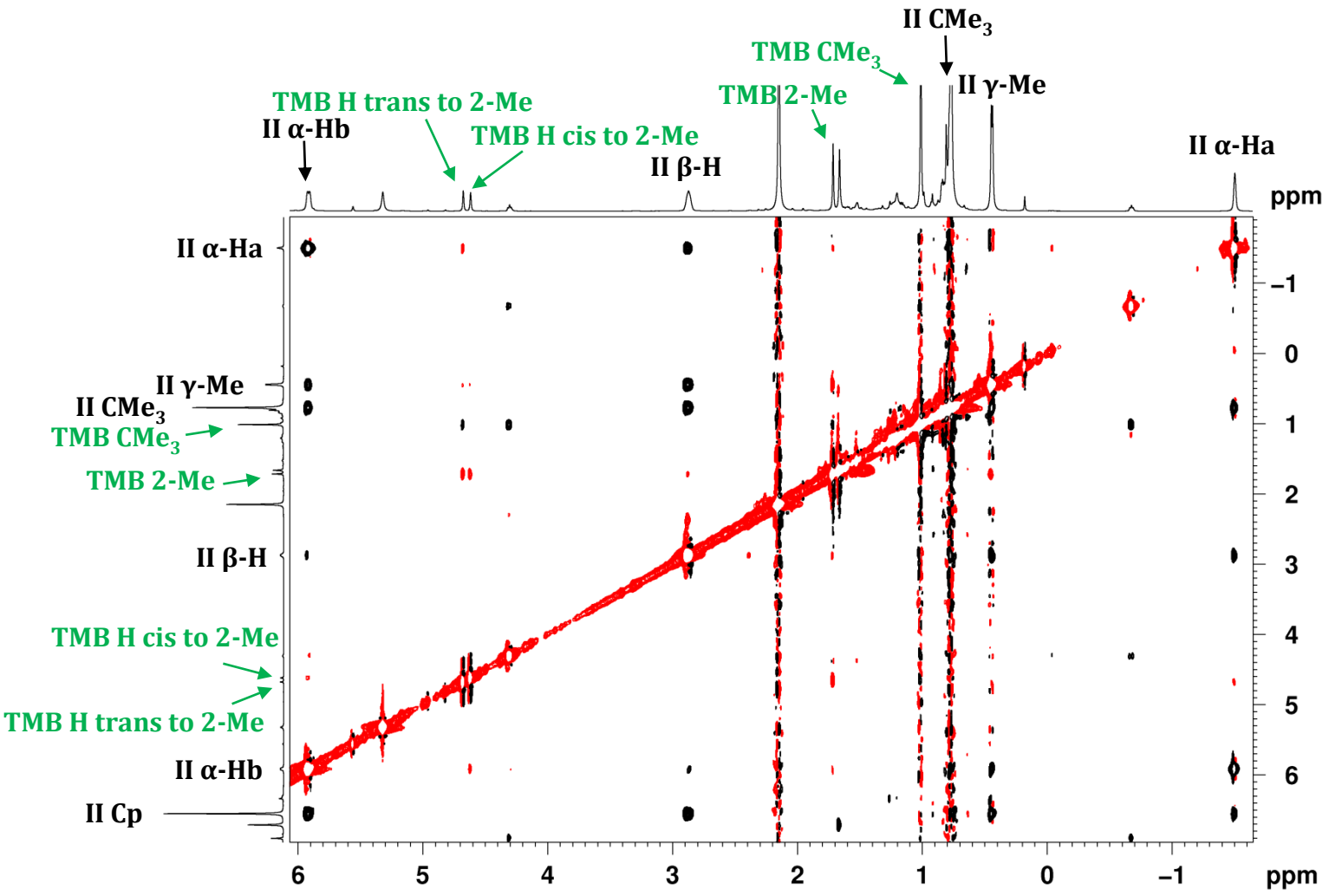

Figure D5a. NOESY spectrum of a solution containing **II** and TMB at 235 K. Of significance, note the exchange for TMB, internally and with **II**.

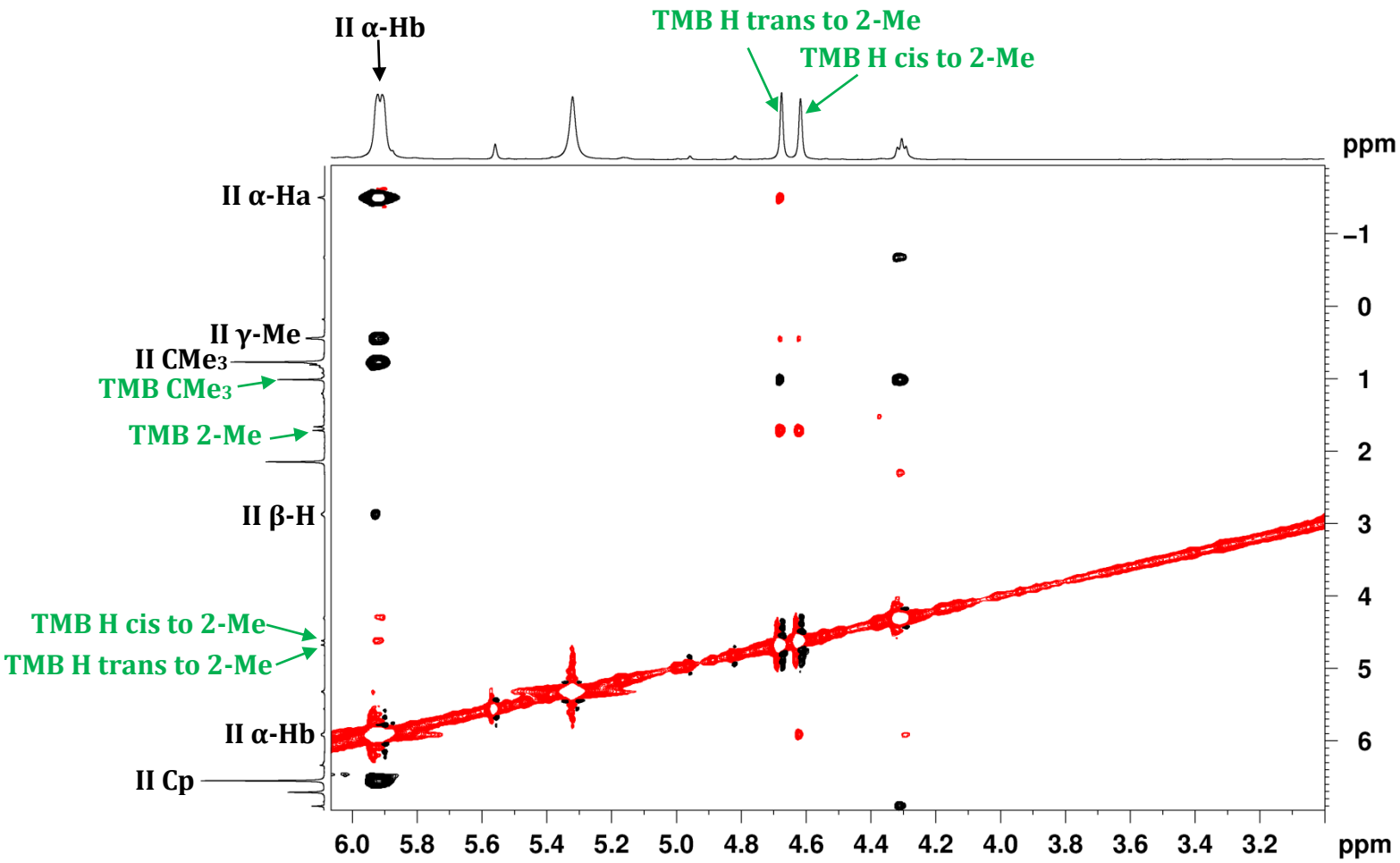

Figure D5b. Inset of Figure D5a. See text for a detailed discussion.

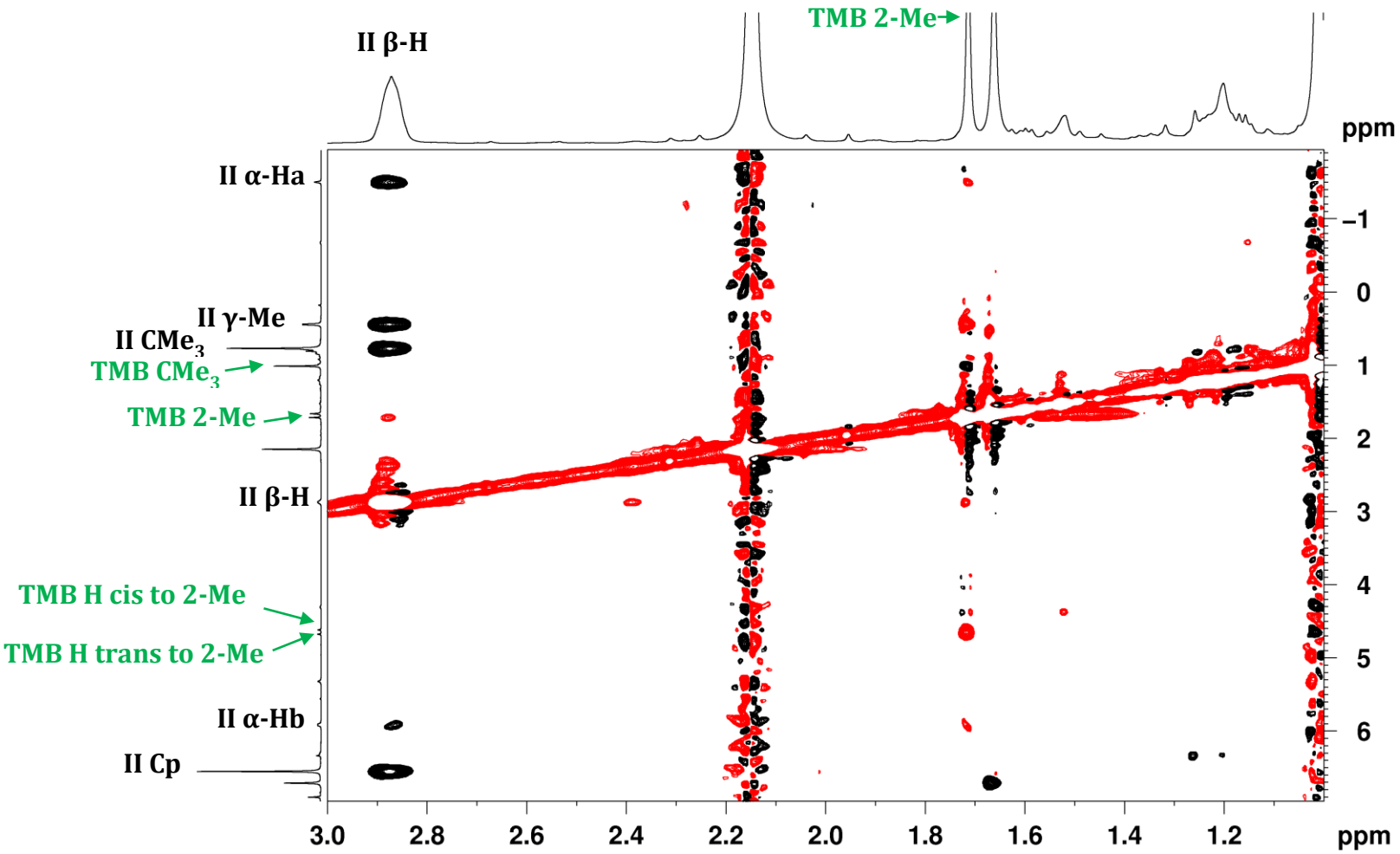

Figure D5c. Inset of Figure D5a. See text for a detailed discussion.

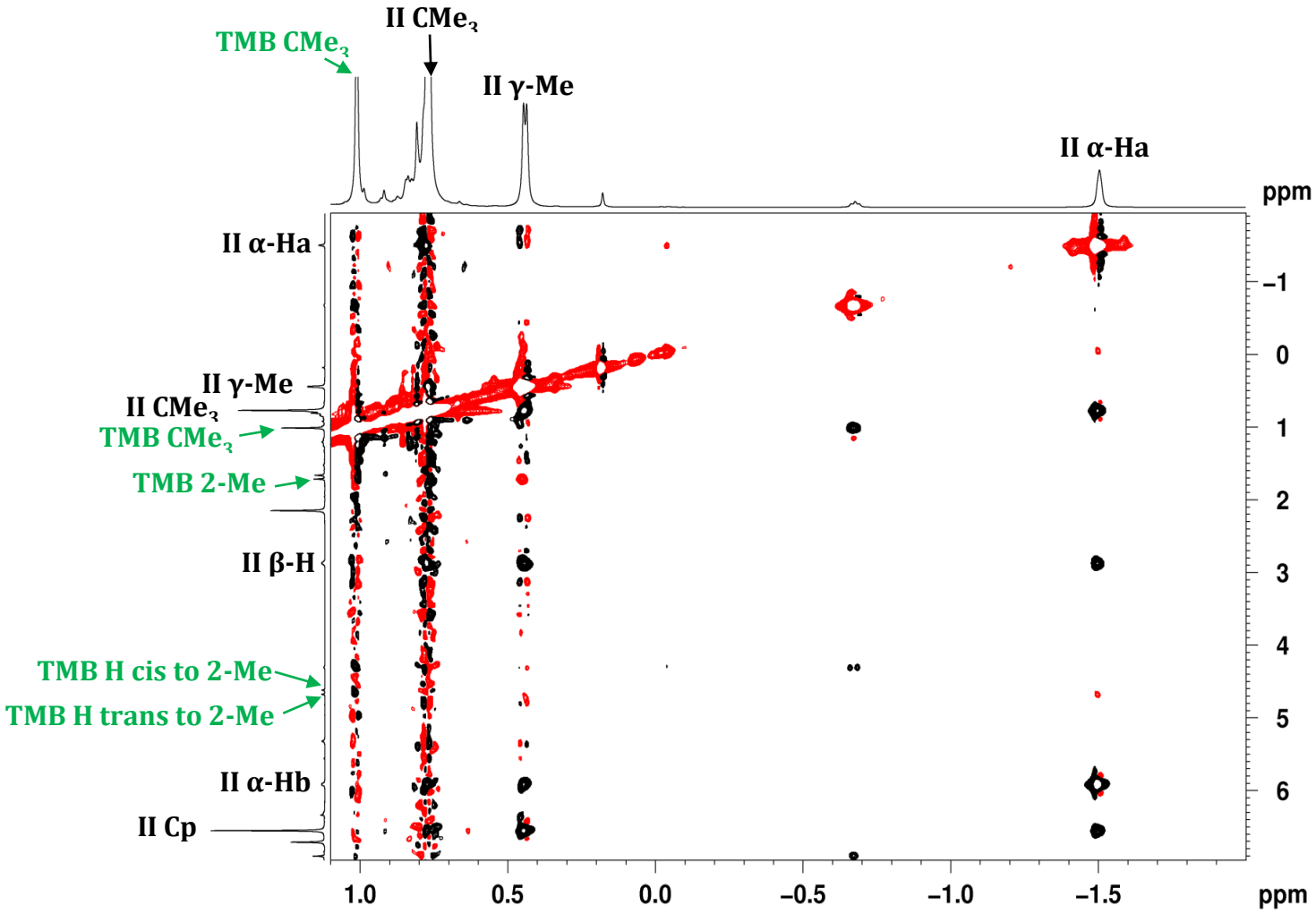

Figure D5d. Inset of Figure D5a. See text for a detailed discussion.

Table D1. Normalized % of H at the α-a-, α-b-, β- and γ- positions of **II**-CD_3 as D is as scrambling occurs at 225 K. Notice the last point was taken at 235 K to evaluate whether the system had reached ~equilibrium after 4 hours.

At 225 K, time (min) =	%H@α-a	%H@α,b	%H@β	%H@γ
0	91.24	86.83	97.09	8.28
11	78.16	72.15	87.27	20.81
17	71.66	71.37	85.36	23.87
25	68.85	66.26	77.99	28.97
39	68.34	58.42	69.26	34.66
98	55.30	50.57	55.74	46.13
149	53.30	50.61	51.15	48.31
251	53.20	48.00	47.50	50.44
289 @235 K	55.34	48.57	44.58	50.50
296 @235 K	54.83	51.34	43.71	50.04

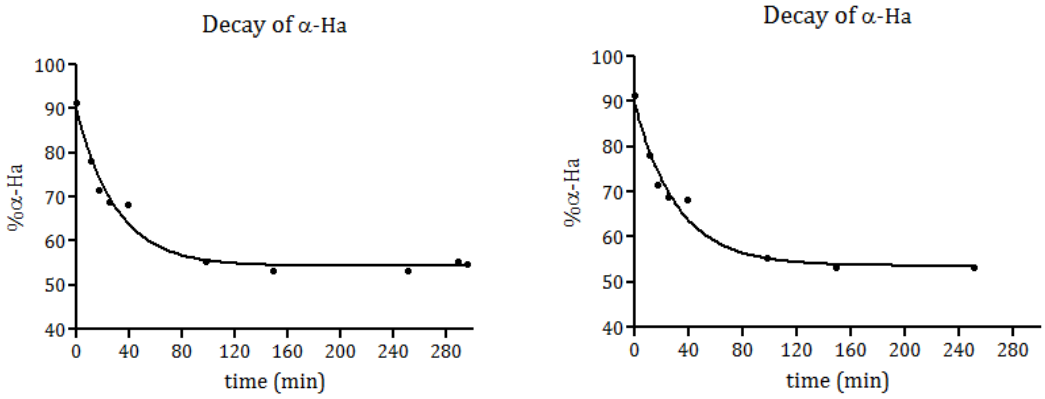

Figure D6a. Exponential decay best fit (from data in Table S1) for the relative population of ^1H at α-a-position as it gets deuterated through D-leakage, with points at 235 K (left) and without (right).

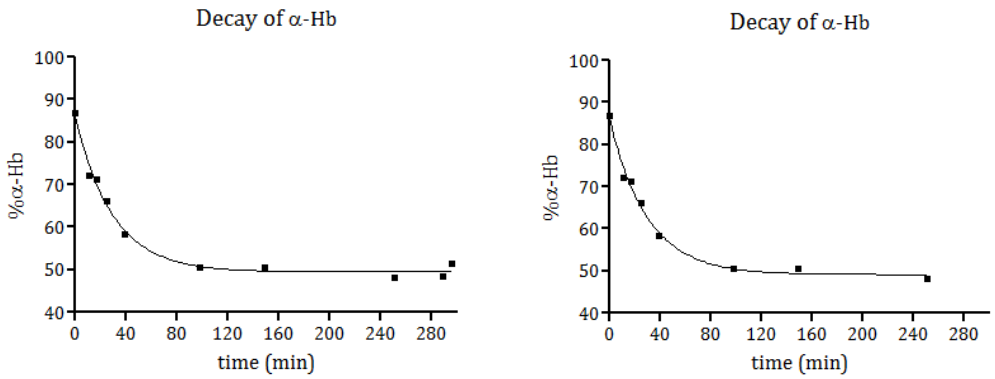

Figure D6b. Exponential decay best fit (from data in table 1) for the relative population of ^{1}H at α-b-position as it gets deuterated through D-leakage, with points at 235 K (left) and without (right).

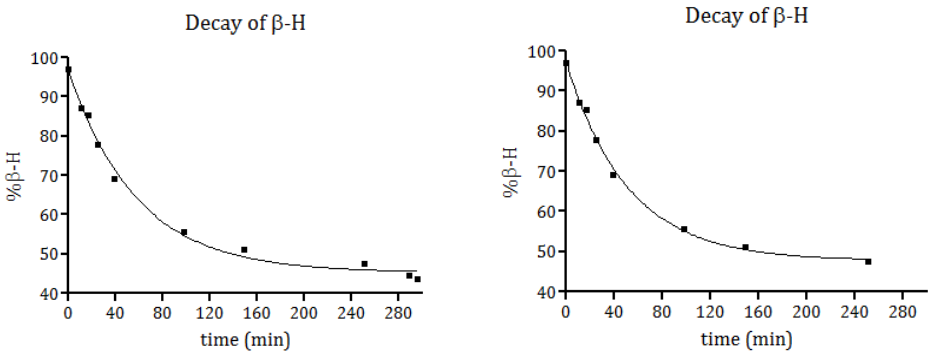

Figure D6c. Exponential decay best fit (from data in table 1) for the relative population of ^{1}H at β- position as it gets deuterated through D-leakage, with points at 235 K (left) and without (right).

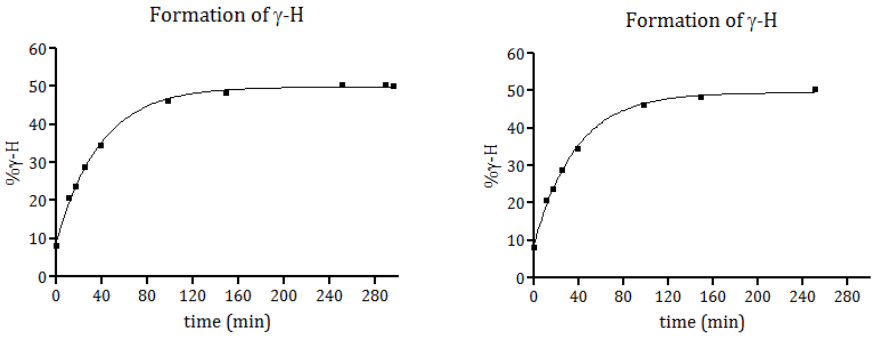

Figure D6d. Exponential decay best fit (from data in table 1) for the relative population of ^{1}H at γ- position as it gets protonated through D-leakage, with points at 235 K (left) and without (right).

Table D2. Calculated total energies and thermal corrections.[a]

Name	Formula	*E* (h)	Δ*H* corr (h)	*TΔS* corr (h)	*G* (h)	On scale (h)	Relative to γ-agostic (kcal/mol)
H2	H2	-1.17803	0.01279	0.01103	-1.17263		
CH2Cl2	CH2Cl2	-959.85681	0.03252	0.02286	-959.83961		
Et2O	C4H10O	-233.76679	0.13927	0.02753	-233.64596		
CH2CHtBu	C6H12	-235.93942	0.16715	0.02892	-235.79164		
CH2CMetBu	C7H14	-275.26819	0.19578	0.03160	-275.09358		
CH3CH2tBu	C6H14	-237.17086	0.19043	0.02979	-237.00039		
CH3CHMetBu	C7H16	-276.49500	0.21893	0.03221	-276.29765		
tBuCMe2_+	C7H15	-275.67021	0.20526	0.03297	-275.48704		
tBuCMe2_+_nonclassical_TS	C7H15	-275.66352	0.20512	0.03184	-275.47973		
Cp2TiEt+_betAgostic	C12H15Ti	-1315.97163	0.23937	0.03843	-1315.75801		
Cp2TiEt+_betAgosticTS	C12H15Ti	-1315.96097	0.23862	0.03831	-1315.74802		
Cp2TiH+_CH2Cl2	C11H13Cl2Ti	-2197.17270	0.21541	0.04383	-2196.98666		
Cp2TiMe+_CH2Cl2	C12H15Cl2Ti	-2236.49693	0.24483	0.04734	-2236.28382		

Cp2TiMe+_CH2Cl2	C12H15Cl2Ti	-2236.49693	0.24483	0.04734	-2236.28382	-1276.44421	5.63
Cp2TiMe+_CH2CHtBu_endo	C17H25Ti	-1512.58082	0.37976	0.05100	-1512.23523	-1276.44359	6.01
Cp2TiMe+_CH2CHtBu_exo	C17H25Ti	-1512.57915	0.37984	0.05181	-1512.23403	-1276.44238	6.77
Cp2TiMe+_CH2CHtBu_insTS	C17H25Ti	-1512.56724	0.37965	0.04689	-1512.21900	-1276.42736	16.20
Cp2TiMe+_CH2CHtBu_21insTS	C17H25Ti	-1512.55658	0.37979	0.04716	-1512.20838	-1276.41674	22.86
Cp2TiCHtBuEt+_betAgostic	C17H25Ti	-1512.5939	0.382125	0.04782	-1512.24386	-1276.45222	0.60
Cp2TiCH2CHMetBu+_alpha_agostic	***C17H25Ti***	***-1512.59237***	***0.38114***	***0.05013***	***-1512.24481***	***-1276.45317***	***0.00***
Cp2TiCH2CHMetBu+_alpha_agostic2	C17H25Ti	-1512.59058	0.38100	0.05061	-1512.24349	-1276.45185	0.83
Cp2TiCH2CHMetBu+_beta_agostic	C17H25Ti	-1512.58822	0.38182	0.04780	-1512.23843	-1276.44679	4.01
Cp2TiCH2CHMetBu+_gamma_agostic	C17H25Ti	-1512.59340	0.38220	0.04823	-1512.24351	-1276.45187	0.82
Cp2TiCH2CHMetBu+_alpalp_agosticTS2	C17H25Ti	-1512.58391	0.37974	0.04964	-1512.23744	-1276.44579	4.63
Cp2TiCH2CHMetBu+_alpbet_agosticTS2	C17H25Ti	-1512.58187	0.38020	0.04942	-1512.23478	-1276.44314	6.30

Cp2TiCH2CHMetBu+_alpgam_agosticTS	C17H25Ti	-1512.58766	0.38004	0.04910	-1512.24051	-1276.44887	2.70
Cp2TiCH2CHMetBu+_betgam_agosticTS	C17H25Ti	-1512.58502	0.38118	0.04786	-1512.23591	-1276.44427	5.59
Cp2TiCH2CHMetBu+_gamma_agosticTS	C17H25Ti	-1512.58680	0.38128	0.04823	-1512.23784	-1276.44619	4.38
Cp2TiCH2CHMetBu+_CH2Cl2	C18H27Cl2Ti	-2472.45123	0.41608	0.06060	-2472.07576	-1276.44450	5.44
Cp2TiCH2CHMetBu+_CH2Cl2_a2	C18H27Cl2Ti	-2472.44804	0.41604	0.06012	-2472.07228	-1276.44103	7.62
Cp2TiCH2CHMetBu_Et2O+	C21H35OTi	-1746.37109	0.52419	0.06194	-1745.88839	-1276.45079	1.50
Cp2TiH+_CH2CMetBu_insTS	C17H25Ti	-1512.57192	0.37773	0.04786	-1512.22626	-1276.43462	11.64
Cp2TiH+_CH2CMetBu	C17H25Ti	-1512.58450	0.37847	0.05067	-1512.23998	-1276.44834	3.03
Cp2TiH+_CH2CMetBu_21insReact	C17H25Ti	-1512.58315	0.37809	0.05146	-1512.23953	-1276.44789	3.31
Cp2TiH+_CH2CMetBu_21insTS	C17H25Ti	-1512.56543	0.37748	0.04620	-1512.21889	-1276.42725	16.26
Cp2TiH+_CH2CMetBu_21insProd	C17H25Ti	-1512.56960	0.38051	0.04611	-1512.21998	-1276.42833	15.59
Cp2TiCMe2tBu_+_2betAgostic	C17H25Ti	-1512.58540	0.38005	0.04668	-1512.23663	-1276.44498	5.14

Cp2TiH+_CH2CMetBu_H2TS	C17H25Ti	-1512.56684	0.37536	0.04640	-1512.22256	-1276.43092	13.96
Cp2TiCH2CtBuCH2_+_H2	C17H25Ti	-1512.56935	0.37751	0.04664	-1512.22308	-1276.43144	13.64
Cp2TiCH2CtBuCH2_+_H2rotTS	C17H25Ti	-1512.56392	0.37591	0.04670	-1512.21930	-1276.42766	16.01
Cp2TiCH2CtBuCH2_+	C17H23Ti	-1511.38664	0.35953	0.04646	-1511.05824	-1276.43922	8.75
Cp2TiH+_CH2CMetBu_H2yReact	C17H25Ti	-1512.57910	0.37821	0.05048	-1512.23471	-1276.44307	6.34
Cp2TiH+_CH2CMetBu_H2TSy	C17H25Ti	-1512.55982	0.37461	0.04838	-1512.21762	-1276.42598	17.06
Cp2TiH+_CH2CMetBu_H2yProd	C17H25Ti	-1512.56196	0.37603	0.04875	-1512.21859	-1276.42695	16.45
Cp2TiH+_CH2Cl2	C11H13Cl2Ti	-2197.17270	0.21541	0.04383	-2196.98666	-1276.44899	2.63
Cp2TiH+_CH2CHtBu	C16H23Ti	-1473.25791	0.35024	0.04811	-1472.93990	-1276.45020	1.86
Cp2TiH+_CH2CHtBu_insTS	C16H23Ti	-1473.25724	0.34911	0.04629	-1472.93914	-1276.44944	2.34
Cp2TiCH2CH2tBu+_alpha_agostic	C16H23Ti	-1473.26973	0.35265	0.04820	-1472.94938	-1276.45968	-4.08
Cp2TiCH2CH2tBu+_beta_agostic	C16H23Ti	-1473.27824	0.35311	0.04672	-1472.95643	-1276.46673	-8.51

Cp2TiCH2CH2tBu+_alpalp_agosticTS2	C16H23Ti	-1473.26365	0.35140	0.04867	-1472.94485	-1276.45515	-1.24
Cp2TiCH2CH2tBu+_alpbet_agosticTS2	C16H23Ti	-1473.26621	0.35182	0.04766	-1472.94631	-1276.45661	-2.16
Cp2TiCH2CH2tBu+_betAgosticTS	C16H23Ti	-1473.27155	0.35285	0.04628	-1472.94971	-1276.46001	-4.29
Cp2TiCH2CH2tBu+_CH2Cl2	C17H25Cl2Ti	-2433.13167	0.38786	0.05869	-2432.78314	-1276.45382	-0.41
Cp2TiCH2CH2tBu+_CH2Cl2_a2	C17H25Cl2Ti	-2433.12537	0.38754	0.05808	-2432.77674	-1276.44743	3.60
Cp2TiCH2CH2tBu_Et2O+	C20H33OTi	-1707.05163	0.49585	0.06043	-1706.59627	-1276.46061	-4.67
Cp2TiCH2CtBuCH2_H	C17H24Ti	-1512.1279	0.366124	0.045922	-1511.79254	-1276.39436	36.91

[a] Geometry optimization and vibrational analysis at b-p/TZVP. Final total energies at b-p/TZVPP using the TZVP-optimized geometries, with a COSMO solvent correction ($\varepsilon = 9.1$, CH_2Cl_2). Free energies calculated from TZVPP total energies combined with thermal corrections for 225K, entropy scaled by 0.67 to allow for reduced freedom of motion in solution.

EXSYCalc software data

The software requires two experiments to be done, one with the proper mixing time (0.4 s) that allows exchange detection and another with identical parameters as the former, but with a mixing time of near 0 s (for measuring reference diagonal integrations). Mathematical and theoretical details of the methods the software can be found in the user's guide. The shortest value allowed by the Topspin software (developed by Bruker to run the NMR spectrometer) for the mixing time was 0.0024 s and this value was used for the reference spectrum. Degradation of **II** and 2,3,3-TMB occurred through the course of these experiments at 235 K, and a correction factor was applied to the diagonal peaks of the EXSY performed second to obtain integration of the diagonal peaks at mixing time ~0 s. The correction factor was based on the integration ratios for **II** (1.13607846679395) and 2,3,3-TMB (1.02134370982119) of ^{1}H-NMR spectra before each experiment. Because of degradation (**II** was over 80% gone after ~2 hours at 235 K), it was unfortunately impossible to get EXSY data at higher temperatures (to obtain a better signal to noise ratio and more reliable rate constants), to perform more scans or to use longer mixing times. Additionally, the extent of partial EXSY signal cancellation due to NOE contribution is unknown. It is thus realized that the rate constants (and derived $\Delta G^{\ddagger}$) obtained here represent an approximation only, and are to be interpreted with caution. The reactions of interest are quite slow at 235 K unfortunately leading to poor signal to noise ratio and large uncertainty on the rate constants obtained.

The exercise is nevertheless useful for providing an estimate of $\Delta G^{\ddagger}$ of interest and it also provides indications of rate ratio between the different exchange processes, giving a qualitative description of the mechanisms of reaction at action.

Table D3. Raw integration data for EXSYCalc software used to obtained exchange rates

Specific H being scrutinized (exch. from this H to that in column)	info	II-α-Ha	II-α-Hb	II-β-H	II-γ-H	TMB-α-Ha	TMB-α-Hb	TMB-γ-H	I_D at ~0 s mix. Time	I_D at ~0 s mix. Time with degradation correction
II-α-Ha	I_D	-7928525							-17513951.25	-19897222.88
	I_C	-7928525				-21553.38		-12520.75		
II-α-Hb	I_D	-7901990							-17928920.12	-20368660.08
	I_C		-7901990				-20646.38	-10084.12		
II-β-H	I_D	-9836446							-18203844.38	-20680995.61
	I_C			-9836446				-14392.12		
II-γ-H	I_D	-16308912							-17344053.04	-19704205.19
	I_C				-16308912	-8240.38	-8417.88	-24788.54		
TMB-α-Ha	I_D	-3552900							-5112151.88	-5807805.67
	I_C	-14607.75			-10637.88	-3552900		-61008.25		
TMB-α-Hb	I_D	-3470941							-5064147.00	-5753268.36
	I_C		-19005		-7963.5		-3470941	-50790.75		
TMB-γ-H	I_D	-10823694							-14764028.75	-16773095.15
	I_C	-10837	-11204.5	-19834.5	-18585.793	-46507.12	-38237.38	-10823694		

I_D = integration of the diagonal peak (same as the I_C correlation in gray cells), I_C = integration of the measured correlation, TMB-α-Ha (the hydrogen trans to the 2-methyl group) and TMB-α-Hb (the hydrogen cis to the 2-methyl group) are the olefinic protons of 2,3,3-TMB, TMB-γ-H is the Me group of 2,3,3-TMB and the degradation factors used for obtaining the degradation corrected value of I_D at ~0 s of mixing time for **II** and 2,3,3-TMB are 1.13607846679395 and 1.02134370982119, respectively.

Table D4. Rate constants (k) returned by the EXSYCalc software from the data input found in table D3. Are also presented here the Calculated $\Delta G^{\ddagger}$ (in kcal/mol) for each rate constant obtained by plugging this latter directly in the Eyring equation ($\Delta G^{\ddagger} = R \times T \times LN\left(\frac{hk}{k_B T}\right)$, where k is the rate constant obtained, h is the Planck's constant, k_B is the Boltzmann's constant, R is the gas constant and T the temperature).

Exchange process probed	k (Hz)	k (Min^{-1})	Calc. $\Delta G^{\ddagger}$ (kcal/mol)
II-α-Ha --> TMB-α-Ha	0.006	0.36	16.03
II-α-Ha --> TMB-γ-H	0.003	0.18	16.36
II-α-Hb --> TMB-α-Hb	0.006	0.36	16.03
II-α-Hb --> TMB-γ-H	0.003	0.18	16.36
II-β-H --> TMB-γ-Me	0.003	0.18	16.36
II-γ-H -->TMB-α-Ha	0.002	0.12	16.55
II-γ-H -->TMB-α-Hb	0.002	0.12	16.55
II-γ-H -->TMB-γ-H	0.005	0.30	16.12
TMB-α-Ha --> II-α-Ha	0.012	0.72	15.71
TMB-α-Ha --> II-γ-H	0.006	0.36	16.03
TMB-α-Ha --> TMB-γ-H	0.042	2.52	15.13
TMB-α-Hb --> II-α-Hb	0.016	0.96	15.58
TMB-α-Hb --> II-γ-H	0.004	0.24	16.22
TMB-α-Hb --> TMB-γ-H	0.035	2.10	15.21
TMB-γ-H --> II-α-Ha	0.003	0.18	16.36
TMB-γ-H --> II-α-Hb	0.003	0.18	16.36
TMB-γ-H --> II-β-H	0.005	0.30	16.12
TMB-γ-H --> II-γ-H	0.003	0.18	16.36
TMB-γ-H --> TMB-α-Ha	0.011	0.66	15.75
TMB-γ-H --> TMB-α-Hb	0.009	0.54	15.85